THE UNIVERSITY
of EDINBURGH

Coordination of Distributed Battery Energy Storage Systems in Networks with High Penetration of Photovoltaics

Obinna Unigwe

A thesis submitted for the degree of

Doctor of Philosophy

The University of Edinburgh

February 2020

THE UNIVERSITY *of* EDINBURGH
School of Engineering

Abstract

The use of battery energy storage system (BESS) in the electricity grid is growing in popularity as a major player in facilitating the integration to greater levels of renewable energy sources (RES) into the electricity network. Photovoltaic (PV) in particular, has seen the highest increase in deployed capacity in recent years as a result of falling costs. However, high levels of penetration of PV into the network, can lead to technical challenges such as harmonics, flickers, reverse power and overvoltage. Among these challenges, overvoltage constitutes the major limitation to the increase in RES penetration. Overvoltage can be managed through adequate utilisation of BESS on the network, but BESS are still expensive. Because the health and lifespan of a BESS is dependent on the way it is cycled during its operating life, it is important that BESS is operated in a way that promotes its longevity. This thesis proposes strategies for the coordination of operations of multiple BESS in networks with high penetration of PV. It presents techniques for mitigating resultant overvoltage situations, while operating the BESS in ways that maximise their lifespans.

Control strategies used are based on the use of voltage sensitivities of the network buses for the estimation of charge and discharge powers of the participating BESS at different times. The flat structure sensitivity scheme (FSSS) is the basic coordination scheme that considers the entire network in a flat non-heirarchical structure. The neighbourhood schemes include the uniform neighbourhod participation scheme (UNPS) and the rotational neighbourhood participation scheme (RNPS). These neighbourhood schemes involve the segmentation of the network into neighbourhoods to promote more effective participation of the BESSs. In this thesis, implementation of the schemes on different networks was carried out and simulation results also presented. The results demonstrate that with the proposed strategies, BESS can be effectively used to achieve higher levels of penetration of PV in the power networks, while maximising the BESS lifetime.

Acknowledgements

I would like to express my gratitude to my supervisor, Dr. Aristides Kiprakis for his guidance, support and encouragement throughout the course of this PhD research. Many thanks also to my second supervisor, Dr. Jonathan Shek, for his support.

Special thanks to the Petroleum Technology Development Fund (PTDF), an initiative of the Federal Government of Nigeria. PTDF provided the full funding for this programme and the staff discharged their duties professionally and with great care.

I am grateful to friends from the office. Thanks to John, Joe and Monika for the discussions, company and for reviewing my papers. Thanks to Gbolahan, Godwin and Joe for reviewing this thesis.

This journey would not have been successful without the prayers and support of my family. I wish to thank my father Cyprian (Chukwuebuka) and mother Esther (O-mummy-mi!), for their love and care; my sisters Chinonye (Noss), Uchechukwu (Ponto) and Onyema (Emerson); and my brother Chiemezie (Meemee) for their words of encouragement all along. I also wish to very specially thank my girlfriend, Esther, for her encouraging words, prayers and company from miles away.

I am grateful to all the folks from Kings Church Edinburgh, who helped make Edinburgh a home for me. Thanks to the members of my Small Group for their prayers and encouragement. Special thanks to Peter and Fiona for their kindness and generosity towards me, and for the many trips all around Scotland and the UK.

To my friends before, during and after Edinburgh: Martin, Chuks, Onyeka, Stanley, Chisom, Anayo and Arinze. Thanks for being there always.

Finally, my deepest gratitude, which encompasses others, goes to God - the author and finisher.

Declaration

I declare that this thesis has been composed solely by myself and that it has not been submitted, either in whole or in part, in any previous application for a degree. Except where otherwise acknowledged, the work presented is entirely my own.

Obinna Unigwe

16th February, 2020

Contents

Abstract ii

Acknowledgements iii

Declaration iv

Contents v

List of Tables x

List of Figures xi

List of abbreviations xv

List of mathematical symbols xvii

1 Introduction **1**

1.1 Background of thesis 1

1.2 Research objectives and scope 2

1.3 Thesis statement 3

1.4 Contribution to knowledge 3

1.5 Publications from the research 4

1.5.1 Journal publication 4

1.5.2 Conference publications 4

1.6 Thesis structure 5

2 Literature Review **7**

2.1 Introduction 7

2.2 Evolution of the distribution network 7

2.3 Technical challenges of renewable energy PV connection on the distribution network 10

2.3.1 Voltage rise 10

2.3.2 Voltage unbalance 13

2.3.3 Harmonic distortions 13

2.4 Overvoltage mitigation in distribution networks with high PV penetration 13

2.4.1 Infrastructure upgrade . . . 13
2.4.2 Reactive power control . . . 14
2.4.3 Active power curtailment . . . 15
2.4.4 On load tap changer transformer . . . 15
2.4.5 Use of battery energy storage system . . . 16
2.5 Battery energy storage system technologies . . . 17
2.6 Applications of BESS in the electricity network . . . 20
2.6.1 Renewables integration . . . 20
2.6.2 Power system reliability . . . 20
2.6.3 Voltage regulation . . . 21
2.6.4 Shaving of peak load . . . 21
2.6.5 Frequency response . . . 21
2.6.6 Network upgrade deferral . . . 22
2.6.7 Energy arbitrage . . . 22
2.7 Costs and drivers of BESS . . . 23
2.8 Coordination of BESS operations . . . 24
2.8.1 Decentralised control . . . 25
2.8.2 Centralised control . . . 26
2.8.3 Coordinated control . . . 27
2.9 Research gap . . . 30
2.10 Chapter summary . . . 30

3 Distributed voltage control with PV inverter and BESS 32
3.1 Introduction . . . 32
3.2 Overview and description of problem . . . 32
3.3 Battery energy storage model . . . 36
3.4 Distributed control scheme . . . 37
3.4.1 Normal operations state . . . 38
3.4.2 BESS charging state . . . 39
3.4.3 PV power curtailment state . . . 39

3.4.4 Reactive power absorption . . . 40
3.4.5 BESS peak-shave discharging . . . 42
3.5 Control scheme implementation . . . 44
3.5.1 Implementation tools . . . 44
3.5.2 Test network . . . 44
3.5.3 Load demand and PV profile inputs . . . 45
3.6 Simulation results . . . 46
3.6.1 Case 1 - without distributed control . . . 46
3.6.2 Case 2 - with distributed control . . . 48
3.6.3 Case 3 - distributed control with reactive power action . . . 49
3.7 Discussion . . . 51
3.8 Conclusion . . . 52

4 Dispatch scheduling for BESS in networks with PV penetration 53
4.1 Introduction . . . 53
4.2 Context and presentation of problem . . . 53
4.2.1 Factors affecting battery life . . . 55
4.2.1.1 State of charge (SOC) . . . 55
4.2.1.2 Depth of discharge (DOD) . . . 55
4.2.1.3 State of health (SOH) . . . 56
4.2.1.4 Calendar losses . . . 56
4.2.1.5 Cycle loss . . . 57
4.3 Time-of-use and other electricity pricing schemes . . . 57
4.4 Mathematical model . . . 58
4.4.1 Modelling the BESS . . . 59
4.4.2 Linear program optimisation . . . 60
4.5 Implementation of algorithm . . . 63
4.5.1 Network description . . . 64
4.5.2 Description of profiles . . . 64
4.6 Simulation results and discussions . . . 67

4.7 Conclusion 71

5 Flat-structure sensitivity scheme 73

5.1 Introduction 73
5.2 Background and context 73
5.3 Methodology of the flat-structure sensitivity scheme 74
5.3.1 Voltage sensitivity for BESS selection 75
5.3.2 Description of sets used in formulation 78
5.4 Flat structure sensitivity scheme operation 79
5.5 Implementation of FSSS 84
5.5.1 Implementation tools 84
5.5.2 Description of distribution network 84
5.5.3 Demand and generation profiles 85
5.6 Simulation results and discussions 85
5.6.1 Case 1 - 100% of planned PV capacities 87
5.6.2 Case 2 - 85% of planned PV capacities 91
5.6.3 Case 3 - 70% of planned PV capacities 93
5.7 Conclusion 96

6 Neighbourhood-based coordination schemes 99

6.1 Introduction 99
6.2 Context and presentation of problem 99
6.3 Uniform neighbourhood participation scheme 100
6.3.1 Network segmentation 101
6.3.2 Operation of the uniform neighbourhood participation scheme 103
6.4 Rotational neighbourhood participation scheme 104
6.4.1 Operation of the rotational neighbourhood participation scheme 104
6.5 Implementation of uniform neighbourhood participation scheme . . . 106
6.5.1 Case study network description 106
6.5.2 Simulation results of UNPS 106

6.6 Implementation of rotational neighbourhood participation scheme . . 107
6.6.1 Simulation results of RNPS 110
6.7 Evaluation of performance of neighbourhood schemes 113
6.7.1 Battery lifetime degradation 113
6.7.2 Simulation for battery lifetime 115
6.7.3 Evaluation for UNPS 117
6.7.4 Evaluation for RNPS 118
6.7.4.1 BESS-18 119
6.7.4.2 BESS-17 121
6.7.4.3 BESS-16 121
6.7.5 Comments on evaluation 123
6.8 Conclusion 123

7 Conclusions, recommendations and future work 125
7.1 Introduction 125
7.2 Summary of chapters 125
7.3 Major results and contribution to knowledge 128
7.4 Limitations of work 129
7.5 Suggestions for further research 131

References 132

Appendices 146

A Publications 147
A.1 List of publications 147
A.1.1 Journal publication 147
A.1.2 Conference publications 147

List of Tables

2.1 Comparing chemical batteries based on different metrics 19

4.1 Cable parameters for network used 64

4.2 Energy arbitrage values 71

6.1 BESS and PV installation ratings on test network after modifications . 116

6.2 Frequency of different depths of discharge for the BESS in Zone-1, operating under UNPS 118

6.3 Frequency of different depths of discharge for the BESS-18 in Zone-1, operating under RNPS 120

6.4 Frequency of different depths of discharge for the BESS-17 in Zone-1, operating with RNPS 121

6.5 Frequency of different depths of discharge for the BESS-16 in Zone-1, operating with RNPS 122

List of Figures

2.1 Traditional electricity grid 8
2.2 Modern electricity grid 8
2.3 Renewable generation capacity growth since 2000 9
2.4 Renewable energy sources growth rates 10
2.5 Cost trends for photovoltaic 11
2.6 Voltage rise along the feeder 12
2.7 Sizes and applications of different energy storage technologies 18
2.8 Benefits-stacking for BESS in multiple applications 23
2.9 Global electrochemical storage capacity, 1996-2016 23
2.10 Volume-weighted average prices for Lithium-ion 25
2.11 Decentralised control 26
2.12 Centralised control 27
2.13 Coordinated control 28
3.1 Renewable generation sources and capacities 33
3.2 Model of storage element 36
3.3 Flowchart of the control scheme 38
3.4 Inverter reactive capability curve 40
3.5 Reactive power methods. Upper figure: Fixed $cos\phi$. Middle figure: $cos\phi(P)$. Bottom figure: Q(U) 43
3.6 Single distribution network feeder 45
3.7 Demand and PV profiles 45
3.8 Feeder voltages for case 1. Here, there is no control action in place . . 47
3.9 Feeder voltage when curtailment of active power alone is implemented on the network to maintain network voltages 47

3.10 Active power curtailed. This is when curtailment is the only control measure taken. The blue line shows the total PV power that the PV generator is capable of generating, while the red line shows the power the PV eventually generated, as a result of curtailment 48
3.11 Feeder voltage profiles for case 2. The charging of BESS is implemented here during high PV generation, and discharging of BESS is performed during peak loading period 49
3.12 Active power curtailed for case 2. The blue line shows the total PV power that the PV generator is capable of generating, while the red line shows the power the PV evetually generated, as a result of curtailment. Take note that the red line lies on the blue line for most parts of the figure. 50
3.13 Voltage profile for Case 3. Here, both BESS charging and discharging, and also reactive power absorption are implemented. 50
3.14 Active power that could have been curtailed for Case 3, if the reactive power mode was not activated. The blue line shows the total PV power that the PV generator is capable of generating, while the red line shows the power the PV would have eventually generated, as a result of curtailment. 51
4.2 Test network diagram 65
4.3 Load and PV generation profiles 66
4.4 TOU electricity price profile 66
4.5 Feeder voltage profiles without PV and BESS 68
4.6 Power flows measured at the feeder head 68
4.7 24-hour BESS dispatch, grid energy import, load demand and PV power utilisation using LP algorithm 69
4.8 24-hour profile of SOC of BESS 69
5.1 Flowchart of the FSSS for overvoltage 80
5.2 Flowchart of the FSSS for undervoltage 81

5.3 Diagram of test network 86
5.4 Load and demand profiles 87
5.5 Feeder voltage profile without controls 88
5.6 Feeder voltage profile with coordination control 89
5.7 SOC of network BESS 89
5.8 Power flows measured at the feeder head 90
5.9 Feeder voltage profile without control - case 2 91
5.10 Feeder voltage profile with FSSS - case 2 92
5.11 SOC of network BESS - Case 2 93
5.12 Power flows measured at the feeder head - Case 2 94
5.13 Feeder voltage profile without control - case 3 94
5.14 Feeder voltage profile with FSSS - case 3 95
5.15 SOC of network BESS - Case 3 96
5.16 Power flows measured at the feeder head - Case 3 97
6.1 IEEE 33-bus distribution network 103
6.2 Feeder voltage profile with UNPS 108
6.3 voltage legends 108
6.4 SOC of zone A and zone B with UNPS 109
6.5 Feeder voltage profile with RNPS 110
6.6 Rotational order and SOC at zone A 111
6.7 Zoomed-in rotational order and SOC at zone A. Rank 6 in the represents the position with the highest priority for charging, while rank 1 represents the lowest priority 112
6.8 Curve showing the relationship between number of cycles to failure and fractional depth of discharge 116
6.9 The distribution of frequency of different depths of discharge identified through the rainflow algorithm for UNPS 119
6.10 The distribution of frequency of different depths of discharge identified through the rainflow algorithm using RNPS for BESS-18 in Zone-1 . 120

6.11 The distribution of frequency of different depths of discharge identified through the rainflow algorithm using RNPS for BESS-17 in Zone-1 . 122
6.12 The distribution of frequency of different depths of discharge identified through the rainflow algorithm using RNPS for BESS-16 in Zone-1 . 123

List of abbreviations

BESS . . . . . battery energy storage system/s

CC . . . . . cluster connectedness

COM . . . . . component object model

CPP . . . . . critical peak pricing

CSI . . . . . cluster size index

CT . . . . . cluster tightness

DER . . . . . distributed energy resource

DG . . . . . distributed generation

DOD . . . . . depth of discharge

EV . . . . . electric vehicle

FSSS . . . . . flat structure sensitivity scheme

GHG . . . . . greenhouse gas

LCT . . . . . low carbon technology

LP . . . . . linear program

LV . . . . . low voltage

MV . . . . . medium voltage

OLTC . . . . . on-load tap changer

PV . . . . . photovoltaic

PCC . . . . . point of common coupling

pu . . . . . per unit

RA . . . . . rotation array

RES . . . . . renewable energy source

RNPS . . . . . rotational neighbourhood participation scheme

SE . . . . . sensitivity evaluator

SOC . . . . . state of charge

SOH . . . . . state of health

TOU . . . . . time of use

UNPS . . . . . uniform neighbourhood participation scheme

USD . . . . . united state dollars

VPP . . . . . variable peak pricing

ZN . . . . . zonal neighbourhood

List of mathematical symbols

S_{max} . . . . . maximum apparent power

P_G . . . . . active power generated

Q_G . . . . . reactive power generated

R . . . . . resistance

X . . . . . reactance

P_{PV} . . . . . active power generated by PV

Q_{PV} . . . . . reactive power generated by PV

V_{PV} . . . . . voltage at bus of PV connection

P_L . . . . . load active power

V_{meas} . . . . . measured voltage

V_{UTH} . . . . . upper threshold voltage

V_{LTH} . . . . . lower threshold voltage

P_{DEM} . . . . . demand power

P_{BATT} . . . . . battery active power

q_k . . . . . reactive power available

p_k . . . . . active power from inverter

C_1 . . . . . constant term denoting fixed power factor

C_{ref} . . . . . capacity of battery at the time of estimation

$C_{ref,nom}$ . . . . nominal capacity of reference available by manufacturer

E_{BESS} . . . . . energy state of BESS

P_B . . . . . charge or discharge power of BESS

η_c . . . . . charge efficiency

η_d . . . . . discharge efficiency

P_G . . . . . power drawn from the grid

w_g . . . . . price of electricity purchased from the grid

w_{PV} . . . . . operating cost of PV

w_b . . . . . operating cost of BESS

E_t . . . . . current capacity of battery

E_t0 . . . . . initial capacity of battery

CR_n . . . . . charge rate of nth selected battery

V_{diff} . . . . . difference between measured and threshold voltage

Z_{nbr} . . . . . set containing neighbourhood zones

Chapter 1

Introduction

1.1 Background of thesis

Globally, there has been an increasingly strong drive towards decarbonisation of all aspects of energy. The motivation for this drive stems largely from the realisation of the negative impacts of carbon on the planet. Consequently, huge efforts have been made in investments, research and development of various renewable energy resources (RES), resulting in significant success. The costs of installation of solar photovoltaic (PV) and wind energy sources have fallen consistently in the last decades [1]. This is one of the reasons PV has the largest yearly growth rate for installed capacity out of all the RES [2].

However, RES are highly variable, intermittent and dependent on weather conditions. A significant proportion of PV installations is located on the distribution network. This is a deviation from the classical design of the distribution network, whose function simply was to deliver electric energy to consumers from the transmission network. Furthermore, the distribution network, in this classical role, was designed to be passive. With the installation of the new low carbon technologies (LCT) into the distribution network, there is a necessity for the network to become more active, especially to handle the power flows which have changed from unidirectional to multi-directional.

The installation of renewable distributed generators (DG) gives rise to technical challenges such as harmonics, flickers, reverse power flows and overvoltage [3, 4]. Of these challenges, overvoltage forms a major limitation to increased penetration of PV in the distribution network, therefore inhibiting the goal of achieving total green energy. Many methods have been proposed to solve the overvoltage problem, and to

consequently increase penetration of PV in the distribution network. One promising solution is the use of battery energy storage systems (BESS). The installation of BESS for use in the electricity networks has gained prominence in recent years. A major reason for this, is the falling costs of BESS [5]. An upsurge in demand for batteries for consumer electronics and for transportation has driven both governments and the private sector to invest huge resources into the research and development of improved battery technologies. Despite the consistent falling costs of BESS, installing them in the electricity networks still comes at a huge cost, leading to the need for economic justifications for their deployments. The way BESS is cycled has a direct relationship to their health, and consequently on their lifespan [6] . Therefore, there is a need to operate the BESS in the most efficient and effective way, or to optimally coordinate the operations of the BESS in cases where there are multiple installations on the network, as projected to be the case in the future.

1.2 Research objectives and scope

As the network transformations continue with increased penetration of PV and BESS, there is need for more sophisticated ways of coordinating the operations of the BESS on the network. This is in order to derive economic justification for installation, and also to meet the technical objectives for installation. The aim of this research is to develop strategies for the optimal coordination of the operations of multiple BESS on the network, on order to meet the objectives of installation while maximising economic benefits for the installation. Within this aim is the utilisation of BESS to encourage higher penetration of PV on the distribution network. The specific objectives of this research are summarised as follows:

1. To develop algorithms for the coordination of multiple BESS on the distribution network.
2. To investigate the performances of the proposed algorithms in meeting specific objectives for installation.

3. To explore the behaviour of the algorithms over the lifetime of the BESS.
4. To carry out assessments on the economic benefits of the algorithms and to draw recommendations on the optimal strategies for different network situations.

1.3 Thesis statement

The thesis statement for this research is as follows:

In electricity distribution networks with installations of PV and multiple BESS, the high installation and replacement costs of the BESS is a major limiting factor. The flat structure sensitivity scheme, uniform neighbourhood participation scheme and the rotational neighbourhood participation scheme help to solve this problem by taking smart and efficient measures while selecting, operating and cycling the BESS to achieve technical objectives for installation.

1.4 Contribution to knowledge

This thesis proposes schemes for more efficient operation of multiple BESS in ditribution networks in such a way that maximises the lifespans of the BESS by ensuring effective cycling. The impact of the results from this thesis is the reduction in the overall cost of having BESS on a network, especially a reduction in the replacement costs. This reduction in cost makes a case for the installation of greater capacities of BESS, which in turn encourages greater penetration of clean renewable energy sources, such as PV, into the networks.

The contributions of this research are summarised as follows:

1. Development of control algorithm for uniform control of BESS on a network with high penetration of PV, where the PV inverters have reactive power capability.
2. Development of control algorithm for coordination of multiple BESS in a

distribution network based on the voltage sensitivity of the buses.

3. Development of uniform neighbourhood participation scheme (UNPS) and rotational neighbourhood participation scheme (RNPS). Both are new methods proposed in this thesis, and their objectives are the sharing of network responsibilities by BESS in order to maximise their lifetimes.
4. Evaluation of the performance of various coordination schemes considering the lifetime of the battery and the economic objectives for installation.

1.5 Publications from the research

The results from this thesis have been presented in the following publications:

1.5.1 Journal publication

1. O. Unigwe, D. Okekunle, A. Kiprakis, "Smart Coordination Schemes for Multiple Battery Energy Storage Systems for Support in Distribution Networks with High Penetration of Photovoltaics", *IET Smart Grid*, vol. 2, no. 3, pp. 347-354, 2019.

1.5.2 Conference publications

1. O. Unigwe, D. Okekunle, A. Kiprakis, "Towards benefit-stacking for grid-connected battery energy storage in distribution networks with high photovoltaic penetration", *Proceedings of 11th APSCOM, Hong Kong*, 2018.
2. O. Unigwe, D. Okekunle, A. Kiprakis, "Smart Coordination of Battery Energy Storage Systems for Voltage Control in Distribution Networks with High Penetration of Photovoltaics", *Proceedings of 7th Int'l Conference on Renewable Power Generation, Copenhagen*, 2018.
3. O. Unigwe, D. Okekunle, A. Kiprakis, "Economical Distributed Voltage Control In Low-voltage Grids with High Penetration of Photovoltaic", *Proceedings of*

CIRED 24th Int'l Conference on Electricity Distribution, Glasgow, 2017.

1.6 Thesis structure

This thesis is organised as follows:

Chapter 1 has so far provided an introduction to the thesis, the motivation and objectives of the study, published work from the research and the structure of the thesis.

In Chapter 2, a literature review is presented, which provides an overview of the challenges of the distribution network in the face of high penetration of PV and motivation for increased installation of BESS. In addition, an overview of BESS technologies, characteristics and limitations to penetration of BESS in power networks was presented. The chapter finishes with a conclusion.

Chapter 3 presents an algorithm for the uniform operation of BESS on a distribution network with PV using inverters that possess reactive power capability. An extensive description of the scheme's methodology is presented, followed by their implementation on test cases.

In Chapter 4, optimisation scheduling for dispatch of BESS used for energy arbitrage. A linear program is proposed for the solution of the dispatch problem. Factors affecting BESS life and different electricity tariffs that could affect arbitrage were discussed. Implementation of the program was carried out, followed by discussion of results.

Chapter 5 presents the flat structure sensitivity scheme (FSSS) for coordination of multiple BESS in distribution network with high PV penetration. The methodology of the FSSS is presented, followed by the operation of the scheme. The scheme is implemented on a distribution network and results form different test cases are presented and discussed.

Chapter 6 presents the two neighbourhood schemes proposed in this thesis - the uniform neighbourhood participation scheme (UNPS) and the rotational neighbourhood participation scheme (RNPS). The methodology of both schemes are discussed, followed by implementation of the schemes. Network segmentation, which is a key aspect of the neighbourhood schemes, are also discussed. Results form simulations are presented in this chapter. The chapter concludes with evaluation of performance of the neighbourhood schemes with respect to BESS lifetime.

Chapter 7 provides the conclusions of the thesis. Here, the major contributions of the thesis are highlighted and recommendations are made on the best coordination strategies for different scenarios. Furthermore, limitations of this research are presented along with the potential impacts that this study can have on modern distribution networks. The chapter concludes by recommending further studies to be carried out to further advance the objectives of the study.

Chapter 2

Literature Review

2.1 Introduction

This chapter presents the review of key literature that exists around the subject of this thesis. It starts with an overview of the evolution of the distribution network and continues by detailing the technical challenges present in networks as a result of installation of distributed renewable generators. The challenge of overvoltage is introduced, with methods existing in literature that are proposed to overcome the overvoltage challenge. BESS is introduced, followed by literature review on methods for the coordination of BESS in the power network. The chapter concludes with identification of gaps in literature that this thesis proposes to fill.

2.2 Evolution of the distribution network

The electric power network, in its classical form, was designed with power being produced at generating plants situated long distances away from the points of consumption. A network of transmission and distribution lines are then used to deliver electricity to consumers. Most of these generating plants were powered by fossil fuels, with the accompanying consequences of global warming and pollution. Figure 2.1 [7] shows a typical traditional network.

The power network has evolved since then, with increasing installation of distributed energy resources (DER) on the network. There has been a shift from the the classical unidirectional flow of electric power from distant generators to loads, to a more

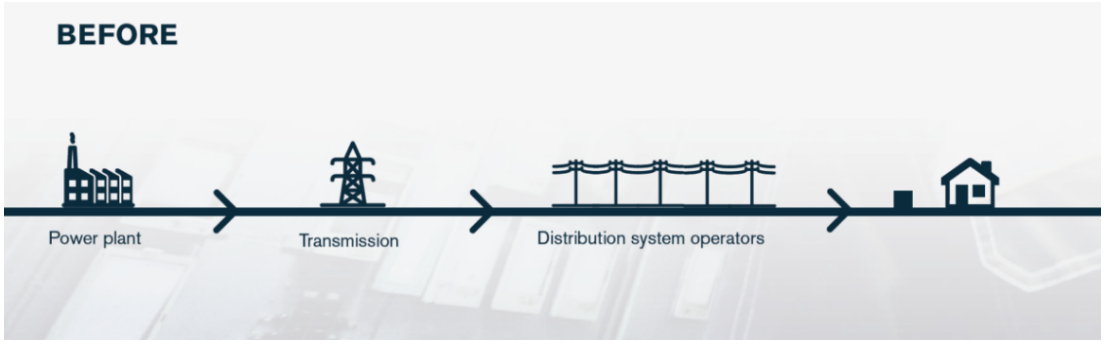

Figure 2.1: Traditional electricity grid [7]

complex network that has power flowing in multiple directions as a result of DER installations. A typical network that has evolved as described is shown in Figure 2.2 [7].

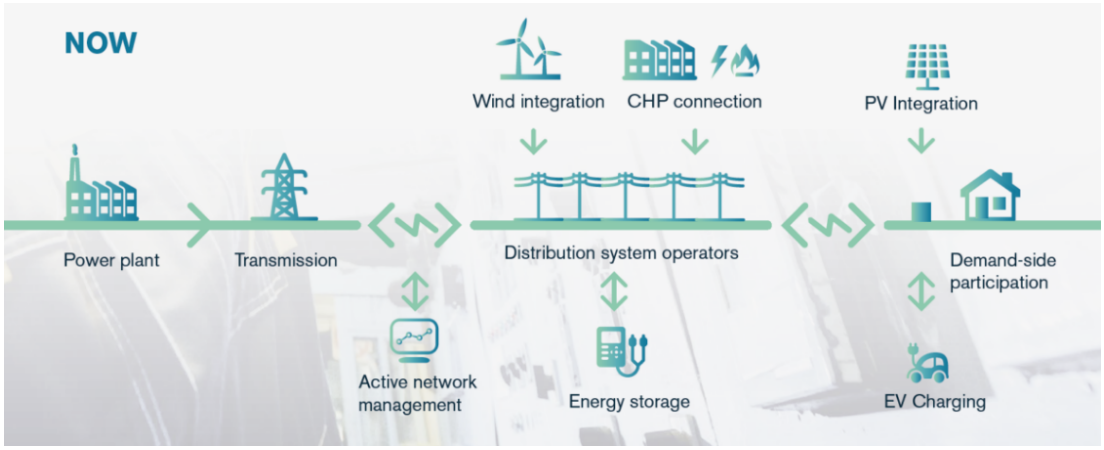

Figure 2.2: Modern electricity grid [7]

DER can be grouped under two major categories: conventional energy sources and renewable energy sources [8]. Conventional energy sources include diesel generators, gas turbines, hydro power plants and fuel cells while renewable energy sources include wind turbines and PV.

Of the two categories of DER, renewable energy sources are of great interest globally. The increase in the installation of renewable energy sources is partly driven by global climate change policies aimed at reducing emission of green house gases (GHG) into the environment. The Kyoto protocol [9] by the United Nations Framework

Convention on Climate Change (UNFCCC) sets out to reduce the rate of global warming by reducing the concentrations of GHG in the atmosphere. Many countries, subsequently, have set carbon targets to reduce carbon emission into the environment. The United Kingdom (UK), in 2016, set new carbon targets to reduce emissions by 57% by 2030 on 1990 levels. [10]. These targets encouraged increase in investments, research and development of renewable energy technologies, with interests coming from governments and the private sector. In 2019, the government of United Kingdom passed into law the amendment of the Climate Change Act of 2008. The new policy introduced a target for at least 100% reduction of greenhouse gas emissions (compared to 1990 levels) in the UK by 2050 [11]. The result of these efforts is the steady growth of global installation capacities of RES since 2000 [2], as shown in Figure 2.3.

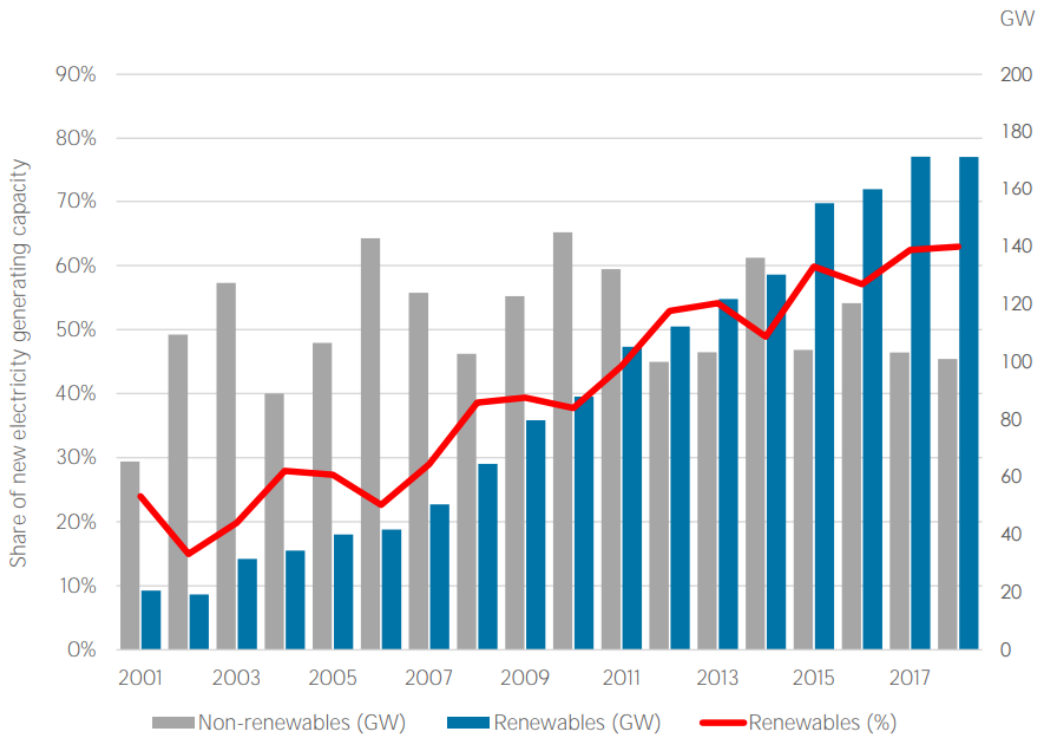

Figure 2.3: Renewable generation capacity growth since 2000 [2]

Of the renewable energy technologies installed on the electricity network, PV constitutes the source with the largest growth rate of installation [2], as shown in Figure 2.4. One reason for this is the consistent fall in the cost of PV as shown in Figure 2.5 [12]. PV also has the advantage of being easily scalable, having less

complex technical installation procedures and having low operations maintenance costs [13].

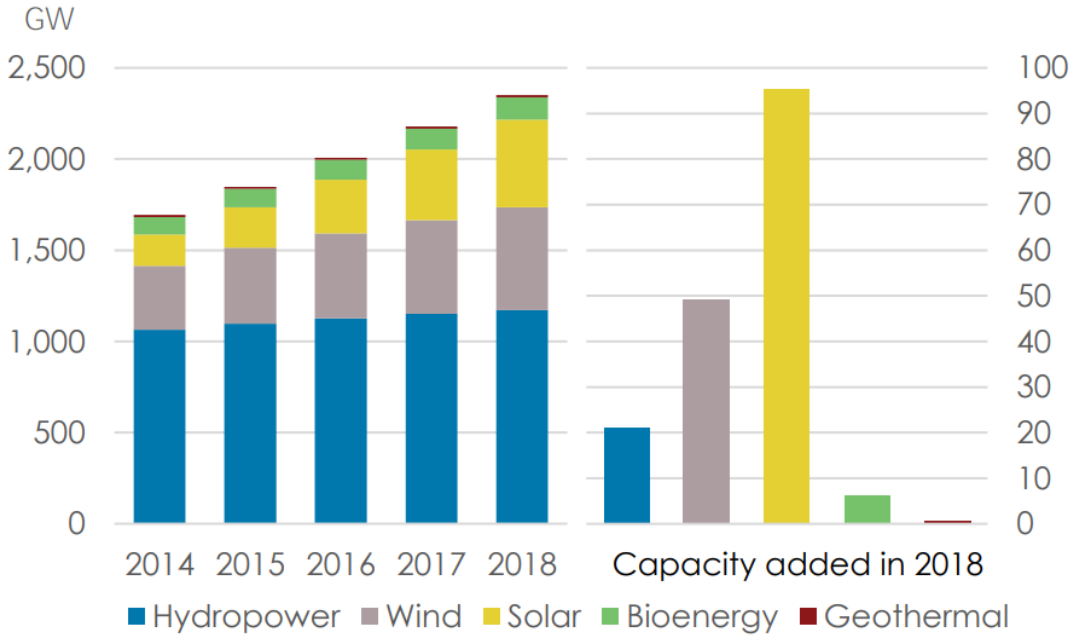

Figure 2.4: Renewable energy sources growth rates (The unit for both charts is GW) [2]

2.3 Technical challenges of renewable energy PV connection on the distribution network

Despite the benefits that accompany the PV and the increase in installations, connection to the network has some technical challenges and negative impacts on the grid. The major technical challenges that arise as a result of PV installation in the distribution network are voltage rise, voltage unbalance and harmonic distortions.

2.3.1 Voltage rise

According to the EN50160 regulation for distribution network voltages in Europe [14], the voltage supplied to electricity consumers are to be maintained at statutory levels. The EN50160 was originally mandated for low and medium voltage distribution

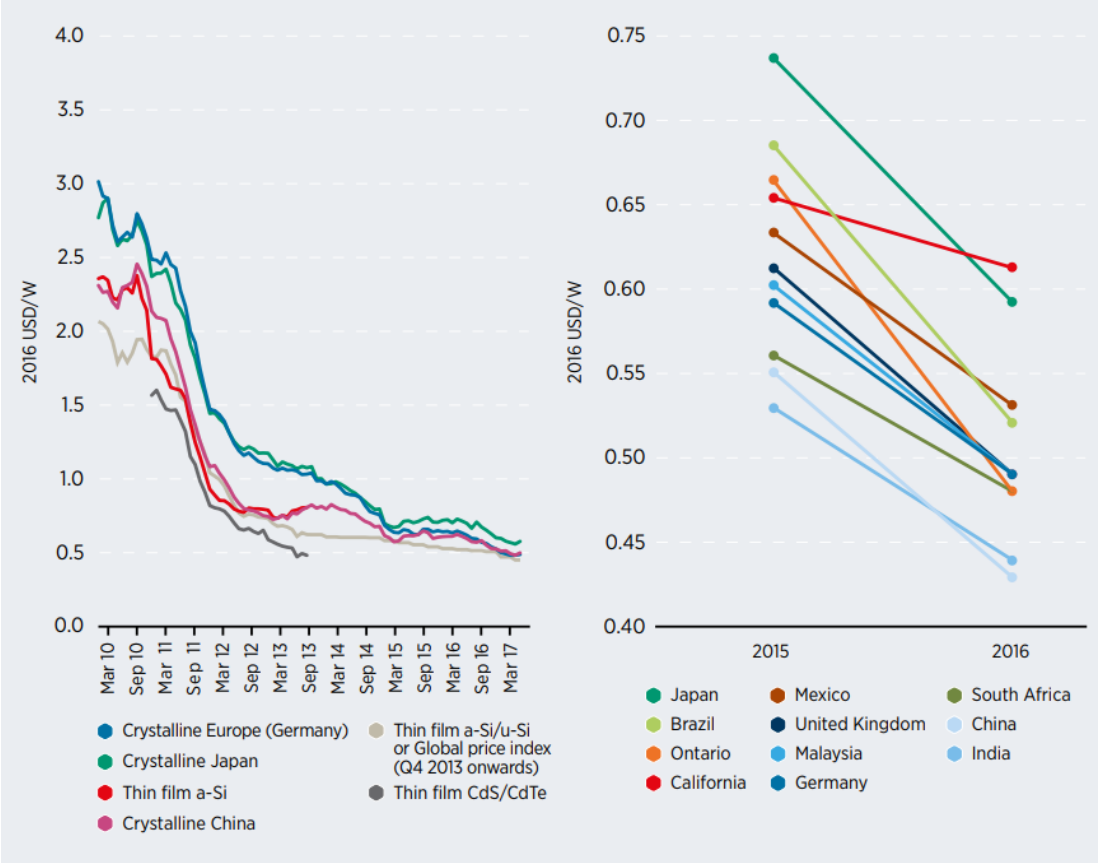

Figure 2.5: Cost trends for photovoltaic [13]

systems for frequency, magnitude waveform and symmetry of supply voltage. There are other standards such as the Norwegian NVE compliance standard, which apply to all network voltage levels [15]. There is also the grid power management requirements by the State Grid Corporation of China for the regulation of voltages within the country. The EN50160 was considered in this research because it deals with supply voltage in the distribution network within Europe and provides general limits which are technically and economically possible for the supplier to maintain in public distribution systems.

During periods of high PV power production on the network, the challenge of voltage rise occurs, especially during times of low consumption on the network. For a radial network without distributed generation (DG), voltage magnitude decreases gradually when moving from the substation down the feeder; the substation has the

highest voltage magnitude while the bus farthest from the substation has the lowest voltage magnitude. In this configuration, there is also unidirectional power flow from substation to the buses down the feeder. With the introduction of DG - such as PV - on the network, there is power flow in multiple directions [16]. Voltages on the buses with DG could rise above statutory levels, to magnitudes greater than the substation voltage and leading to power flowing upstream in the reverse direction. Power flow is also influenced, not just by voltage magnitudes, but by phase angle. Power flows from leading voltage to lagging voltage. Power angles can be manipulated by the use of phase advancers. Multi-directional power flow constitutes technical issues for many network devices since the network was traditionally designed for unidirectional power flow from the medium voltage (MV) network to the low voltage (LV) networks [17]. Figure 2.6 [18] shows voltage rise along a feeder. The voltage rise problem is discussed further in Section 3.2

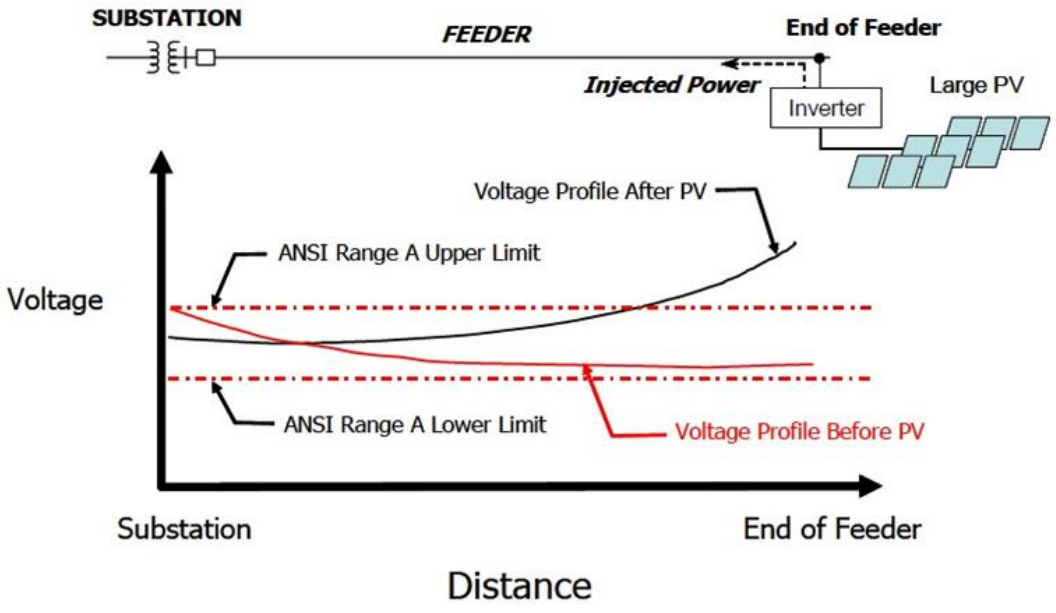

Figure 2.6: Voltage rise along the feeder [18]

2.3.2 Voltage unbalance

Voltage unbalance is often caused when single-phase loads are unevenly distributed within the network, resulting in adverse effects on the power system and on the connected equipment [19, 20]. Voltage unbalance is also caused by asymmetric transformer windings or transmission lines. PV installation is another factor that contributes to unequal voltage magnitudes or angles in the network, when single-phase PV installations are unevenly distributed across the network [21].

2.3.3 Harmonic distortions

Renewable energy sources are connected to grid using power electronic inverters. The main functions of the power electronic inverters, for example the PV's, are to extract maximum power from the PV units while converting direct current (DC) to alternating current (AC). These inverters introduce harmonics into the power networks that lead to distortion of both current and voltage [22]. Harmonics impact the quality of power by causing tripping of circuit breakers, overheating of transformers and reduction in lifespan of devices connected to the network.

2.4 Overvoltage mitigation in distribution networks with high PV penetration

Overvoltage is a major limitation to increased penetration of PV on the network and hence, poses the biggest challenge to connecting RES to distribution networks. Some approaches employed to solve the overvoltage issue are described as follows:

2.4.1 Infrastructure upgrade

A simple and straightforward way of approaching the overvoltage problem is to upgrade some network infrastructure, such as increasing the cross-sectional area of

the cables, and upgrading of transformers [23, 24]. This solution, however, is cost intensive, making it difficult to justify spending [25]. In [23], the maximum possible PV penetration on a distribution network was estimated while upgrading the spans of some selected conductors and the transformer. The investigations revealed that increasing cable sizes increased the network's capacity to host distributed generation, or mitigate overvoltage for already installed PV generators. It was also uncovered that there are optimal locations of the transformer that could help defer the investment in upgrade of cables. This solution is not always trivial, especially in networks that did experience a gradual addition of components and loading over a period of time. Thermal limit is also an important factor affecting power transfers, which can be improved through infrastructure upgrade.

2.4.2 Reactive power control

Reactive power can be used to mitigate overvoltage on the distribution network by the use of PV inverter to absorb reactive power during overvoltage, reducing the magnitude of the voltage as a result [26, 27]. The inverters regulate the power factors to the limit of the inverters' capabilities, given in (2.1)

$$-\sqrt{(S_{max}^2 - P_G^2} \leq Q_G \leq \sqrt{(S_{max}^2 - P_G^2)} \tag{2.1}$$

where S_{max} represents the maximum apparent power of the PV inverter, Q_G is the reactive power and P_G is the active power of the PV. The reactive power capability of the inverter is only as good as its ratings and the current carrying capability of the semiconductor switches used in the construction. The maximum power point tracking (MPPT) of the inverter enables it to produce as much real power as possible. The rest of the current capacity of the inverter can be used to produce reactive power [28]. On the network, however, there is usually a constraint on the power factor of the inverters, enforced by grid operators. This limit varies from region to region. Studies show that

if properly controlled, the PV inverters, through their reactive power capabilities, are able to efficiently achieve volt-VAr control in a distribution network [29–31].

2.4.3 Active power curtailment

Active power curtailment occurs when there is an intentional reduction in the active power output of a generator from what the generator is capable of producing at any given time [32]. With this approach, active power from PV is fully or partially curtailed in the distribution network when there is higher PV power production than load consumption. The voltages are monitored to check when voltage threshold violation occurs. The threshold in this case is the statutory upper limit set for voltages, above which is unacceptable by regulations due to the danger on the network. When the overvoltage is detected, PV power is reduced in discrete blocks of 10% of the capacity of the PV. This continues until there is no more occurrence of overvoltage.

This also means, however, that the revenue gained by PV owners is reduced over a period of time if this intervention continues to be deployed [33]. The economics of installing PV is such that the owners are dependent on maximising the outputs from the installations in order to cover installation and maintenance costs [32]. This is a major disadvantage of active power curtailment for overvoltage mitigation.

2.4.4 On load tap changer transformer

The use of on-load tap changers (OLTC) in networks with DG installation is another way of mitigating overvoltage along the feeders connected to the OLTC [34]. The OLTC is an autotransformer with a number of steps that are automatically adjusted to maintain the voltage within the stipulated lower and upper boundaries. Down the feeder from the substation, voltage generally decreases, except when there is significant presence of DG within the network. The OLTC therefore functions to maintain the voltage at the end of the feeder at a level higher than the minimum stipulated voltage, while maintaining voltages closer to the OLTC at levels lower than

the maximum stipulated voltage [35]. The variability of PV power on a network with high penetration of PV, therefore, leads to frequent switching operations of the OLTC, increasing the overall maintenance and overhaul cost of the OLTC. In [36], a study was carried out to investigate the possibilities of increasing PV hosting capacity of a distribution network. OLTC was utilised and results presented showed that the network's capacity to host PV was increased from 40 to 60. With a resultant increase in total cost, the hosting capacity of the network was further increased to 100% when a remote end voltage-based control was implemented for the operation of the OLTC. In [37], a UK underground low voltage network was examined while implementing a coordinated use of OLTC and three phase capacitor banks. In this study, the capacitors were designed to switch into action before the action of the OLTC, where possible. This combination of reactive power and OLTC action resulted in a reduction in voltage variations on the network. A study carried out in [34] had a Danish underground low voltage network simulated, for investigation of the impact of OLTC and reactive power control on network voltages. For higher levels of PV penetration, OLTC controls alone were insufficient for maintaining network voltages.

2.4.5 Use of battery energy storage system

In distribution networks with high penetration of PV, BESS can be used to mitigate the overvoltage occurrence to which such networks are susceptible. The deployment of BESS in power networks has been increasing over the last decade. This is as a result of the multiple functions that the BESS can perform, in addition to the reality of gradually falling costs of BESS [5]. The central basis of BESS application across the power network, especially networks with installations of renewable energy resources, is the concept of charging the batteries with cheap, available and often surplus energy from the renewable energy sources and discharging during times of costly and insufficient power production [38]. Among the multiple functions of the BESS, overvoltage mitigation is achieved by charging the BESS during periods of high PV power production and lower load consumption. In this application, the BESS

acts as extra load on the network and therefore prevents the situation where voltages rise beyond statutory levels. Further insight on the BESS functions, technologies, costs and challenges are provided in Section 2.5.

2.5 Battery energy storage system technologies

There are several types of energy storage systems. These can be broadly categorised under thermal, mechanical, electrochemical, electromagnetic and biological energy storage. Examples of mechanical energy storage include pumped hydroelectric, flywheel, compressed air, and gravitational potential storage [39]. Electrochemical energy storage includes flow batteries and metal oxide batteries. Thermal storage includes solar pond, brick storage heater and molten salt heater. Electromagnetic storage includes supercapacitors and capacitors. Mechanical storage accounts for the largest proportion of energy storage deployed in electric power networks, with pumped hydroelectric storage being the highest of all energy storage deployed, in terms of capacity [40] as shown in Figure 2.7.

Battery energy storage is a type of electrochemical storage. Three components constitute the typical battery storage namely: cathode, anode and electrolyte. Battery energy storage is the most popular form of storage for smaller scale applications among all the other sotrage technologies. A comparison made in [39] between the common battery storage technologies with respect to the metrics described above is given in Table 2.1 .

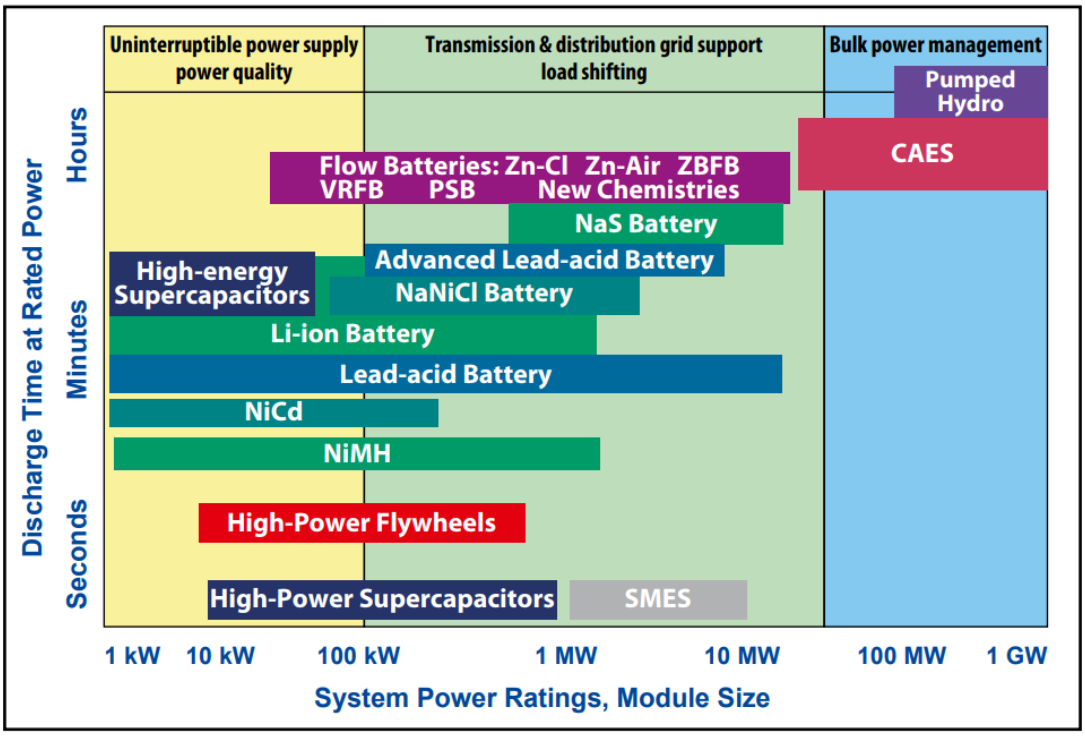

Figure 2.7: Sizes and applications of different energy storage technologies [40]

Table 2.1: Comparing chemical batteries based on different metrics [41].

Specifications	**Lead Acid**	**NiCd**	**NiMH**	**Li-ion**		
				Cobalt	Manganese	Phosphate
Specific energy (Wh/kg)	30-50	45-80	60-120	150-250	100-150	90-120
Internal resistance	Very low	Very low	Low	Moderate	Low	Very low
Cycle life (80% DoD)	200-300	1000	300-500	500-1000	500-1000	1000-2000
Charge time	8-16h	1-2h	2-4h	2-4h	1-2h	1-2h
Overcharge tolerance	High	Moderate	Low	Low. No trickle charge		
Self-discharge/month (room temp)	5%	20%	30%	<5% Protection circuit consumes 3%/month		
Cell voltage (nominal)	2V	1.2V	1.2V	3.6V	3.7V	3.2-3.3V
Charge cutoff voltage(V/cell)	2.40 Float 2.25	Full charge detection by voltage signature		4.20 typical Some go to higher V		3.60
Discharge cutoff voltage (V/cell, 1C)	1.75V	1.00V		2.50V - 3.00V		2.50V
Peak load current **Best result**	5C 0.2C	20C 1C	50C 0.5C	2C <1C	>30C <10C	>30C <10C
Charge temperature	-20 to 50^oC	0 to 45^oC		0 to 45^oC		
Discharge temperature	-20 to 50°C	-20 to 65^oC		-20 to 60^oC		
Maintenance requirement	3-6 months	Fully discharge every 90 days in full use		Maintenance-free		
Cost	Low	Moderate		High		

2.6 Applications of BESS in the electricity network

In the electric power network, the energy storage is employed for a number of applications. The different applications are available at different levels of the network, from generation to transmission and distribution networks, down to the load level [42]. These applications are summarised in the following subsections.

2.6.1 Renewables integration

Solar and wind power generation, which are the most deployed renewable energy sources, are intermittent and non-dispatchable [43]. Therefore, to effectively integrate these sources into the network, the BESS is useful for balancing up the variability caused as a result of integration [43, 44]. This improves the power system's reliability. In addition, profitability of solar and wind installations can be improved by incorporating BESS [45]. In this study, BESS incorporation caused an increase of 18% in revenue made every 48 hours. Using the BESS for renewables integration applies both for large scale systems like solar and wind farms, and for smaller scale systems like the residential rooftop applications. The BESS enables owners to produce and consume electricity at times of the day most convenient to their needs and in the most economical way.

2.6.2 Power system reliability

BESS can be dispatched in a very short time and therefore can be used in applications that require fast response. BESS is therefore made available to be used in response to contingencies on the network. In addition, reliability of power networks with large conventional power generators can be improved with incorporation of BESS. The study in [46] compared the reliability of the power supply in a network using conventional power plants with and without BESS. The metrics for this comparison were Energy Index of Reliability (EIR), Loss of Load Expectation (LOLE), Expected Energy Not

Supplied (EENS) and Loss of Expected Energy (LOEE). It was demonstrated that the use of BESS resulted in the improvement of 10.9% in LOLE and an improvement of 50% in the LOEE reliability metrics of the power supply on the network.

2.6.3 Voltage regulation

In networks with renewable energy power sources, BESS can be used to regulate voltages, especially mitigating overvoltage. Overvoltage arises during times of high power production compared to lower loading value. Also, voltage regulation through reactive power can be provided to the network using the inverters of BESS. In [47], the BESS was employed to provide voltage support at the site of a large electricity consumer that experienced motor start problems caused by voltage drop as a result of faults. As a result of initial current surge during electric motor start, consumers use motor soft starters to reduce mechanical stress on the motor, the shaft and the electric distribution network.

2.6.4 Shaving of peak load

BESS finds useful applications in networks by reducing load demand on the network during peak times. BESS is charged during periods of low load demand, low electricity prices or high production from renewable energy sources. The stored energy is made available at peak loading periods to alleviate congestion on the network. Results of the study carried out in [48] shows that employing BESS in networks with PV penetration was successful in significantly reducing the peak electricity demand on the network.

2.6.5 Frequency response

As a result of increasing deployment of intermittent renewable energy resources on the network, frequency events (increase above and decrease below maximum and minimum regulation frequencies respectively) on the network are expected to increase.

This expectation is also supported by the reduction in system inertia as a result of decommissioning of large conventional power plants that provided inertia support [49]. BESS are able to dispatch energy very fast, and therefore are a good option for the use in frequency response ancillary services. Provision of this service by BESS, however, comes with a few factors that must be considered [50]. Factors such as the SOC at which the BESS should be maintained, the right size of BESS to be used, the best location to site the BESS and the economic cost justifications for the owners of the BESS.

2.6.6 Network upgrade deferral

Upgrading transmission or distribution networks, for example, changing to larger size cables or transformers, is a cost-intensive endeavour [51]. Grid reinforcement, which is often done as a result of growth in annual loading or peak loading on a network, could be deferred by the installation of BESS on the network. As the peak load rises, the components of the network approach their rated capacities and operating close to this rate often reduces the lifespan of these components [52].

2.6.7 Energy arbitrage

In some electricity markets, there could be significant difference between electricity prices at different times of the day. This difference can be taken advantage of, using BESS, to purchase electricity during periods of lower prices and then sell during periods of higher prices [53]. Some energy is lost in conversion between charging and discharging, and this constitutes a limitation. In many use cases, energy arbitrage using BESS is not significantly profitable when deployed as a standalone application, Therefore, energy arbitrage is often deployed alongside other BESS applications in a structure referred to as ”benefits-stacking”. Figure 2.8 [42] shows the concept of benefits-stacking, using BESS for multiple applications on the network.

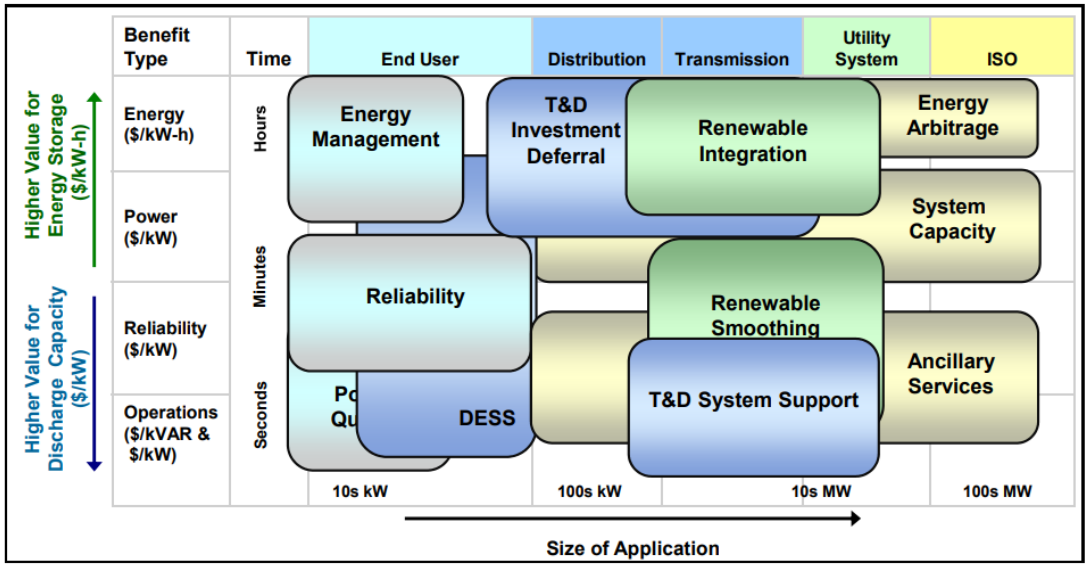

Figure 2.8: Benefits-stacking for BESS in multiple applications [42]

2.7 Costs and drivers of BESS

BESS has many promises and potential areas of application in the power network, as seen in Section 2.6. In the last few decades, there has been a steady increase in the capacities of BESS installed for stationary applications on the electric power grid [40], as shown in Figure 2.9.

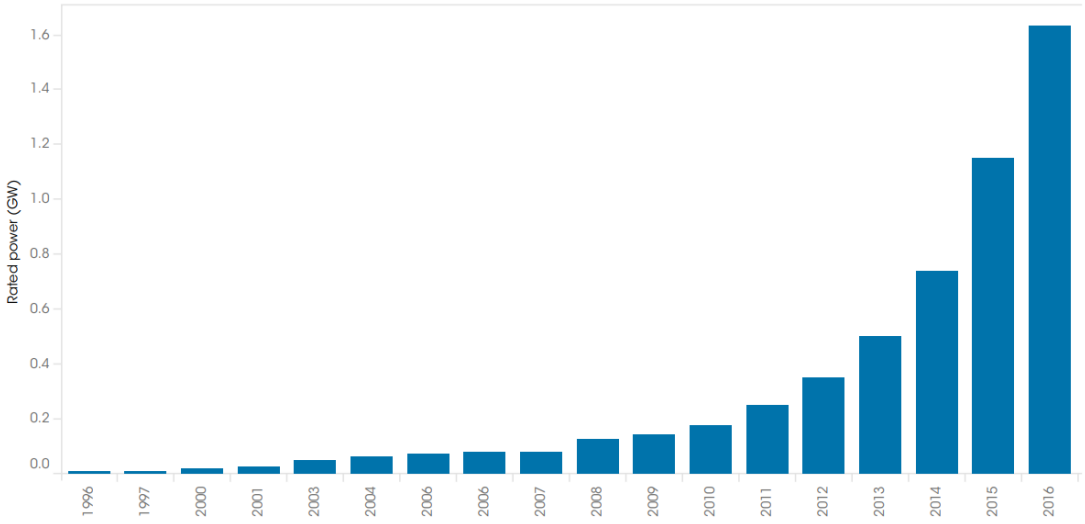

Figure 2.9: Global electrochemical storage capacity, 1996-2016 [40]

A major motivation for the increased deployment of BESS on the network is the steady fall in prices of the systems [5]. There is a high interest in the development of batteries, not only for stationary applications in power systems, but for applications in consumer electronics and electrification of transportation using the electric vehicles (EV). The disruption in the electricity industry, occasioned by the uptake of renewable energy sources, will be advanced by the increased and rapid deployment of BESS on the power networks.

The lithium ion (Li-ion) battery, in particular, has huge potential for cost reduction. The major drivers for this cost reduction include economies of production scale, improvements in materials, performance improvement and more competitive supply chains [40]. The potential for reduction in cost is greater for the Li-ion battery than for other technologies as a result of the dominance of Li-ion in the EV market and collaborations for Li-ion production, both for EV and stationary applications.

Despite the falling costs of BESS and the expectations for the costs to continue dropping in the coming years [54], the present cost of BESS is still high. Some applications of BESS are still not able to economically justify the costs for their installation. Figure 2.10 shows that the volume weighted average battery pack fell 85% from 2010 to 2018 [55].

2.8 Coordination of BESS operations

Given that the costs for installation of BESS are still high, there is therefore a need for optimal operation of the BESS within the network. The pattern of operation of the BESS impacts the health and lifespan of the BESS. Any scheme for coordination of operations of BESS that helps to prevent the shortening of the lifespan of the BESS, improves the chances of profitability of BESS investments.

Three high level methods of control of the BESS in networks can be identified. These are decentralised, centralised and coordinated control methods.

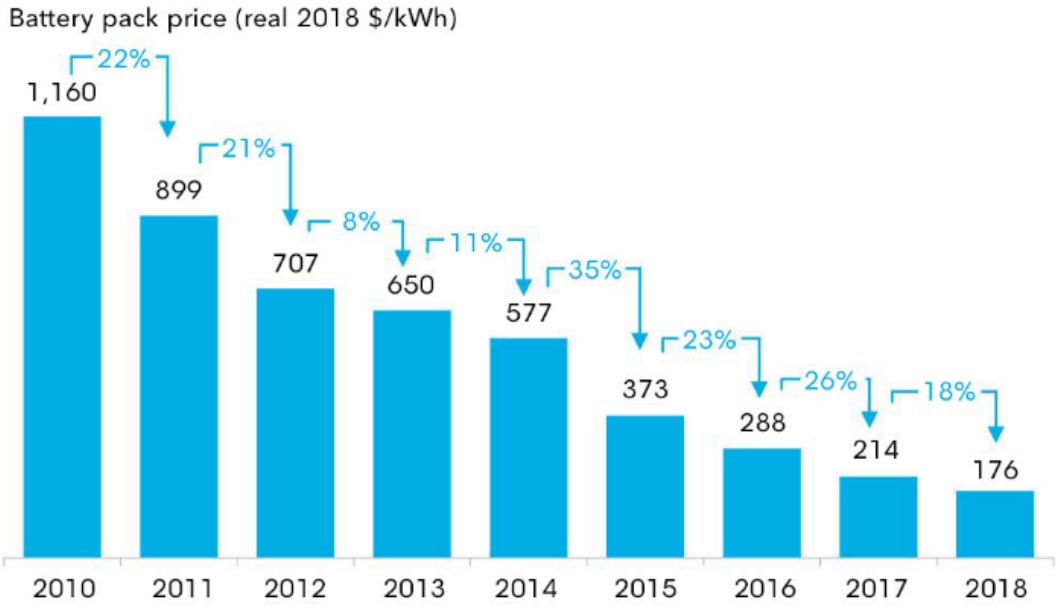

Figure 2.10: Volume-weighted average prices for Lithium-ion [55]

2.8.1 Decentralised control

For the decentralised method, shown in Figure 2.11, there is a reliance on the local bus voltage measurements for the control of the operations of the BESS. This is often a cheap solution since there is no need for investment in communication infrastructure for its operation. Authors in [56] implemented a decentralised voltage control for distributed generators. They controlled the on-load tap changer (OLTC) capacitor banks and distributed generators in the network using localised fuzzy logic controllers. In their work, the measurements were obtained from the local buses and the aim of the controllers was to maintain the local bus voltages within target limits. In [57], a strategy for the decentralised operation of multiple energy storage systems was presented for frequency regulation. A droop controller was used for the management of the state of charge of the BESS to regulate frequency in the network by adding a frequency offset in accordance with the measured frequency.

One downside to the use of the decentralised method is that the structure of the decentralised method, having no communication between network buses, does not

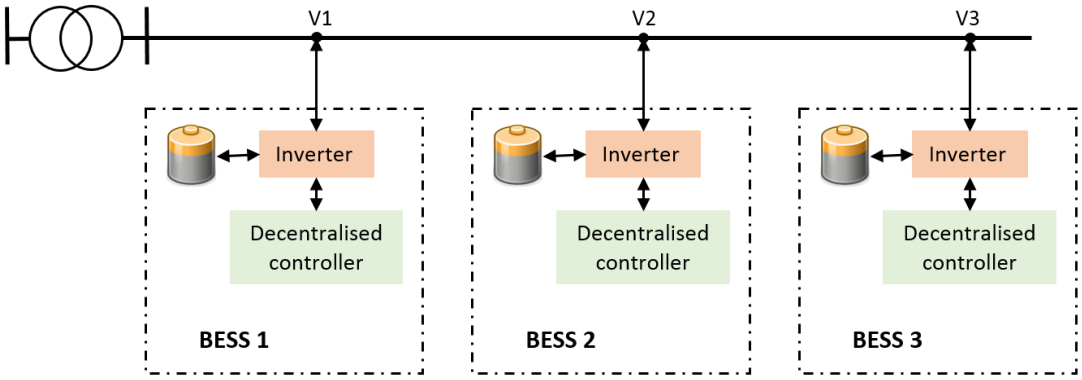

Figure 2.11: Decentralised control

permit the support of other buses by neighbouring buses. A bus that is distressed by overvoltage, as a result of the co-located BESS being fully charged, or due to insufficient power capacity to deal with a situation, cannot get support from other BESS in the decentralised control scheme.

2.8.2 Centralised control

In the centralised control method, the set-points, charge and discharge signals of the BESS are determined and set by a central controller. The central controller knows the state of the network and voltages at every node, at every point in time. This requires, therefore, that a fast and reliable communication infrastructure exists in the network between the controller and other network components. The centralised control is shown in Figure 2.12.

In microgrids, the use of centralised control with dedicated communication channels can help to enhance the stability of the grid [58]. In [59], a proposal was made for a centralised coordination scheme for small control of energy storage and distributed generation in microgrids. The aim was to use the control to limit the generation of renewable energy sources in the microgrid, in order to avoid overcharging of the energy storage systems while disconnecting loads at the appropriate times, in order to avoid deep discharge of the energy storage systems [60]. As a result of the requirement for

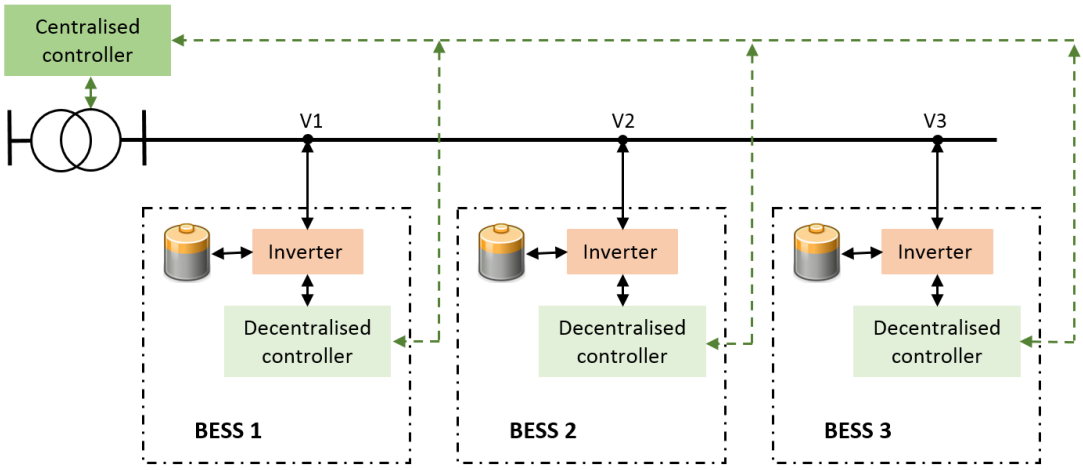

Figure 2.12: Centralised control

communication infrastructure, the centralised control method can be capital intensive. Another disadvantage is that there is a single point of failure in the system.

2.8.3 Coordinated control

The coordinated control scheme attempts to combine desirable features of the distributed control and the centralised control to deliver best results. Figure 2.13 shows the coordinated control structure.

Many studies have been carried out in the area of coordinated control of BESS in power networks. In [61], a control algorithm was proposed for the coordination of BESS used in low voltage distribution networks in networks with rooftop PV. BESS was used to mitigate occurrence of overvoltage and undervoltage on the network in the presence of high penetration of PV. Consensus control was used in this work to share the action responsibilities among the participating BESS on the network. A strategy for optimally integrating BESS on a distribution network to improve the capacity to host load and other distributed generators was developed in [62]. It takes into account the system of cycling the batteries in a way to protect battery health. In [60], a battery aging model was incorporated into the coordination strategies developed for the operation of BESS on a low voltage network. Voltage sensitivity analysis was the basis of the scheme,

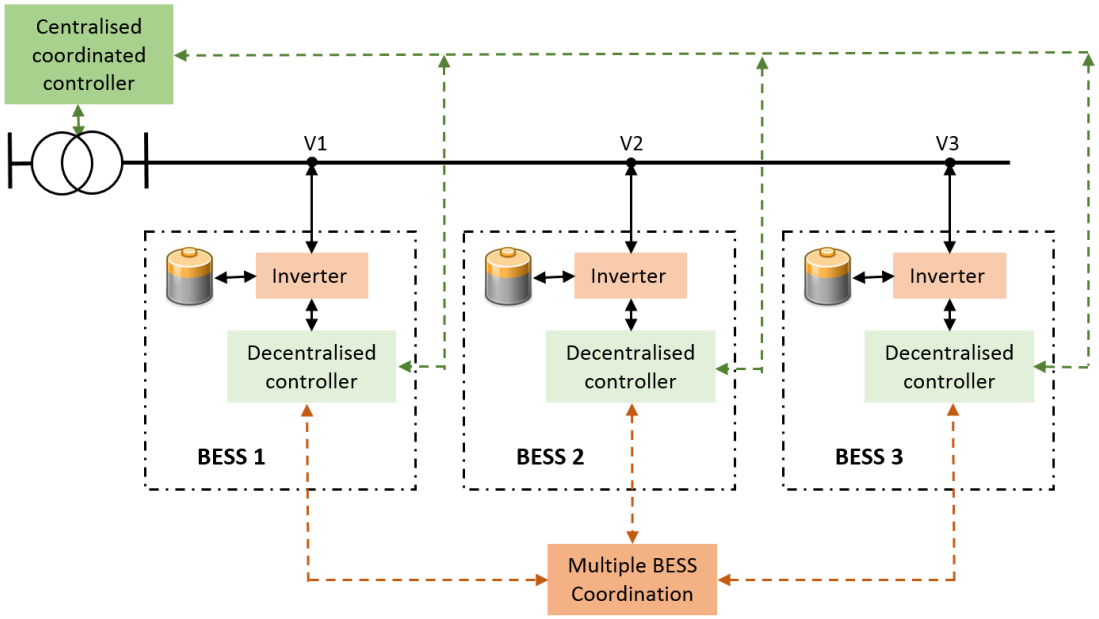

Figure 2.13: Coordinated control

which is aimed at maintaining the voltages along the feeder within statutory limits. Reactive power is one of the solutions available for the control of network voltages within this study. The reactive power injection and absorption are controlled locally at the buses, using voltage sensitivity to estimate the quantity needed. This is the same for active power dispatch. A central controller handles the task of appointing which BESS is to be selected, depending on capacity availability, aging and outage condition.

The study carried out in [63] proposed a coordinated control algorithm for the control of multiple BESS in a distribution network. The algorithm involves a central controller where network information resides and from where charge/discharge control action signals are sent to the network BESS. The central controller has information on voltage, state of charge of the batteries and frequency. The major objective of the algorithm is to mitigate frequency and voltage deviations of the network by coordinating the operations of the participating BESS. In [64], the profitability of stacking multiple applications of BESS in a network is evaluated. Consideration was given to the often-overlooked situation that the BESS cannot always be available at every time to provide the services for which they have been contracted. Provision of one service

often means unavailability for the provision of another service, due to limitation in the capacity of the BESS. Reliability of components was also factored in while carrying out the evaluations in this work. In [65], the authors explored the performances of different strategies for the control of BESS that are co-located with PV. In these strategies, mitigation of overvoltage and deriving benefits for BESS owners were the main objectives. The amount of reactive power required for the operation of the systems was also considered for reduction. The distributed scheme, which was one of the strategies explored, showed superior performance in reducing voltage imbalance and line losses.

In [66], a coordinated control of BESS and PV to achieve voltage control was proposed for the control of voltages on residential networks. In this study, advanced metering infrastructure or any extensive communication was not required, since there was placement of local droop controllers on every bus where BESS is installed. The charging and discharging operations of the BESS are dependent on the measured voltages at the residential locations. The impact of line characteristics on the effectiveness of reactive power control was also evaluated. Authors in [67] proposed a method for the coordination of multiple BESS in a network to control voltage and manage loading in distribution networks. It uses a combination of loaclised and centralised approaches to manage the dispatch of reactive power for voltage control. A consensus algorithm is used in a centralised control scheme to achieve coordinated operation of the installed BESS in a way that distributes the network burdens across the participating BESS according to their availability and power capacities. One of the demerits of this method is the possibility of using same BESS, or same set of BESS, more frequently than others, as a result of the position of these victim BESS being located on critical buses on the network that are susceptible to overvoltage. In [68], energy storage was used to mitigate fluctuations in power output from PV using ramp rate control. The energy storage units used in this work can be made available for other services such as voltage control.

2.9 Research gap

In the literature examined so far, one of the major challenges encountered while coordinating multiple energy storage in power networks is the susceptibility of some BESS to over-cycling when compared to other BESS on the same network. Since the topology of a network and other network parameters such as line impedance and lengths do not change very much over time, it means that some BESS located at certain buses in the network will be candidate BESS selected for solutions on the network. This is what the uniform neighbourhood participation scheme (UNPS) introduced in Chapter 6 of this thesis proposes to solve. In addition to the UNPS, a second method is proposed in this thesis - the rotational neighbourhood participation scheme. This method approaches the problem from a different perspective by keeping track of the cycling of BESS in particular zones and rotating the operations of participating BESS in the zones.

Solving the challenge of coordinated control by using efficient cycling methods leads to longer lifespan for the BESS as a result of more even use and cycling of the BESS. For power networks in general, this helps to reduce the overall cost of installation and use of BESS by delaying replacement costs, thereby paving the way for installation of cleaner distributed renewable energy sources in the power networks.

2.10 Chapter summary

This chapter reviewed the changes that have occured in recent years in the way electric power is produced, transported and used. Some of the technical challenges network operators are faced with as a result of increased installation of intermittent distributed energy resources in the network were examined. Energy storage use for various applications on the power network was also reviewed, with particular attention to the BESS, which is the energy storage technology used throughout the

thesis. Furthermore, the chapter highlighted the challenges that inhibit the growth and prevalence of BESS installations in the power network. This focused mostly on the trends of BESS cost and the drivers for the BESS market. The importance of coordination of BESS operations was emphasised in this chapter and a review of studies carried out in this area was also presented. The chapter concludes with the identification of research gaps that form the motivation for this thesis.

Chapter 3

Distributed voltage control with PV inverter and BESS

3.1 Introduction

This chapter presents a scheme for distributed control of voltages on distribution networks with high penetration of PV. The chapter begins with an overview of relevant literature and presentation of problem, followed by a description of BESS model used in the rest of the thesis. The control scheme is described with its various features. The chapter continues with description of simulations for the implementation of the scheme, followed by presentation of results. Results are discussed and conclusions are drawn to end the chapter.

3.2 Overview and description of problem

Considerable research and investment have gone into the development of cleaner Renewable Energy Sources (RES) such as PV. The penetration of PV in the distribution network has also experienced a significant increase as a result of this. The distribution network was originally designed to be a passive network that only facilitates the transport of generated power from the transmission network to the final consumers [69]. However, increased penetration of RES into the traditional grid gives rise to technical challenges with power quality, especially in distribution networks where a significant portion of these RES are connected. The power quality issues include voltage unbalance, overvoltage, line flickering and harmonics. Among these problems, overvoltage presents the major limiting factor to increased levels of penetration of

RES into the grid. Overvoltage arises when the consumption on a feeder is below the production, causing voltages to increase beyond statutory levels and power to flow in the reverse direction from the low voltage network in to higher voltage networks [70]. In some countries like Japan, such reverse power flows are totally prohibited due to adverse effects that often arise [71]. In Germany, the maximum allowed voltage increase on the low voltage network as a result of distributed generation is 0.02 per unit (pu) [72]. This implies that there is a limitation on the amount of PV generation that can be installed on the network, and in some cases, the installed PV generators are not able to generate to their maximum capacities.

Typical radial networks with no DG along the feeders have unidirectional power flow from the substation down to the end of the feeder. For such networks, voltage magnitudes also decrease from the substation down along the feeder. With the introduction of DG such as PV, the feeder voltage behaviour changes. Consider the simple network depicted in Figure 3.1.

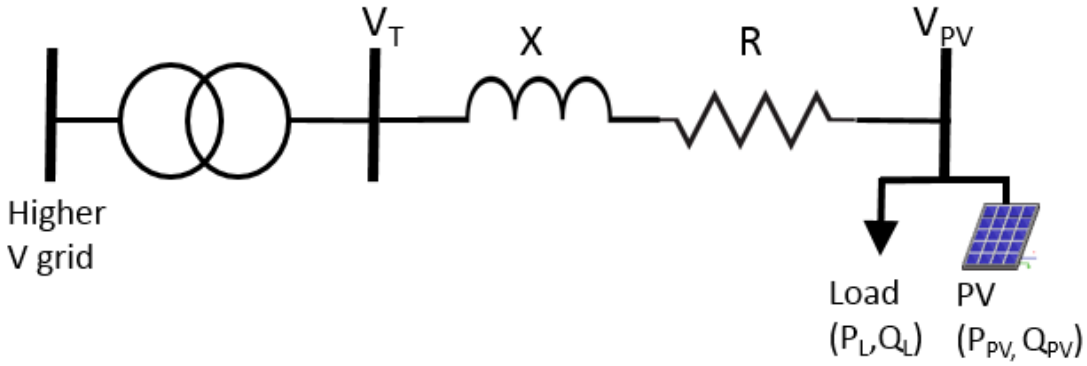

Figure 3.1: Renewable generation sources and capacities

The network consists of the substation and power line connecting the substation to the load. On the same bus as the load is connected a PV generator. An expression for the voltage across the network with respect to the buses is given in (3.1)

$$V_{PV} - V_T = \Delta V = \frac{R(P_{PV} - P_L) + X(Q_{PV} - Q_L)}{V_{PV}} \tag{3.1}$$

where R and X are the resistance and reactance of the line respectively. P_{PV} and Q_{PV} are the active and reactive power of the PV generation, V_T and V_{PV} are the voltages at the substation and the bus of PV connection respectively while P_L and Q_L are the load active and reactive powers. In the event of any unbalance between P_{PV} and P_L, or Q_{PV} and Q_L, voltage rise along the feeder may be experienced and thus violating statutory voltage thresholds for operation on the network. Electricity networks are operated and managed within voltage bands [14]. Other impacts of high PV penetration are investigated in the work done in [73]. Continued violation of these thresholds could lead to disconnection of the distributed generators from the network [74].

Many approaches to solving this problem have been proposed in the literature. Upgrade of network infrastructure, like the cross-section of cables is a straightforward way of achieving this [23]. In [36], a study was carried out to investigate the possibilities of increasing PV hosting capacity of a distribution network. OLTC was utilised and results presented showed that the network's capacity to host PV was increased from 40% to 60%. With a resultant increase in total cost, the hosting capacity of the network was further increased to 100% when a remote end voltage based control was implemented for the operation of the OLTC. Using step voltage regulators (SVR) and on-load tap changers (OLTC) are traditional voltage control methods. However, these technologies, in the presence of high PV penetration are exposed to stress, leading to degradation and reduced lifetimes [75].

The cables in the distribution network have high resistance to reactance ratio, (R/X), which makes real power control of voltages to have significant effect on distribution network voltages [76–78]. Incorporating BESS into networks with PV systems is a promising solution to the overvoltage problem as it provides flexible real power control within the network. In [79], a distributed control was developed for sharing of power using droop control without the communication connections.

Use of the reactive power capabilities of the PV inverters, alongside active power curtailment is one method for solving the overvoltage problem. For this method,

reactive power absorption is employed during overvoltage, followed by active power curtailment if the reactive power absorption is insufficient [80]. The limitation of this approach is that curtailment of active power means that the gains from investment in PV are not maximised. In the literature, a number of works have utilised the capability of the PV power electronic inverters to produce reactive power, alongside active power. Network bus voltages are controlled, not only be active power, but by reactive power injection and absorption [29–31, 81].

Active power curtailment is one of the methods of mitigating overvoltage that results from distributed PV installations. In [82], an adaptive droop based control was implemented for the management of active power curtailment in the distribution network. The adaptive method reduces the occurrence of unnecessary curtailment of PV power. In [83], a droop based active power control scheme was implemented for the prevention of overvoltage on buses of a distribution network with high levels of PV penetration.

In countries like Germany and Italy, there has been a drive to involve prosumers in the low voltage (LV) distribution networks to actively participate in network management, instead of remaining passive [84]. The inverters of PV systems are capable of providing reactive power services to the networks to which they are connected. This feature can be further explored in achieving voltage control together with the use of BESS. This is achieved by varying the reactive power being exchanged between the inverters and the grid.

This chapter presents a control scheme that utilises the reactive power capabilities of PV, battery energy storage and active power curtailment to maintain network voltages within statutory limits for networks with high penetration of PV. In this scheme, during high PV generation that leads to overvoltage, the BESS is brought into action by the controllers. The reactive power resource of the PV inverters is then utilised if the BESS action fails to solve the overvoltage problem. Curtailment of PV active power (P_{PV}) is carried out as a last resort if the previous measures failed.

3.3 Battery energy storage model

BESS use converters for connection to the grid and for the control of charge and discharge operations of the batteries. In general, the power electronics contained within the converters are made up of DC-DC converters and power factor correction (PFC) devices [85–87]. The DC-DC converters are useful for providing voltage supply to the battery at desired levels while the PFC devices are used to provide reactive power capabilities to the system. The storage element used in the rest of this thesis is shown in Figure 3.2. It can be considered a generator dispatching power during discharging and as a load when consuming power during charging.

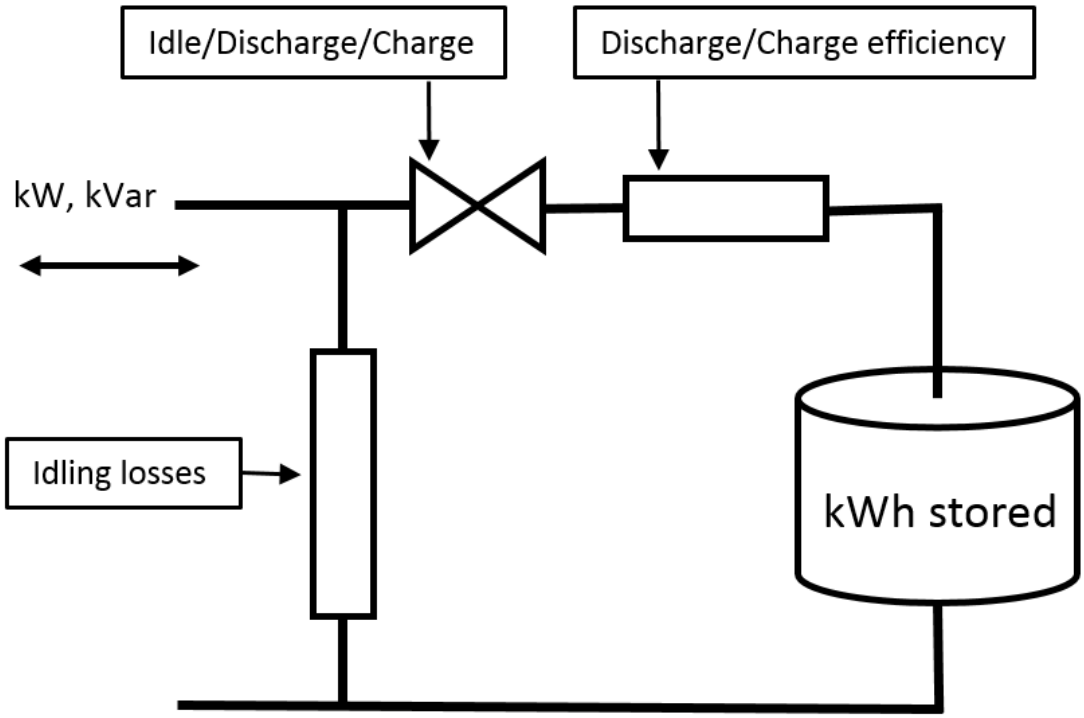

Figure 3.2: Model of storage element

The storage element has a maximum capacity, rated in kilowatt-hours (kWh) and a maximum charge/discharge rate, rated in kilowatts (kW). The amount of charge, in kWh, in the battery at any point is defined as the state of charge (SOC). During discharging of the battery, the level to which the battery is discharged is the depth

of discharge (DOD). A battery that is fully discharged from 100% SOC is said to have been discharged with a DOD of 100%. The terms SOC and DOD are often used interchangeably. Depending on specific applications and use cases, a constraint is placed on how deep the battery could be charged or discharged $SOC_{min} \leq SOC \leq SOC_{max}$. This measure is taken to protect the battery and prolong its lifetime. The losses in the system as a result of charging and discharging of the battery are accounted for by the charge efficiency η_c and discharge efficiency η_d.

3.4 Distributed control scheme

A distributed control scheme is used for the management of the network to keep voltages within designated limits. With this distributed control, only local measurements are utilised for making control decisions. For the scheme implemented in this chapter, the controllers are located on every node where PV is installed. Minimal communication is required for the distributed control scheme since inverters on the same feeder only need to send distress signals across the feeder using cheap and available Power Line Communication (PLC). An advantage of the distributed control is that there is no singular possible point of failure for the entire network. This feature makes the distributed control differ form the centralised control where there is such possibility. Another advantage of the distributed scheme is that knowledge of the entire network state is not needed for the control. This scheme depends only on local measurement of voltages (V_{meas}) at the nodes for decisions and actions of the controllers. Figure 3.3 illustrates the different sections of the control scheme.

The distributed control scheme consists of a number of operational states. These states are activated according to the prevailing conditions on the network at any time. The operational states of the scheme are described in the following.

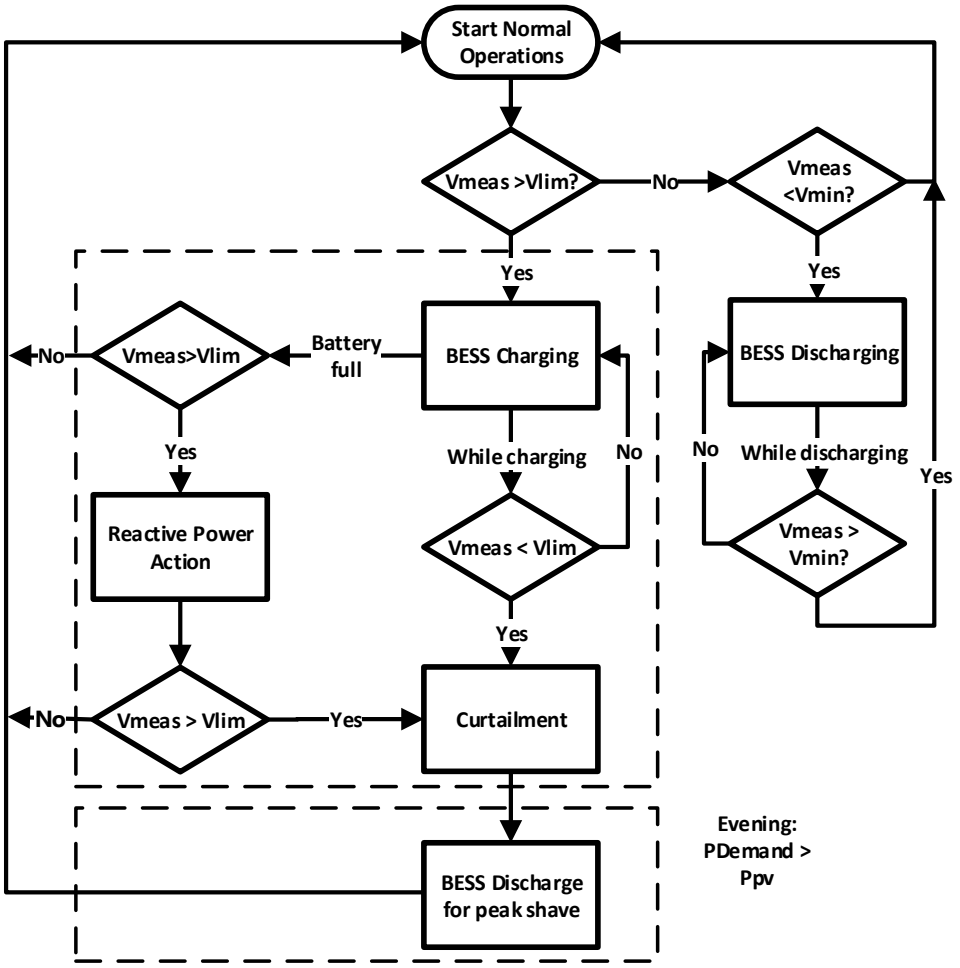

Figure 3.3: Flowchart of the control scheme

3.4.1 Normal operations state

The Normal operating state is active when the measured bus voltage V_{meas} is within the set upper voltage limit (V_{UTH}) and the lower voltage limit V_{LTH}. The normal operations state is an ”inaction state” because in this state, there is no action required on the part of the distributed controllers since there is no violation of any voltage limits.

This state would normally be active during periods of the day when power generated from PV is less than the total load demand on the network ($P_{PV} \leq P_L$). As seen in Figure 3.3, there is a constant check on the bus voltages for voltage violations. When no violation is detected on any of the buses, the power flows are recalculated and the process program loops within this stage.

3.4.2 BESS charging state

A local controller switches to the BESS charging state of operation when the condition $V_{meas} \leq V_{UTH}$ is violated. This state is typical in the daytime when PV generation is higher than load consumption $P_{PV} > P_L$. When this occurs, an overvoltage signal is sent across the feeder by the controller located at the node of occurrence of overvoltage, to notify other controllers. BESS charging starts in a bid to consume the excess PV power, thereby preventing overvoltage.

3.4.3 PV power curtailment state

The controllers switch to the PV power curtailment state as a result of one of two conditions. The first condition is when BESS charging occurs simultaneously with overvoltage. In this condition, $(P_{PV} > P_{BATT} + P_L)$, where P_{BATT} refers to the power of the BESS. Here, the BESS is unable to take up all the excess PV power that is not consumed by the load. The second condition is when batteries are full, reactive power action has been taken (described in Section 3.4.4), and yet an overvoltage signal persists. For any of these two conditions, a curtailment algorithm is run by the controllers to determine the minimum amount of active power to be curtailed so that voltages are maintained within desired ranges. This is not a favourable approach from an economic standpoint because it reduces the profits that owners of PV installations would have otherwise made. It also leads to loss of green energy that would otherwise have been harnessed for use. Active power curtailment, therefore, is deferred as much as possible and used as a last option when other alternatives are not available.

3.4.4 Reactive power absorption

The reactive power absorption state is activated when the batteries are fully charged and an overvoltage signal is still being received. Power quality - in this case, appropriate voltage levels – on the distribution network can be improved by the use of PV inverters. The use of PV inverters for this purpose, however, comes under regulations by different countries. The specific country grid code defines whether this feature is allowed or not, as well as the permitted capability curve to be used. Figure 3.4 shows the capability curve of for a typical PV inverter. PV inverters do not infinitely sink or source reactive power [88]. The maximum reactive power q_{max} which can be provided by the inverter is limited by the inverter's rated apparent power s_{PV} and the current active power generation $p_{(k)}$.

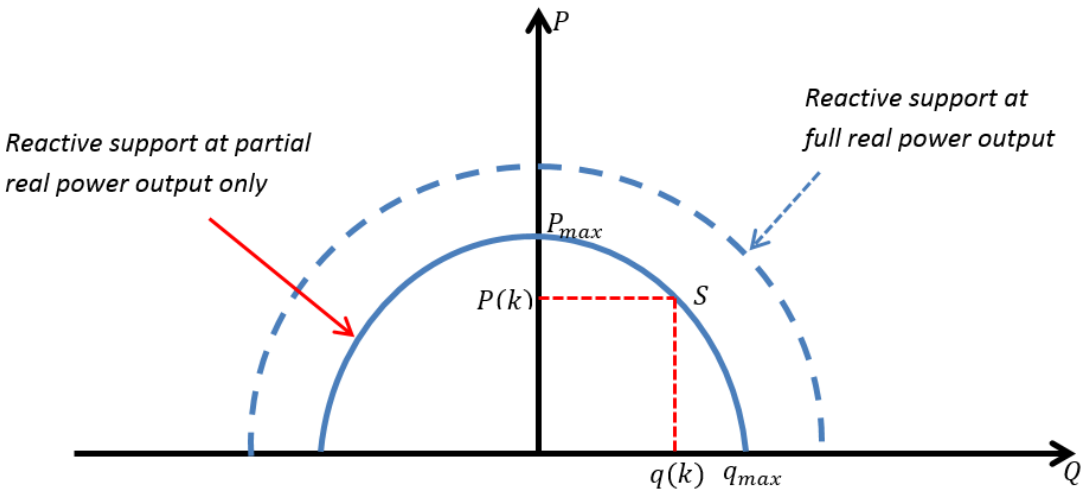

Figure 3.4: Inverter reactive capability curve

The relationship between these quantities is given as

$$q_{(k)} \leq \sqrt{(s_{PV}^2 - p_{(k)}^2)} = q_{max} \tag{3.2}$$

where $q_{(k)}$ is the reactive power available during real power output $p_{(K)}$. An oversized inverter, indicated by the dashed semi-circle in Figure 3.4, is capable of reactive power

support even when active power production is at maximum. It must be remembered that the R/X ratio of distribution networks is higher than that of transmission networks, so that the impact of reactive power on voltages on the distribution network is less than what is obtainable in transmission networks. The methods for the absorption of reactive power locally in networks can be divided into three classes: fixed power factor, reactive power as a function of active power, and reactive power as a function of voltage at the point of connection [89].

The fixed power factor method has the reactive power proportional to the generated PV active power. There is a set power factor that must be implemented by the controller, irrespective of the magnitude of the active power generated. This is expressed in (3.3)

$$C_1 = \frac{Q}{P} \tag{3.3}$$

where C_1 is a constant term that denotes the fixed power factor, PF is the power factor while P and Q are active and reactive power. This method has a major drawback, experienced especially during periods of low PV generation. During low PV generation, there is a lower risk of overvoltage on the network and there is sufficient load on the network to consume the generated PV power. But due to the fixed power factor, the controller continues to absorb reactive power, leading to increased grid losses.

For the method involving reactive power as a function of voltage $Q(U)$, the measured voltage at the point of common coupling (PCC) is used as as a reference for implementation of a droop control. Reactive power is absorbed when the PCC voltage exceeds a set point and the amount of reactive power absorbed follows the droop control curve. This method is especially useful because during periods when high PV generation coincides with demand on the network, there might be no need for reactive power action. This is expressed in (3.4).

$$Q = \begin{cases} Q_{max} & U < U_1 \\ \frac{Q_{max}}{U_1 - U_2}(U - U_1) + Q_{max} & U_1 \leq U \leq U_2 \\ 0 & U_2 < U < U_3 \\ \frac{Q_{max}}{U_3 - U_4}(U + U_3) & U_3 < U < U_4 \\ -Q_{max} & U > U_4 \end{cases} \tag{3.4}$$

The third is the method which applies reactive power as a function of active power, which is similar to the fixed power factor method, but changes the constant term C_1 to another predetermined constant term C_2, during periods of low production of active power form the PV. This is expressed in (3.5).

$$\cos\phi = \begin{cases} C_1 & P < P_1 \\ \frac{C_1 - C_2}{P_1 - P_2}(P - P_1) + C_1 & P_1 \leq P \leq P_2 \\ C_2 & P > P_2 \end{cases} \tag{3.5}$$

The three methods are depicted in Figure 3.5.

For the purpose of the study presented in this chapter, the reactive power as function of active power was used, since high PV power production periods do not often coincide with high network demand periods.

3.4.5 BESS peak-shave discharging

The controllers switch to the BESS peak-shave discharging state when the power demand on the network exceeds a set power threshold P_{TH}. This occurs during times when P_L is much higher than P_{PV}. For this work, P_{TH} is measured at the substation

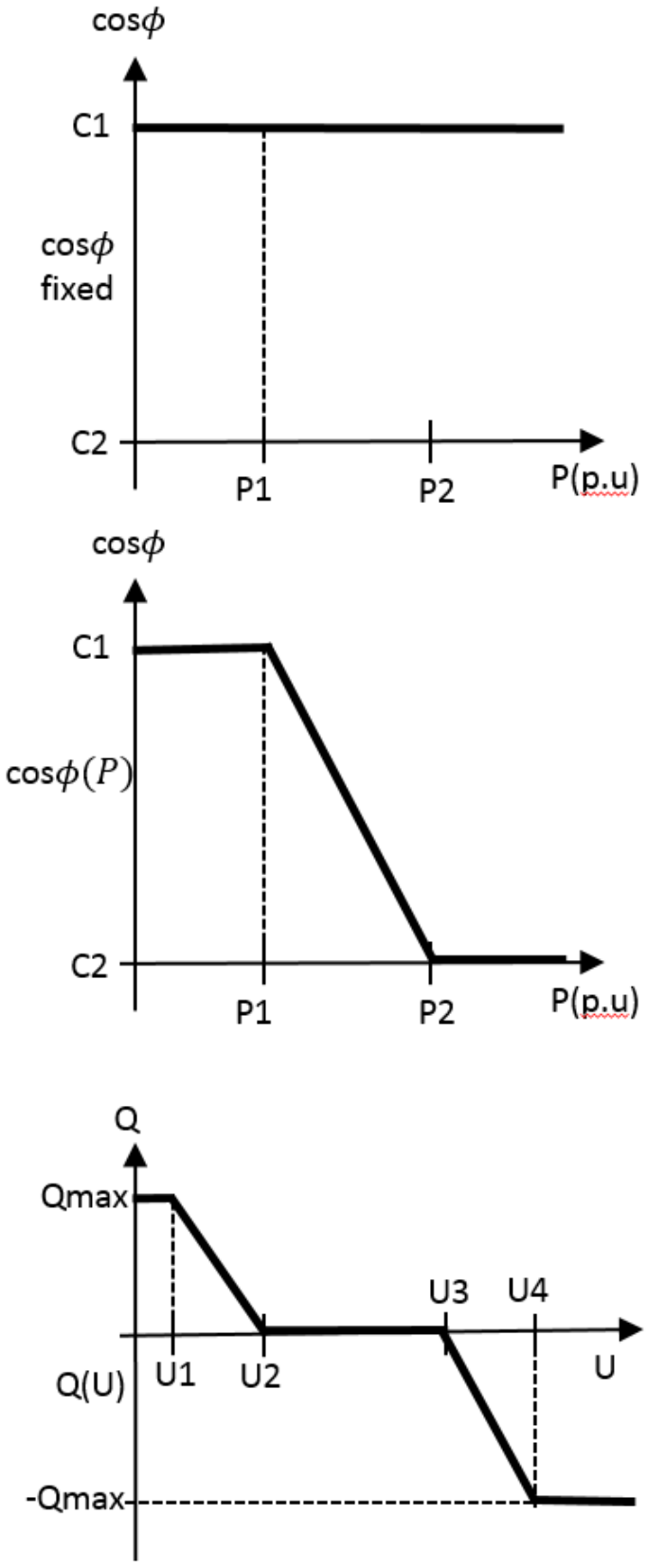

Figure 3.5: Reactive power methods. Upper figure: Fixed $cos\phi$. Middle figure: $cos\phi(P)$. Bottom figure: Q(U)

bus. The BESS start discharging during this peak loading period. This operation during peak period is especially useful because it can prevent the need to upgrade the network infrastructure as a result of peak loads.

3.5 Control scheme implementation

This section describes the tools, data and test network used to illustrate the distributed control scheme.

3.5.1 Implementation tools

The algorithm for the distributed control scheme was developed in MATLAB and the distribution network models and resources were developed using OpenDSS. OpenDSS is an open source distribution network systems tool developed by Electric Power Research Institute (EPRI). It has the Component Object Model (COM) which enables it to interact with MATLAB and other similar programming tools. MATLAB was further utilised for all the analysis carried out in this work.

3.5.2 Test network

The operation of the control scheme is illustrated using a single feeder distribution network, which is a section of the network presented in [90]. It has been modified for the purpose of this implementation. The line diagram of the feeder is shown in Figure 3.6.

The single feeder consists of 10 nodes with PV units and loads installed on each of the nodes. The PV units are each rated 32.5 kWp and the equivalent load on a single node is rated at maximum 15 kVA apparent power. BESS are added on different nodes of the network to create different scenarios. Each BESS is rated at 120kWh with initial state of charge (SOC) of 30% and an external dispatch mode. $V_{lim} = 1.07$ pu is used as the upper voltage threshold for this study.

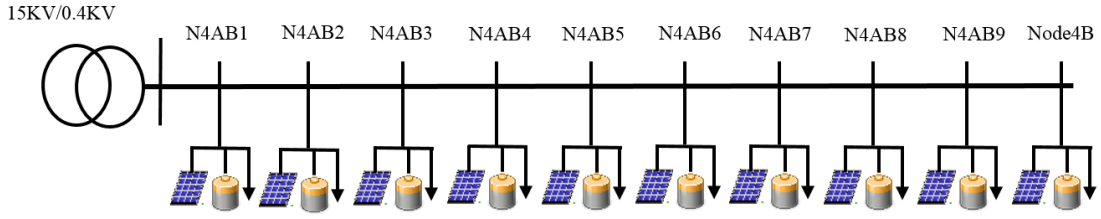

Figure 3.6: Single distribution network feeder

3.5.3 Load demand and PV profile inputs

The load demand and PV power profiles used for the simulations are shown in Figure 3.7.

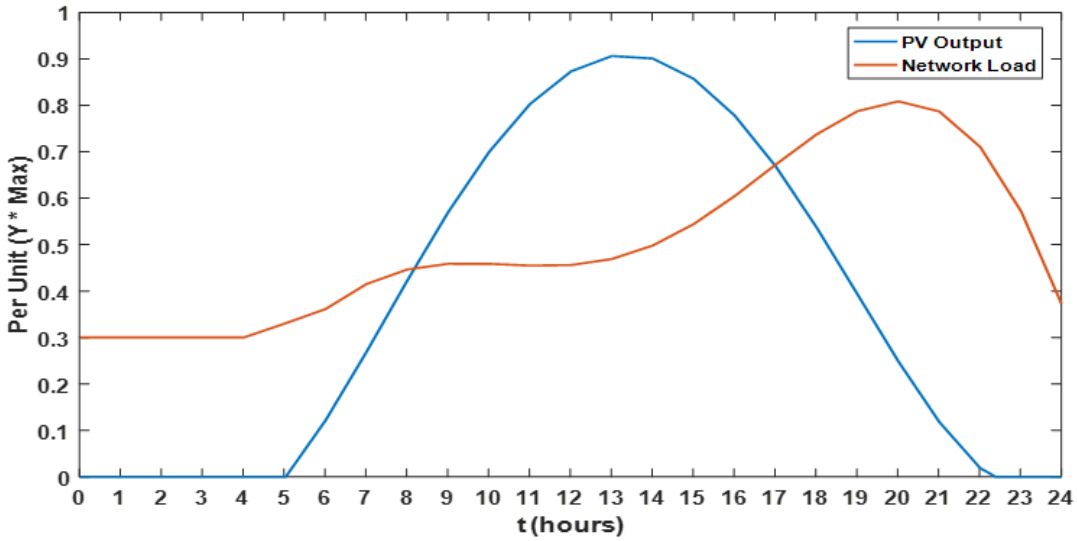

Figure 3.7: Demand and PV profiles

The maximum PV value is 32.5 kWp while the maximum load value is 15 kVA. Both profiles are generic, representing typical characteristics of daily PV power output and daily residential demand. Therefore the high variability and intermittent nature of load demand and PV output power respectively have not been considered. This notwithstanding, the profiles provide a fair representation of PV generation and demand on a typical network. The profiles here are typical of European countries with higher demands in the evening. These profiles could change for different countries. Real generation and demand profiles have not been used in the implementation of this

scheme, since the emphasis is on demonstrating the operation of various components available for mitigating overvoltage on distribution networks with high levels of installed PV. More realistic demand and generation profiles are utilised in subsequent chapters of this thesis.

3.6 Simulation results

Daily simulations of 1-minute resolution (1440 minutes) are used throughout the study. P_{PV} and demand data are therefore also in 1-minute resolutions. The simulation cases highlight effects on the network characteristics (especially voltage) for different combinations of control. Knowledge of the amount of active power curtailed for each case is also important as this is a good metric for estimating the benefits of having the control.

3.6.1 Case 1 - without distributed control

In this case, the network behaviour is observed with the penetration of PV, without application of the distributed control scheme. A plot of the voltage profile is shown in Figure 3.8. This is the voltage of the network buses without any controls in place. Overvoltage occurs on most of the nodes when no control actions are taken. With this situation, if no control actions are taken to mitigate the overvoltage, the grid code regulations will demand that generated PV active power will be curtailed. Curtailment is undesirable, as it makes it difficult to economically justify the investment on PV installations. For this network, if active power is to be curtailed in order to achieve voltages occurring at or below the upper voltage limit, then about 94.5 kWh of PV power would have to be curtailed. The voltage profile if curtailment alone is implemented on the network is shown in Figure 3.9, while Figure 3.10 shows the amount of excess PV energy that is being curtailed. V_{meas} for Node4B reaches V_{lim}. at $t = 485$ mins (just after the 8th hour), and this is the time when the curtailment was commenced.

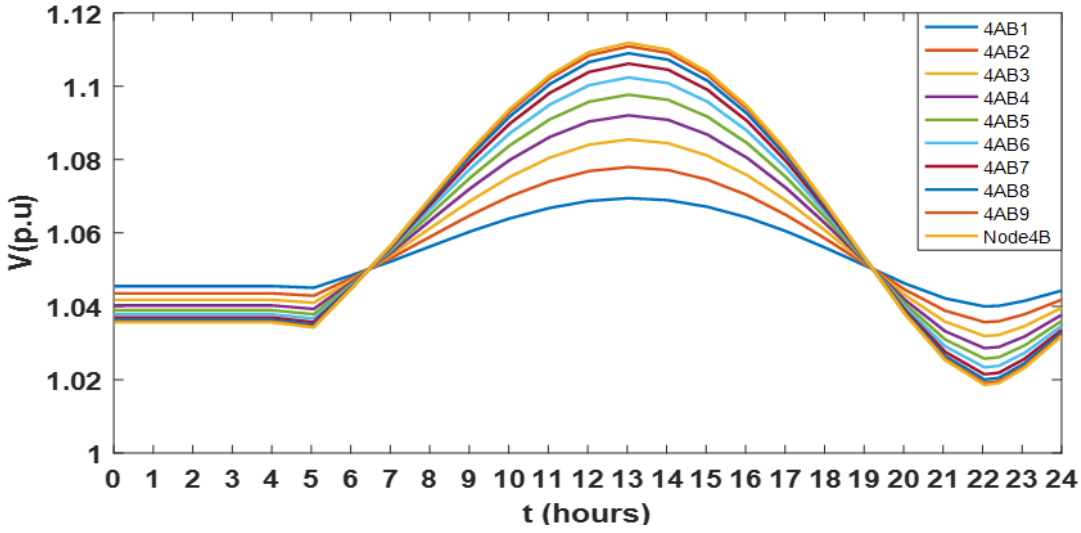

Figure 3.8: Feeder voltages for case 1. Here, there is no control action in place

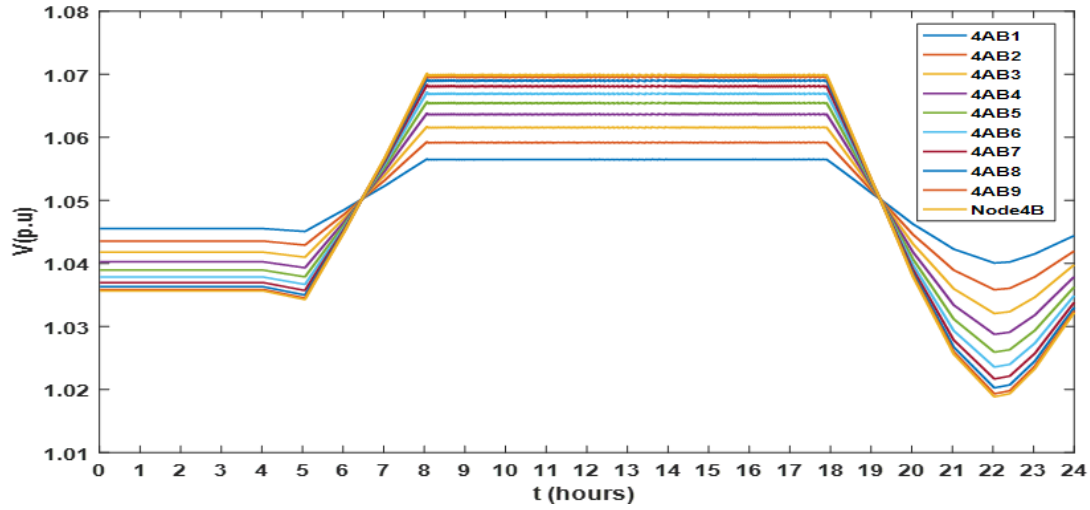

Figure 3.9: Feeder voltage when curtailment of active power alone is implemented on the network to maintain network voltages

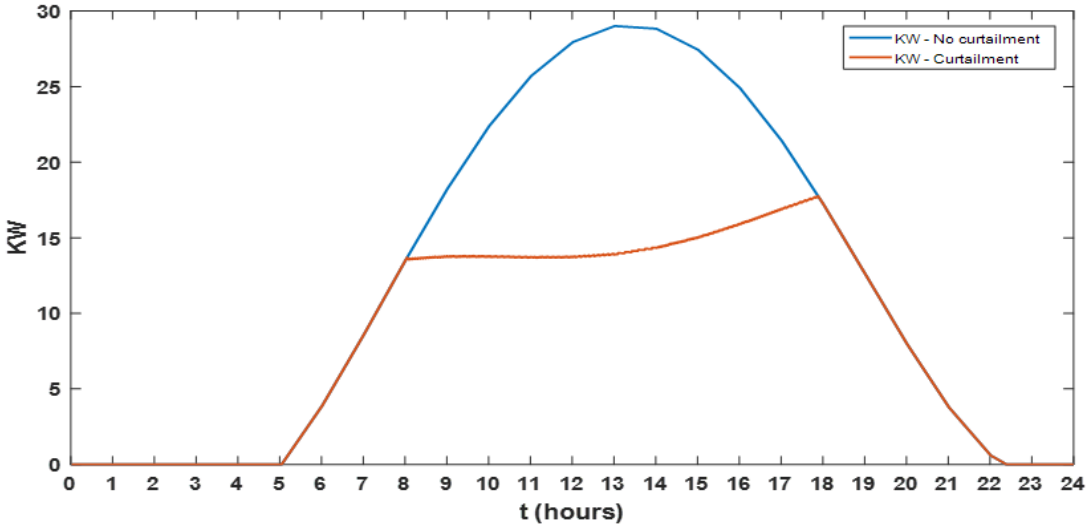

Figure 3.10: Active power curtailed. This is when curtailment is the only control measure taken. The blue line shows the total PV power that the PV generator is capable of generating, while the red line shows the power the PV eventually generated, as a result of curtailment

3.6.2 Case 2 - with distributed control

In this case, the distributed control algorithm is deployed with BESS installed on all the nodes on the feeder. The reactive power action has been disabled for this case, to represent a possible real life scenario where the PV systems do not have this reactive power injection and absorption capabilities. Figure 3.11 shows the voltage profile for this case while Figure 3.12 shows that most of the of the PV power generated was utilised, and only a small portion was curtailed.

Again, V_{meas} for Node4B reaches V_{lim}. at $t = 485$ mins (after the 8th hour) and the controllers switch to the BESS charging state. The batteries are fully charged at time $t = 1024$ mins (just after the 17th hour) and a small curtailment is observed in this case (Figure 3.12). The curtailment is small because at this time of the day, P_{PV} is decreasing and tending towards zero. Node4B is the node located at the end of the feeder, and therefore is the critical node on this network, since overvoltage occurs first on this node.

BESS discharge to ease loading on the network starts at time $t = 1025$ mins (after the 17th hour), when the threshold power P_{TH} is reached as a result of high load demands on the network during this period (see Figure 3.7 that shows the periods of high loading on the network).

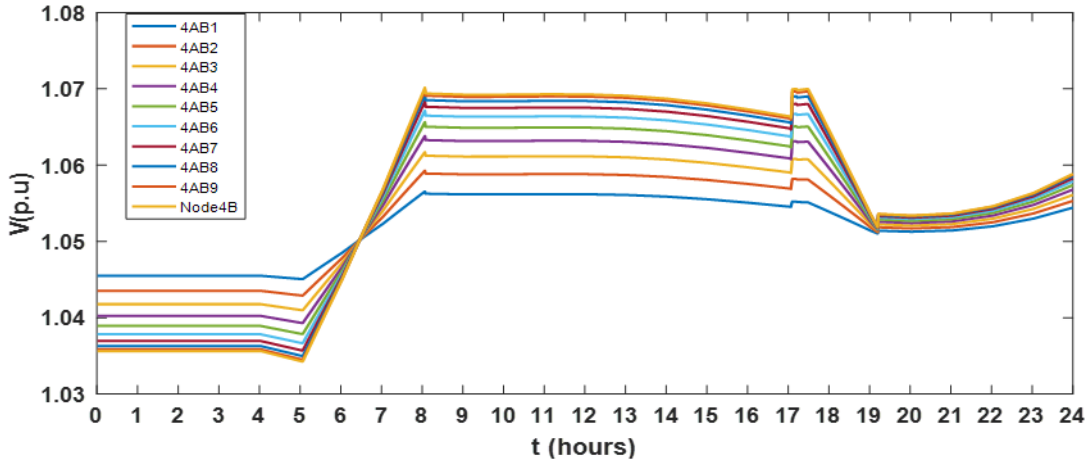

Figure 3.11: Feeder voltage profiles for case 2. The charging of BESS is implemented here during high PV generation, and discharging of BESS is performed during peak loading period

3.6.3 Case 3 - distributed control with reactive power action

In this case, the distributed control scheme is again deployed on the test feeder as in Case 2, but this time, with the reactive power action enabled. Another difference between Case 2 and Case 3 is that fewer BESS have been installed on the nodes of the test feeder. BESS installations for this case are only on nodes 4AB2, 4AB4, 4AB6, 4AB8 and Node4B. This is to represent a possible real life scenario where an attempt is made to cut the cost of installation of BESS units. These nodes have been randomly selected. The voltage profile after simulation is shown in Figure 3.13.

The batteries start charging and are fully charged at times $t = 485$ mins (after the 8th hour) and $t = 774$ mins (before the 13th hour) respectively. The reactive power action takes up the control immediately the batteries are fully charged. The maximum amount of reactive power that can be absorbed by the inverters at this time is given

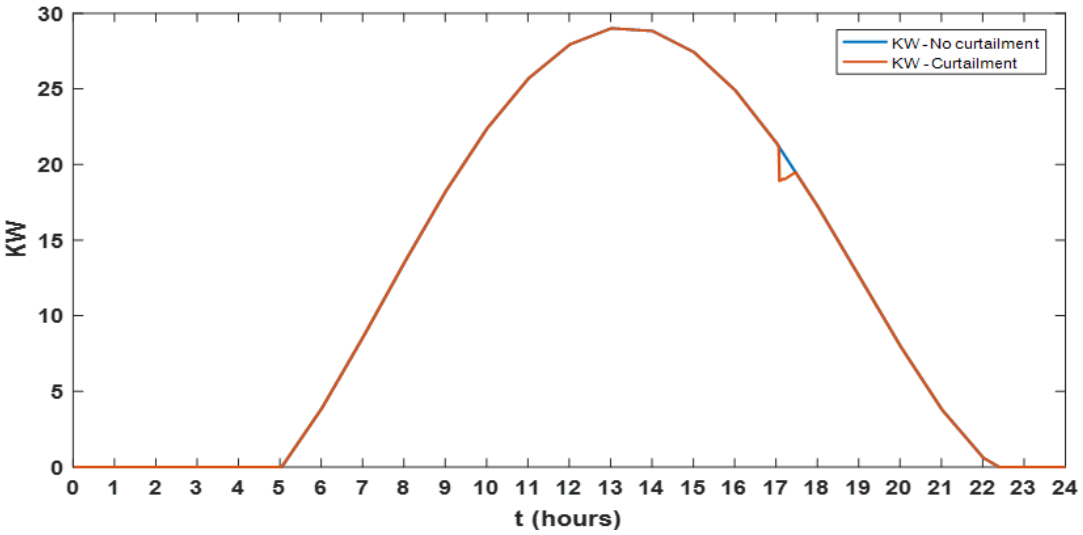

Figure 3.12: Active power curtailed for case 2. The blue line shows the total PV power that the PV generator is capable of generating, while the red line shows the power the PV evetually generated, as a result of curtailment. Take note that the red line lies on the blue line for most parts of the figure.

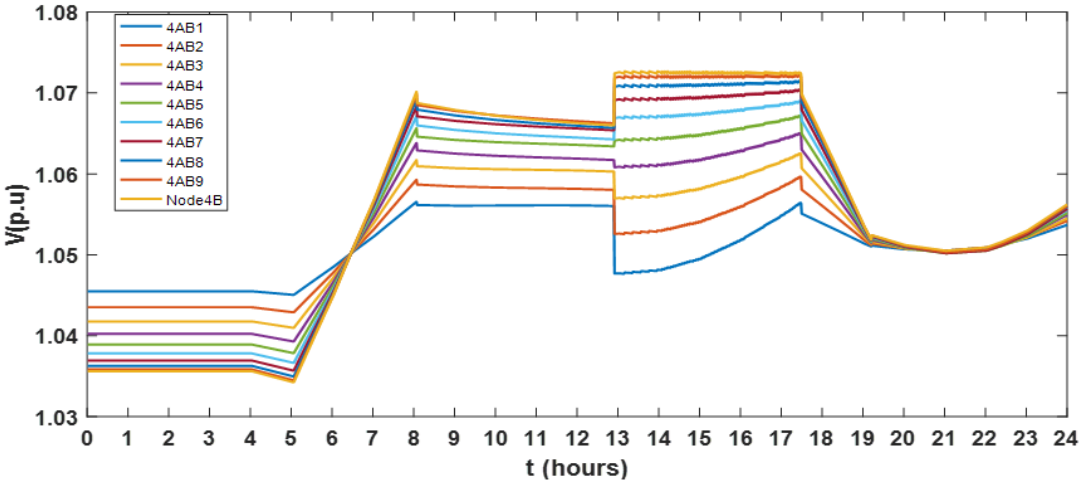

Figure 3.13: Voltage profile for Case 3. Here, both BESS charging and discharging, and also reactive power absorption are implemented.

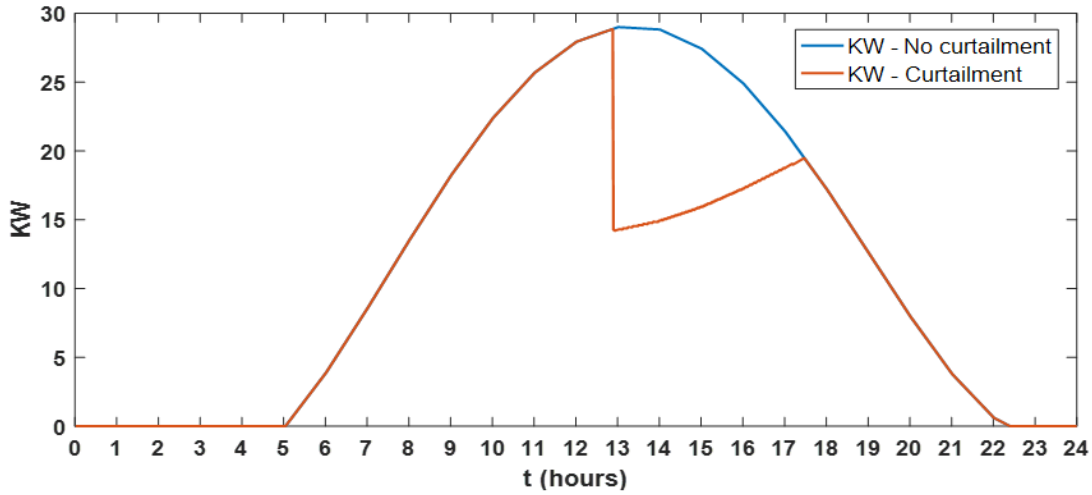

Figure 3.14: Active power that could have been curtailed for Case 3, if the reactive power mode was not activated. The blue line shows the total PV power that the PV generator is capable of generating, while the red line shows the power the PV would have eventually generated, as a result of curtailment.

by (3.2). The voltage dip that can be observed at the point of reactive power action, especially for the nodes closer to the substation, is because for this implementation, the same amount of reactive power is injected or absorbed at every bus. This therefore has different impacts on the terminal voltage of different nodes on the feeder. Reactive power absorption has been useful in this case to mitigate overvoltage and eliminate possible active power curtailment that would have resulted after the BESS got fully charged. If the reactive power action was not activated for this case, the amount of active power curtailment that would have been experienced is depicted in Figure 3.14.

3.7 Discussion

This scheme has demonstrated the use of BESS and reactive power to mitigate overvoltage on the distribution network. The tests however, were carried out without consideration of the variability of load and intermittency of PV power. The methodology was kept simple to obtain preliminary results and information for further development, which are presented in subsequent chapters of this thesis. Using this scheme, it is possible to have no curtailment of active power. This maximises the

benefits of investment in PV systems and reduction in greenhouse gas emissions, but it comes at the cost of having to install BESS, which are cost intensive. Holistic cost-benefit assessments are important in order to ascertain the exact economic benefits of using BESS versus curtailing active power. Optimum BESS sizing and location are also important factors to consider if this scheme is to be deployed in a larger network. This is to avoid situations where BESS are oversized, as this would lead to greater costs. Losses on the power lines due to use of reactive power for voltage control is a factor that should also be considered.

3.8 Conclusion

This chapter presented a distributed control scheme for mitigation of overvoltage on low voltage distribution networks with high penetration of PV using BESS and reactive power capability of PV inverter . The scheme was tested on a single feeder distribution network. BESS was employed to accommodate excess PV production, especially during the day when there is light loading and high PV power production. Simulations show that this scheme successfully keeps voltages within statutory limits. Fewer numbers of BESS were installed on selected nodes and this achieves almost the same results as when BESS are installed on all the nodes. The control scheme therefore is economical in this sense.

Chapter 4

Dispatch scheduling for BESS in networks with PV penetration

4.1 Introduction

This chapter presents a scheme for the optimisation of dispatch of BESS used for energy arbitrage. A linear program is proposed for the solution of the dispatch problem. The chapter begins with an overview and presentation of problem. It continues with description of factors that affect the life of BESS. The linear program with a mathematical model of the battery is presented next, followed by the implementation of the algorithm. Simulation results are presented, followed by discussions on the results. The chapter ends with a conclusion on the findings that emanated from studies on the chapter.

4.2 Context and presentation of problem

As the applications of BESS in the electricity network gain popularity, the need to optimise the benefits of the BESS also increases. For networks with PV installations where BESS is installed, a common aim is to utilise BESS to maximise the use of PV power produced. This is in line with the goal of achieving power networks where consumption of renewable energy is promoted. For these networks, the purchase of electricity from the grid is minimised, especially during peak periods when the price of electricity is high and the electricity source is often peaker plants (plants that generally run only during periods of high demand) that are fossil fuel powered.

The BESS when deployed in networks can generate value for investors in a number

of ways. Some of the value streams for BESS include energy arbitrage, frequency response, demand charge management, peak shaving, network upgrade deferral, loss reduction and voltage management [91]. BESS installation cannot commit to the provision of all the services at the same time, since the commitment to one or a few often means the system is not available to provide other services. Therefore, it is important to evaluate the benefits from the various value streams available to the BESS and to optimise its usage for maximum gains.

Various studies have been carried out on cost-benefit assessment of BESS in power networks using different methods. Authors in [92] evaluated the use of BESS specifically for provision of primary and secondary frequency control. In [93], economic analysis was performed on different use cases of BESS, examining both lithium-ion and lead acid battery applications. The economic benefit of BESS due to deferral of network infrastructure upgrade was studied in [52]. Different methods are also employed in the solution of the BESS scheduling problem, with most of them involving some optimisation within constraints. In [94], mixed integer linear programming was used to evaluate the economic benefits of combining BESS and PV in commercial buildings while interior point method was used in [62] to improve distributed generation and load hosting capability of distribution networks using BESS. The majority of work in this area focus on maximising the benefits gained by installation of BESS, while making the BESS operate in a way that prioritises longevity. In [95], the authors considered the profitability of investments on the part of battery energy storage owners. A model was proposed for the stochastic formulation of profit maximisation for storage owners through energy arbitrage in both real-time and day-ahead market prices, under uncertainty. The model aims to assist storage owners to bid and make operational decisions. Several studies have been carried out in the area of use of battery storage for arbitrage in the power networks. In [96], a battery energy storage sizing methodology was proposed for the maximisation of the economic benefit to the consumers as a result of employing battery storage for reduction of power demand payment. In addition to this, an optimal operating strategy

was also implemented which was based on dynamic programming. The aim was to minimise the cost of energy for the consumers while obeying the physical constraints of the battery.

The work in this chapter presents a linear program (LP) optimisation technique to manage the scheduling of BESS in distribution networks with high PV penetration. The focus is scheduling assignment by the optimiser to maximise the economic benefits gained through energy arbitrage, while simultaneously maximising the use of available PV power. Satisfaction of network load demand using the cheapest energy sources available, is also an objective.

4.2.1 Factors affecting battery life

In literature, a distinction is often made between battery aging and battery wear. Battery aging refers to processes or factors that affect the BESS physically, limiting the battery's ability to perform intended functions. Battery wear refers to the processes or factors that limit the amount of electric energy the battery can store up [97]. Battery wear is a function of the manner the battery is charged/discharged through the duration of its lifetime.

4.2.1.1 State of charge (SOC)

The state of charge (SOC) is an indication of the battery charge as a fraction of its maximum capacity. This quantity is often expressed as a percentage.

4.2.1.2 Depth of discharge (DOD)

The depth of discharge (DOD) of a battery, indicates the capacity of discharged as a fraction of the initial capacity. The DOD is very similar to the SOC and both terms are often used interchangeably. Over a discharging interval, the DOD can be calculated from the battery discharge current as shown in (4.1)

$$DOD = \frac{\int_{t_i}^{t_f} I_{dis}.dt}{C_0} \tag{4.1}$$

where C_0 is the initial battery capacity, t_f is the time at the end of the evaluation period, t_i is the initial time and I_{dis} is the current from the battery.

4.2.1.3 State of health (SOH)

This describes the condition of the battery at any time, compared to its ideal conditions [98]. This is given in the expression (4.2)

$$SOH(t) = \frac{C_{ref}(t)}{C_{ref,nom}} \tag{4.2}$$

where $C_{ref,nom}$ is the nominal capacity of reference available by manufacturer and $C_{ref}(t)$ is the capacity at the time of estimating the SOH. Therefore, it is expected that the SOH of BESS is 1 after manufacture and before use.

4.2.1.4 Calendar losses

Capacity fading is a term used to refer to the irreversible loss in the usable capacity of the BESS as a result of operating conditions.

The factors that lead to the deterioration of BESS, and hence these losses, include the number of cycles, the depth of discharge and the operating temperature. These factors are grouped into two classes. The first is calendar losses, to account for the occurrence of these losses when the BESS is not in operation. The second class is the cycling losses that captures the occurrence of these losses when the BESS is in operation [99].

4.2.1.5 Cycle loss

The number of cycles and the DOD of these cycles affect the life of the battery. A dimensionless parameter, Z quantifies the loss of capacity per equivalent full charge.

4.3 Time-of-use and other electricity pricing schemes

Time-of-use (TOU) pricing is a pricing model designed to incentivise various categories of electricity consumers to use energy more efficiently by consuming less energy during peak demand periods than off-peak periods. TOU offers time-differentiated pricing schemes rather than flat single pricing. Two or more prices are fixed in advance, which apply at different intervals of the day, usually in hours [100]. The broad advantages of TOU are that demand is better managed on the electricity networks, and electricity consumers can benefit from lower electricity prices as a result. A study carried out in [101] found that electricity consumers are able to reduce their electricity consumption to periods of moderate network loading or periods of low network loading. The motivation for the electricity utilities for using TOU pricing is primarily for reducing the economic cost of running the network and also to improve network stability [102, 103].

The proposed benefits of TOU pricing notwithstanding, one of the challenges faced is that the shifting of consumption from higher electricity prices to lower electricity prices often conflicts with the schedules, and therefore convenience, of the consumers. This makes a good case for the use of BESS to maximise the goals of TOU electricity pricing. Consumers can buy electricity during periods of low prices for charging of the batteries, and consume the stored energy during periods of high electricity prices. Because the continuous charging and discharging of the BESS leads to degradation, there is a need to evaluate the value gained as a result of using BESS for energy arbitrage.

In addition to TOU pricing there are also other tariff types that are supposed to be flexible. The critical peak pricing (CPP) scheme is an improved TOU tariff that dynamically traces critical supply periods, the periods which have extremely high unit price of electricity, and can change from one day to another. Electricity consumers are notified of these periods at least one day ahead. The CPP is offered to customers who are most likely to contribute to load relief. CPP is often targeted at large residential electricity users who are likely to have the greatest demand response and greatest bill saving [104]. Real time pricing is the method that directly reflects the dynamics of the wholesale electricity price each day all year round. Real-time prices vary every hour or half-hour. It also constitutes the maximum uncertainty for users due to its dynamic nature. Some real-time pricing schemes will require advanced technology to communicate and manage the frequent price changes [105, 106].

Variable peak pricing (VPP) is similar to critical peak pricing, with the difference that peak prices vary from day to day. Superpeak time-of-use is another tariff scheme similar to TOU, but differs from TOU due to the peak window being shorter in duration in order to give stronger price signals. Seasonal tariffs observe the different seasons in the year that corresponds with different levels of demand on the network. Electricity prices are then charged at higher rates during seasons of high demand, and at lower rates during low-demand seasons.

4.4 Mathematical model

This section presents the mathematical modelling involved in the BESS scheduling problem. First, the modelling of the BESS operation and characteristics is presented, followed by the setting up of the linear program for optimisation

4.4.1 Modelling the BESS

BESS operation is modelled considering the energy storage capacity, charge/discharge limits, maximum and minimum depth of discharge (DOD), and efficiencies during charging/discharging. The DOD is the limit to which the BESS has been discharged, expressed as a percentage of the total capacity. Often, there is a specified constraint on the DOD to prevent damage of the energy storage.

The state of energy in the battery at any instant in time $E_{BESS}(t)$ is determined by the change in energy from the previous time instant, as expressed in (4.3).

$$\Delta E_{BESS} = E_{BESS}(t) - E_{BESS}(t-1) \tag{4.3}$$

The change in energy is dependent on the charge/discharge power of the BESS.

$$P_B(t) = \begin{cases} \frac{\Delta E_{BESS)}}{\Delta t}.\eta_c^{-1}, & P_B(t) > 1 \\ \frac{\Delta E_{BESS)}}{\Delta t}.\eta_d^{-1}, & P_B(t) < 1 \end{cases} \tag{4.4}$$

where $P_B(t)$ is the charge or discharge power of BESS (positive for charging and negative for discharging), and Δt is the sampling or operation interval, η_d is the discharge efficiency and η_c is the charge efficiency. P_B will be the solution of the scheduling problem, containing the optimised power dispatch values for the period under consideration, given in (4.5).

$$P_B = \begin{bmatrix} P_B(1) \\ . \\ . \\ P_B(q) \end{bmatrix} \tag{4.5}$$

where q is the number of sampling instants within the period considered. For 15-minute and hourly sample intervals in a day, for example, $q = 96$ and $q = 24$ respectively.

4.4.2 Linear program optimisation

A linear program is set up to optimise the scheduling of BESS in the network. The objective of the optimisation is to achieve maximum benefit from arbitrage, charging from cheapest electricity sources and discharging during high electricity prices, while obeying network constraints. This objective also coincides with peak shaving objective since peak load periods are also periods of higher electricity prices.

The objective function minimises the cost of delivering power to the network load, charging the BESS at minimum cost, especially during periods of high PV power production and discharging during peak demand periods. The objective function is presented in (4.6).

$$min \sum_{t=1}^{q} \left[P_G(t).w_G(t) + \sum_{r=1}^{y} P_{PV}^{r}(t).w_{PV}^{r} + \sum_{s=1}^{z} [P_B^s(t).w_B^s \right] \tag{4.6}$$

P_G is the power drawn from the grid, P_{PV} is the power from the PV while P_B is the charge or discharge power of the BESS. w_{PV} and w_B are the operating costs of the PV and the BESS respectively, while w_G represents the price of electricity purchased from the grid. y and z respectively are the total numbers of PVs and BESSs on the network. $r = 1, 2 \ldots y$ and $s = 1, 2 \ldots z$.

The objective function is subject to the following constraints:

$$SOC_{min}^{S} \leq SOC^{S} \leq SOC_{max}^{S} \tag{4.7}$$

$$P_L(t) = P_G(t) + \sum_{r=1}^{y} P_{PV}^{r}(t) + \sum_{s=1}^{z} P_B^s(t) \tag{4.8}$$

$$P^{r}_{PV}(t) \leq P^{r}_{PV.PEAK} \tag{4.9}$$

$$P^{S}_{B,D.MAX} \leq P^{s}_{B} \leq P^{s}_{B,C.MAX} \tag{4.10}$$

$$P^{S}_{B,D}(t) = \frac{\Delta E_{BESS}}{\Delta t}.\eta_d \tag{4.11}$$

$$P^{S}_{B,C}(t) = \frac{\Delta E_{BESS}}{\Delta t}.\eta_c \tag{4.12}$$

$$P_G(t) \leq P_{G.PEAK} \tag{4.13}$$

$$\sum_{t=1}^{q}\left[\sum_{s=1}^{z}[P^{S}_{B,D}(t) \leq P^{S}_{B,C}(t)]\right] \tag{4.14}$$

The constraints for the DOD of the BESS are given in (4.7), where SOC^{S}_{min} and SOC^{S}_{max} are the minimum and maximum SOC of the S^{th} BESS respectively. The power flow balance equation is given in (4.8), where P_L is the network load demand. The constraint on the amount of power produced by the PV is presented in (4.9), where $P_{PV.PEAK}$ is the kilowatt peak rating of the PV. The constraint on the rate of charge or discharge of the BESS is given in (4.10), where $P^{S}_{B,D.MAX}$ and $P^{S}_{B,C}$ are the maximum discharge and charge rates respectively. The charge and discharge rates are given in (4.11) and (4.12) where η_d and η_c are the discharge and charge efficiencies respectively. In (4.13), the constraint for the maximum power drawn from the grid at the bulk supply point is given, where $P_{G.PEAK}$ is the peak power. This constraint ensures peak shave. Constraint (4.14) specifies that during the given operation period, the amount of energy delivered by the BESS is not greater than the amount stored.

In this formulation, excess energy from the PV generators during high production periods are utilised for charging of the BESS, rather than exporting back to the grid

after meeting the network load demand. In a time of use (TOU) electricity market, electricity prices at different times of the day vary according to the cost of providing power during those times. In this scheme, prices are taken to be highest during peak demand periods than otherwise. This means that overall, the BESS is charged at cheaper costs and discharged during peak periods when electricity prices are higher. This difference provides the energy arbitrage value, which is computed as

$$\Omega_{TOU} = \sum_{t=1}^{q} \sum_{s=1}^{z} \left[P_{B,D}^{S}(t) - P_{B,C}^{S}(t) \right] . w_G(t) \tag{4.15}$$

where Ω_{TOU} is the value obtained from arbitrage.

The lifetime of a BESS is represented by the total number of charge and discharge cycles of the unit before end-of-life is reached. This information is often provided by the manufacturer, and for most batteries, this represents the number of times the battery is cycled before it reaches 80 per cent of its initial energy capacity, expressed as

$$E_t \leq 0.8 E_{t_0} \tag{4.16}$$

where E_t and E_{t_0} are the present and initial (immediately after manufacture) capacities, in Coulombs, of the BESS respectively. The total number of cycles of BESS before (4.16) becomes satisfied is also a function of the DOD. The lower the DOD, the higher the number of cycles. Curves showing this relationship between the number of cycles to failure and the DOD are normally provided by the battery manufacturers, or can be estimated from field measurements. Figure 4.1 [107] shows typical DOD/number of cycles relationship curve.

Depending on application, there could be varying and overlapping DOD during the operations of the BESS, rather than a constant DOD. For example, a cycle of 50% DOD could be followed by another cycle with 70% DOD. This makes it challenging to count accurately the number of cycles to end-of-life. In this situation, the rainflow counting algorithm [108] is used to capture the various cycle depths and therefore

estimate more accurately the number of cycles to end-of-life. The expression for the rainflow counting is given by

$$C_F = a_1 + a_2 e^{a_3 R} + a_4 e^{a_5 R} \tag{4.17}$$

where C_F is the number of cycles to failure, a_1, a_2, a_3, a_4, a_5 are fitting constants, and R is the fractional depth of discharge. Further discussions and implementation of this, including constant values, are presented in 6.7.1

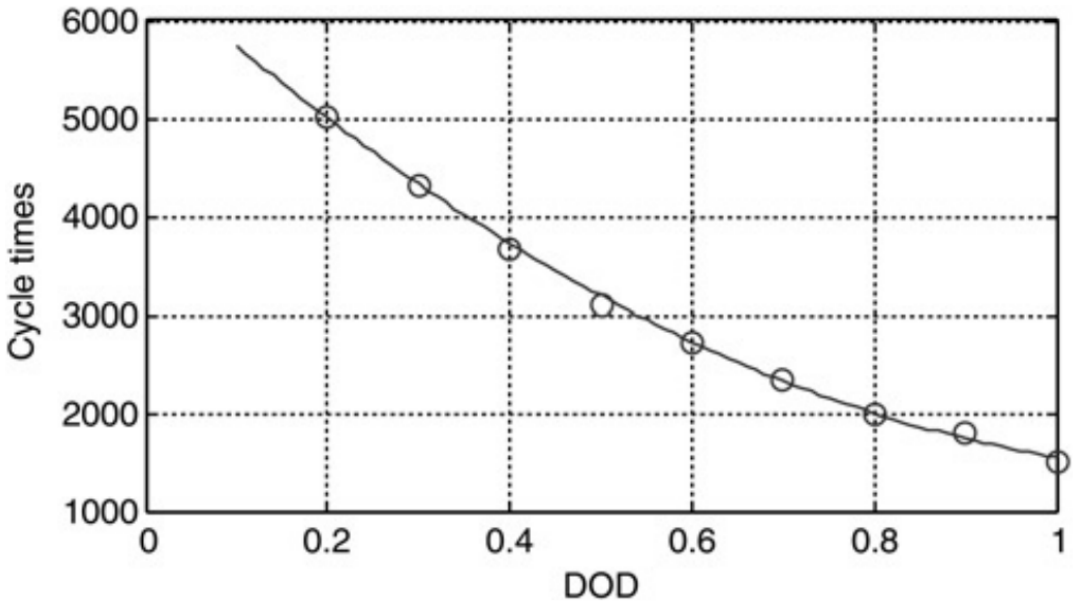

Figure 4.1: Number of cycles to failure vs depth of discharge [107]

4.5 Implementation of algorithm

This section describes the test network and data used in the implementation of the linear program.

4.5.1 Network description

The distribution network shown in Figure 4.2 is used [61]. It is a radial network with PV and BESS installations as shown. A $22/0.4kV$ transformer supplies the feeder and 33 residential houses are connected to the feeder. The network comprises NA2XRY type low voltage cables and the parameters of the cables are given in Table 4.1

Table 4.1: Cable parameters for network used

No of conductors and cross sectional area (mm^2)	**Maximal resistance of conductor at** 20^0 (Ω/km)	**Reactance of conductor** (Ω/km)
1X95	0.3211	0.0892
4X95	0.3211	0.0691
4X120	0.2539	0.0691
4X150	0.2060	0.0691

For demonstrating the performance of the scheduling linear program, aggregated values for the load, PV and BESS are used in the simulations. The aggregate load values for the load and PV power respectively are $P_L = 66.75kW$ and $P_{PV} = 70kWp$. The BESS is also taken to be aggregated, with $P_B = 44kW$ and $E_{BESS} = 310kWh$. The discharge efficiency of the BESS is $\eta_d = 0.9$.

4.5.2 Description of profiles

The computational model developed by Centre for Renewable Energy Systems Technology (CREST) [109] was used to create the load profile. The tool was used to generate realistic demand profiles for 100 residential houses. Typical demand profile was obtained by averaging out 50 different profiles obtained from 100 residential houses. The resulting load shape is used as multiplier on the loads of the test network. Summer time profile generated using this method and used for this implementation is shown in Figure 4.3.

A typical summer-time PV profile, also shown in Figure 4.3 is used in the

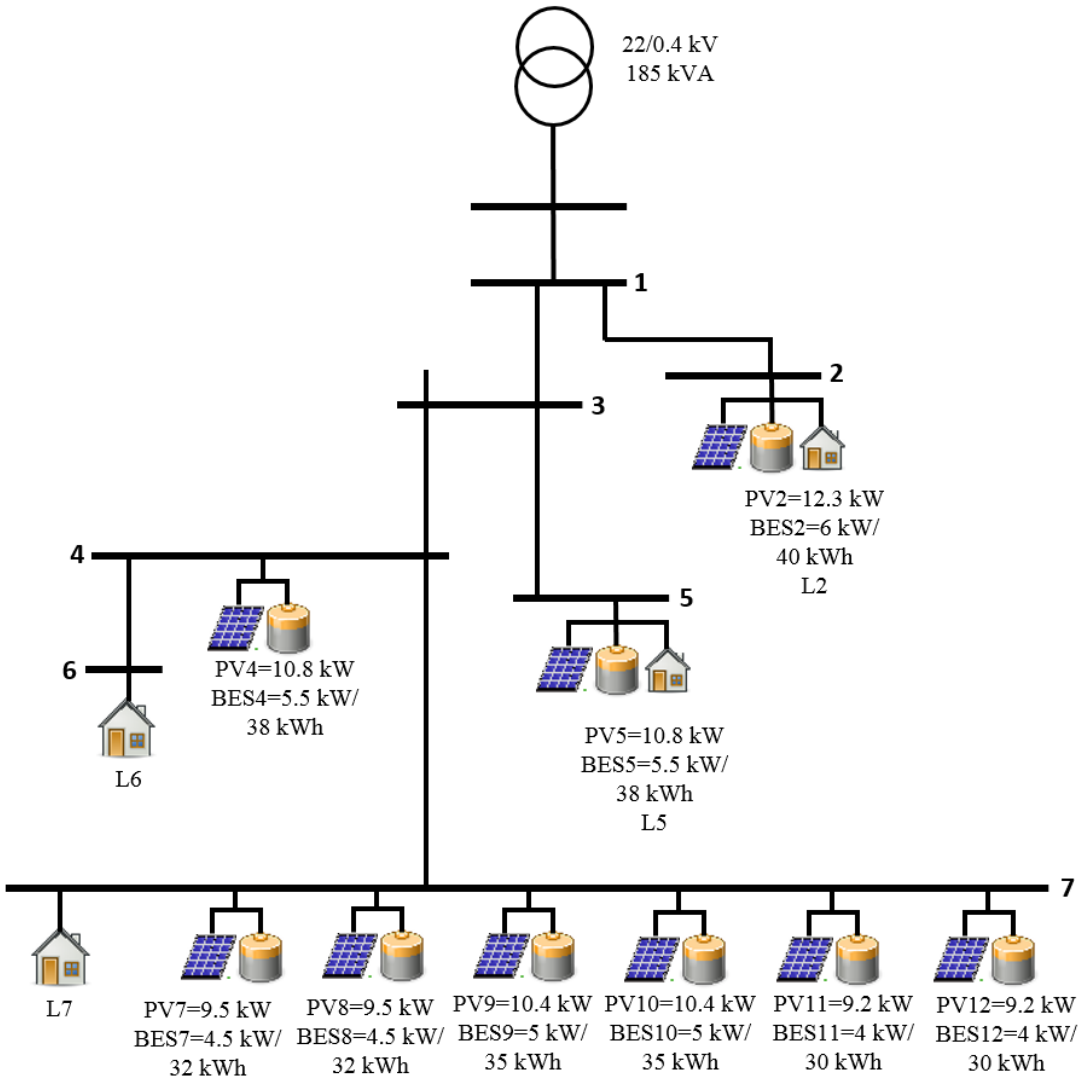

Figure 4.2: Test network diagram

implementation. The values of the PV profile, like the load profile, are per unit and used as multipliers for the actual kWp ratings of the PV units.

In the LP formulation, the prices of the electricity from the grid, PV and BESS are essential for decision making, since the objective is to supply load to the network using the cheapest available power resource. Day-ahead TOU prices for energy purchased from the grid is shown in Figure 4.4 [110].

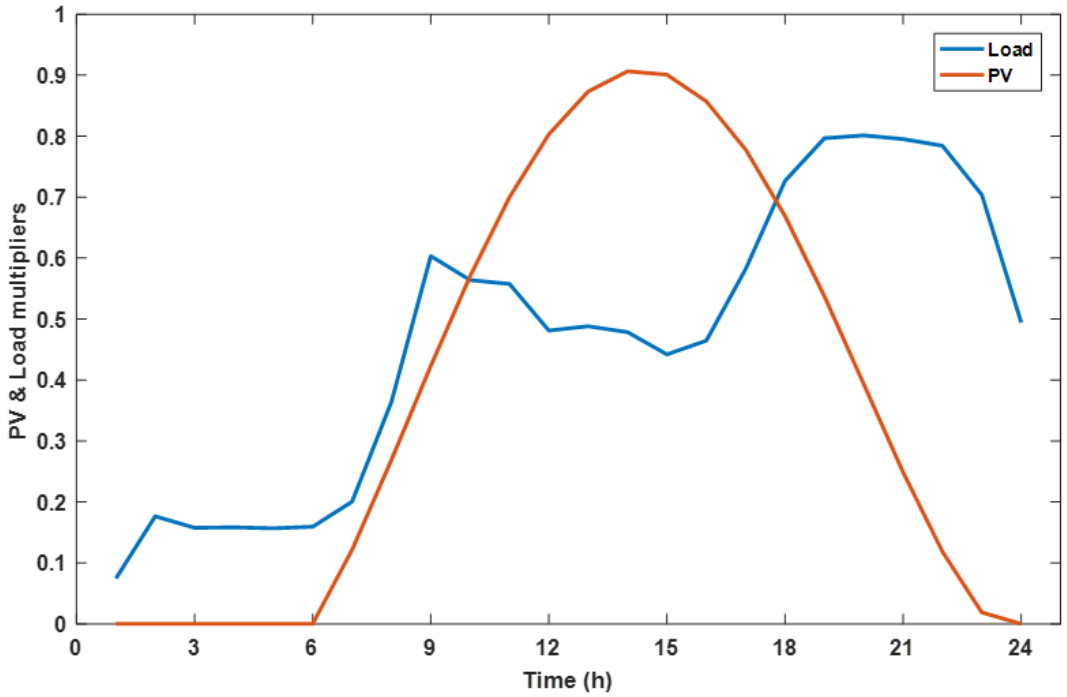

Figure 4.3: Load and PV generation profiles

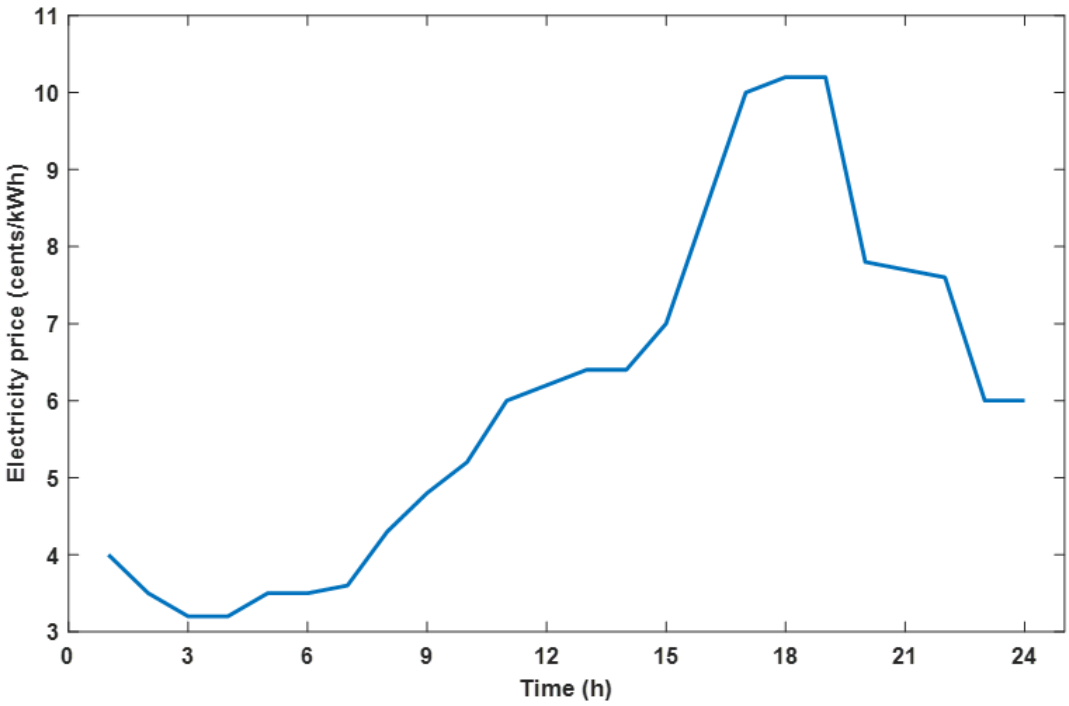

Figure 4.4: TOU electricity price profile [110]. This is w_G in (4.6)

4.6 Simulation results and discussions

Hourly simulations were carried out for a full day and the linear program was set up and solved using MATLAB software. The DOD of the BESS used is 0.9. Maximum charge and discharge rates were both 44kW. The unsubsidised cost of energy for the PV used in this analysis was taken to be $w_{PV} = 4.6$ cents/kWh [111]. The low voltage network has been considered as an aggregate network, represented by singular load, PV generator and BESS when considered from the medium voltage network level. In a medium voltage network, there could be a number of such low voltage feeders connecting to the medium voltage network, and therefore experienced as aggregates at this level. Figure 4.5 shows the voltage profile of the network without PV and BESS installations. It can be seen that before high penetration of PV and BESS, the voltage profile of the feeder fall within the regulatory upper and lower limits of 1.05 p.u and 0.95 p.u respectively (red dashed lines). In Figure 4.6, the power drawn from the grid, as measured at the feeder head, is shown. Relatively higher amounts of power can be seen drawn during peak demand periods. Only the feeder head power profile is shown here since the study in this paper focuses on the aggregate demand.

Figure 4.7 shows plots of the optimal dispatch scheduling of the BESS, the power drawn from the grid, utilised PV power and the load. The optimisation aims to utilise all the available PV power produced during high solar irradiation, since this is cheaper, and also promotes the case for economic justification for PV installations. PV power is utilised, firstly to meet demand, followed by the use for BESS charging. Subsequently, any excess PV is either curtailed or exported back to the grid. In this LP formulation, excess PV is exported to the grid. However, for the case study presented, all the PV power is fully utilised, and no power is returned back to the grid.

To maximise the arbitrage gain Ω_{TOU}, the BESS prioritises the use of the excess PV power for charging.

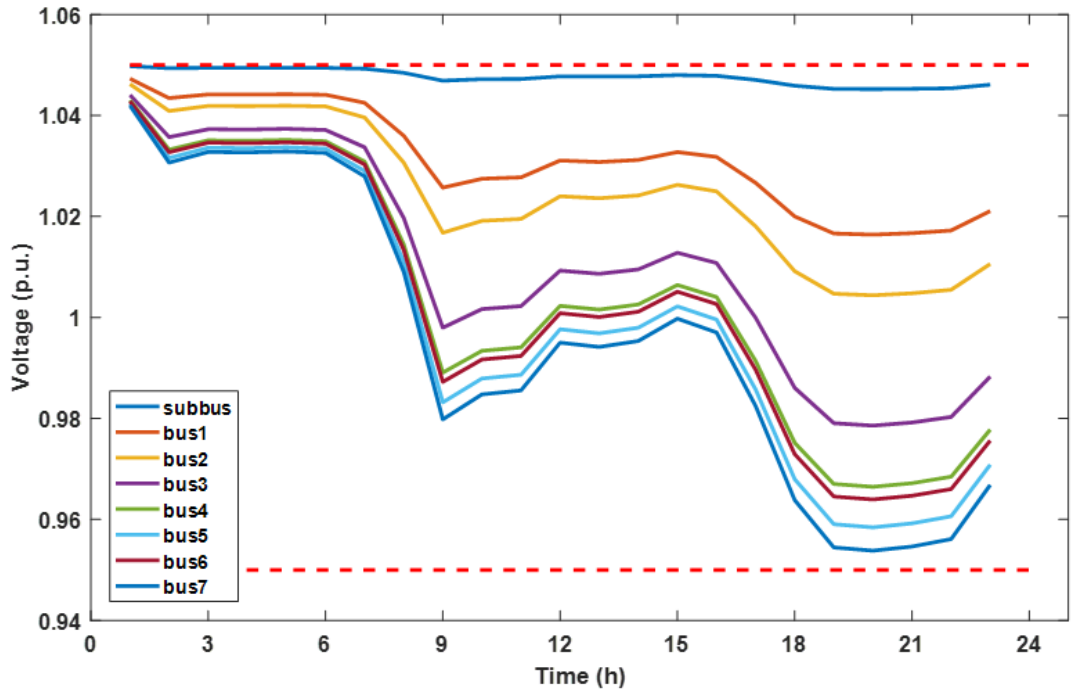

Figure 4.5: Feeder voltage profiles without PV and BESS

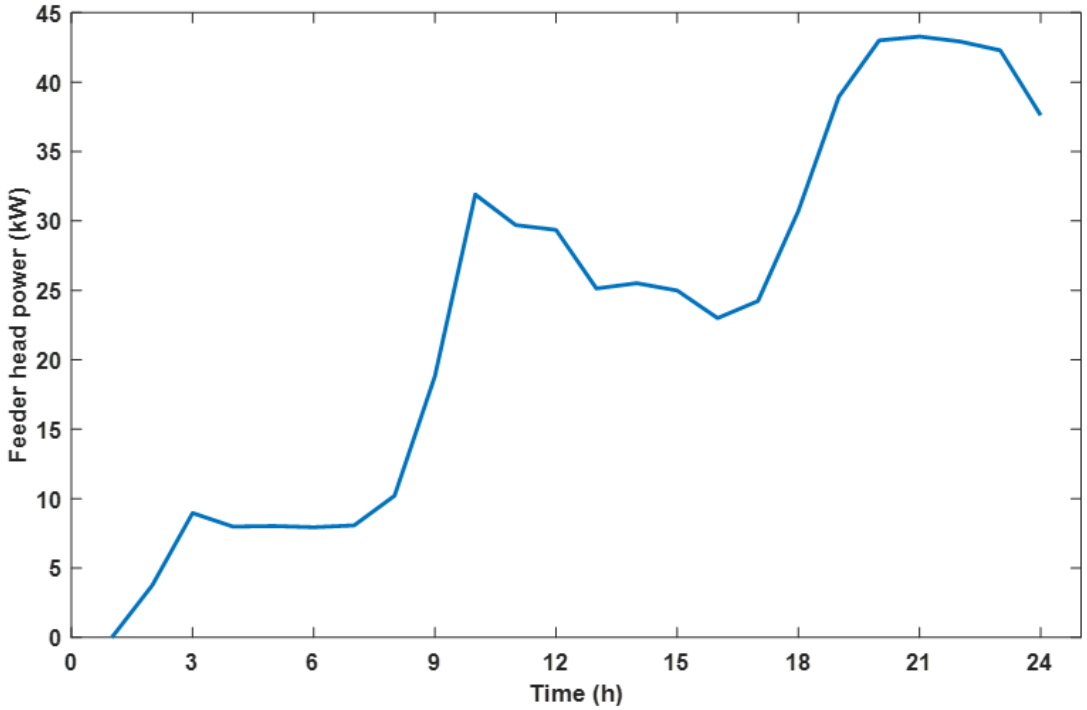

Figure 4.6: Power flows measured at the feeder head

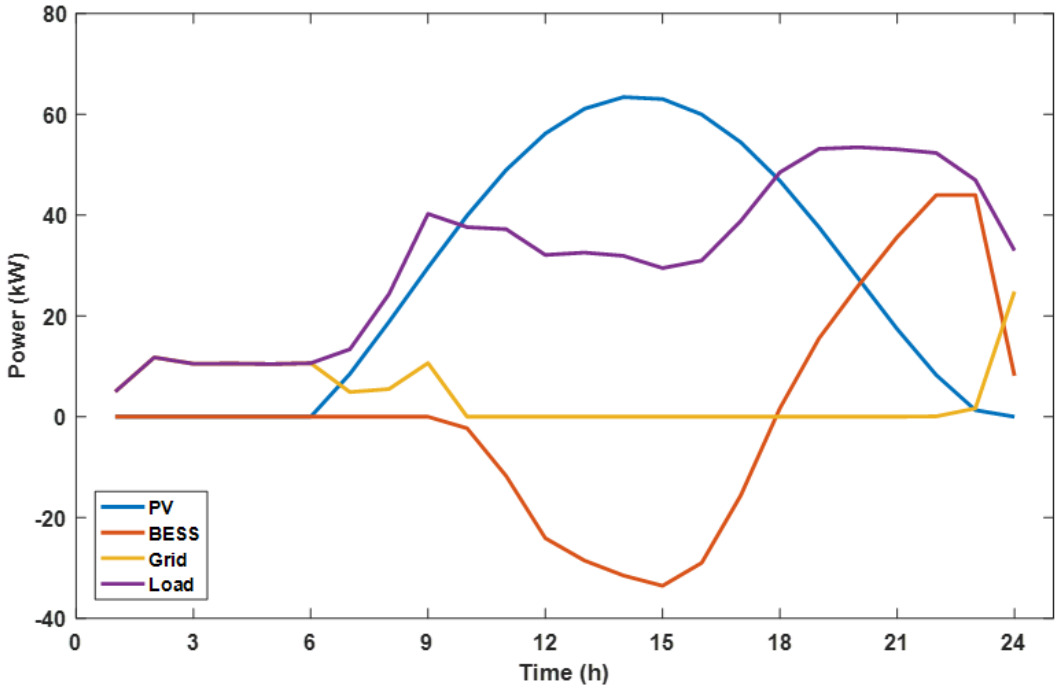

Figure 4.7: 24-hour BESS dispatch, grid energy import, load demand and PV power utilisation using LP algorithm

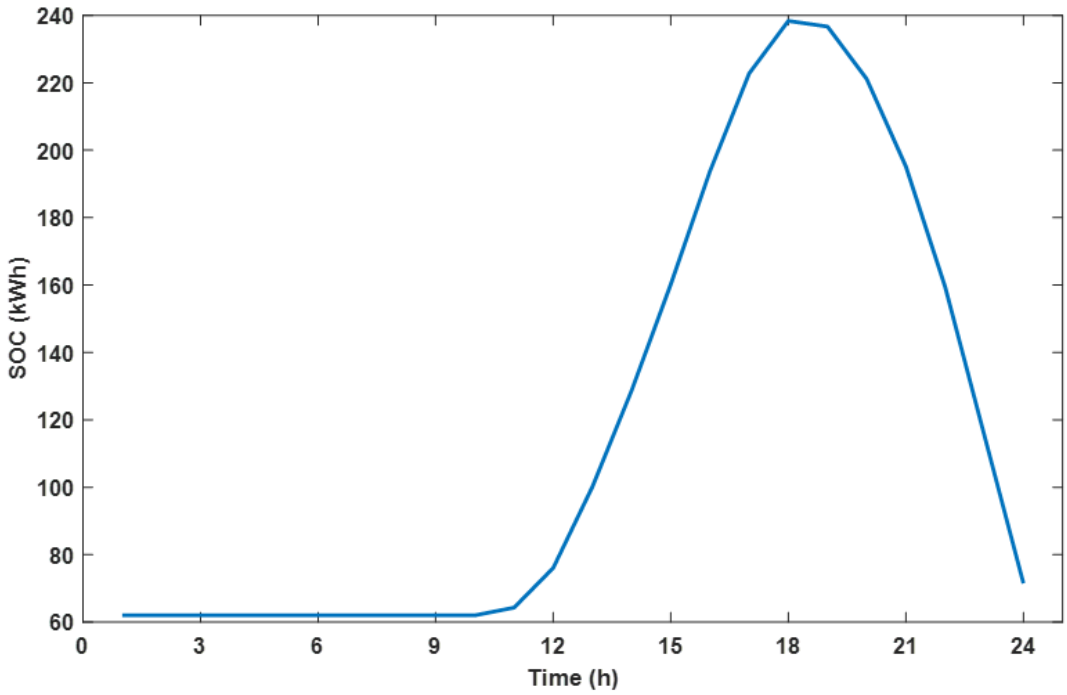

Figure 4.8: 24-hour profile of SOC of BESS

Figure 4.7 shows that between 00:00 and 09:00, the BESS does not start charging with power from the grid. Charging only starts when excess PV power is available after meeting load demand. BESS is also incentivised to discharge during times of high electricity prices, which coincides with peak load periods, which is seen between 18:00 to 23:00.

At 23:00, the maximum discharge power of the BESS (44kW) is not sufficient to meet demand, hence from this point, power is purchased from the grid. The minimal exchange of power between the network and the grid implies that the voltage profile of the network is maintained within regulatory limits, even with the high PV penetration, as there is no reverse power flow at any time.

The life characteristic curve for the typical lithium-ion battery used in this work adheres to the curve shown in Figure 4.1. With an average single cycle per day at 80% DOD, the number of cycles to failure is estimated as 2000, corresponding to a period of 5.48 years. Hence, the rainflow algorithm given in (15) is not employed at this stage of the work. Life cycle counting methods for varying BESS cycles are implemented in the later parts of this thesis when comparisons between different control schemes in relation to BESS lifespan will be made. This will also include yearly simulations on the network with BESS. The SOC of the BESS during the simulation period is shown in Figure 4.8. The BESS in this case gets fully charged and discharged within the course of the day. Observe that the SOC of the BESS begins at 62kWh because the BESS has a minimum depth of discharge of 20%.

For a 24-hour period and lifetime of the BESS, the arbitrage gain Ω_{TOU} is calculated by solving (4.15), and results are presented in Table 4.2. The results show a total energy arbitrage gain of USD 21,900. This is the value gained when exclusively considering purchasing energy at cheaper rates and delivering at higher rates. This result is dependent, firstly, on the TOU prices used in the study. A single TOU price has been used for the analysis, but this could change from day to day. In addition, there will also be variations in TOU tariffs in different countries. Secondly, the result

is dependent on the cost of PV power used for charging of the BESS. There will be different solar irradiation values for different geographical areas during different seasons of the year. This means that the quantity of PV power generated on different days may be inadequate to charge the BESS to sufficient levels so that the BESS is utilised during periods of the day when the electricity prices are high.

Table 4.2: Energy arbitrage values

	Daily ($)	Lifetime ($)
Cost of charging: $\sum_{t=1}^{q} P_{B,C}^{S}(t)$	8.04	16,080
Cost of discharging: $\sum_{t=1}^{q} P_{B,D}^{S}(t)$	18.99	37,980
Arbitrage gain: Ω_{TOU}	10.95	21,900

4.7 Conclusion

This chapter presented a linear program optimisation for scheduling BESS in a network with high penetration of PV, in order to maximise arbitrage gains. This is achieved while satisfying all the BESS characteristic constraints and also meeting the network load demand using the cheapest available energy source at different times of the day. Overall, minimal energy was imported from the grid into the test network since the PV power was efficiently utilised by the optimisation.

The results obtained are based on the assumption that the day-ahead network load and PV power have been forecast accurately. However, this is hardly the case in practice and therefore is a limitation of this work. Practical systems will have to employ some control systems to handle variability of load and PV generation. The network losses are also considered to be part of the base load demand, and are therefore not accounted for separately in this work.

As stated previously, BESS commitment to provision of one or more services results to unavailability to participate in the provision of some others. The end-goal is to develop a scheme that optimises the operation of the BESS to yield maximum benefit from several value streams in order to justify investment. Other factors that affect

the overall economic valuation are load growth rate, cost of BESS installation and economies of scale.

Chapter 5

Flat-structure sensitivity scheme

5.1 Introduction

This chapter presents the flat structure sensitivity scheme (FSSS) for the coordination of multiple BESS in a distribution networks with high PV penetration. The chapter starts off with some background and a presentation of the problem. The methodology of the FSSS is presented next, followed by the operation of the scheme. The chapter continues with presentation of the implementation of the FSSS. Simulation results were presented for the different test cases considered, followed by a discussion of the results. Conclusions are drawn at the end of the chapter.

5.2 Background and context

One of the reasons for the growth in interest in the installation of the BESS is because it provides fast and flexible active and reactive power dispatch, which is then used for a variety of functions such as frequency support, voltage support and for arbitrage purposes. Even though the initial installation cost of BESS is still high, this is changing as a result of increased investment into the research and development of cheaper and more efficient BESS technologies. This drive comes especially from the increasing demand for BESS for consumer electronics and for electric vehicles [5]. The high cost of BESS installation has placed a huge demand on the efficiency of operations and use of BESS, to ensure BESS lifetime is maximised before any need for replacement.

In low voltage distribution networks with high penetration of PV, overvoltage remains

a power quality issue, and therefore a major limitation to growth of penetration. When the power generated exceeds demand, there is reverse power flow to the MV distribution network and also overvoltage. Curtailment of excess PV power in this case is common, but this threatens the economic justification for installation of PV. BESS installation in scenarios such as described, is a widely-used method to try to mitigate overvoltage while fully utilising the power from the PV. The BESS in this case works to store energy from the PV during the periods of high production, and to make the stored energy available to the network during periods of high load demand. In networks where there exists multiple BESS installations, there is the challenge of appropriate coordination of the operations of the BESS installed, in order to achieve set technical objectives of installation. This coordination should also control the BESS operations in such a way that the BESS has maximum possible lifetime.

In this chapter, a coordination algorithm is presented for the control of BESS on a low voltage distribution network with high penetration of PV. The algorithm is developed based on the voltage sensitivity of the network buses. Through the efficient selection, coordination and timing of the charge and discharge operations of the BESS, the scheme maintains bus voltages within statutory ranges during both periods of high PV power generation and high network load demand. The scheme also prevents sudden voltage rise, which usually occurs in such networks immediately a BESS reaches full charge. Simulations were carried out on a real LV distribution network and the results were analysed and discussed thereafter.

5.3 Methodology of the flat-structure sensitivity scheme

For multiple BESS connected in a network, a major objective of the coordination scheme is to resolve the challenge of BESS selection for operations at different times for different network conditions, and also to determine how the selected BESS behaves – charge/discharge rates and DOD. The flat-structure sensitivity scheme

(FSSS) utilises the voltage sensitivities of the network nodes to coordinate the operations of participating BESS, in a way that considers the entire network as a flat non-hierarchical and non-segmented structure. The method of derivation and use of voltage sensitivity, including the operational principles of the flat-structure scheme are presented in this section.

5.3.1 Voltage sensitivity for BESS selection

The relationship between the changes in voltage at the buses, as a consequence of the changes in active or reactive power at other buses on the network is provided by the voltage sensitivity factor (VSF). The Jacobian matrix in (5.2) presents this relationship.

$$\begin{bmatrix} \Delta\theta \\ \Delta|V| \end{bmatrix} = J^{-1} \begin{bmatrix} \Delta P \\ \Delta Q \end{bmatrix} \tag{5.1}$$

where

$$J^{-1} = \begin{bmatrix} \frac{\delta\theta}{\delta P} & \frac{\delta\theta}{\delta Q} \\ \frac{\delta V}{\delta P} & \frac{\delta V}{\delta Q} \end{bmatrix} \tag{5.2}$$

$\Delta\theta$ is the change in bus voltage angle, ΔQ is the change in reactive power, ΔV is the change in bus voltage, and ΔP is the change in active power. (5.1) and (5.2) present expressions for the sensitivities of both voltage angle and magnitude. Of particular interest to this work is ΔV and this is expressed as

$$\Delta|V| = \begin{bmatrix} \frac{\delta V}{\delta P} & \frac{\delta V}{\delta Q} \end{bmatrix} . \begin{bmatrix} \frac{\Delta P}{\Delta Q} \end{bmatrix} \tag{5.3}$$

Under network conditions of overvoltage, undervoltage and during periods where peak shaving is required, the voltage sensitivity is utilised in the appointment of BESS and determination of charge and discharge rates. In this scheme, in relation to (5.3), ΔP represents the charge or discharge power of the operational BESS, which can be converted to respective charge/discharge rates, while ΔV is considered at the node where the voltage change is desired. This method of selection ensures that the selected BESS has the most effective desired effect on the voltage of the target node.

A drawback of using the Jacobian matrix method for obtaining voltage sensitivity is the computational complexity that is involved in the process. Other methods have been proposed in literature for the evaluation of network sensitivities different from the use of the Jacobian. In [112], first-order sensitivity relationships for current and voltage of buses were developed and used to evaluate constants for sensitivities at different buses and branches as a result of variation of active or reactive power at other buses. In [113], an approximate method was proposed that required the power flow to be computed only once. This method also involves only a single topology search and the sensitivities could be obtained that require less computational complexity.

A method of sensitivity evaluation was presented in [114], and this method provides an alternative computationally less intense way of obtaining the sensitivity matrix. The method is an approximate evaluation, however, the results obtained are close to those obtained by using (5.1) directly. This method is summarised in (5.4) and (5.5).

$$\frac{\delta E_i}{\delta P_j} = -\frac{1}{E_n}\left[\sum_{hk \in PT_{i,j}} R_{hk}\right] \tag{5.4}$$

$$\frac{\delta E_i}{\delta Q_j} = -\frac{1}{E_n}\left[\sum_{hk \in PT_{i,j}} X_{hk}\right] \tag{5.5}$$

R_{hk} and X_{hk} are the resistance and reactance of branch hk respectively; E_n is the approximate rated voltage of the network; $PT_{i,j}$ is the set of nodes contained in the path connecting the medium voltage (MV) busbar to nodes i and j, and at the same time common to both nodes. Sensitivity ranking tables B_P and B_Q for real and reactive power respectively are formed using (5.4) and (5.5). These are presented in (5.6) and (5.7)

$$B_P = \begin{bmatrix} \frac{\delta E_1}{\delta P_1}\Delta P_1 & \dots & \dots & \frac{\delta E_1}{\delta P_N}\Delta P_N \\ \dots & \dots & \dots & \dots \\ \dots & \dots & \dots & \dots \\ \frac{\delta E_N}{\delta P_1}\Delta P_1 & \dots & \dots & \frac{\delta E_N}{\delta P_N}\Delta P_N \end{bmatrix} \tag{5.6}$$

$$B_Q = \begin{bmatrix} \frac{\delta E_1}{\delta Q_1}\Delta Q_1 & \dots & \dots & \frac{\delta E_1}{\delta Q_N}\Delta Q_N \\ \dots & \dots & \dots & \dots \\ \dots & \dots & \dots & \dots \\ \frac{\delta E_N}{\delta Q_1}\Delta Q_1 & \dots & \dots & \frac{\delta E_N}{\delta Q_N}\Delta Q_N \end{bmatrix} \tag{5.7}$$

N represents the total number of buses on the network and $n = 1, 2...N$ represents any specific bus on the network. The rows of B_P represent the node voltages while the columns represent the BESS locations. When the voltage of a particular bus (along rows) is of interest for change, the column (representing BESS installation location) with the highest value is selected as the best suited for affecting the required voltage change. This selected BESS is designated $BESS_{sel}$ for the time instant that this evaluation is carried out. The selection according to ranking is carried out by the selection evaluator (SE) within the algorithm. When there is no BESS installation on a particular bus, the position of that bus in (5.6) or (5.7) is designated zero and therefore cannot be selected.

5.3.2 Description of sets used in formulation

The algorithm, during operation, maintains and updates the following sets at each time step.

1. **Power ratings set** (P_{BES})**:** This is the set of active power ratings of all BESS on the network.

$$P_{BES} = P_{BES_n} : n = 1, 2, \ldots N \tag{5.8}$$

   where P_{BES_n} is the active power rating of the BESS connected to bus n, N is the total number of buses on the network. Observe that $P_{BES_n} = 0 \; \forall n \in Z$ holds true, where Z is the set of all buses that have no BESS installation.

2. **Selected BESS set** (BES_{sel})**:** This is the set of all BESS that have been selected by the SE and activated for charging or discharging.

$$BES_{sel} = BES_{sel_n} : n = 1, 2, \ldots N \tag{5.9}$$

   where BES_{sel_n} is an output from the SE which denotes the BESS that has been selected for charging. $BES_{sel} = \phi$ holds true as an initial condition at the start of operations. BES_{sel_l} is used to denote the last BESS that has been added to BES_{sel}.

3. **Charge rates set** (CR)**:** This is a set of the charge or discharge rates of corresponding selected BESS contained in BES_{sel}

$$CR = CR_n : n = 1, 2, \ldots N \tag{5.10}$$

   where CR_n is the charge rate of the corresponding BES_{sel_n}. Similar to BES_{sel}, $CR = \phi$ holds true at the start of operations. CR_l is used to denote the charge rate of BES_{sel_l} and CR_{max} denotes the maximum charge rate of any BESS.

4. **State of charge set** (Ω_{soc})**:** This set contains the varying SOC of all the BESS

on the network. The algorithm uses this to have knowledge of which BESS are fully charged, or nearly fully charged in order to take proactive actions. The latter is one of the objectives the scheme aims to achieve.

5.4 Flat structure sensitivity scheme operation

The flowchart in Figure 5.1 shows the operation of the flat-structure sensitivity scheme (FSSS). In this work, the algorithm coordinates multiple BESS on a network with the objectives of mitigating overvoltage during periods of high PV generation and mitigating undervoltage during high loading periods. High loading periods often coincide with periods of low PV generation, usually in the evening. The bus voltages are maintained within set upper and lower limits, $V_{LTH} \leq V_m \leq V_{UTH}$. V_m is the monitored bus voltage, V_{LTH} is the statutory lower threshold voltage and V_{UTH} is the statutory upper threshold voltage.

Figure 5.2 shows the flow of operations of the FSSS for undervoltage scenarios. In this work, the algorithm coordinates multiple BESS on a network whose needs are to mitigate overvoltage and undervoltage, and also for peak-shave during periods of high network loading. Therefore, the algorithm becomes operational when the condition $V_{LTH} \leq V_m \leq V_{UTH}$ is violated, where V_m is monitored bus voltages, V_{LTH} is the statutory lower threshold voltage and V_{UTH} is the statutory upper threshold voltage.

Following a scenario where the algorithm is initialised at the start of the day (midnight), then $V_m > V_{UTH}$ is likely to occur first as a result of possible overvoltage due to high PV power generation in the day when load demand is low. Upon overvoltage, the SE executes an evaluation and the output from the SE is BES_{sel_n}, which is a BESS selected for operation at that point. This BESS goes into charging mode. V_{diff} is the difference between the measured bus voltage V_m and the statutory threshold voltage V_{UTH} or V_{LTH}. The amount of power that keeps V_{diff} at zero (CR_n), is also derived for BES_{sel_n}. CR_n, which is the charge rate of the BESS, is derived from (5.6) as

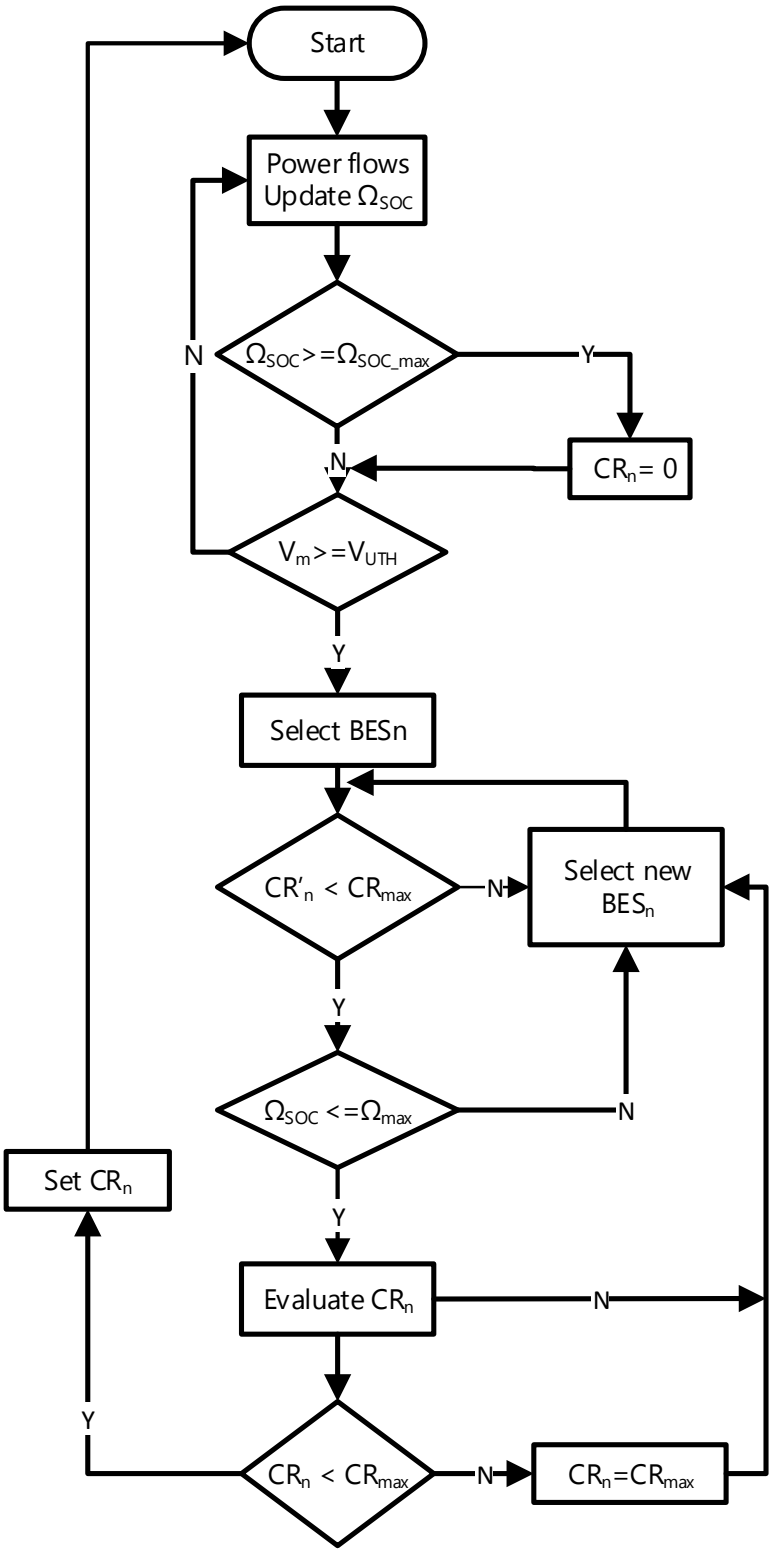

Figure 5.1: Flowchart of the FSSS for overvoltage

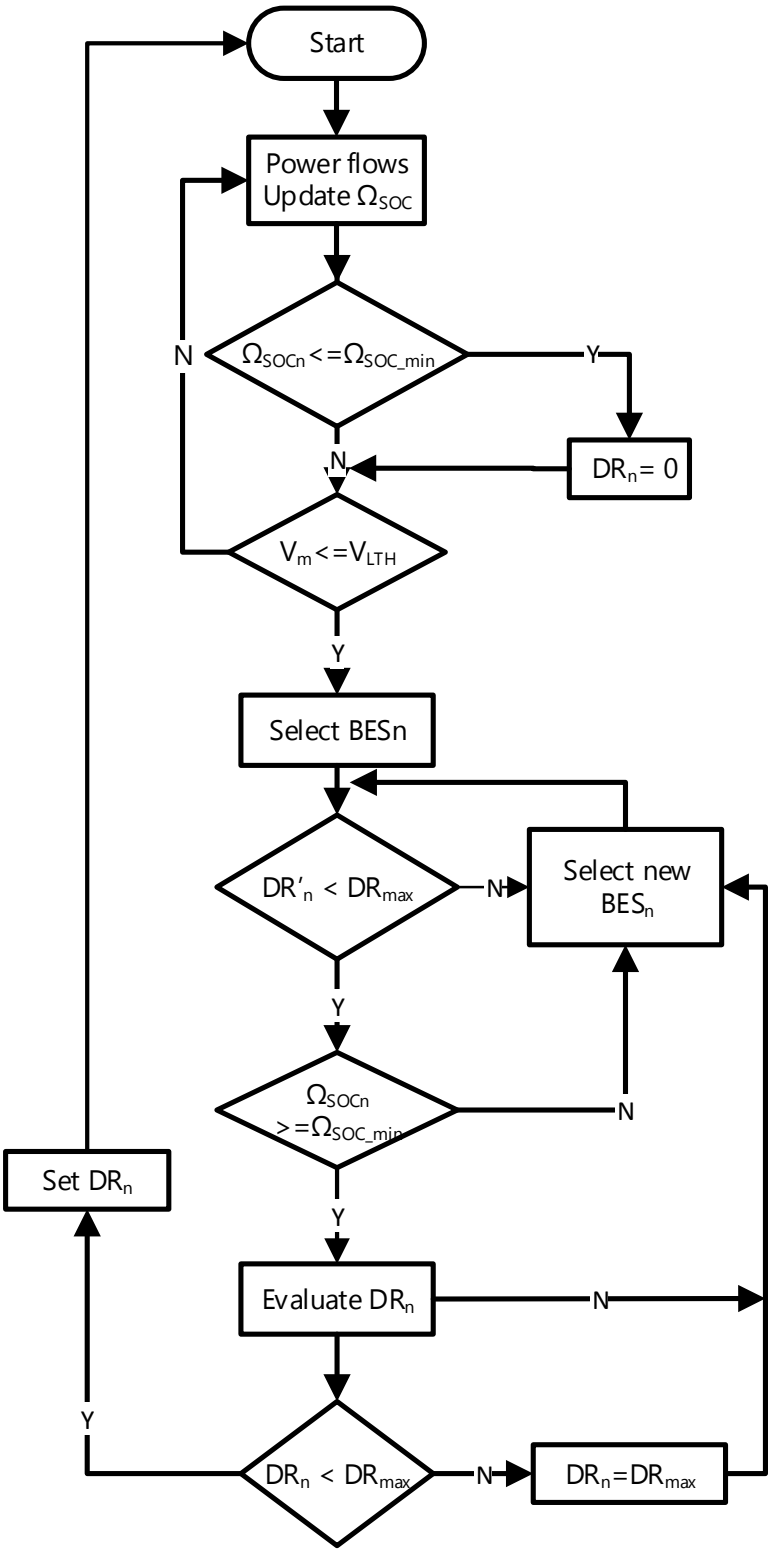

Figure 5.2: Flowchart of the FSSS for undervoltage

$$CR_n = V_{diff}.(\frac{\delta V_m}{\delta P_n})^{-1} \tag{5.11}$$

where $(\frac{\delta V_m}{\delta P_n})$ is the sensitivity V_m to the bus where BES_{sel_n} is connected. During operation, given the situation where the CR of BES_{sel_n} stops being large enough to maintain $V_{diff} = 0$, possibly as a result of sustained increase in PV active power generation, new BESS are added, one at a time, to the BES_{sel} set. The selection this time will exclude from the ranking, any BESS that is already contained in BES_{sel}.

The SOC of participating BESS are known, since Ω_{SOC} (a set containing the SOCs) is updated at every time step. Having this information from Ω_{SOC} helps the controller to add new BESS to the set of active BESS, BES_{sel}, in time enough to mitigate the possible undesirable occurrence of voltage excursions as a result of a BESS becoming fully charged or fully discharged. When the power required from a BESS in order to respond to a voltage issue is larger than the maximum charge rate of the BESS, the BESS is assigned to charge at its maximum charge rate while the SE selects the next best BESS to be added to BES_{sel}. However, if the charge rate of the BESS is greater than the required power, the charge rate for this BESS is set, the BESS goes into charging at the estimated rate and the algorithm advances to the next time step. When any of the participating BESS reaches maximum SOC, charging is discontinued. In Figure 5.1, CR'_n is used to represent the current charge rate prior to estimation of new charge rates.

During peak loading times, the algorithm switches to discharge mode for the BESS. During this period in the day, there is little or no PV power generated, and therefore the stored charge in the BESS is utilised. This is shown in Figure 5.2. Upon the occurrence of undervoltage ($V_m < V_{LTH}$), the SE selects the best BESS ($BESS_{sel}$) for discharge and the discharge rate is calculated according to (5.12).

$$DR_n = V_{diff}.(\frac{\delta V_m}{\delta P_n})^{-1} \tag{5.12}$$

V_{diff} in this case is estimated as $V_{diff} = V_m - V_{LTH}$. This is the amount of power required by the selected BESS to restore V_{diff} to zero. In Figure 5.2, the discharge rate is represented as DR_n. If the estimated required power is greater than the discharge rate of the selected BESS, then the selected BESS is discharged at maximum discharge rate possible, while the algorithm selects the next best BESS to add to the $BESS_{sel}$ set. But if the required power is less than the maximum discharge rate of the selected BESS, the estimated discharge rate is set for this BESS and it goes into discharging mode. In Figure 5.2, DR'_n is used to represent the current discharge rate prior to estimation of new discharge rates.

For the discharge mode, in addition to being triggered by undervoltage, the scheme can be set to trigger the discharge mode when the amount of power imported from the grid into the network under consideration exceeds a predetermined threshold. This threshold could be measured at the head of the feeder or substation delivering power to the network. In this situation, the BESS discharge in response of both undervoltage and violation of set threshold power. When any BESS reaches minimum depth of discharge, discharge is discontinued.

With the Jacobian sensitivity method, an increase in the size of the power network leads to a corresponding increase in the complexity of computation. This increase in complexity could lead to time delays in operations, depending on the particular operation the method is being deployed for. This statement is a judgement based on expected behaviour that accompanies increase in system size and complexity. There has not been any comparative study carried out in this research to provide empirical evidence to this statement. There could also arise a need to invest more into computational resources as a result of this complexity. The FSSS overcomes

this limitation by being faster, and therefore, suitable for implementation on large networks.

5.5 Implementation of FSSS

This section describes the tools, test network and implementation considerations made in demonstrating the performance of the coordination scheme.

5.5.1 Implementation tools

The distribution network used as a case study in the implementation of the coordination scheme was built using OpenDSS software [115], an open source tool developed by Electric Power Research Institute (EPRI). The algorithm for the coordination control was developed using MATLAB software. The Component Object Model (COM), which is made available in OpenDSS, was used as an interface to effect the controls on MATLAB to the network model on OpenDSS.

5.5.2 Description of distribution network

The scheme is demonstrated using a Belgian low voltage residential network [61], earlier presented in Section 4.5.1. The network is a radial 7-bus feeder with 4 out of the 7 buses (buses 2, 4, 5 and 7) having PV installations. The feeder is supplied through a 22/0.4 kV transformer rated 185 kVA. The network diagram is shown in Figure 5.3. 33 residential houses are connected on the feeder, with PV installations that total 42.6 kW. Six PV installations are located on bus 7 while buses 2, 4 and 5 contain single installations each. The values of the installations are as shown in Figure 5.3. On each bus containing PV, BESS is installed and the capacities are also shown in Figure 5.3. For adaptation of the network to the structure of the algorithm, the BESS on the network are named according to the buses they are connected to. Multiple BESS on bus 7 are numbered from 7 to 12.

5.5.3 Demand and generation profiles

The load profile was created using the computational model developed by Centre for Renewable Energy Systems Technology (CREST) [109]. The CREST tool generates realistic daily profiles with one minute resolution for residential loads. Load profiles for an aggregate of 100 houses were generated using the CREST tool. A total 50 different aggregations were averaged out to obtain a typical representation of demand in a residential low voltage distribution network. The resulting load shape was applied as multipliers on the test network loads. The demand profile is shown in Figure 5.4. Summer-time load profile was generated to capture period of high PV generation.

The PV profile used in this work, as shown in Figure 5.4, is a generic summer-time solar irradiation profile and represents average typical behaviour of PV output power. Similar to the demand profile, the PV profile is applied to the kWp values of the PV on the test network.

5.6 Simulation results and discussions

Simulations were run for an entire day to demonstrate the operation of the algorithm, with a resolution of one minute. This also formed the time step for the algorithm – a total of 1440 time steps – since the PV and demand data were both obtained at resolutions of one minute. Other configuration parameters used in the simulations are as follows: $V_{UTH} = 1.05$ p.u, $V_{LTH} = 0.98$ p.u, $CR_{max} = 90\%$, $20\% \leq DOD \leq 90\%$. The substation voltage was set at 1.04 p.u in order to accommodate the voltage drop along the feeder. Three different cases were explored to observe the behaviour of the schemes. Each case has a different level of penetration of PV generators. In this study, the level of penetration refers to the capacities of the PV generators on the network. The results obtained for the three cases are presented in the following sections.

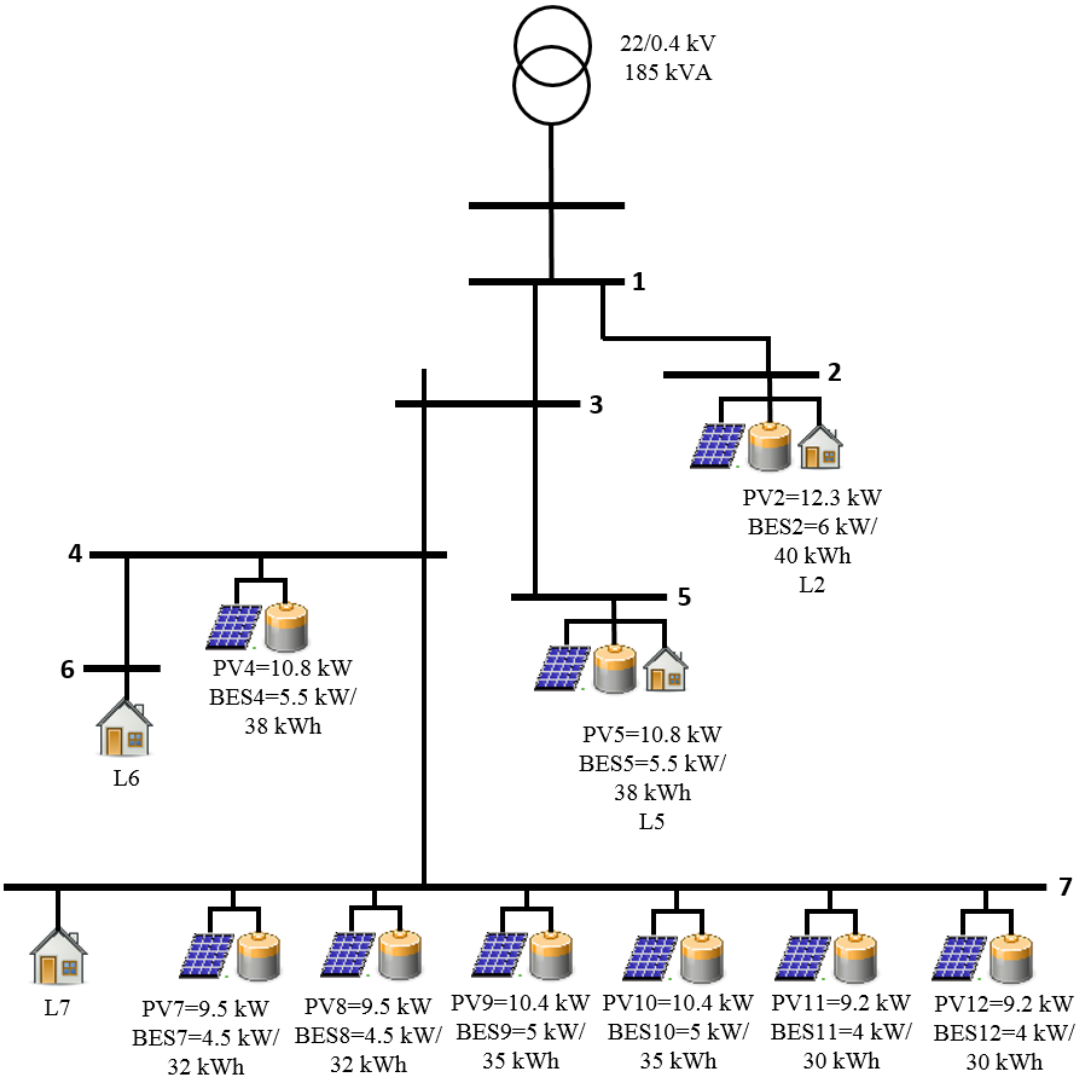

Figure 5.3: Diagram of test network

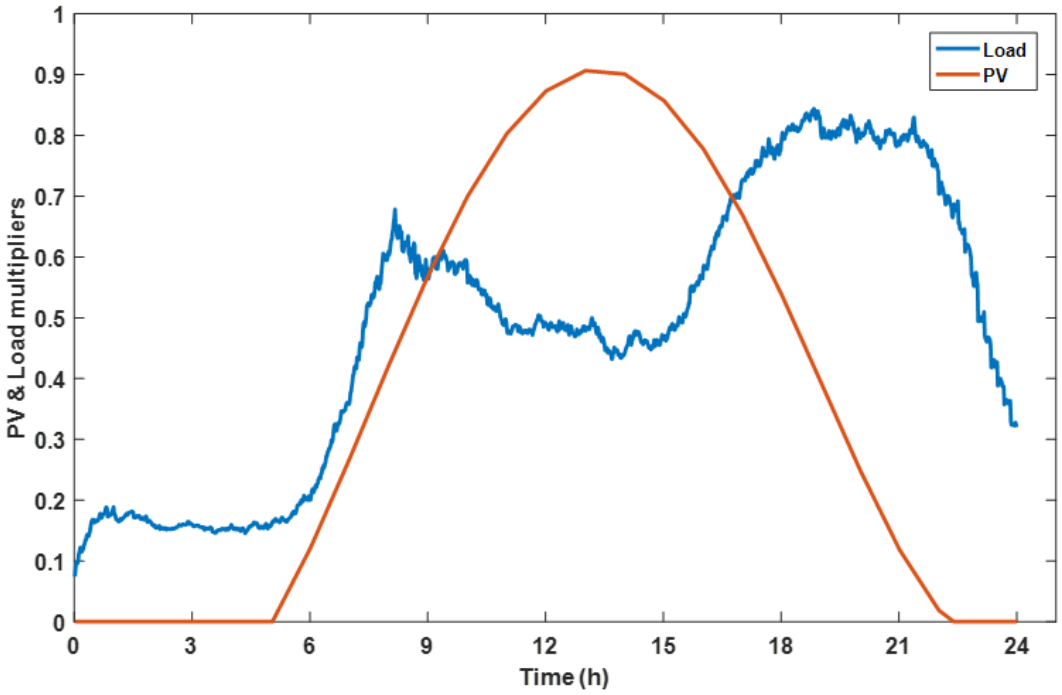

Figure 5.4: Load and demand profiles

5.6.1 Case 1 - 100% of planned PV capacities

For this case, the FSSS is implemented on the test network with PV capacities that are equal to the rated capacities given in Section 5.5.2. This case represents a practical scenario where investment in PV is sufficient enough to meet the planned maximum capacity of PV installations on the network. Figure 5.5 shows the voltage profile of the network when there is no control scheme in place. It can be seen that the voltages exceed the statutory V_{TH} during the period of high PV production. This situation will lead to curtailment of excess active power, thereby reducing the economic benefits of PV installation. Also during the peak load period, there is occurrence of undervoltage on the network.

Figure 5.6 shows the voltage profile of the network with the coordination algorithm in operation. Bus 7 is the end bus on this network and the first to experience voltage excursion. The coordination algorithm is activated when the voltage at bus 7 exceeds

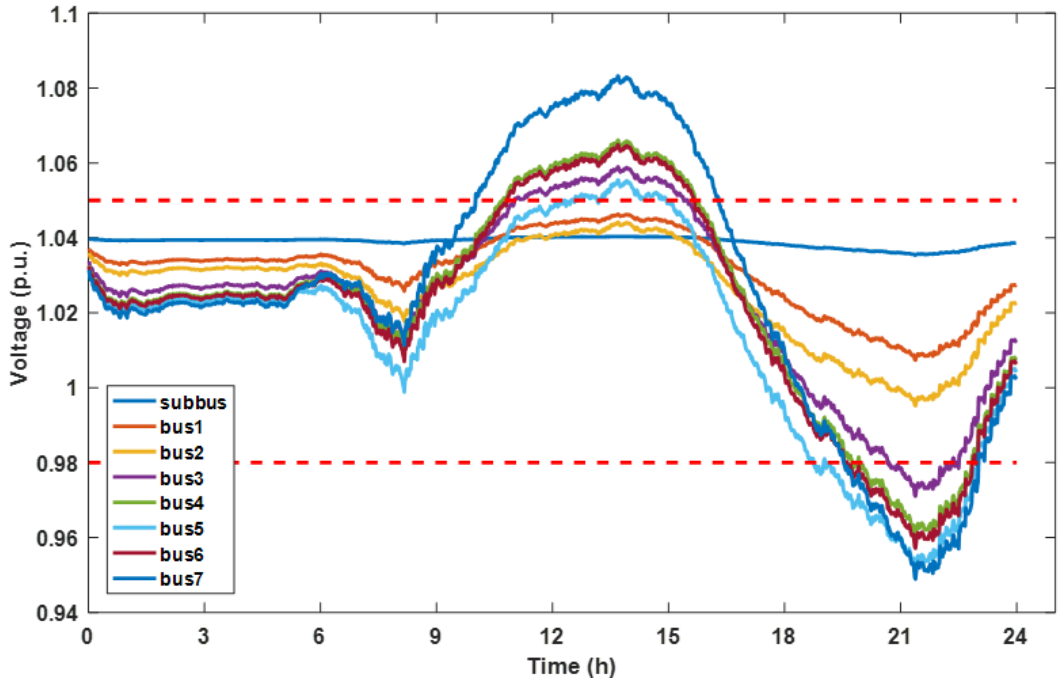

Figure 5.5: Feeder voltage profile without controls

the upper threshold $V_{m_7} > V_{UTH}$. This occurs around the 10th hour, as shown in Figure 5.6. BES_9 is switched to charging mode first as it is the highest ranking on the SE. BES_{10} could also have been switched first since it has the same ranking as BES_9, given that they both have the same power ratings, availability according to ω_{SOC} and are both positioned on the same bus. BES_{10} is switched to charging mode shortly after BES_9. This happens after CR_9 reaches CR_{max}, and $V_{diff} > 0$ still persists.

The other BESS are sequentially switched to charging mode as PV power production continues to increase. The coordination control algorithm also ensures there are no sudden voltage rises, especially when a BESS charges to maximum capacity. This accomplishes one of the aims of this work. Figure 5.6 also shows that the regulation of the voltage at the boundary is not exact but very close. This can be attributed to the fact that the method used to obtain the sensitivity matrix is an approximation. The benefit of the method, however, is its low computational complexity. Another reason is non-linearity of the elements of the distribution network.

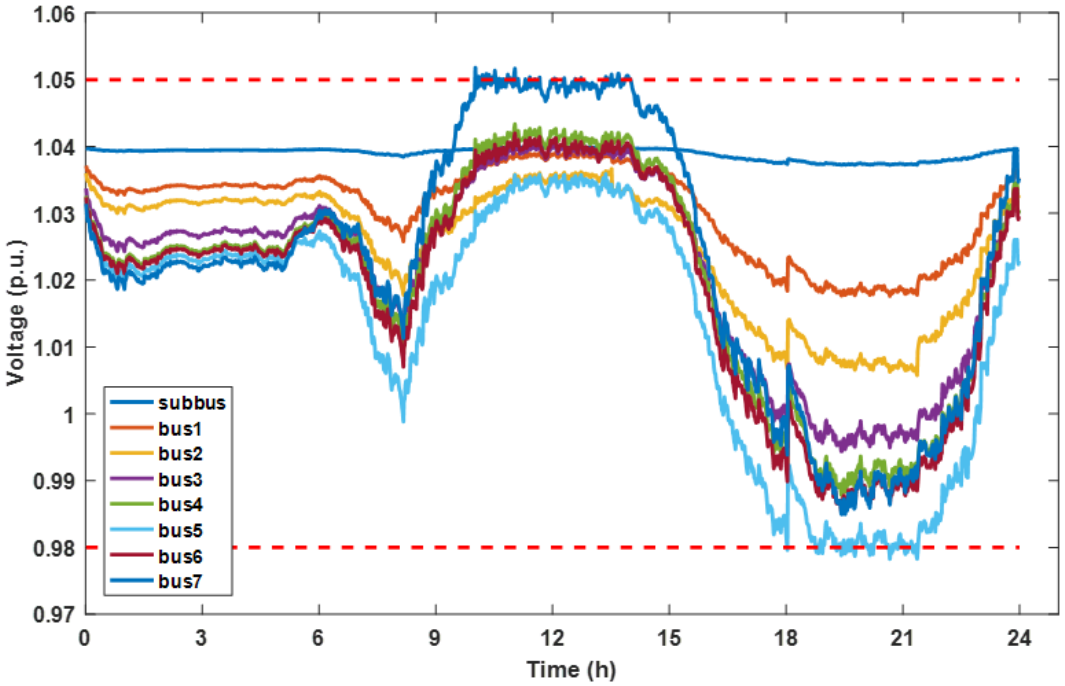

Figure 5.6: Feeder voltage profile with coordination control

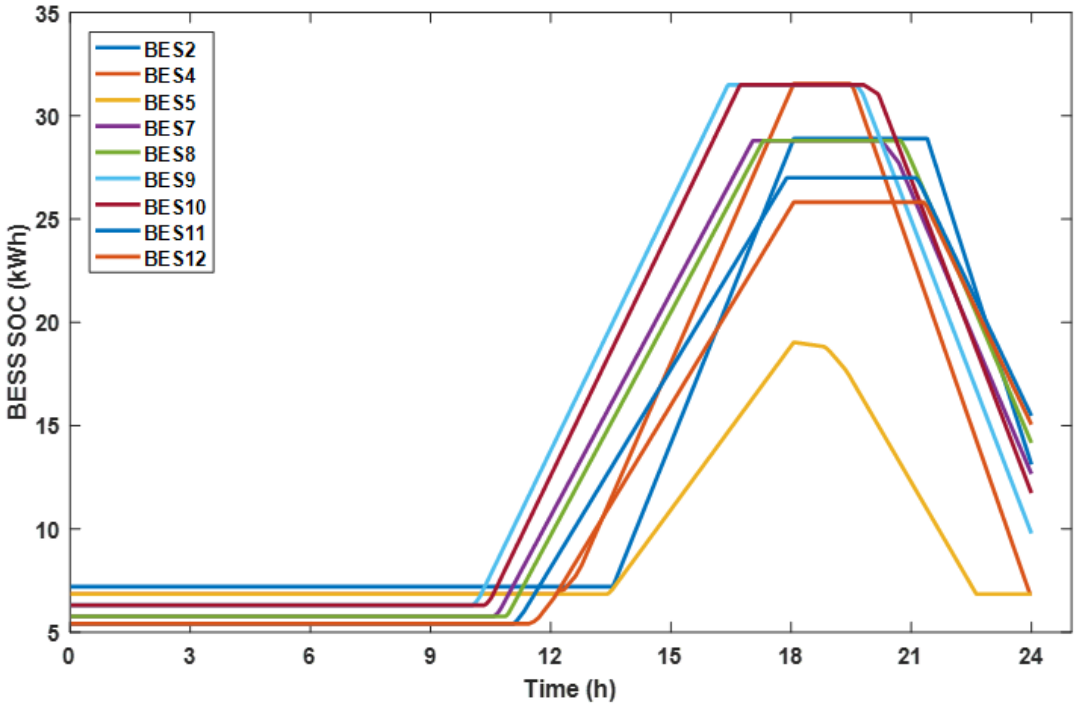

Figure 5.7: SOC of network BESS

During periods of heavy loading on the network, discharge signals are sent to appropriate BESS. As seen in Figure 5.6, this is activated around the $18th$ hour when $V_5 < V_{LTH}$ occurs. BES_5, which is the most effective BESS for impact on bus 5, is switched to discharge mode first. Charging is discontinued for any BESS still in charging mode (BES_2 for example), and other BESS are sequentially switched to discharge mode according to the results of the evaluation in the SE at each time step. Undervoltage is prevented with the coordination control on the network.

The SOC of the BESS for the simulation period are presented in Figure 5.7. This shows the times when charge and discharge begin and end for the BESS. The Figure also shows the BESS during periods of full charge, as indicated by the flat lines at the top. Figure 5.8 shows that there is reverse power flow from the LV network to the MV network without the coordination control.

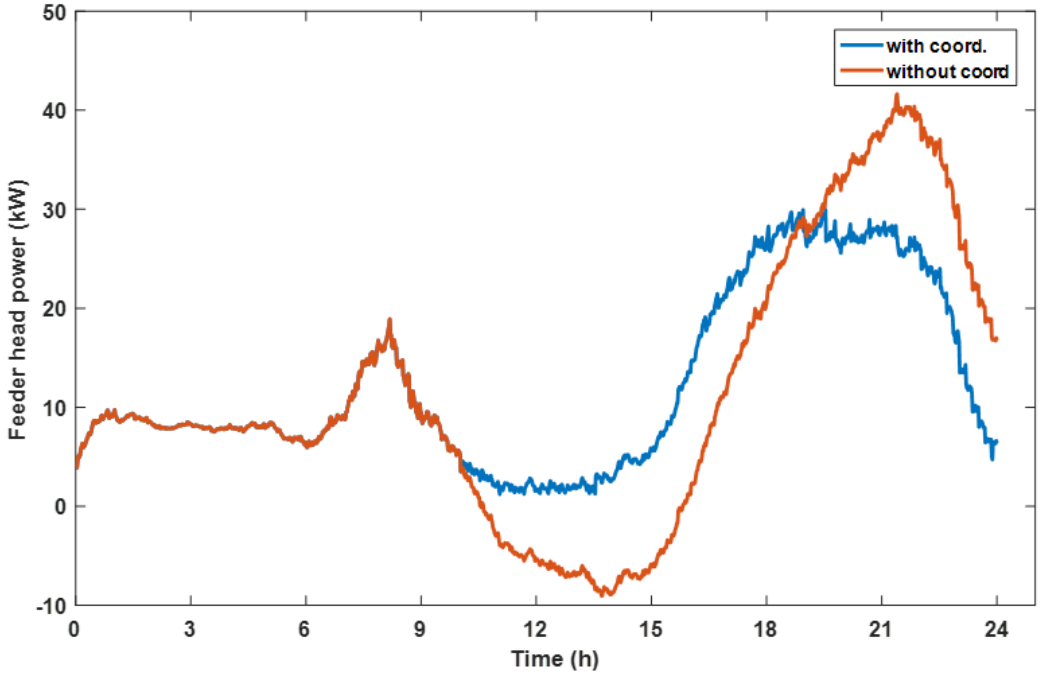

Figure 5.8: Power flows measured at the feeder head

There is also large power drawn from the MV network during peak periods, which could lead to thermal ratings being exceeded or the need for infrastructure upgrade. There is a significant difference from this when the coordination control is deployed

on the network.

5.6.2 Case 2 - 85% of planned PV capacities

In this case, the capacities of the PV installations on the network are only 85% of the PV capacities described in Section 5.5.2. This represents a real life situation where the available resource for investment in PV installations for the network is less than planned. In the absence of the actions of the FSSS in this case, the voltage profile of test network is as presented in Figure 5.9, which shows there is a violation of regulation voltage boundaries. In this case, $V_m > V_{UTH}$ occurs halfway between the 10th and 11th hour as a result of higher PV power generation when compared to network load. Bus 7 is the first bus to experience overvoltage.

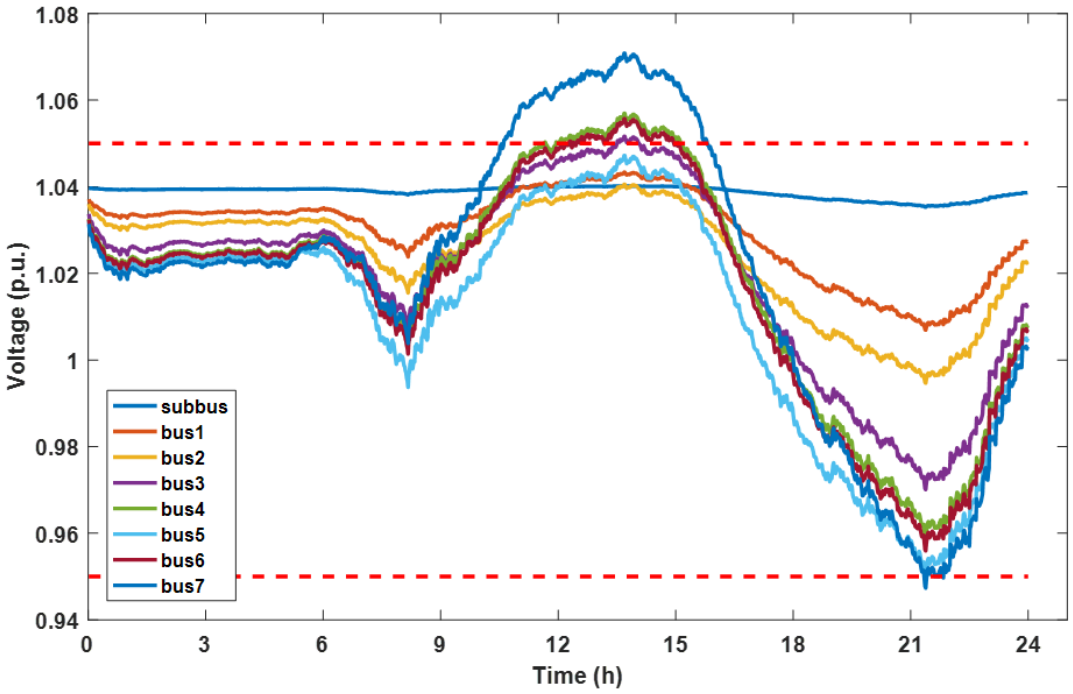

Figure 5.9: Feeder voltage profile without control - case 2

The situation therefore calls for curtailment of PV power, as a drastic and final measure, or for other control actions to be taken. Figure 5.10 shows the voltage profile of the network buses when the FSSS is in action. BES_9 is activated for charging operation, since it is the most effectvie BESS to handle voltage excursions occurring at bus 7,

given its capacity, as estimated by the SE. In this situation, the SE also has the option of activating BES_{10}, since it has the same ratings of power as BES_9. Both BESS also have the same availability according to Ω_{SOC} and are positioned on the same bus on the network. BES_{10} can be seen activated shortly after, when BES_9 did not have sufficient capacity to handle the persistent overvoltage situation on the bus.

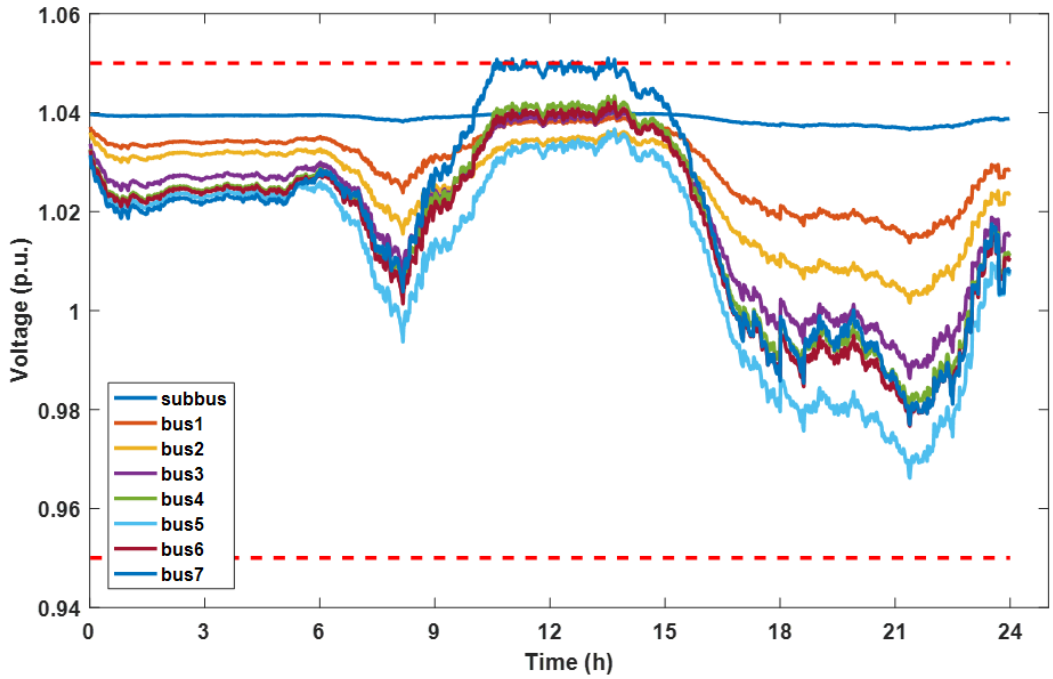

Figure 5.10: Feeder voltage profile with FSSS - case 2

Other BESS are sequentially switched to charging mode as needed on the network. Unlike the condition with Case 1 (with 100% PV capacity), with lower levels of PV power injected into the network and with same load profiles, the voltage violations as a result of PV were reduced. This also means that some of the BESS on the network did not need to be switched to charging. During peak loading periods, the charged-up BESS are made to discharge, both to ease network loading and to get the BESS in a ready state for operations on the next day, in expectation for overvoltage during high PV power generation. Therefore for this case, the discharge signals were not dependent on occurrence of undervoltage.

Figure 5.11 shows the SOC of the BESS on the network during the day, with their

charge and discharge times. $BESS_2$, $BESS_4$ and $BESS_5$ did not need to be activated for charging at any time within the simulation period.

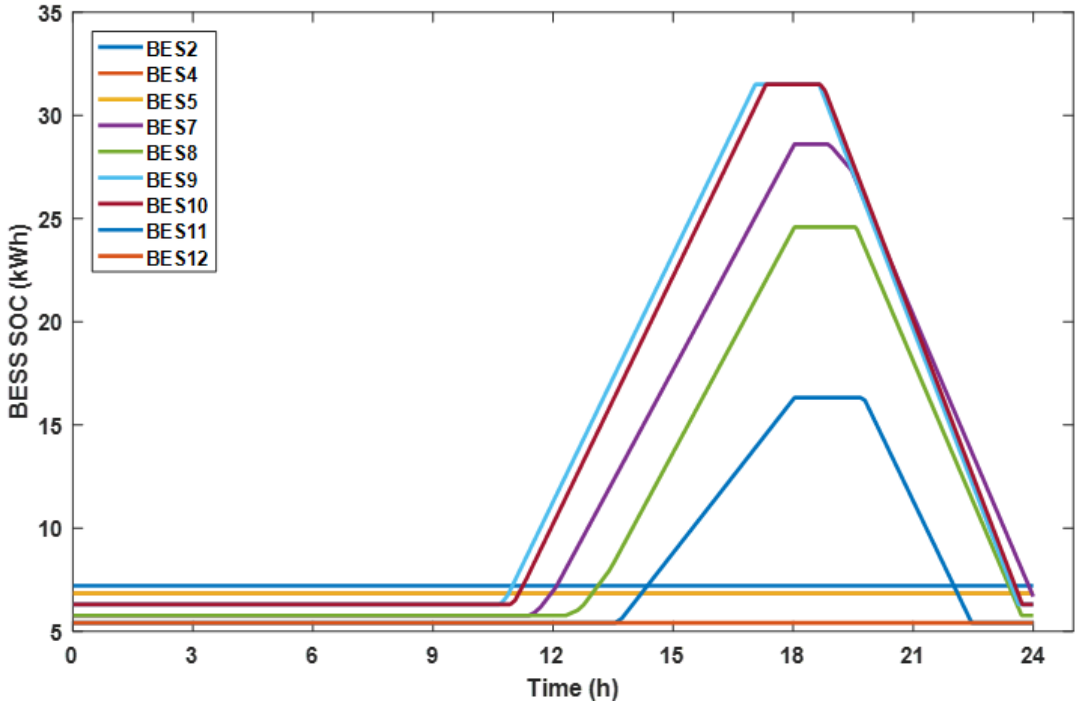

Figure 5.11: SOC of network BESS - Case 2

The power drawn from the MV grid during the day, as measured at the feeder head, is shown in (5.12). Reverse power flow is prevented by the action of the charging BESS during the simulation period.

5.6.3 Case 3 - 70% of planned PV capacities

In this last case, a scenario is considered where only 70% of capacities of PV installations outlined in Section 5.5.2 are installed on the network. The simulation result presented in Figure 5.13 shows the voltage profiles of the buses when the FSSS is not in action. Overvoltage is seen in to occur on bus 7 just before the 12th hour, when the voltage exceeds V_{UTH}. A short period of undervoltage can also be seen in this figure just after the 21st hour.

Figure 5.14 shows the bus voltages with the FSSS in operation. At the same time

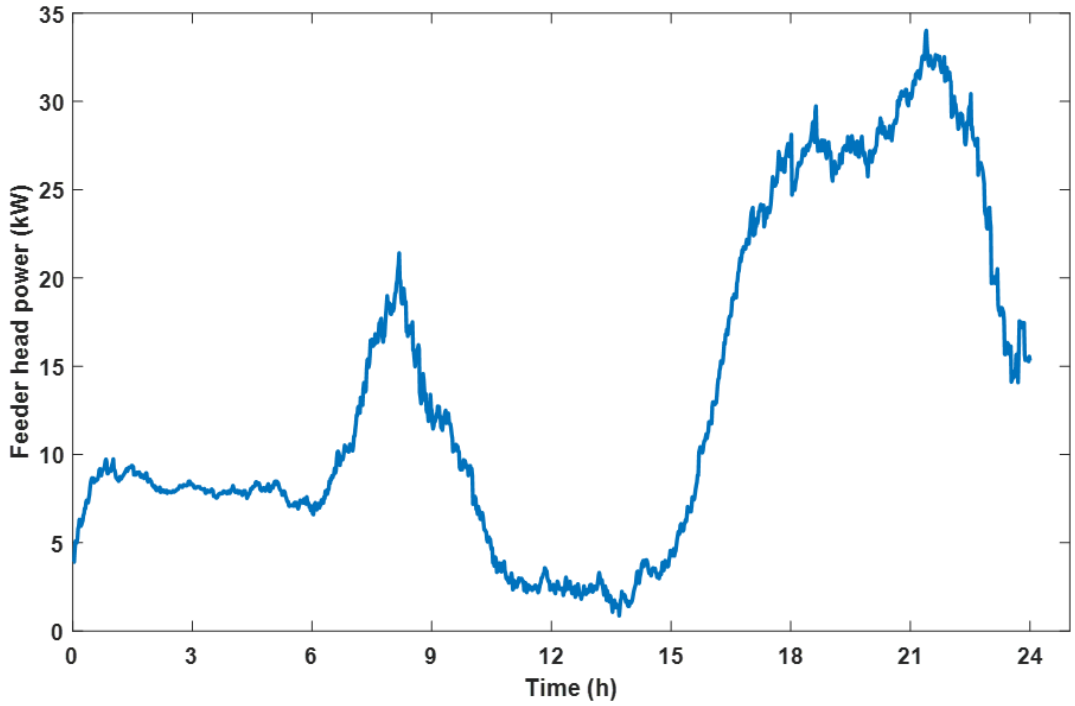

Figure 5.12: Power flows measured at the feeder head - Case 2

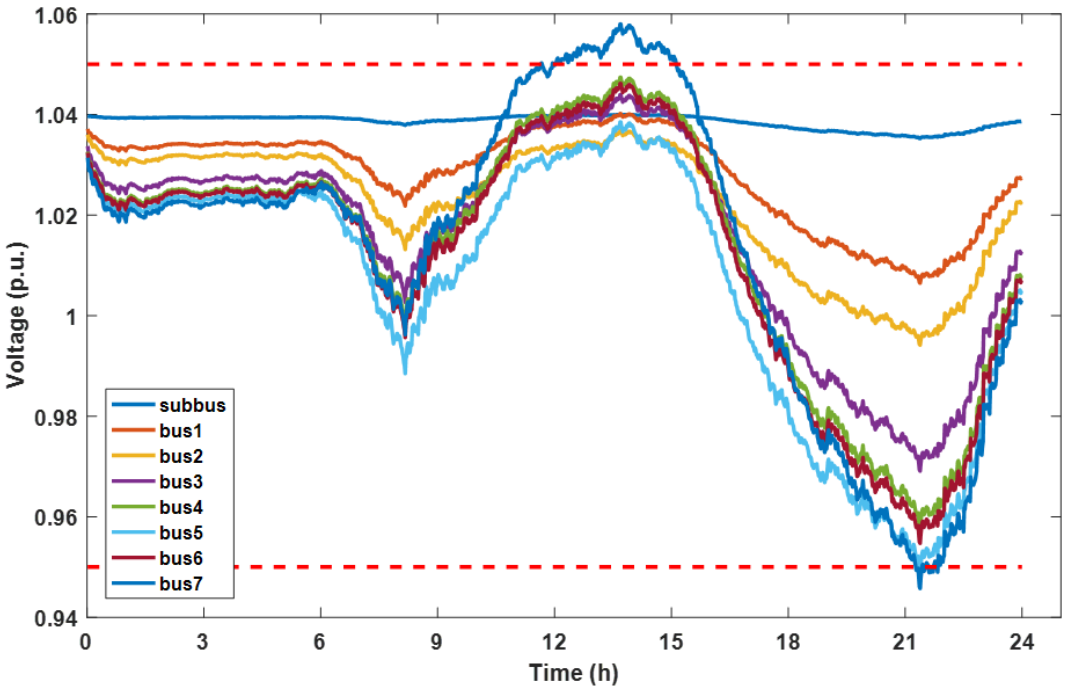

Figure 5.13: Feeder voltage profile without control - case 3

of occurrence of overvoltage, seen in Figure 5.13, a charging operation is activated for BES_9. BES_9 is the most effective BESS to handle the overvoltage situation, as nominated by the SE. BES_{10} is activated around the 13.5th hour when BES_9 is found not to be able to handle the voltage excursion.

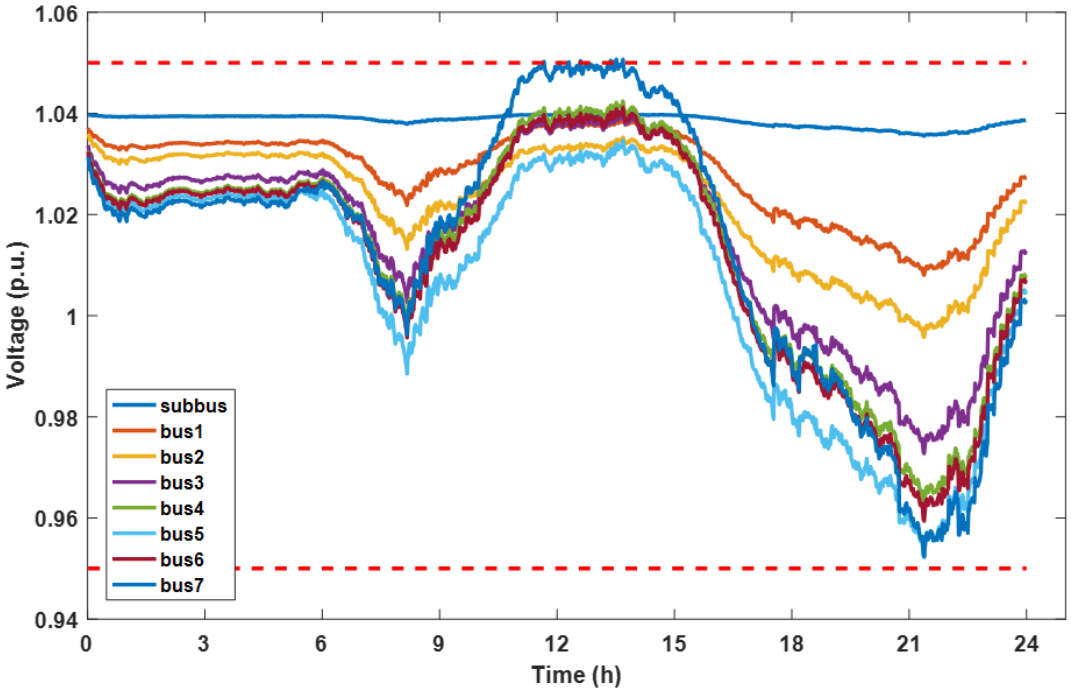

Figure 5.14: Feeder voltage profile with FSSS - case 3

During periods of high demand on the network, both charged BESS ($BESS_9$ and BES_910) discharge to ease the loading stress on the network. It can be seen that undervoltage, which was shown in Figure 5.13 does not occur. However, since only few BESS on the network charged during the day, then there is actually a chance of recording undervoltage for bus 7 if the loading on the network went above what was recorded. This is because for this level of PV capacity and generation, only few BESS are charged.

The SOCs of the network BESS are shown in Figure 5.15. Only BES_9 and BES_{10} participated in charging and discharging, in response to the needs of the network, given the prevailing conditions.

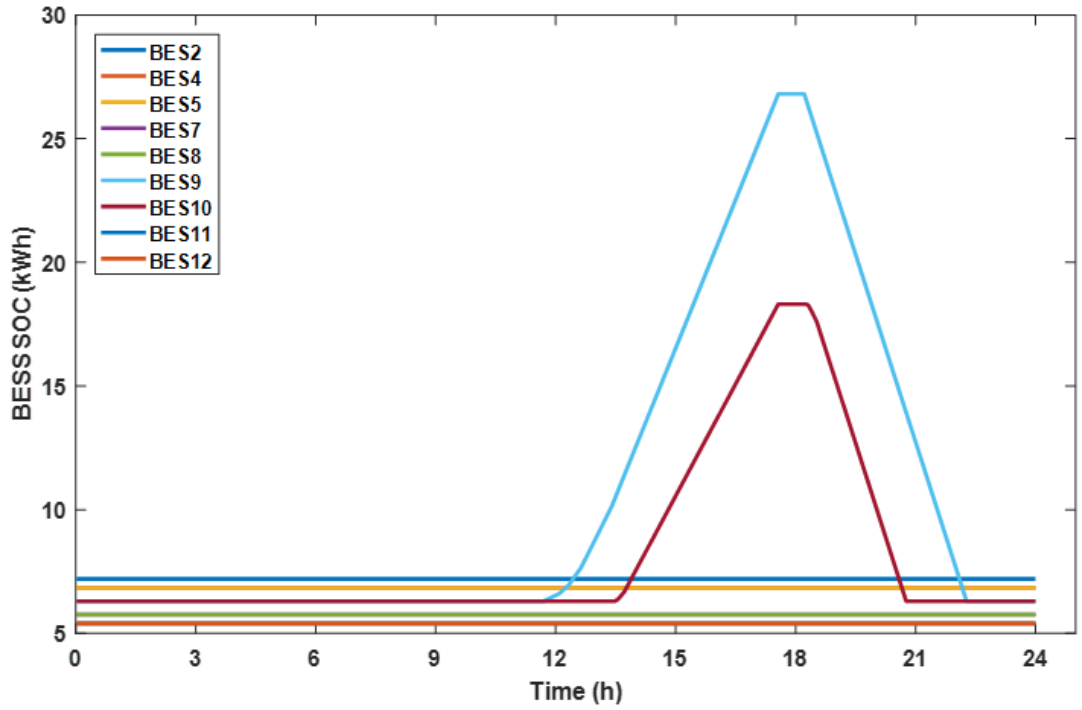

Figure 5.15: SOC of network BESS - Case 3

In Figure 5.16, the power imported from the MV grid is presented, measured at the head of the feeder. Reverse power flow is mitigated, a deviation from the behaviour observed when there was not control on the network.

5.7 Conclusion

In this chapter, an approximate method of voltage sensitivity evaluation was used to obtain a sensitivity ranking matrix, and based on this, a BESS coordination algorithm was developed for use in LV distribution networks with high PV penetration and multiple BESS. The algorithm was demonstrated to be effective in coordinating the selection of BESS for charging or discharging at different times during operation.

The coordination control scheme also successfully mitigated overvoltage on the network during periods of high PV generation and prevented undervoltage from occurring during periods of high load demand on the network. Finally, the scheme

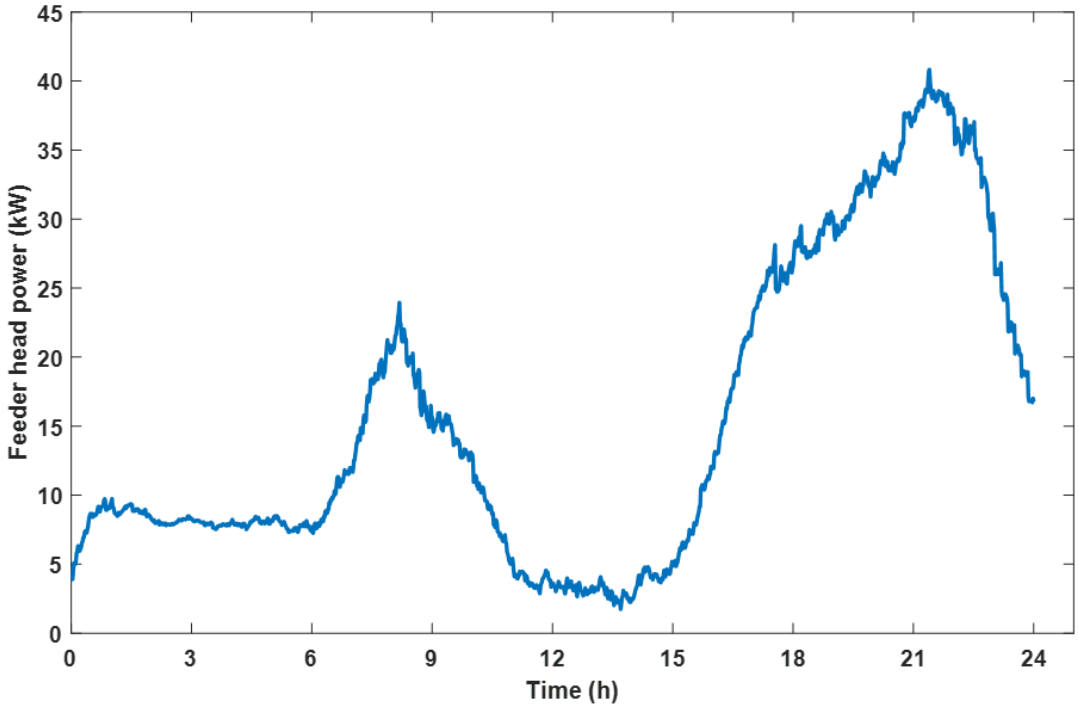

Figure 5.16: Power flows measured at the feeder head - Case 3

was effective in preventing reverse power flows into the MV network and also reducing the power drawn from the MV network. The latter benefits the network by ensuring thermal limits are not exceeded and that infrastructure upgrades are not needed immediately.

Since the method presented in this chapter is based on the voltage sensitivity characteristics of the network, the sensitivity matrix will need to be recomputed and updated in the event of any significant modifications on the network, or if the method were to be applied on a different network.

One of the limitations of this scheme is that there is a high tendency that a particular BESS or a set of BESS are selected first each time as a result of the topology and characteristics of the network. This will lead to such BESS being cycled more frequently, with the consequence being that these BESS will reach their end of life earlier, and therefore require replacements. This adds to the overall cost of having BESS on networks. Possible solutions to this challenge are some of the aims of the

schemes proposed in Chapter 6 of this thesis.

Chapter 6

Neighbourhood-based coordination schemes

6.1 Introduction

This chapter presents the neighbourhood schemes proposed in this thesis for the coordination of multiple BESS in distribution networks with high PV penetration. The chapter begins with some context which includes some limitations of the FSSS presented in Chapter 5. Uniform neighbourhood participation scheme (UNPS) is presented next, including discussion on the need for network segmentation. This is followed by the presentation of the rotational neighbourhood participation scheme (UNPS). The implementation of both schemes on a test network is carried out and results from simulations are presented. An evaluation for the lifetime performance of BESS using each of the schemes was carried out, and results were compared. The chapter ends with a conclusion on the major findings.

6.2 Context and presentation of problem

The cost of BESS is the major limitation to increased installations on power networks. It is therefore necessary that initial cost of installation be justified, as well as delaying, as much as possible, any future replacement costs. Because the length of life of the battery is a function of the way it is operated during its lifetime, it then follows that the systematic operation in a manner to promote good health and prolong the lifetime, while satisfying the technical aims of installation of BESS, is an important objective.

One common scenario encountered in networks with BESS installations is where, due

to network topology and structure, BESS connected to certain buses end up being cycled more frequently than others, as a result of their locations. Such BESS therefore reaches end-of-life quicker, thereby subjecting owners and operators to replacement costs, while some other BESS are not being put to use as much. Such replacements do not benefit from the advantages of economy of scale, among other undesirable consequences. In Chapter 5 where the FSSS was presented, it was observed that the FSSS design is prone to this type of limitation.

The challenge of unbalanced cycling as a result of network topology, and other factors that result in wildly disproportionate cycling across multiple BESS in the same network, is what the two neighbourhood-based coordination schemes presented in this chapter aim to address. The schemes are the uniform neighbourhood participation scheme (UNPS) and the rotational neighbourhood participation scheme (RNPS). The methodology, operations and implementation of both schemes are provided in the rest of the chapter. The results from simulations are also presented and discussed along with the concluding remarks.

6.3 Uniform neighbourhood participation scheme

In this scheme, the network is segmented into BESS operational zones. The BESS in each zone operate in a cooperative and uniform manner to respond to events within the zone with charge and discharge operations as required. The sensitivity method introduced in Section 5.3.1 is applied to determine the charge and discharge rates of the BESS for any active zone. A zone becomes active when the voltage on any bus in the zone exceeds the defined thresholds. This means that more than one zone can be active at any time. Zonal neighbours (ZN) are zones configured with the ability to respond to distress signals from each other, when the source zone for the distress is unable to sufficiently deal with the undesirable event. Every zone therefore possesses a hierarchical set, Z_{nbr}, that contains a list of every zone that it shares zonal neighbourhood with. The hierarchical structure of Z_{nbr} means that the first zone in the

set is given priority appointment to attempt to resolve the distress. Only after the first element in Z_{nbr} is unable to resolve the problem is the second zone appointed, then the third, and so on. For example, the zonal neighbourhood set for zone B in a network is given by

$$Z_{nbr|B} = [D, C, A, E] \tag{6.1}$$

Zone D is the priority zone to respond to distress signals from zone B when the BESS in zone B are not sufficient to resolve the problem, followed by zone C, zone A and then zone E.

6.3.1 Network segmentation

Network segmentation has been used for various applications in power systems. One of the applications is in utility planning procedures, such as load deliverability assessment. In [116], a set of metrics for the quality of zones were laid out. Definition for zones should reflect high level of electrical connectivity. Zonal boundaries were defined for the network using three methods. Hierarchical clustering, which employs a bottom-up approach or agglomerative approach was utilised. This works by linking two clusters that have the smallest distance apart. The process is run iteratively, with each iteration yielding one less cluster than the previous step. This continues until the entire network is grouped under one cluster, or until a cut-off value is encountered. Typical cut off values are maximum number of clusters, maximum/minimum distance and maximum distance. Another method of zonal segmentation is the K-means and spectral clustering. K-means clustering, unlike the hierarchical clustering, uses a top-down approach. The algorithm begins with the entire network and divides it into K clusters in such a way that the within cluster sum of squares is minimised [117]. The third method for segmentation is the use of genetic algorithm. In [118], a

conventional graph partitioning was combined with an evolutionary algorithm to partition a power network to obtain segments based on electrical distances, cluster sizes, number of clusters and connectednes of clusters. For the purpose of voltage assessment, network segmentation was implemented in [119–121].

Some metrics used for evaluating the performance of network segmentation include clustering tightness index (CTI), cluster count index (CCI), cluster size index (CSI) and cluster connectedness (CC). These metrics are combined to form the overall evaluation metric. CTI measures the within-cluster electrical proximity of the buses in each cluster. CCI measures the proximity of the number of clusters in a given clustering to an exogenously provided ideal number of clusters. CSI, on the other hand, measures the extent to which the cluster sizes deviate from the ideal cluster sizes. CC is an evaluation of the connectedness of all the buses on the same cluster. In the study in [116], a binary representation was used for CC, with a value of 1 when all the buses within a cluster are fully connected, and a 0 when the buses are not fully connected.

The segmentation of the network into zones for the implementation of the neighbourhood scheme considers the electrical distances between the buses. With the increase in the length of the lines between buses comes a corresponding increase in the resistance between them.

The sensitivity values for buses electrically closer to each other are higher than that for buses that are farther apart, and therefore can more easily affect the voltages of each other. When using BESS active power for voltage control in the neighbourhood scheme, the aim therefore is to minimize the distances between the participating BESS in each zone. Areas of the network with shorter line distances apart are likely to be placed in the same zone while longer line distances are likely to form inter-zone boundaries. For implementation of the ZN feature, zones with shorter inter-zonal distances are likely to belong to the same zonal neighbourhoods. Segmentation of the test network used to demonstrate the scheme is shown in Figure 6.1.

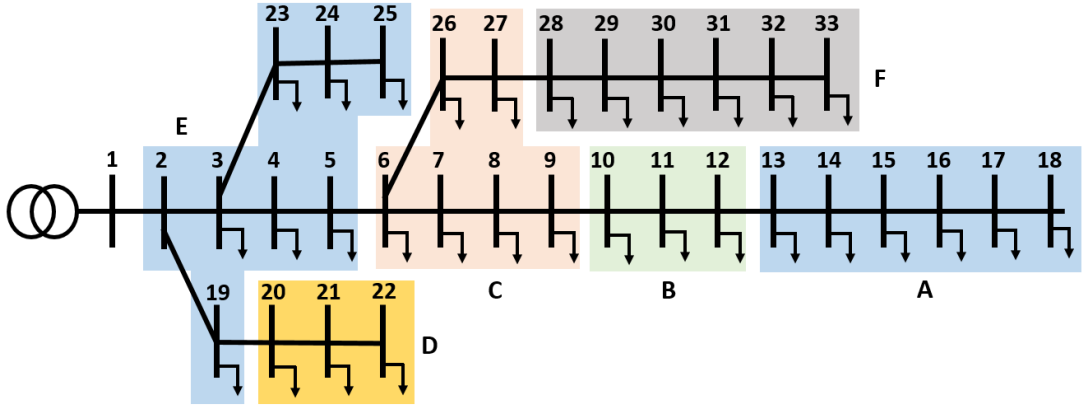

Figure 6.1: IEEE 33-bus distribution network

6.3.2 Operation of the uniform neighbourhood participation scheme

Let the network be segmented into ϕ zones, where $\phi = A, B, C....$ Each zone can contain any number of BESS, depending on unique network features considered during segmentation, described in Section 6.3.1. Let the number of BESS in each zone be $1, 2, 3 \ldots K$, so that if zone A and B, for example, have 4 and 5 BESS respectively, then the zones will be:

$$A = [A1, A2, A3, A4]; B = [B1, B2, B3, B4, B5] \tag{6.2}$$

Z_{sel} is a set of all active zones and is updated at every time step of operations. The scheme switches the BESS into charge or discharge operation mode for any zone when the condition $V_{LTH} \leq V_m \leq V_{UTH}$ ceases to remain true for any bus in the zone. This means overvoltage or undervoltage on a single bus switches all the BESS in the zone from where the signal was sent. The BESS charge and discharge rates change in a uniform fashion until the distress signal discontinues. The algorithm also updates the Z_{nbr} for each zone according to availability at any given time. The Z_{nbr} is used when

distress signal persists in an operational zone, even when all the participating BESS in the operational zone are charging or discharging at maximum possible rates. When this happens, the first zone in Z_{nbr} for the zone in question is checked for availability and then appointed if available. If unavailable, the second zone in Z_{nbr} is checked, and so on. The newly-appointed zone is added into the Z_{sel} set. The zone goes into operation, despite the condition $V_{LTH} \leq V_m \leq V_{UTH}$ not violated on any of the buses in its zone.

6.4 Rotational neighbourhood participation scheme

The rotational neighbourhood participation scheme (RNPS) is a hybrid combination of the FSSS and UNPS. Like the UNPS, the segmentation of the network into zones, described in Section 6.3.1 is maintained; and like the FSSS, within each active zone, the BESS charge and discharge in turns, and not necessarily uniformly. Section 6.4.1 further describes other features and operations of the RNPS.

6.4.1 Operation of the rotational neighbourhood participation scheme

In the RNPS, the BESS in each zone also belong to the same neighbourhood and only respond to events within the zones, except in cases where the Z_{nbr} is used to appoint a neighbour zone as a result of an active zone not being able to deal with events independently. BESS in the active zone are added to BES_{sel}, one at a time, depending on the severity of the event. The gradual addition of BESS in a zone to the BES_{sel} is similar to that seen in the FSSS. In other words, only the number of BESS required to make $V_{diff} = 0$ at every bus in the zone are sequentially added to the BES_{sel}. A unique feature of the RNPS is the use of a rotation array (RA) for charging and discharging operations in the zones. Each zone has two RAs; RA_C for charging operations and RA_D for discharging operations. The RA is the tool used by the RNPS to mitigate disproportionate cycling among BESS in any zone.

Each of RA_C and RA_D for each zone contains all the BESS in the zone, in the order to be followed for charging or discharging operations. The first BESS in RA_C and RA_D are the ones to respond to any charge or discharge signals respectively, received at any bus in the zone. This is followed by the second BESS in the RAs when the first is unable to make $V_{diff} = 0$, as a result of insufficient available capacity or persistence of distress signal despite charging or discharging at maximum rates. The third, then fourth, and so on, are subsequently appointed following same rules. Once a BESS has been added to BES_{sel}, the RA is updated with the same BESS moved from the first to the last position in the rank, while other BESS move up one step in the rank. This sequence is the same for RA_C and RA_D.

For example, $RA_{C|B}$ is the rotation array for charging operations in zone B and contains the BESS in zone B, in the order in which they will respond to charge signals. On receipt of a charge signal on any bus in zone B, $BESS_{B1}$ is added to B_{sel} and at the same time, moved to the last rank position in $RA_{C|B}$, which is then updated as presented in (6.3).

$$RA_{C|B} = \begin{bmatrix} BES_{B1} \\ BES_{B4} \\ BES_{B5} \\ BES_{B2} \\ BES_{B3} \end{bmatrix} ...to.. \begin{bmatrix} BES_{B4} \\ BES_{B5} \\ BES_{B2} \\ BES_{B3} \\ BES_{B1} \end{bmatrix} \tag{6.3}$$

$BESS_{B4}$ becomes the next BESS to respond to charge signal from Zone B, and this happens when $BESS_{B1}$ is fully charged or B1 is unable to bring $V_{diff} = 0$ operating alone. A similar sequence is maintained in $RA_{D|B}$. Note that in $RA_{D|B}$, the BESS can be ranked in an order different from $RA_{C|B}$, but must contain the same BESS as $RA_{C|B}$. The rotation of the BESS within the RA ensures that the charge/discharge responsibilities are evenly distributed among the participating BESS when assessed

over a long period of time, such as during their entire lifetime.

6.5 Implementation of uniform neighbourhood participation scheme

6.5.1 Case study network description

The hypothetical IEEE 33-bus distribution network [122] is used for the implementation of the UNPS and RNPS. The network was developed in OpenDSS while the algorithm implementation was built in Python. The COM interface of the OpenDSS was used for connecting Python to the OpenDSS model. The substation voltage is $12.66kV$ with total load demand of 3715 kW. Each bus of the network has PV installation of $70kWp$ with co-located BESS of $50kW/50kWh$. This network is shown in Figure 6.1. Following the segmentation considerations described in Section 6.3.1, the network is segmented as shown in Figure 6.1. The load and generation profiles created in Section 5.5.3 are used as multipliers on the actual loads and PV respectively. The voltage at the feeder head is set at $1.05pu$. The BESS are named both according to their operational zones and the bus number to which they are connected. The bus number follows the zone identifier in this naming convention. For example, the BESS in zone A are named as follows:

$$[BES_{A13}, BES_{A14}, BES_{A15}, BES_{A16}, BES_{A17}, BES_{A18}] \tag{6.4}$$

The zonal neighbourhood sets for zones A and B, which are the zones used for illustration of the scheme, are: $Z_{nbr|A} = [B, C, E]$ and $Z_{nbrA|B} = [A, C, E]$.

6.5.2 Simulation results of UNPS

Simulations were run for an entire day with a 1- minute resolution. The simulation was initialised with $SOC = 100\%$ for BES_{A18}, in order to capture the variations

that might be encountered in real operations where a BESS does not have capacity for charge prior to periods of high PV generation. Voltage profile of the network with UNPS in operation is shown in Figure 6.2. Voltage violation ($V_{m18} > V_{UTH}$) occurs in zone A at about the $12th$ hour at bus 18 and the zone is switched to charge mode. Without the control in place, this overvoltage event will persist. The BESS in zone A charge uniformly, with charge rates determined by the magnitude of V_{diff} on the overvoltage bus. Figure 6.4 shows the SOC of the BESS in zones A and B. The SOC for each zone can be seen varying uniformly throughout the duration of the simulation. In the evening during periods of high loading on the network, the BESS are switched to discharge mode. Around the $22nd$ hour, zone A BESS become fully charged, even though there is still need for maintaining the voltages in zone A within the set range. The algorithm, at this stage, uses $Z_{nbr|A}$, (the zonal neighbourhood set for zone A) to appoint a neighbour zone that switches into operation for the purpose of maintaining voltages. Zone B is the first element in Z_{nbr} and is appointed. As seen in Figure 6.2, zone B's BESS ($BES_{B10}, BES_{B11}, BES_{B12}$), start discharging at about the same time that zone A BESS become fully charged (around the $22nd$ hour).

6.6 Implementation of rotational neighbourhood participation scheme

The same network, zone segmentation, load and generation profiles used in 6.5 are also used in this section for the demonstration of the operations of the RNPS. To demonstrate the rotational sequencing of the BESS using the RNPS, zone A will be focused on for simplicity. Behaviours in other zones of the network will be similar to zone A's. The initial RAs for zone A are given by

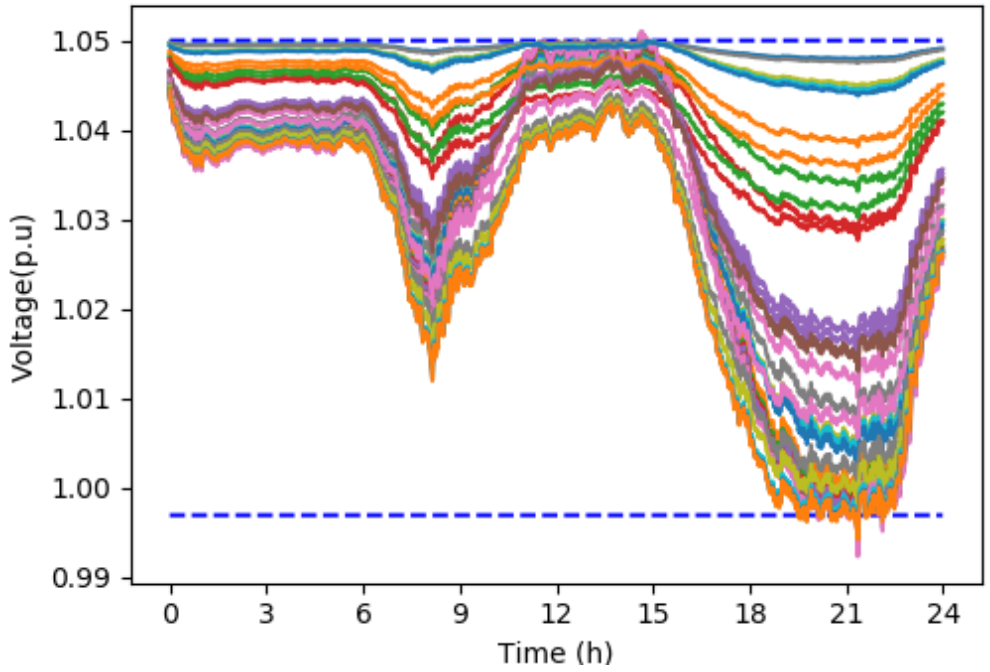

Figure 6.2: Feeder voltage profile with UNPS

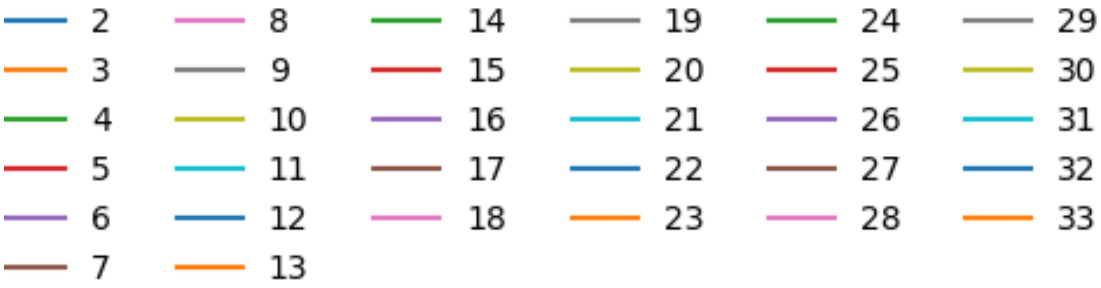

Figure 6.3: voltage legends

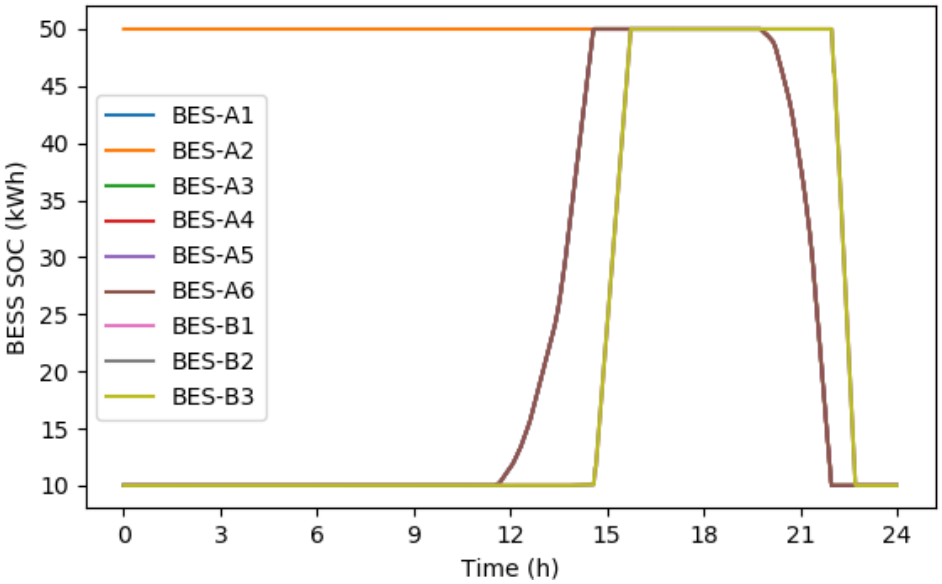

Figure 6.4: SOC of zone A and zone B with UNPS

$$RA_{C|A} = \begin{bmatrix} BES_{A18} \\ BES_{A17} \\ BES_{A16} \\ BES_{A15} \\ BES_{A14} \\ BES_{A13} \end{bmatrix} \quad RA_{D|A} = \begin{bmatrix} BES_{A17} \\ BES_{A18} \\ BES_{A16} \\ BES_{A15} \\ BES_{A14} \\ BES_{A13} \end{bmatrix} \tag{6.5}$$

Observe that in 6.5, BES_{A17} and BES_{A18} are swapped in $RA_{C|A}$ and $RA_{D|A}$. Also, the initial SOC values of the BESS in zone A are 20% (minimum SOC), except BES_{A17} which starts at 100%. These have been done for initial conditions, to ensure that the there is discharge availability at the start of the operation.

6.6.1 Simulation results of RNPS

Figure 6.5 shows the voltage profile of the feeder with the RNPS in operation. The legend and colour schemes are the same as those used in Figure 6.2. As PV power generation increases, bus 18 at the end of the feeder is the first to have its voltage exceed the upper threshold ($V_{m18} > V_{UTH}$) around the 12th hour. BES_{A18} is switched to charge mode, being the top ranked in $RA_{C|A}$. Figure 6.6 shows how the orders of the BESS are changing as their SOC change. A zoomed-in view is presented in Figure 6.7 for clearer details. The magnified area is indicated by the block dotted oval on Figure 6.6. Rank 6 in the figure represents the position with the highest priority for charging while rank 1 represents the lowest priority.

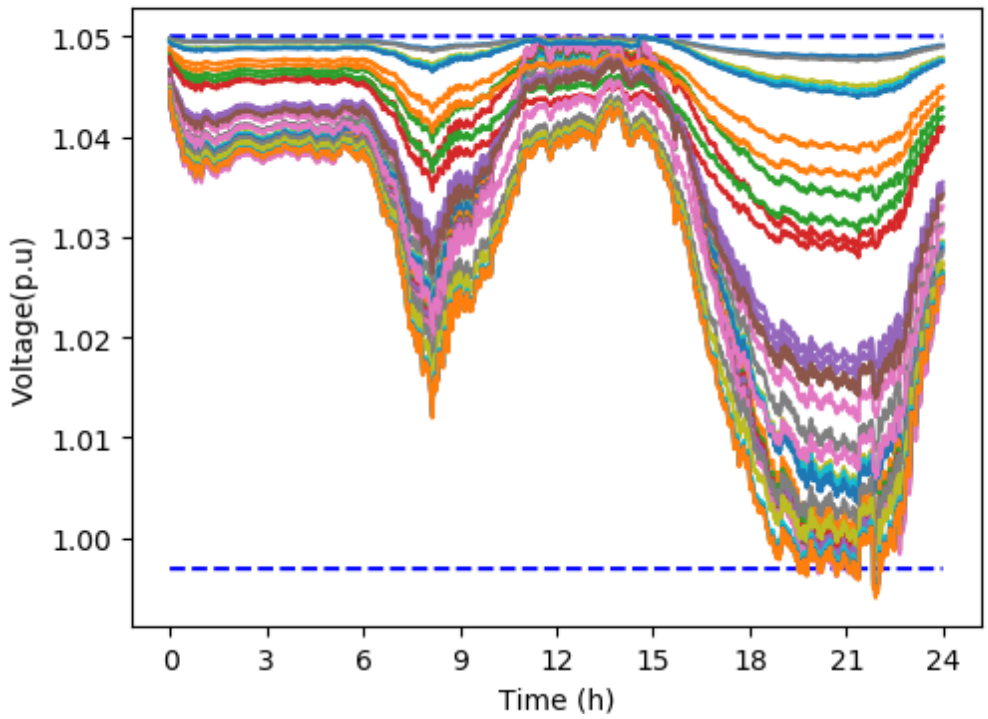

Figure 6.5: Feeder voltage profile with RNPS

When BES_{A18} reaches maximum SOC, it is moved to the bottom of $RA_{C|A}$ and other BESS in the set move up one step. The new highest-ranked BESS becomes

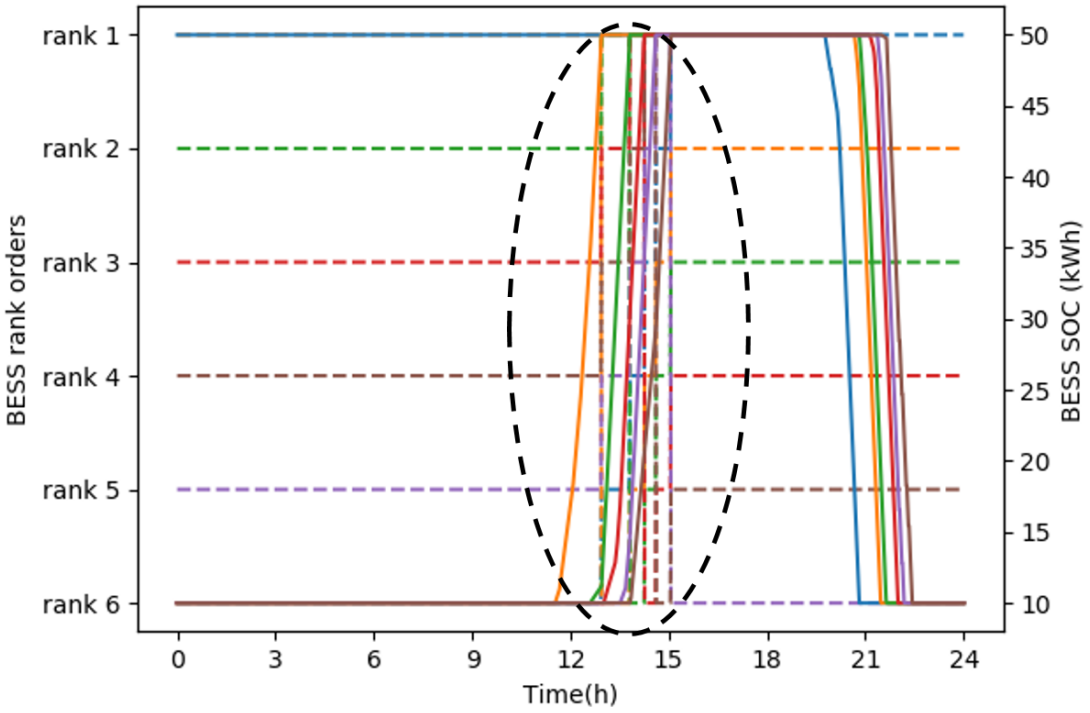

Figure 6.6: Rotational order and SOC at zone A

BES_{A16} because the algorithm detects that BES_{A17} is fully charged (from initial settings), moves it to the bottom of the set and makes BES_{A16} the priority for charging. The BESS are brought to charge sequentially according to the ranking in $RA_{c|A}$ until a signal for discharge is received around the 20th hour. $BESS_{17}$, being the highest-ranked in $RA_{D|A}$ is the first to start discharging. The other BESS in the zone follow according to their positions on $RA_{D|A}$.

Around the 14th hour, a situation arises where all the BESS in zone A are either fully charged, or charging at maximum rates but not able to mitigate the distress signal. The algorithm uses the Z_{nbr} of zone A, which has zone B as the first element, to solve the problem. BES_{B12} is switched to charging, followed by BES_{B11}. The voltage along the feeder is maintained during the period of high PV generation and high network loading. Two possible objectives could be set as target for the BESS discharge – a power threshold at the secondary of the substation or undervoltage at the buses. The latter has been used in this simulation and was set at $0.999Vp.u.$

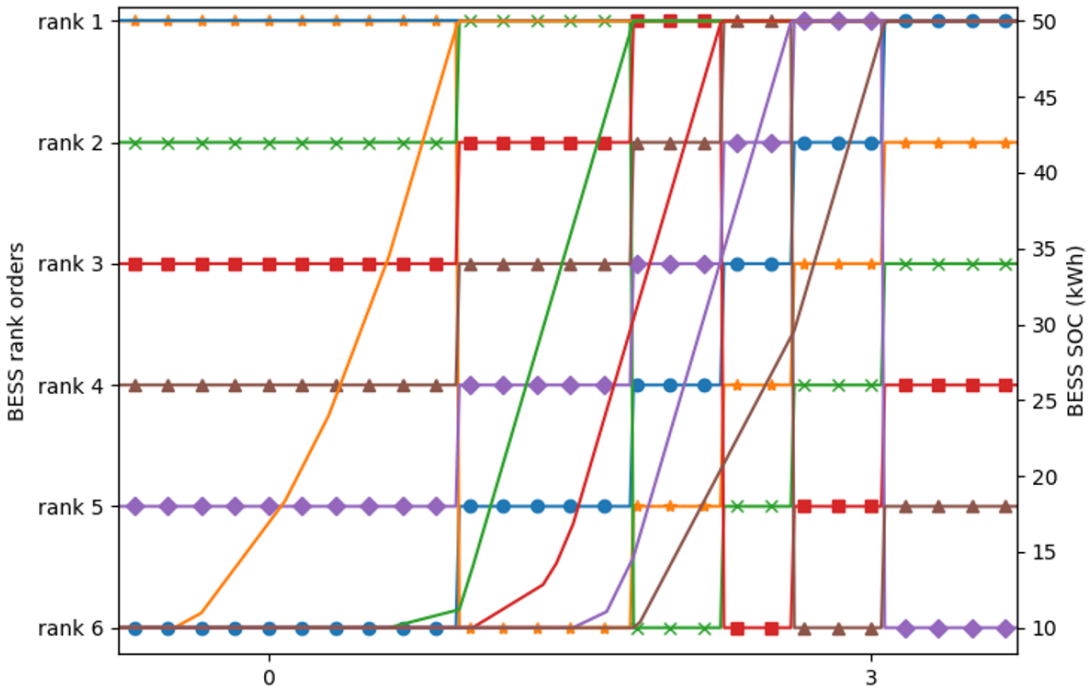

Figure 6.7: Zoomed-in rotational order and SOC at zone A. Rank 6 in the represents the position with the highest priority for charging, while rank 1 represents the lowest priority

Legend for the rotational orders. The shapes represent, from left to right, BES_{A18}, BES_{A16}, BES_{A15}, BES_{A14}, BES_{A13} *and* BES_{A17}.

6.7 Evaluation of performance of neighbourhood schemes

In this section, the UNPS and RNPS will be evaluated for performance. The objective of both schemes was to cycle the BESS in such a way that lifetime is prolonged. Therefore, performance evaluation is carried out by estimating the remaining useful life of the battery after a specified long period. This is synonymous to estimating the time duration before the end of life of the battery. A few concepts around battery lifetime evaluation will be presented, followed by the methodology chosen in this work.

6.7.1 Battery lifetime degradation

For BESS deployed in power networks, a trade-off has to be made between the availability of the BESS to provide power whenever needed, and concerns over the lifetime duration of the BESS. Two major factors affecting the life of the battery are the number of cycles-to-failure of the battery and the fractional depth of discharge (DOD) during cycling. A full cycle occurs when the battery's DOD has returned to the same point it was before the commencement of discharge and charge operations.

Battery life can be modelled with the assumption of nominal lifetime. This assumption is too simplistic and does not nearly capture the effects on the battery as a result of the manner of operation and cycling of the battery during the life of the battery. For the life of the battery to be modelled to a better degree of accuracy, considerations must be given to the irregular and overlapping charge and discharge cycles with variable depths. Such scenarios are common where BESS is used in applications involving PV systems, which are characterised by high variability. For example, a shallow cycle might be immediately followed by long deep cycles. A battery life estimation model that considers this irregularity in cycling adopts Miner's rule [123]. Miner's rule has been popularly implemented in the "Rainflow Counting" algorithm. The rainflow

counting algorithm was initially used to identify individual stress cycles in a given time-series history of irregular stress cycles in metal fatigue analysis [124]. This method has also been used in electronics and in power engineering for evaluations such as the estimation of semiconductor lifetime [125, 126]. Other applications for BESS lifetime estimation are reported in [127, 128].

Since battery life is a function of the depth of charge/discharge cycles, battery lifetime can be based on the empirical curves that relate the number of cycles to battery failure as a function of the magnitude of the depth/magnitude of the curves. The double exponential curve fit presented in (6.6) gives this relationship.

$$C_F = a_1 + a_2 e^{a_3 R} + a_4 e^{a_5 R} \tag{6.6}$$

where C_F is the number of cycles to failure, a_1, a_2, a_3, a_4, a_5 are fitting constants, and R is the fractional depth of discharge (see Figure 6.8). This curve is often obtained from empirical methods. Values in literature, [60], for fitting constants that apply to a suitable valve-regulated lead-acid battery are presented in (6.7) .

$$C_F = 12500 e^{-0.1158R} + 2070 e^{-0.01537R} \tag{6.7}$$

During a charge/discharge cycle, the fraction of life used up is $1/C_F$. If the cycling continues, a point is reached where these multiple fractions sum up to 1.0. At this point, the BESS is considered to be dead and replacement is required. Suppose there are n total number of cycles with N_i cycles to k different fractional DODs. If there corresponds a number of cycles to failure $C_{F,i}$ to each of these discharge depths, then the total factional damage to the battery by the cycles under consideration would be estimated by (6.8). When the partial cycles have been determined, the total degradation

of the battery can be estimated by (6.8).

$$D = \sum_{i=1}^{k} N_i \frac{1}{C_{F,i}} \tag{6.8}$$

6.7.2 Simulation for battery lifetime

For the performance evaluation carried out for the UNPS and RNPS, yearly simulations were run on the test network. The purpose of the year-long simulation is to observe how each of the schemes performs over a long period of time when the same BESS on the same network are exposed to similar network conditions (demand and generation). Some modifications were made in order to streamline the focus of this study. The first modification made was the use of generation and demand profiles with a resolution of 1-hour. This differs from the 1-minute resolution profiles used in Section 6.6. This modification was done to reduce the simulation time, since simulation was run for an entire year. The second modification made was the use of fewer number of PV and BESS installations on the IEEE 33-bus network shown in 6.1. The PV and BESS installations on this network, after modification, is presented in Table 6.1. BESS-16, BESS-17 and BESS-18 are grouped in the same Neighbourhood Zone (Zone-1). The load values on the network remain unchanged.

There could exist an infinite number of possible DOD values between 0% and 100%. This will possibly result to a very large number of categories of DOD when the entire simulation period is considered. To avert this, for the purpose of this evaluation, a discrete and finite number of possible DOD bins have been used. The DOD is split into k equally-sized intervals. The bins each cover the same interval size, but could have different number of elements, depending on the number of DOD values that eventually fall within the range covered by each particular bin.

Table 6.1: BESS and PV installation ratings on test network after modifications

Bus ID	BESS name	BESS rating(kW/kWh)	PV(kWp)
Bus 10	BESS-10	50/200	152
Bus 11	BESS-11	50/200	76
Bus 12	BESS-12	50/200	190
Bus 16	BESS-16	60/300	152
Bus 17	BESS-17	60/300	
Bus 18	BESS-18	60/300	152
Bus 31	BESS-31	60/200	266
Bus 32	BESS-32	60/200	152
Bus 33	BESS-33	60/200	76

A plot of (6.7) for values of DOD between 0% to 100% is presented in Figure 6.8. The curve show the relationship between the DOD and the number of cycles to failure of the BESS for each DOD.

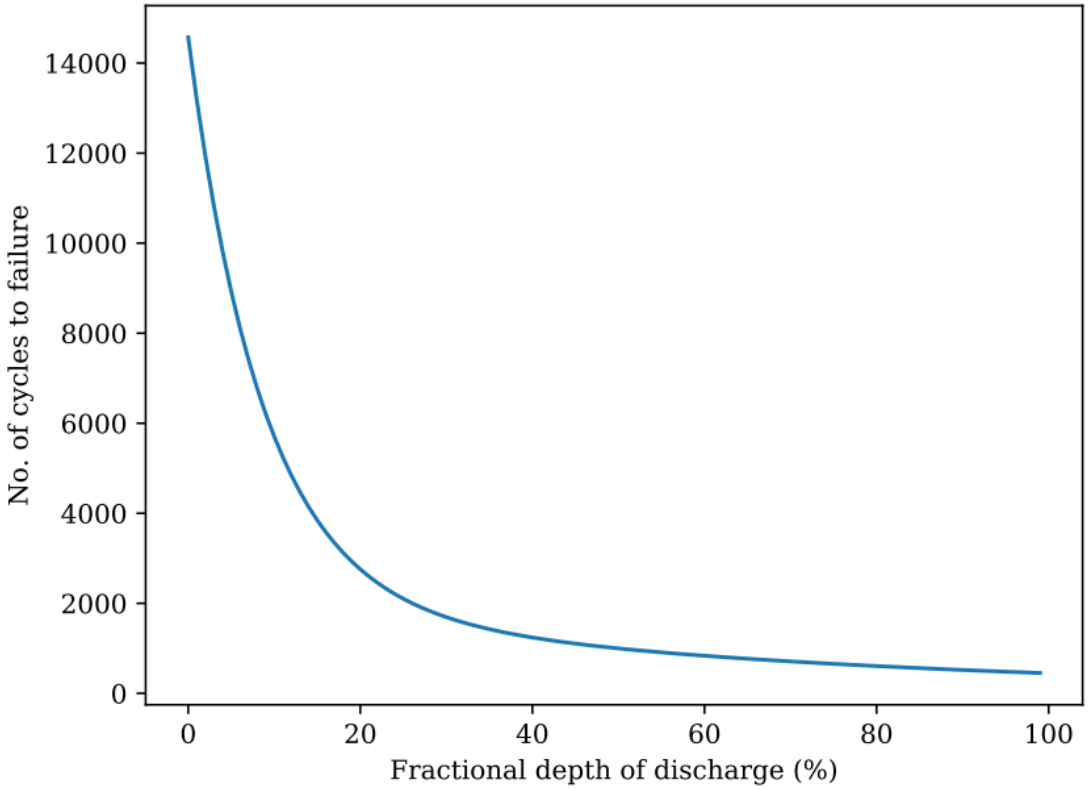

Figure 6.8: Curve showing the relationship between number of cycles to failure and fractional depth of discharge

6.7.3 Evaluation for UNPS

The evaluation carried out for the UNPS is focused on Zone-1. The UNPS operates by making the BESS in each zone to charge and discharge uniformly according to the demands of the network at different times. Since the BESS in zone-1 have the same rating for maximum capacity (kWh) and maximum charge/discharge power (kW), the SOC of the BESS are approximately the same.

The BESS in this zone are rated 300kWh, with rated maximum charge/discharge power of 60kW. The state of charge constraints for the BESS for the year-long simulation is $20\% \leq SOC \leq 100\%$. Load and generation profiles are at 1-hour intervals, which gives a total of 8760 simulation time steps. The rainflow algorithm was used to collect the different depths of charge/discharge cycles. Table 6.2 presents the different cycle depths identified.

DOD values were grouped into categorical bins, so that there is a finite number of categories of depth of discharge. The size of each bin is a range of 3, as shown in the "Range" column of Table 6.2. The ranges start from $[0, 3], [3, 6], ..., [237, 240]$. The maximum of 240 is as a result of the constraint on maximum DOD of 80% ($20\% \leq SOC \leq 100\%$). The ranges that do not appear in the table are the ones that did not occur during the period of operation of the BESS. Table 6.2 shows that there were more deep cycles (represented by $DOD = 80\%$), than other shallower cycles. A plot of the frequency of the different DOD for the UNPS is presented in Figure 6.9.

Applying (6.8) to the data, the total fractional damage at the end of the year for BESS in Zone-1 is 0.257. This implies that it will take approximately $\frac{1}{0.257} = 3.89$ years before these BESS are to be replaced, under the specific network conditions that they are being used.

Table 6.2: Frequency of different depths of discharge for the BESS in Zone-1, operating under UNPS

Range	Cycle counts	DOD (%)
(57, 60]	1	20
(78, 81]	1	27
(81, 84]	1	28
(90, 93]	1	31
(93, 96]	1	32
(96, 99]	4	33
(99, 102]	1	34
(102, 105]	4	35
(105, 108]	6	36
(108, 111]	7	37
(111, 114]	3	38
(114, 117]	3	39
(117, 120]	7	40
(120, 123]	9	41
(123, 126]	8	42
(126, 129]	8	43
(129, 132]	3	44
(132, 135]	38	45
(141, 144]	1	48
(198, 201]	25	67
(213, 216]	4	72
(237, 240]	99	80

6.7.4 Evaluation for RNPS

For evaluating performance under RNPS, BESS in Zone-1 were examined, so that the results can be compared to those obtained from evaluation of UNPS. The RNPS has Zone-1 BESS taking turns to charge and discharge in a rotational fashion. Therefore, the cycling of the BESS are not uniform and will vary according to the requirements of the network at different times. The cycles of each BESS in Zone-1 are analysed separately, and the lifetime performances are presented.

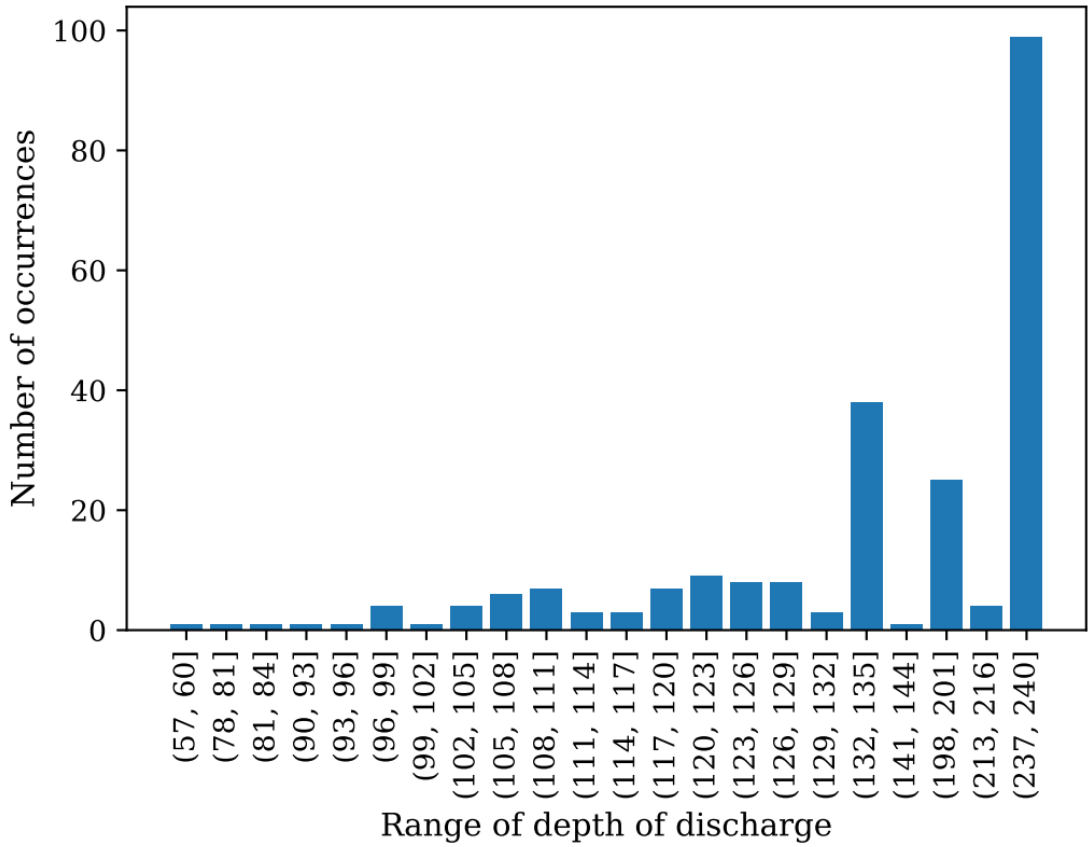

Figure 6.9: The distribution of frequency of different depths of discharge identified through the rainflow algorithm for UNPS

6.7.4.1 BESS-18

BESS-18 is the BESS located on the 18th bus of the IEEE 33-bus network. This bus is an end node and therefore is very susceptible to overvoltage during times of high PV power generation. Table 6.3 presents the different DOD for BESS-18 when operating under RNPS.

Table 6.3 shows that there are more cycles at full depth (80% DOD) than other discharge depths. This data is presented in the bar graph in Figure 6.10.

Using the identified DOD and applying (6.8), the total fractional degradation of BESS-18 after operating for a year is 0.203. The implication of this is that if BESS continues to operate with the RNPS under similar network conditions, it will take

Table 6.3: Frequency of different depths of discharge for the BESS-18 in Zone-1, operating under RNPS

Range	Cycle counts	DOD (%)
(12, 15]	13	5
(21, 24]	13	8
(24, 27]	12.5	9
(48, 51]	0.5	17
(57, 60]	1	20
(96, 99]	4	33
(99, 102]	1	34
(141, 144]	12	48
(153, 156]	26	52
(237, 240]	102.5	80

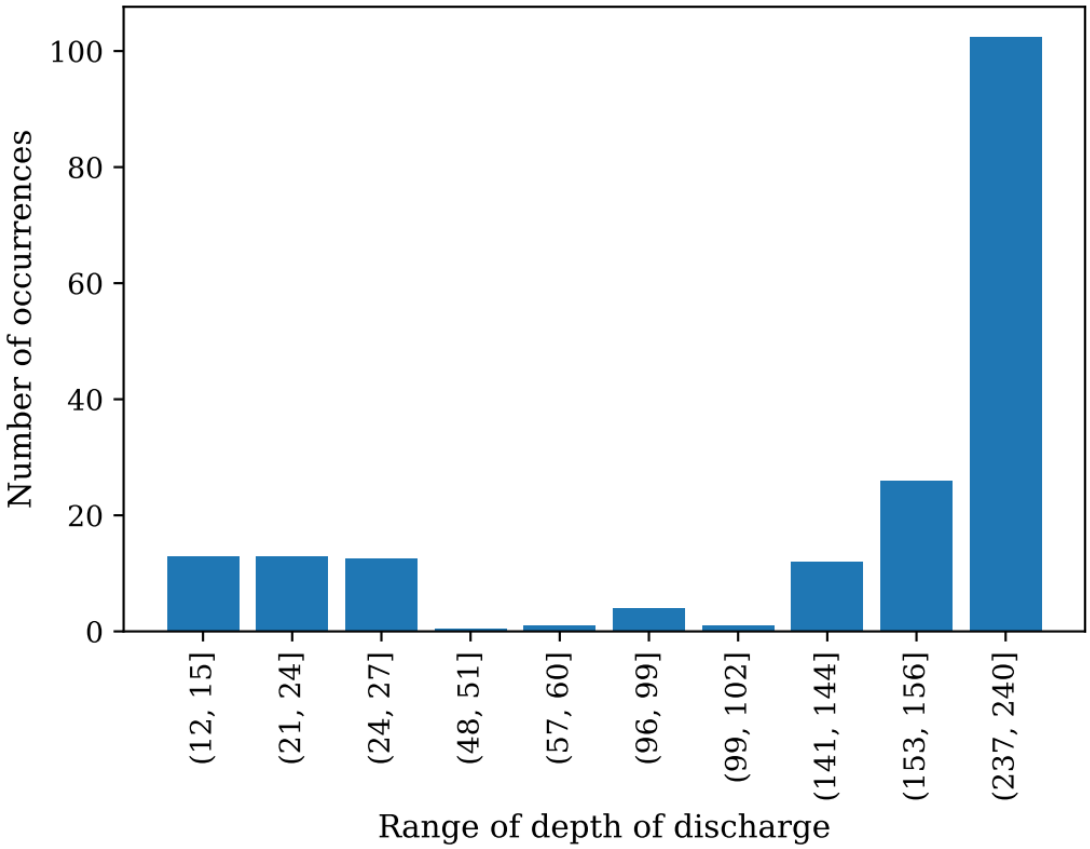

Figure 6.10: The distribution of frequency of different depths of discharge identified through the rainflow algorithm using RNPS for BESS-18 in Zone-1

approximately $\frac{1}{0.203} = 4.93$ years before replacement would be required.

6.7.4.2 BESS-17

BESS-17 is the second BESS in Zone-1, located on the 17th bus of the IEEE 33-bus network. The results of the rainflow counting performed on the various partial cycles of BESS-17 during simulation is presented in Table 6.4.

Table 6.4: Frequency of different depths of discharge for the BESS-17 in Zone-1, operating with RNPS

Range	Cycle counts	DOD (%)
(15, 18]	13	6
(81, 84]	1	28
(96, 99]	4	33
(102, 105]	4	35
(105, 108]	6	36
(183, 186]	1	62
(201, 204]	12.5	68
(207, 210]	13	70
(237, 240]	114.5	80

A significant portion of the DODs fall in the range of [237-240], corresponding to 80% DOD. The bar graph in 6.11 is a visual presentation of the distribution of different DODs for BESS-17.

Applying (6.8) on the identified DODs yield a yearly degradation of 0.23 for BESS-17. This implies that if, over the years, the conditions of demand, PV generation and network parameters remain similar to the ones used for this simulation, the it will take $\frac{1}{0.23}$ = 4.34 years before BESS-17 reaches its end of life.

6.7.4.3 BESS-16

BESS-16 is located on the 16th bus of the IEEE 33-bus network. This is the third and last BESS in Zone-1. The results obtained by counting the cycles of BESS-16 is presented in Table 6.5 while 6.12 presents a visual representation.

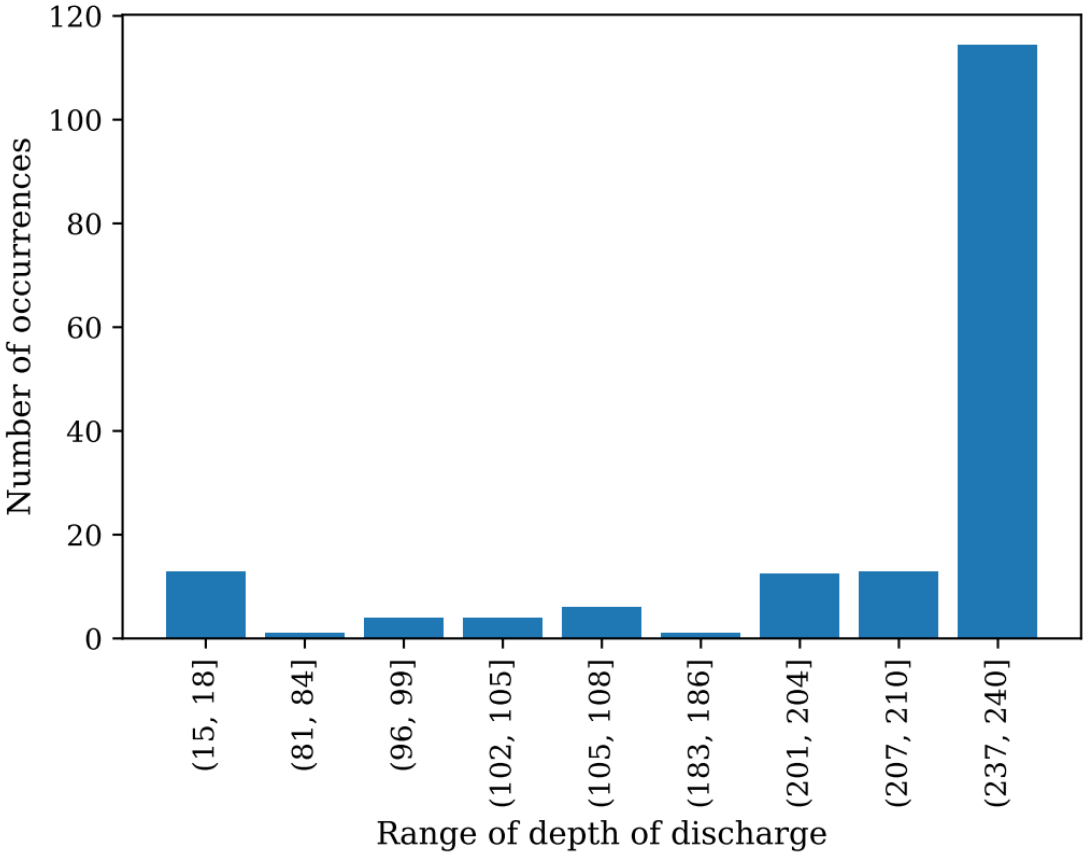

Figure 6.11: The distribution of frequency of different depths of discharge identified through the rainflow algorithm using RNPS for BESS-17 in Zone-1

Table 6.5: Frequency of different depths of discharge for the BESS-16 in Zone-1, operating with RNPS

Range	**Cycle counts**	**DOD (%)**
(9, 12]	12.5	4
(12, 15]	13	5
(30, 33]	13	11
(117, 120]	1	40
(129, 132]	11	44
(159, 162]	13	54
(171, 174]	13	58
(237, 240]	89.5	80

The fractional damage to BESS-16 at the end of the operation year with UNPS is 0.18. This corresponds to a lifetime of 5.55 years before the BESS will have to be replaced, as long as the network and operating conditions do not very wildly over time.

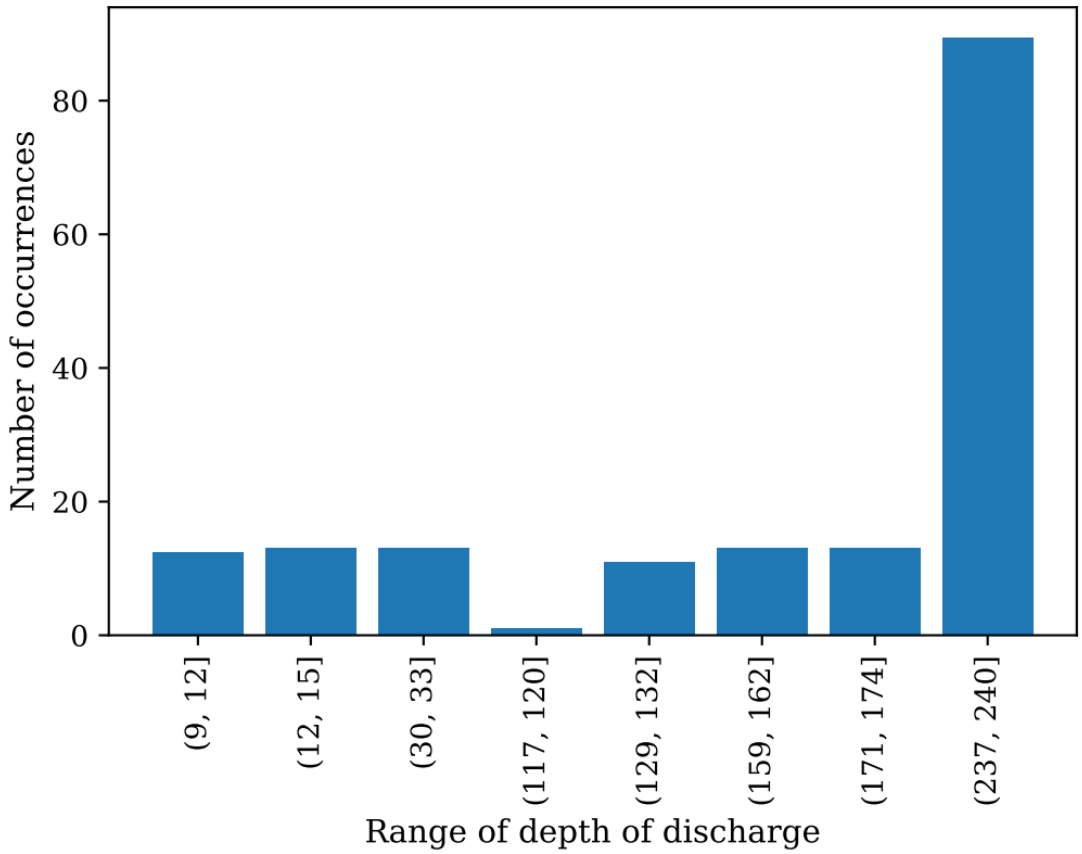

Figure 6.12: The distribution of frequency of different depths of discharge identified through the rainflow algorithm using RNPS for BESS-16 in Zone-1

6.7.5 Comments on evaluation

From the results of the evaluation of UNPS and RNPS presented in Section 6.7.4, the RNPS has a slightly better performance than UNPS in maximising the lifetime of BESS. Most of the DODs are observed to fall close to the maximum possible DOD.

6.8 Conclusion

In this chapter, the uniform neighbourhood participation scheme (UNPS) and the rotational neighbourhood participation scheme (RNPS) were presented. Both schemes require a segmentation of the network into neighbourhood zones. Methods

for segmentation were reviewed and the method used in the implementation was provided. Simulations were carried out using the IEEE 33-bus network and results were presented and discussed.

The UNPS and RNPS differ from the FSSS presented in Chapter 5 primarily because they both require no network segmentation. The BESS in each zone of the segmented network, when using the FSSS, participate in a single objective that is common to the zone. However, the concept of zonal neighbourhoods (ZN) has the zones being able and ready to respond to distress signals from neighbouring zones. This occurs when the distressed neigbouring zone is not able to handle the undesirable situation by itself. Similar pattern as the FSSS is followed by the UNPS, except that for the UNPS, the BESS follow a rotational pattern for operations, according to the rotation array (RA) for the zone.

A performance evaluation was carried out for the UNPS and RNPS and results obtained showed that UNPS performed better than the RNPS, for the network conditions that were considered in the simulation. Overall, the results show that both schemes achieve the purpose of mitigating overvoltage in the network, with the added advantage of systemic cycling that enables the prolonged lifetime for the BESS.

Chapter 7

Conclusions, recommendations and future work

7.1 Introduction

This thesis has presented research on coordination schemes for multiple BESS in networks with high penetration of PV. This chapter summarises the major findings from the research, and highlights the key contributions of the work. The limitations of the work are also discussed, and recommendations for future work are stated.

7.2 Summary of chapters

Chapter 1 introduced the thesis and provided some background on the work. The objectives of the research were stated, as well as the contribution to knowledge the thesis proposes to make. Publications that came out from the research work were presented and the chapter concluded with laying out of the structure that the rest of the thesis follows.

Chapter 2 presented a review of literature relevant to the thesis. The evolution of the network from classic traditional unidirectional power flow structure, to the multi-directional structure of the smart grid. Challenges of the smart grid were discussed, especially technical challenges as a result of penetration of low carbon technologies in the networks. Overvoltage, being one of the major limitations to the higher penetration of renewable generators in the distribution network, was discussed in detail. Ways of mitigating this technical challenge, found in literature, were also presented and a case was made for the use of the BESS in solving this problem.

Methods of coordination of operations of BESS, as found in literature, were presented. The chapter is concluded by identifying the gaps in research, which the research presented in this thesis proposes to solve.

In chapter 3, a study was presented that investigated the potentials of use of BESS and reactive power capability of PV inverters to solve voltage excursion problem. The network considered had a high level of penetration of PV. A combination of BESS for active power and PV power electronics inverter for reactive power on the network helped mitigate overvoltage and reduce the curtailment of active power. A model of the BESS used throughout the thesis was also presented in Chapter 3. Three cases were considered for this work. First, the case with PV but without any controls. The second was the case where BESS was used to mitigate overvoltage but without use of reactive power. The final case employed the use of reactive power, but with fewer BESS installations on the network. The BESS was charged with excess PV generated power during the day and discharged during peak loading periods in the evening.

The focus of Chapter 4 was the scheduling of BESS in networks with high penetration of PV for energy arbitrage. The purpose of the work in this chapter was to bring the other potential benefits of the BESS to light, and to highlight how energy arbitrage could play a part in the economic justification for the installation of BESS. Time-of-use (TOU) electricity tariff, on which the scheme is based, was discussed alongside other tariff systems available. A linear optimisation was set up that optimised the dispatch of the BESS throughout the day. The objective of the optimisation was to minimise the purchase of electricity from the grid during times of high electricity prices and to use stored BESS instead. The program also prioritises the use of PV power charging of the BESS. Results showed that, given favourable TOU profiles, economic gains from the use of the BESS for energy arbitrage can be maximised.

In chapter 5, the new flat structure sensitivity scheme (FSSS) for the coordination of multiple BESS in distribution networks with high PV penetration was presented. This is a contribution of this research. The scheme used the voltage sensitivity of the

buses of the network do implement a charging and discharging scheme for the BESS, for the mitigation of overvoltage on the network. An approximate method was used, which reduces computational complexity of the algorithm when compared to the use of Jacobian matrix. The sensitivity evaluator (SE) was responsible for the ranking of the BESS in order of priority for selection for particular voltage excursion problems. The BESS were monitored during operations, to update their state of charge so that new BESS are appointed in time before the BESS under operation gets fully charged or fully discharged.

The FSSS coordinated the operation of the BESS both for overvoltage and undervoltage conditions. Implementation was carried out on a real low voltage distribution network. Three cases were considered, each case different from the others due to different levels of planned penetration of PV on the network. 100%, 85% and 70% of planned PV penetration levels on the network were examined. Results showed that the FSSS was able to cooridinate the operations of the BESS to mitigate overvoltage and undervoltage on the test network. Import of power from the MV grid was also minimised, especially during periods of high demand.

Chapter 6 built upon the work in Chapter 5 and extended it to consider some of the limitations of the FSSS. Two neighbourhood participation schemes, which are new contributions of this research, were presented, namely: the uniform neighbourhood participation scheme (UNPS) and the rotational neighbourhood participation scheme (RNPS). The objectives of the neighbourhood schemes were to ensure that the participating BESS are cycled in a way that maximises the lifetime of the BESS while achieving the technical objectives of overvoltage mitigation. Splitting up of the network into segments makes the neighourhood schemes possible. The concept of neigbourhood zones was also introduced so that zones found in the same neighborhood zones are able to be activated when the active zone lack sufficient resources to handle distress within the active zone. Both schemes were implemented on a medium voltage distribution network and results showed that the schemes are

able to meet the proposed objectives.

The chapter continued with the evaluation of performance of the UNPS and RNPS with respect to the longevity of the participating BESS. This was implemented by using the rainflow counting algorithm to identify the various DODs. These DODs were subsequently used for evaluating the lifetime of the BESS operating under both schemes.

7.3 Major results and contribution to knowledge

The objectives of this thesis, outlined in chapter 1, included the development of algorithms for the coordination of multiple BESS installations in distribution networks with high penetration of PV. At the end of this thesis, three key schemes were developed in accordance to the thesis statement and objectives of the thesis. These outcomes extend the body of knowledge in this area of research.

Firstly, in Chapter 5, the development of the flat structure sensitivity scheme was presented. This scheme involved the use of an approximate method to reduce possible computational complexity as a result of the use of the Jacobian matrix. The approximate method was then utilised for the selection of BESS and also the calculation of charge and discharge rates of the participating BESS on the network. This scheme is applicable in large networks that have a high number of buses, where increased number of network buses potentially lead to increase in computation time.

Secondly, in Chapter 6, the uniform neighbourhood participation scheme (UNPS) was presented. This scheme insists on the uniform operation of BESS in a given network zone. The uniform participation ensures that BESS are not cycled unevenly. This reduces the frequency of replacement of the BESS on the network. This scheme can be applied in networks where the installed BESS are not very far apart from each other in terms of electrical distance. Another major advantage of this scheme is that benefits from economy of scale can be maximised, since the BESS reach their end of life at

approximately the same time.

Thirdly, in Chapter 6, the rotational neighbourhood participation scheme (RNPS) was presented, whose aim, like the UNPS, is prevention of uneven cycling for the participating BESS, and hence, extension of the time period before there is need for replacement. This scheme has the participating BESS following an order for charging and discharging over the lifetime of the BESS. The RNPS is applied in networks with a large number of buses, where the time taken to solve the circuit grows as the number of buses increase. An evaluation was carried out to obtain the performance of both neighbourhood schemes.

7.4 Limitations of work

At the end of the work carried out in this research, some limitations of this work have been identified. These limitations are outlined in this section. The limitations outlined include both limitations to practical application or deployment of the concepts proposed in this research, and limitations around implementation and simulation of the methods. Some of these limitations would have been considered for improvement, but for the time constraints on the length of time for the research.

As a result of segmentation of the network into neighbourhood zones, the performances of the UNPS and RNPS are dependent on how close to each other (in electrical distance) the BESS in each zone are. The longer the distance, the more losses would be incurred in transporting the power, which in turn reduces efficiency. Therefore, the UNPS and RNPS may not be very efficient when deployed in networks with long power lines separating the installed BESS if the aim is to have a coordinated operation among these BESS. For such networks, when the network segmentation step for the UNPS and RNPS is carried out, the result will be having the number of zones that equals the number of BESS. This means that the BESS belong to different neighbourhoods, and that interactions across across neighbourhoods will be minimised

in order to reduce losses incurred while transporting power during these interactions.

The demand and generation profile data used in Chapter 3 to implement the distributed scheme were not real dataset. The data used are only generic and representative data. Also in Chapter 3, consideration was not given for the cost of installation of the BESS.

The work in Chapter 4, where scheduling of BESS was presented, depended on very favourable TOU profiles in order to yield significant benefits from the use of BESS for arbitrage. In addition, the work in Chapter 4 considered the network as an aggregate, from the point of view of the medium voltage network. Also, the profiles demand and generation profile used in this chapter were generic representative profiles and not real profile data generated from existing network.

In implementation of the FSSS in Chapter 5, a case was made for the suitability of the FSSS for similar operations in larger networks. Even though this statement remains true, simulations were not conducted for larger network to demonstrate this. In addition to these, the PV generation profile was generic and representative, and not from real PV generators. The FSSS also has a limitation that specific BESS are cycled more frequently than others, depending on their locations on the network and the topology of the network. The FSSS also depends on the electrical parameters of the network, like line impedance, capacitance and length. The implication of this is that the selection evaluation would have to be updated anytime the network is changed or upgraded.

For the entire thesis, there is a need for communication on the network for the transfer of charge/discharge signals to the BESS from the controllers, and for the communication of BESS SOC to the controllers. The possible implication of communication medium, in terms of cost and latency, have not been considered in-depth in this thesis.

7.5 Suggestions for further research

During the course of this project, a number of areas were identified that will benefit from further research in order to extend the work. These areas for further research are enumerated below:

1. The work carried out in Chapter 3 for distributed control using reactive power and BESS, and in Chapter 4 for the scheduling of BESS were carried out using generic profiles for generation and demand. An improvement of this would be repeating the simulation with real profiles.

2. In chapter 4 where BESS scheduling was presented, simulation was carried out for a single day using the TOU pricing for the day. This methodology did not account for the variability of TOU prices across different days. An extension of this work will be running daily simulation for a year, using different TOU profiles that correspond to the different days.

3. This thesis has been focused on distribution networks. However, the simulations carried out in this project have used balanced three phase distribution networks. This can be different in real distribution network, which are often characterised by unbalances, as a result of single phase connections. A worthy extension of the studies done in this thesis would be be the consideration of distribution networks that are unbalanced.

4. Another way to extend the findings from this project is the implementation of the FSSS on a larger network. A case was made for the potential of the FSSS to be faster when the size of the network grows.

5. For the coordination schemes developed and presented in this thesis, knowing how differently they perform across different battery technologies could further uncover useful findings that can form a template for recommending battery technologies to be used for particular applications and network situations.

Bibliography

[1] International Renewable Energy Agency (IRENA), *The Power to Change: Solar and Wind Cost Reduction Potential to 2025 (www.irena.org/publications)*, 2016, vol. 978-92-951, no. June. [Online]. Available: http://www.irena.org/DocumentDownloads/Publications/IRENA{_}Power{_}to{_}Change{_}2016.pdf

[2] IRENA, "Renewable Capacity 2016 - Highlights," no. March, 2016.

[3] A. Gabash and P. Li, "Active-reactive optimal power flow in distribution networks with embedded generation and battery storage," *IEEE Transactions on Power Systems*, vol. 27, no. 4, pp. 2026–2035, 2012.

[4] R. Walling, R. Saint, R. C. Dugan, J. Burke, and L. A. Kojovic, "Summary of distributed resources impact on power delivery systems," *IEEE Transactions on power delivery*, vol. 23, no. 3, pp. 1636–1644, 2008.

[5] B. Nykvist and M. Nilsson, "Rapidly falling costs of battery packs for electric vehicles," *Nature Climate Change*, vol. 5, no. 4, pp. 329–332, apr 2015. [Online]. Available: http://www.nature.com/articles/nclimate2564

[6] B. Xu, J. Zhao, T. Zheng, E. Litvinov, and D. S. Kirschen, "Factoring the cycle aging cost of batteries participating in electricity markets," *IEEE Transactions on Power Systems*, vol. 33, no. 2, pp. 2248–2259, 2017.

[7] E.DSO. (2016) Why smart grids? [Online]. Available: https://www.edsoforsmartgrids.eu/home/why-smart-grids/

[8] A. Asrari, T. Wu, and S. Lotfifard, "The Impacts of Distributed Energy Sources on Distribution Network Reconfiguration," *IEEE Transactions on Energy Conversion*, vol. 31, no. 2, pp. 606–613, jun 2016. [Online]. Available: http://ieeexplore.ieee.org/document/7386646/

[9] S. Oberthür and H. E. Ott, *The Kyoto Protocol: international climate policy for the 21st century*. Springer Science & Business Media, 1999.

[10] S. Vaughan, Adamür and H. E. Ott, "Uk sets ambitious new 2030s carbon target," 30 June 2016.

[11] U. Legislature. (2019) The climate change act 2008 (2050 target amendment) order 2019. [Online]. Available: https://www.legislation.gov.uk/ukdsi/2019/9780111187654

[12] IRENA(2018), *Power Generation Costs in 2017,*, 2018, vol. Abu Dhabi.

[13] D. A. Jacques, J. Gooding, J. J. Giesekam, A. S. Tomlin, and R. Crook, "Methodology for the assessment of pv capacity over a city region using low-resolution lidar data and application to the city of leeds (uk)," *Applied energy*, vol. 124, pp. 28–34, 2014.

[14] H. Markiewicz and A. Klajn, "5.4.2 Standard EN 50160 Voltage Characteristics in Public Distribution Systems," 2004. [Online]. Available: http://www.cdtechnics.be/542-standard-en-50160-voltage-characteristics-in.pdf

[15] ERGEG, "European regulators' group for electricity and gas (ERGEG): Towards Voltage Quality Regulation In Europe: An ERGEG Public Consultation Paper," 2006.

[16] F. Camilo, R. Castro, M. E. Almeida, and V. Fernão Pires, "An Assessment of Overvoltage Mitigation Techniques in Low Voltage Distribution Networks with High Penetration of Photovoltaic Microgeneration," *IET Renewable Power Generation*, vol. 12, pp. 649–656, 2018. [Online]. Available: http://digital-library.theiet.org/content/journals/10.1049/iet-rpg.2017.0482

[17] R. Online, M. J. E. Alam, K. M. Muttaqi, D. Sutanto, and &. D. Sutanto, *Distributed energy storage for mitigation of voltage-rise impact caused by rooftop solar PV Publication Details Publication Details*, 2012. [Online]. Available: http://ro.uow.edu.au/eispapers/254

[18] G. Blog. (2016) High penetration of solar photovoltaic in an electricity distribution feeder. [Online]. Available: https://germipower.wordpress.com/2015/04/24/high-penetration-of-solar-photovoltaic-in-an-electricity-distribution-feeder/

[19] K. Chua, Y. S. Lim, P. Taylor, S. Morris, and J. Wong, "Energy storage system for mitigating voltage unbalance on low-voltage networks with photovoltaic systems," *IEEE Transactions on power delivery*, vol. 27, no. 4, pp. 1783–1790, 2012.

[20] R. Yan and T. K. Saha, "Voltage variation sensitivity analysis for unbalanced distribution networks due to photovoltaic power fluctuations," *IEEE Transactions on Power Systems*, vol. 27, no. 2, pp. 1078–1089, 2012.

[21] A. von Jouanne, “Closure on ”assessment of voltage unbalance”,” *IEEE Transactions on Power Delivery*, vol. 17, no. 4, pp. 1176–1177, 2005.

[22] Y. Du, D. D. C. Lu, G. James, and D. J. Cornforth, “Modeling and analysis of current harmonic distortion from grid connected PV inverters under different operating conditions,” *Solar Energy*, vol. 94, pp. 182–194, 2013. [Online]. Available: http://dx.doi.org/10.1016/j.solener.2013.05.010

[23] T. Aziz and N. Ketjoy, “Enhancing pv penetration in lv networks using reactive power control and on load tap changer with existing transformers,” *IEEE Access*, vol. 6, pp. 2683–2691, 2017.

[24] M. Bollen and A. Sannino, “Voltage control with inverter-based distributed generation,” *IEEE transactions on Power Delivery*, vol. 20, no. 1, pp. 519–520, 2005.

[25] A. Safayet, P. Fajri, and I. Husain, “Reactive power management for overvoltage prevention at high pv penetration in a low-voltage distribution system,” *IEEE Transactions on Industry Applications*, vol. 53, no. 6, pp. 5786–5794, 2017.

[26] J. Schiffer, T. Seel, J. Raisch, and T. Sezi, “Voltage stability and reactive power sharing in inverter-based microgrids with consensus-based distributed voltage control,” *IEEE Transactions on Control Systems Technology*, vol. 24, no. 1, pp. 96–109, 2015.

[27] W. Zheng, W. Wu, B. Zhang, H. Sun, and Y. Liu, “A fully distributed reactive power optimization and control method for active distribution networks,” *IEEE Transactions on Smart Grid*, vol. 7, no. 2, pp. 1021–1033, 2015.

[28] A. Safayet, P. Fajri, and I. Husain, “Reactive Power Management for Overvoltage Prevention at High PV Penetration in a Low-Voltage Distribution System,” *IEEE Transactions on Industry Applications*, vol. 53, no. 6, pp. 5786–5794, 2017.

[29] R. Moghe, D. Divan, D. Lewis, and J. Schatz, “Turning Distribution Feeders into STATCOMs,” *IEEE Transactions on Industry Applications*, vol. 53, no. 2, pp. 1372–1380, 2017.

[30] D. Shah and M. L. Crow, “Online Volt-Var Control for Distribution Systems with Solid-State Transformers,” *IEEE Transactions on Power Delivery*, vol. 31, no. 1, pp. 343–350, 2016.

[31] H. V. Padullaparti, Q. Nguyen, and S. Santoso, "Advances in volt-var control approaches in utility distribution systems," *IEEE Power and Energy Society General Meeting*, vol. 2016-November, pp. 1–5, 2016.

[32] L. Bird, J. Cochran, and X. Wang, "Wind and Solar Energy Curtailment: Experience and Practices in the United States," Tech. Rep., 2014. [Online]. Available: www.nrel.gov/publications.

[33] R. Tonkoski and L. A. Lopes, "Impact of active power curtailment on overvoltage prevention and energy production of PV inverters connected to low voltage residential feeders," *Renewable Energy*, vol. 36, no. 12, pp. 3566–3574, 2011. [Online]. Available: http://dx.doi.org/10.1016/j.renene.2011.05.031

[34] J. Hu, M. Marinelli, M. Coppo, A. Zecchino, and H. W. Bindner, "Coordinated voltage control of a decoupled three-phase on-load tap changer transformer and photovoltaic inverters for managing unbalanced networks," *Electric Power Systems Research*, vol. 131, pp. 264–274, 2016.

[35] Y. P. Agalgaonkar, B. C. Pal, and R. A. Jabr, "Distribution voltage control considering the impact of PV generation on tap changers and autonomous regulators," *IEEE Transactions on Power Systems*, vol. 29, no. 1, pp. 182–192, 2014.

[36] A. Navarro-Espinosa and L. F. Ochoa, "Increasing the pv hosting capacity of lv networks: Oltc-fitted transformers vs. reinforcements," in *2015 IEEE Power & Energy Society Innovative Smart Grid Technologies Conference (ISGT)*. IEEE, 2015, pp. 1–5.

[37] C. Long and L. F. Ochoa, "Voltage control of pv-rich lv networks: Oltc-fitted transformer and capacitor banks," *IEEE Transactions on Power Systems*, vol. 31, no. 5, pp. 4016–4025, 2015.

[38] X. Li, D. Hui, and X. Lai, "Battery energy storage station (BESS)-based smoothing control of photovoltaic (PV) and wind power generation fluctuations," *IEEE Transactions on Sustainable Energy*, vol. 4, no. 2, pp. 464–473, 2013.

[39] S. Sabihuddin, A. E. Kiprakis, and M. Mueller, "A numerical and graphical review of energy storage technologies," *Energies*, vol. 8, no. 1, pp. 172–216, 2015.

[40] International Renewable Energy Agency (IRENA), "Electricity Storage and Renewables : Costs and Markets To 2030," no. October, 2017.

[41] E.DSO. (2016) Comparison table of secondary batteries. [Online]. Available: https://batteryuniversity.com/learn/article/secondary_batteries

[42] D. Rastler, "EPRI Project Manager Electricity Energy Storage Technology Options," Tech. Rep., 2010. [Online]. Available: www.epri.com

[43] A. Castillo and D. F. Gayme, "Grid-scale energy storage applications in renewable energy integration: A survey," *Energy Conversion and Management*, vol. 87, pp. 885–894, 2014.

[44] N. R. Tummuru, M. K. Mishra, and S. Srinivas, "Dynamic energy management of renewable grid integrated hybrid energy storage system," *IEEE Transactions on Industrial Electronics*, vol. 62, no. 12, pp. 7728–7737, 2015.

[45] M. A. Abdullah, K. M. Muttaqi, D. Sutanto, and A. P. Agalgaonkar, "An Effective Power Dispatch Control Strategy to Improve Generation Schedulability and Supply Reliability of a Wind Farm Using a Battery Energy Storage System," *IEEE Transactions on Sustainable Energy*, vol. 6, no. 3, pp. 1093–1102, jul 2015. [Online]. Available: http://ieeexplore.ieee.org/document/6913566/

[46] S. R. Ramavat, S. P. Jaiswal, N. Goel, and V. Shrivastava, "Battery Energy Storage Technology Integrated for Power System Reliability Improvement," in *Advances in Energy and Power Systems*, S. N. Singh, F. Wen, and M. Jain, Eds. Singapore: Springer Singapore, 2018, pp. 131–140.

[47] A. Maitra, J. Smith, B. Jordan, and C. Cryer, "Integrating photovoltaic and storage systems on distribution feeders." [Online]. Available: www.ietdl.org

[48] L. Mardira, T. K. Saha, and M. Eghbal, "Investigating impacts of battery energy storage systems on electricity demand profile," in *2014 Australasian Universities Power Engineering Conference (AUPEC)*. IEEE, sep 2014, pp. 1–5. [Online]. Available: http://ieeexplore.ieee.org/document/6966562/

[49] A. Ulbig, T. S. Borsche, G. Andersson, and E. Zurich, *Impact of Low Rotational Inertia on Power System Stability and Operation*, 2014. [Online]. Available: https://ac.els-cdn.com/S1474667016427618/1-s2.0-S1474667016427618-main.pdf?{_}tid=1d49c464-72c0-4b72-b1f5-9e35b0c79508{&}acdnat=1543599359{_}5444bf38ce50f7530a2e1cfa572ff497

[50] D. Greenwood, K. Lim, C. Patsios, P. Lyons, Y. Lim, and P. Taylor, "Frequency response services designed for energy storage," *Applied Energy*, vol. 203, pp. 115–127, oct 2017. [Online]. Available: https://www.sciencedirect.com/science/article/pii/S0306261917307729{#}b0010

[51] R. Hidalgo-Leon, D. Siguenza, C. Sanchez, J. Leon, P. Jacome-Ruiz, J. Wu, and D. Ortiz, "A survey of battery energy storage system (BESS), applications and environmental impacts in power systems," in *2017 IEEE Second Ecuador Technical Chapters Meeting (ETCM)*. IEEE, oct 2017, pp. 1–6. [Online]. Available: http://ieeexplore.ieee.org/document/8247485/

[52] A. Thomas, T. K. Saha, S. R. Deeba, D. Chakraborty, and R. Sharma, "Evaluation of technical and financial benefits of battery-based energy storage systems in distribution networks," *IET Renewable Power Generation*, vol. 10, no. 8, pp. 1149–1160, 2016. [Online]. Available: http://digital-library.theiet.org/content/journals/10.1049/iet-rpg.2015.0440

[53] R. L. Fares and M. E. Webber, "What are the tradeoffs between battery energy storage cycle life and calendar life in the energy arbitrage application?" *Journal of Energy Storage*, vol. 16, pp. 37–45, 2018. [Online]. Available: https://doi.org/10.1016/j.est.2018.01.002

[54] O. Schmidt, A. Hawkes, A. Gambhir, and I. Staffell, "The future cost of electrical energy storage based on experience rates," *Nature Energy*, vol. 2, no. 8, p. 17110, jul 2017. [Online]. Available: http://www.nature.com/articles/nenergy2017110

[55] L. Goldie-Scot. (2019) A behind the scenes take on lithium-ion battery prices. [Online]. Available: https://about.bnef.com/blog/behind-scenes-take-lithium-ion-battery-prices/

[56] L. J. C. Dela Torre and M. A. A. Pedrasa, "Decentralized voltage control for distribution networks with high penetration of distributed generators," *IEEE PES Innovative Smart Grid Technologies Conference Europe*, pp. 636–641, 2016.

[57] J. W. Shim, G. Verbic, K. An, J. H. Lee, and K. Hur, "Decentralized operation of multiple energy storage systems: SOC management for frequency regulation," *2016 IEEE International Conference on Power System Technology, POWERCON 2016*, pp. 1–5, 2016.

[58] A. D. F. Katiraei, R. Iravani, N. Hatziargyriou, "Gestão de Microgrids," no. june, pp. 54–65, 2008.

[59] N. L. Díaz, A. C. Luna, J. C. Vasquez, and J. M. Guerrero, "Centralized Control Architecture for Coordination of Distributed Renewable Generation and Energy Storage in Islanded AC Microgrids," *IEEE Transactions on Power Electronics*, vol. 32, no. 7, pp. 5202–5213, 2017.

[60] L. Wang, D. H. Liang, A. F. Crossland, P. C. Taylor, D. Jones, and N. S. Wade, "Coordination of Multiple Energy Storage Units in a Low-Voltage Distribution Network," *IEEE Transactions on Smart Grid*, vol. 6, no. 6, pp. 2906–2918, nov 2015. [Online]. Available: http://ieeexplore.ieee.org/document/7172552/

[61] M. Zeraati, M. E. Hamedani Golshan, and J. Guerrero, "Distributed Control of Battery Energy Storage Systems for Voltage Regulation in Distribution Networks with High PV Penetration," *IEEE Transactions on Smart Grid*, pp. 1–1, 2016. [Online]. Available: http://ieeexplore.ieee.org/document/7775016/

[62] N. Jayasekara, M. A. S. Masoum, and P. J. Wolfs, "Optimal Operation of Distributed Energy Storage Systems to Improve Distribution Network Load and Generation Hosting Capability," *IEEE Transactions on Sustainable Energy*, vol. 7, no. 1, pp. 250–261, jan 2016. [Online]. Available: http://ieeexplore.ieee.org/document/7321810/

[63] S.-J. Lee, J.-H. Kim, C.-H. Kim, S.-K. Kim, E.-S. Kim, D.-U. Kim, K. K. Mehmood, and S. U. Khan, "Coordinated Control Algorithm for Distributed Battery Energy Storage Systems for Mitigating Voltage and Frequency Deviations," *IEEE Transactions on Smart Grid*, vol. 7, no. 3, pp. 1713–1722, may 2016. [Online]. Available: http://ieeexplore.ieee.org/document/7115169/

[64] Y. Tian, A. Bera, M. Benidris, and J. Mitra, "Stacked Revenue and Technical Benefits of a Grid-Connected Energy Storage System," *IEEE Transactions on Industry Applications*, vol. 54, no. 4, pp. 3034–3043, 2018.

[65] I. Ranaweera, O.-M. Midtgård, and M. Korpås, "Distributed control scheme for residential battery energy storage units coupled with PV systems," *Renewable Energy*, vol. 113, no. 2, pp. 1099–1110, 2017. [Online]. Available: http://linkinghub.elsevier.com/retrieve/pii/S0960148117305888

[66] M. N. Kabir, Y. Mishra, G. Ledwich, Z. Y. Dong, and K. P. Wong, "Coordinated control of grid-connected photovoltaic reactive power and battery energy storage systems to improve the voltage profile of a residential distribution feeder," *IEEE Transactions on Industrial Informatics*, vol. 10, no. 2, pp. 967–977, 2014.

[67] G. Mokhtari, G. Nourbakhsh, and A. Ghosh, "Smart Coordination of Energy Storage Units (ESUs) for Voltage and Loading Management in Distribution Networks," *IEEE Transactions on Power Systems*, vol. 28, no. 4, pp. 4812–4820, nov 2013. [Online]. Available: http://ieeexplore.ieee.org/document/6571285/

[68] M. J. Alam, K. M. Muttaqi, and D. Sutanto, "A novel approach for ramp-rate control of solar PV using energy storage to mitigate output fluctuations caused by cloud passing," *IEEE Transactions on Energy Conversion*, vol. 29, no. 2, pp. 507–518, 2014.

[69] M. Karimi, H. Mokhlis, K. Naidu, S. Uddin, and A. Bakar, "Photovoltaic penetration issues and impacts in distribution network–a review," *Renewable and Sustainable Energy Reviews*, vol. 53, pp. 594–605, 2016.

[70] R. Tonkoski, L. A. Lopes, and T. H. El-Fouly, "Coordinated active power curtailment of grid connected PV inverters for overvoltage prevention," *IEEE Transactions on Sustainable Energy*, vol. 2, no. 2, pp. 139–147, 2011.

[71] H. Hatta, S. Uemura, and H. Kobayashi, "Cooperative control of distribution system with customer equipments to reduce reverse power flow from distributed generation," *IEEE PES General Meeting, PES 2010*, pp. 1–6, 2010.

[72] A. Woyte, V. Van Thong, R. Belmans, and J. Nijs, "Voltage fluctuations on distribution level introduced by photovoltaic systems," *IEEE Transactions on energy conversion*, vol. 21, no. 1, pp. 202–209, 2006.

[73] R. Tonkoski, D. Turcotte, and T. H. El-Fouly, "Impact of high pv penetration on voltage profiles in residential neighborhoods," *IEEE Transactions on Sustainable Energy*, vol. 3, no. 3, pp. 518–527, 2012.

[74] I. S. C. Committee *et al.*, "Ieee standard for interconnecting distributed resources with electric power systems," *IEEE Std*, pp. 1547–2003, 2009.

[75] Y. Yang, H. Li, A. Aichhorn, J. Zheng, and M. Greenleaf, "Sizing strategy of distributed battery storage system with high penetration of photovoltaic for voltage regulation and peak load shaving," *IEEE Transactions on Smart Grid*, vol. 5, no. 2, pp. 982–991, 2013.

[76] G. Valverde and T. Van Cutsem, "Model predictive control of voltages in active distribution networks," *IEEE Transactions on Smart Grid*, vol. 4, no. 4, pp. 2152–2161, 2013.

[77] E. Demirok, D. Sera, R. Teodorescu, P. Rodriguez, and U. Borup, "Evaluation of the voltage support strategies for the low voltage grid connected pv generators," in *2010 IEEE Energy Conversion Congress and Exposition*. IEEE, 2010, pp. 710–717.

[78] S. Ghosh, S. Rahman, and M. Pipattanasomporn, "Distribution voltage regulation through active power curtailment with pv inverters and solar generation forecasts," *IEEE Transactions on Sustainable Energy*, vol. 8, no. 1, pp. 13–22, 2016.

[79] J. M. Guerrero, J. Matas, L. G. de Vicuna, M. Castilla, and J. Miret, "Decentralized control for parallel operation of distributed generation inverters using resistive output impedance," *IEEE Transactions on industrial electronics*, vol. 54, no. 2, pp. 994–1004, 2007.

[80] F. Olivier, P. Aristidou, D. Ernst, and T. Van Cutsem, "Active Management of Low-Voltage Networks for Mitigating Overvoltages Due to Photovoltaic Units," *IEEE Transactions on Smart Grid*, vol. 7, no. 2, pp. 926–936, 2016.

[81] J. Smith, W. Sunderman, R. Dugan, and B. Seal, "Smart inverter volt/var control functions for high penetration of pv on distribution systems," in *2011 IEEE/PES Power Systems Conference and Exposition*. IEEE, 2011, pp. 1–6.

[82] M. Maharjan, U. Tamrakar, N. Malla, F. B. dos Reis, Z. Ni, T. M. Hansen, and R. Tonkoski, "Adaptive droop-based active power curtailment method for overvoltage prevention in low voltage distribution network," in *2017 IEEE International Conference on Electro Information Technology (EIT)*. IEEE, 2017, pp. 1–6.

[83] R. Tonkoski, L. A. Lopes, and T. H. El-Fouly, "Coordinated active power curtailment of grid connected pv inverters for overvoltage prevention," *IEEE Transactions on Sustainable Energy*, vol. 2, no. 2, pp. 139–147, 2010.

[84] B. Bayer, P. Matschoss, H. Thomas, and A. Marian, "The German experience with integrating photovoltaic systems into the low-voltage grids," *Renewable Energy*, vol. 119, pp. 129–141, 2018. [Online]. Available: https://doi.org/10.1016/j.renene.2017.11.045

[85] I.-O. Lee and J.-Y. Lee, "A high-power dc-dc converter topology for battery charging applications," *Energies*, vol. 10, no. 7, p. 871, 2017.

[86] I.-O. Lee, "Hybrid dc–dc converter with phase-shift or frequency modulation for nev battery charger," *IEEE Transactions on Industrial Electronics*, vol. 63, no. 2, pp. 884–893, 2015.

[87] J.-H. Kim, I.-O. Lee, and G.-W. Moon, "Analysis and design of a hybrid-type converter for optimal conversion efficiency in electric vehicle chargers," *IEEE Transactions on Industrial Electronics*, vol. 64, no. 4, pp. 2789–2800, 2016.

[88] K. Turitsyn, P. Sulc, S. Backhaus, and M. Chertkov, "Options for control of reactive power by distributed photovoltaic generators," *Proceedings of the IEEE*, vol. 99, no. 6, pp. 1063–1073, 2011.

[89] E. Demirok, P. C. González, K. H. Frederiksen, D. Sera, P. Rodriguez, and R. Teodorescu, "Local reactive power control methods for overvoltage prevention of distributed solar inverters in low-voltage grids," *IEEE Journal of Photovoltaics*, vol. 1, no. 2, pp. 174–182, 2011.

[90] B. Otomega and T. Van Cutsem, "Distributed load interruption and shedding against voltage delayed recovery or instability," *2013 IEEE Grenoble Conference PowerTech, POWERTECH 2013*, 2013.

[91] C. A. Hill, M. C. Such, D. Chen, J. Gonzalez, and W. M. K. Grady, "Battery energy storage for enabling integration of distributed solar power generation," *IEEE Transactions on Smart Grid*, vol. 3, no. 2, pp. 850–857, 2012.

[92] M. Benini, S. Canevese, D. Cirio, and A. Gatti, "Battery energy storage systems for the provision of primary and secondary frequency regulation in Italy," in *2016 IEEE 16th International Conference on Environment and Electrical Engineering (EEEIC)*. IEEE, jun 2016, pp. 1–6. [Online]. Available: http://ieeexplore.ieee.org/document/7555748/

[93] N. DiOrio, A. Dobos, and S. Janzou, "Economic Analysis Case Studies of Battery Energy Storage with SAM," *National Renewable Energy Laboratory: Denver, CO, USA*, no. November, 2015.

[94] A. Mariaud, S. Acha, N. Ekins-Daukes, N. Shah, and C. N. Markides, "Integrated optimisation of photovoltaic and battery storage systems for UK commercial buildings," *Applied Energy*, vol. 199, pp. 466–478, 2017. [Online]. Available: http://dx.doi.org/10.1016/j.apenergy.2017.04.067

[95] D. Krishnamurthy, C. Uckun, Z. Zhou, P. R. Thimmapuram, and A. Botterud, "Energy storage arbitrage under day-ahead and real-time price uncertainty," *IEEE Transactions on Power Systems*, vol. 33, no. 1, pp. 84–93, 2017.

[96] A. Oudalov, R. Cherkaoui, and A. Beguin, "Sizing and optimal operation of battery energy storage system for peak shaving application," in *2007 IEEE Lausanne Power Tech*. IEEE, 2007, pp. 621–625.

[97] S. Drouilhet and B. L. Johnson, "A Battery Life Prediction Method for Hybrid Power Applications: Preprint," 1997. [Online]. Available: https://www.nrel.gov/docs/legosti/fy97/21978.pdf

[98] Y. Riffonneau, S. Bacha, F. Barruel, and S. Ploix, "Optimal power flow management for grid connected PV systems with batteries," *IEEE Transactions on Sustainable Energy*, vol. 2, no. 3, pp. 309–320, 2011.

[99] O. Erdinc, B. Vural, and M. Uzunoglu, "A dynamic lithium-ion battery model considering the effects of temperature and capacity fading," *2009 International Conference on Clean Electrical Power, ICCEP 2009*, pp. 383–386, 2009.

[100] E. Celebi and J. D. Fuller, "Time-of-use pricing in electricity markets under different market structures," *IEEE Transactions on Power Systems*, vol. 27, no. 3, pp. 1170–1181, 2012.

[101] O. E. Board *et al.*, "Ontario energy board smart price pilot final report," 2007.

[102] E. Hossain, M. Z. Xahin, K. R. Islam, and M. Q. Akash, "Design a novel controller for stability analysis of microgrid by managing controllable load using load shaving and load shifting techniques; and optimizing cost analysis for energy storage system," *International Journal of Renewable Energy Research*, vol. 6, no. 3, pp. 772–786, 2016.

[103] C. Bartusch, F. Wallin, M. Odlare, I. Vassileva, and L. Wester, "Introducing a demand-based electricity distribution tariff in the residential sector: Demand response and customer perception," *Energy Policy*, vol. 39, no. 9, pp. 5008–5025, 2011.

[104] K. Herter, "Residential implementation of critical-peak pricing of electricity," *Energy Policy*, vol. 35, no. 4, pp. 2121–2130, 2007.

[105] G. Dutta and K. Mitra, "A literature review on dynamic pricing of electricity," *Journal of the Operational Research Society*, vol. 68, no. 10, pp. 1131–1145, 2017.

[106] Z. Yun, Z. Quan, S. Caixin, L. Shaolan, L. Yuming, and S. Yang, "Rbf neural network and anfis-based short-term load forecasting approach in real-time price environment," *IEEE Transactions on power systems*, vol. 23, no. 3, pp. 853–858, 2008.

[107] J. Xiao, L. Bai, Z. Zhang, and H. Liang, "Determination of the optimal installation site and capacity of battery energy storage system in distribution network integrated with distributed generation," *IET Generation, Transmission & Distribution*, vol. 10, no. 3, pp. 601–607, feb 2016. [Online]. Available: http://digital-library.theiet.org/content/journals/10.1049/iet-gtd.2015.0130

[108] J. F. Manwell, A. Rogers, G. Hayman, C. T. Avelar, J. G. Mcgowan, U. Abdulwahid, and K. Wu, "Hybrid2 - A Hybrid System Simulation Model Theory Manual," *National Renewable Energy Laboratory*, 2006. [Online]. Available: http://citeseerx.ist.psu.edu/viewdoc/download?doi=10.1.1.466.731{&}rep=rep1{&}type=pdf

[109] E. McKenna and M. Thomson, "High-resolution stochastic integrated thermal–electrical domestic demand model," *Applied Energy*, vol. 165, pp. 445–461, mar 2016. [Online]. Available: https://www.sciencedirect.com/science/article/pii/S0306261915016621

[110] G. Blog. (2018) Real time hourly prices. [Online]. Available: https://hourlypricing.comed.com/live-prices/

[111] Lazard, "Levelised Cost of Energy Analysis," no. November, pp. 0–21, 2017. [Online]. Available: https://www.lazard.com/perspective/levelized-cost-of-energy-2017/

[112] V. Kumar, I. Gupta, H. Gupta, and C. Agarwal, "Voltage and current sensitivities of radial distribution network: a new approach," *IEE Proceedings - Generation, Transmission and Distribution*, vol. 152, no. 6, p. 813, 2005. [Online]. Available: http://digital-library.theiet.org/content/journals/10.1049/ip-gtd{_}20045068

[113] R. Jamalzadeh and M. Hong, "An approximate method for voltage sensitivity calculation in unbalanced distribution systems," in *2016 IEEE/PES Transmission and Distribution Conference and Exposition (T&D)*. IEEE, may 2016, pp. 1–5. [Online]. Available: http://ieeexplore.ieee.org/document/7519963/

[114] M. Brenna, E. De Berardinis, L. Delli Carpini, F. Foiadelli, P. Paulon, P. Petroni, G. Sapienza, G. Scrosati, and D. Zaninelli, "Automatic distributed voltage control algorithm in smart grids applications," *IEEE Transactions on Smart Grid*, vol. 4, no. 2, pp. 877–885, jun 2013. [Online]. Available: http://ieeexplore.ieee.org/document/6296741/

[115] R. C. Dugan and D. Montenegro, "Reference Guide The Open Distribution System Simulator (OpenDSS)," 2018. [Online]. Available: http://download2.nust.na/pub4/sourceforge/e/el/electricdss/OpenDSS/OpenDSSManual.pdf

[116] S. Blumsack, P. Hines, M. Patel, C. Barrows, and E. C. Sanchez, "Defining power network zones from measures of electrical distance," *2009 IEEE Power and Energy Society General Meeting, PES '09*, pp. 1–8, 2009.

[117] G. A. Wilkin and H. Xiuzhen, "K-means clustering algorithms: Implementation and comparison," *Proceedings - 2nd International Multi-Symposiums on Computer and Computational Sciences, IMSCCS'07*, pp. 133–136, 2007.

[118] E. Cotilla-Sanchez, P. D. Hines, C. Barrows, S. Blumsack, and M. Patel, "Multi-attribute partitioning of power networks based on electrical distance," *IEEE Transactions on Power Systems*, vol. 28, no. 4, pp. 4979–4987, 2013.

[119] H. Liu, A. Bose, and V. Venkatasubramanian, "A fast voltage security assessment method using adaptive bounding," in *Proceedings of the 21st International Conference on Power Industry Computer Applications. Connecting Utilities. PICA 99. To the Millennium and Beyond (Cat. No. 99CH36351)*. IEEE, 1999, pp. 325–330.

[120] J. Zhong, E. Nobile, A. Bose, and K. Bhattacharya, "Localized reactive power markets using the concept of voltage control areas," *IEEE Transactions on Power Systems*, vol. 19, no. 3, pp. 1555–1561, 2004.

[121] Y. Wang, F. Li, Q. Wan, and H. Chen, "Reactive power planning based on fuzzy clustering, gray code, and simulated annealing," *IEEE Transactions on Power Systems*, vol. 26, no. 4, pp. 2246–2255, 2011.

[122] B. Venkatesh, R. Ranjan, H. B. Gooi, and S. Member, "Optimal Reconfiguration of Radial Distribution Systems to Maximize Loadability," vol. 19, no. 1, pp. 260–266, 2004.

[123] M. Miner, "Cumulative damage in fatigue journal of applied mechanics 12 (1945) no. 3, pp," *A159-A164*, 1945.

[124] M. Matsuishi and T. Endo, "Fatigue of metals subjected to varying stress," *Japan Society of Mechanical Engineers, Fukuoka, Japan*, vol. 68, no. 2, pp. 37–40, 1968.

[125] M. Musallam and C. M. Johnson, "An efficient implementation of the rainflow counting algorithm for life consumption estimation," *IEEE Transactions on reliability*, vol. 61, no. 4, pp. 978–986, 2012.

[126] L. R. GopiReddy, L. M. Tolbert, B. Ozpineci, and J. O. Pinto, "Rainflow algorithm-based lifetime estimation of power semiconductors in utility applications," *IEEE Transactions on Industry Applications*, vol. 51, no. 4, pp. 3368–3375, 2015.

[127] M. Chawla, R. Naik, R. Burra, and H. Wiegman, "Utility energy storage life degradation estimation method," in *2010 IEEE Conference on Innovative Technologies for an Efficient and Reliable Electricity Supply*. IEEE, 2010, pp. 302–308.

[128] N. DiOrio, A. Dobos, S. Janzou, A. Nelson, and B. Lundstrom, "Technoeconomic modeling of battery energy storage in sam," National Renewable Energy Lab.(NREL), Golden, CO (United States), Tech. Rep., 2015.

Appendices

Appendix A

Publications

A.1 List of publications

The following publications are the outcomes of this PhD research. A journal paper and three conference papers were produced in the process and are all included at the end of the listing.

A.1.1 Journal publication

1. **O. Unigwe**, D. Okekunle, A. Kiprakis, *"Smart Coordination Schemes for Multiple Battery Energy Storage Systems for Support in Distribution Networks with High Penetration of Photovoltaics"*, in press, DOI: 10.1049/iet-stg.2019.0094, IET Smart Grid Journal

A.1.2 Conference publications

1. **O. Unigwe**, D. Okekunle, A. Kiprakis, *"Towards benefit-stacking for grid-connected battery energy storage in distribution networks with high photovoltaic penetration"*, Proceedings of 11th APSCOM, 2018, Hong Kong.
2. **O. Unigwe**, D. Okekunle, A. Kiprakis, *"Smart Coordination of Battery Energy Storage Systems for Voltage Control in Distribution Networks with High Penetration of Photovoltaics"*, Proceedings of 7th Int'l Conference on Renewable Power Generation, RPG 2018, Copenhagen, Denmark.
3. **O. Unigwe**, D. Okekunle, A. Kiprakis, *"Economical Distributed Voltage Control*

In Low-voltage Grids with High Penetration of Photovoltaic", Proceedings of CIRED 24th Int'l Conference on Electricity Distribution, 2017, Glasgow.

Smart Coordination Schemes for Multiple Battery Energy Storage Systems for Support in Distribution Networks with High Penetration of Photovoltaics

Obinna Unigwe [1*], Dahunsi Okekunle [1], Aristides Kiprakis [1]

[1] School of Engineering, The University of Edinburgh, The King's Building, EH9 3DW, Edinburgh, UK.
*o.unigwe@ed.ac.uk

Abstract: The use of battery energy storage system (BESS) is one of the methods employed in solving the major challenge of overvoltage, experienced on distribution networks with high penetration of photovoltaics (PV). The overvoltage problem limits the penetration levels of PV into the distribution network, and the benefits that could be gained. This paper presents three loosely-related schemes for the coordination of multiple battery energy storage systems (BESS) in such networks. Through the efficient selection, coordination and timing of charge and discharge operations of the BESS, the scheme maintains bus voltages within statutory ranges during periods of high PV power generation and high network load demand. Network segmentation was used in two of the schemes to encourage more even utilisation of the BESS in order to maximise the economic benefits of the BESS. The algorithms for the schemes were implemented and demonstrated on two different distribution networks. Simulation results showed that the schemes met the objectives of mitigating overvoltage and more even cycling of the BESSs during their operating lifetimes.

1. Introduction

The electricity network is currently undergoing transformative changes globally, as it transitions from the more traditional structures that involve unidirectional power flow from large generating plants, often fossil fuel-powered, into more flexible structures. The new structures accommodate multidirectional power flows, newer renewable energy sources (RES) and other low carbon technologies (LCT). Of the RES, the photovoltaic (PV) has experienced the highest capacity of installations in the last decade [1]. A challenge with the transition from classical to so-called "smart grid" is that the grid was not originally designed with these changes in mind. The consequence of this is that technical complications arise, that must be dealt with, in the presence of increasing penetration of RES. Power quality issues such as harmonics, reverse power flow, voltage unbalance and overvoltage are common. Overvoltage, in particular, constitutes a major limitation to higher penetrations of PV in the network, especially because there are many periods with substantially higher PV generation levels when compared to consumption on the network.

Methods such as curtailment, use of reactive power injection and absorption, on-load tap changer operations and battery energy storage system (BESS) have been employed to solve these technical challenges [2]. BESSs have grown in popularity for use in stationary applications in electric network systems. Reasons for the increasing widespread deployment of BESS include flexibility and speed in dispatch of active (sometimes reactive) power when required [3]. Falling costs of BESS also account, in part, for the growth in popularity of BESS use in power systems applications. High interest and demand for batteries for use in consumer electronics and transport have motivated increased investment, research and development in manufacture of cheaper and more efficient batteries [4]. Battery prices are expected to continue falling in the coming years [5].

This favourable trend on battery prices notwithstanding, BESS is still acquired at significant costs in the present, and therefore, justification for such investments becomes necessary. On the other hand, it has been established that the method and manner of operation of BESS have significant impact on the lifespan of BESS [6]. It then follows that there is a need for highly efficient coordination of operations of installed BESSs on the network, to maximise the economic benefits, while meeting the specific objectives of installation.

A number of studies have been carried out to improve the operations of BESS in power networks. In [7], a rule-based strategy was presented for the charging/discharging of BESSs that are co-located with rooftop PVs. The focus was on calculating charge/discharge rates that maintain the state of charge (SOC) of the batteries within range for overvoltage mitigation and peak support in the evening. This paper, however, did not consider the potential uneven cycling of BESSs placed at different locations. In [8]–[11], methods of operation of BESS in power networks were examined for varying objectives. A control algorithm for mitigating frequency and voltage deviations was presented in [12], but this strategy did not consider the effects of daily cycling, and therefore techno-economic justification for installation will be difficult. In [13], a coordination algorithm for control of multiple BESSs was carried out based on voltage sensitivity. Considerations were made to achieve evenly-spread participation of BESSs over time, but this paper did not consider the decrease in sensitivity/impact of the BESS as electrical distance from target bus increases. In [14], a dispatch control strategy for BESS was developed using stochastic programming. The work also involved a ranking order for ensuring even utilisation of BESS across lifetimes – from which some parts have been adopted in our work. [14], however did not consider the reduced impact of the BESS active power as the distance increases.

This paper presents three schemes that coordinate the operations of multiple BESSs installed on a network. The objectives of the schemes are to ensure that BESSs are operated in ways that meet the technical objectives of installation while ensuring they are cycled in manner

favourable to the health and long life of the BESSs. The schemes are presented with their methods and considerations, followed by simulations and analysis of performances. This work is an expansion of the earlier work carried out in [15].

The rest of the paper is organised as follows: Section 2 presents a description of the problem while Section 3 presents the flat structure sensitivity scheme. Section 4 presents the uniform neighbourhood participation scheme while Section 5 has the rotational neighbourhood participation scheme. Section 6 presents the implementation and simulation results of the schemes and finally, conclusion is drawn in section 7.

2. Problem description and BESS characteristics

Typical radial networks with no distributed generation (DG) along the feeders have unidirectional power flow from the substation down to the end of the feeder. For such networks, voltage magnitudes also decrease from the substation down along the feeder. With the introduction of DG such as PV, the feeder voltage behaviour changes. Consider the simple network depicted in Fig. 1.

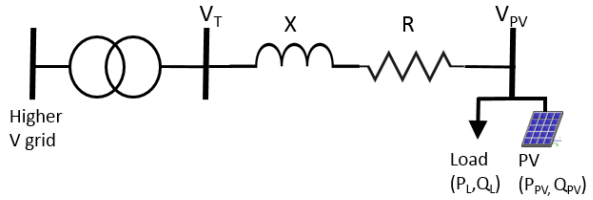

Fig. 1. *Simple radial network with distributed generator*

The network consists of the substation and power line connecting the substation to the load. On the same bus as the load is connected a PV generator. An expression for the voltage across the network with respect to the buses is given in (1).

$$V_{PV} - V_T = \Delta V = \frac{R(P_{PV} - P_L) + X(Q_{PV} - Q_L)}{V_{PV}} \quad (1)$$

where R and X are the resistance and reactance of the line respectively. P_{PV} and Q_{PV} are the active and reactive power of the PV generation, V_T and V_{PV} are the voltages at the substation and the bus of PV connection respectively while P_L and Q_L are the load active and reactive powers. In the event of $P_{PV} > P_L$, voltage rise along the feeder may be experienced and thus violating statutory voltage thresholds for operation on the network. Other impacts of high PV penetration are investigated in the work done in [16]. Continued violation of these thresholds could lead to disconnection of the distributed generators from the network [17]. Reducing the resistance and reactance of the lines is one way to solve this problem, as seen in (1). This can be done by replacing existing lines with larger diameter lines, but this usually comes at high costs. Another solution is increasing the P_L and Q_L and this can be achieved by adding BESS to the network. Due to the dispatchable nature of the BESS, loading on the network can be controlled at different times as required, and network constraint violations can be mitigated. For networks with multiple BESS installations, there arises, therefore, the challenge of coordination of operations of the BESS in such a way that lifespans of the BESSs are preserved for economic reasons, while satisfying the technical objectives of installation.

2.1. BESS characteristics

The state of energy in the battery at any instant in time $E_{BESS}(t)$ is determined by the change in energy from the previous time instant, given in (2)

$$\Delta E_{BESS} = E_{BESS}(t) - E_{BESS}\,(t-1) \quad (2)$$

The change in energy is dependent on the charge/discharge power of the BESS, expressed in (3).

$$P_B(t) = \begin{cases} \frac{\Delta E_{BESS}}{\Delta t}.\eta_c^{-1} & P_B(t) > 1 \\ \frac{\Delta E_{BESS}}{\Delta t}.\eta_d & P_B(t) < 1 \end{cases} \quad (3)$$

where $P_{BESS}\,(t)$ is the charge or discharge power of BESS (positive for charging and negative for discharging), and Δt is the sampling or operation interval, η_d is the discharge efficiency and η_c is the charge efficiency [18]. Constraint on the depth of discharge of the BESS is given in (4).

$$SOC_{min}. \leq SOC \leq SOC_{max}. \quad (4)$$

$SOC_{min}.$ and $SOC_{max}.$ are the minimum and maximum SOC of the BESS. Idling losses in the BESS are considered to be negligible in this work. Equations (2), (3) and constraint (4) describe the behaviour of the battery model used in this work. This model has been chosen because it captures the characteristics of the battery that are of interest.

3. Flat-structure sensitivity scheme

For multiple BESSs connected in a network, a major objective of the coordination scheme is to resolve the challenge of BESS selection for operations at different times for different network conditions, and also the determination of how the selected BESS behaves – charge/discharge rates and depth of discharge (DOD). The flat-structure sensitivity scheme (FSSS) utilises the voltage sensitivities of the network nodes to coordinate the operations of participating BESSs, in a way that considers the entire network as a flat non-hierarchical and non-segmented structure. The method of derivation and use of voltage sensitivity, including the operational principles of the flat-structure scheme are presented in this section.

3.1. Voltage sensitivity for BESS selection

The relationship between the changes in voltage at the buses, as a consequence of the changes in active or reactive power at other buses on the network is provided by the voltage sensitivity factor (VSF). The Jacobian matrix in (5) presents this relationship.

$$\begin{bmatrix} \Delta\theta \\ \Delta|V| \end{bmatrix} = J^{-1} \begin{bmatrix} \Delta P \\ \Delta Q \end{bmatrix} \quad (5)$$

where

$$J = \begin{bmatrix} \frac{\delta P}{\delta \theta} & \frac{\delta P}{\delta V} \\ \frac{\delta Q}{\delta \theta} & \frac{\delta Q}{\delta V} \end{bmatrix} \quad (6)$$

In this equation, Δθ is the change in bus voltage angle, ΔQ is the change in reactive power, ΔV is the change in bus voltage, and ΔP is the change in active power. (5) and (6) present equations for sensitivities of both voltage angle and magnitude. Of particular interest to this work is ΔV and this is expressed in (7)

$$\Delta|V| = \begin{bmatrix} \frac{\delta V}{\delta P} & \frac{\delta V}{\delta Q} \end{bmatrix} \cdot \begin{bmatrix} \Delta P \\ \Delta Q \end{bmatrix} \quad (7)$$

Under network conditions of overvoltage, undervoltage and during periods where peak shaving is required, the voltage sensitivity is utilised in the appointment of BESS and determination of charge and discharge rates. In this scheme, in relation to (7), ΔP represents the charge or discharge power of the operational BESS, which can be converted to respective charge/discharge rates, while ΔV is considered at the node where the voltage change is desired. This method of selection ensures that the selected BESS has the most effective desired effect on the voltage of the target node.

A drawback of using the Jacobian matrix method for obtaining voltage sensitivity is the computational complexity that is involved in that is involved in the process. A method of sensitivity evaluation was presented in [19], and this method provides an alternative computationally less intense way of obtaining the sensitivity matrix. The method is an approximate evaluation, however, the results obtained are close to those obtained by using (1) directly. This method is summarised in (8) and (9).

$$\frac{\delta E_i}{\delta P_j} = -\frac{1}{E_n} \left[\sum_{hk \in PT_{i,j}} R_{hk} \right] \quad (8)$$

$$\frac{\delta E_i}{\delta Q_j} = -\frac{1}{E_n} \left[\sum_{hk \in PT_{i,j}} X_{hk} \right] \quad (9)$$

R_{hk} and X_{hk} are the resistance and reactance of branch hk respectively; E_n is the approximate rated voltage of the network; $PT_{i,j}$ is the set of nodes contained in the path connecting the medium voltage (MV) busbar to nodes i and j, and at the same time common to both nodes.

Sensitivity ranking tables B_P and B_Q for real and reactive power respectively are formed using (8) and (9). Only B_P is shown, since this work considers only active power changes, but the formation of B_Q is in a similar fashion to B_P.

$$B_P = \begin{bmatrix} \frac{\delta E_1}{\delta P_1}\Delta P_1 & \cdots & \cdots & \frac{\delta E_1}{\delta P_N}\Delta P_N \\ \cdots & \cdots & \cdots & \cdots \\ \cdots & \cdots & \cdots & \cdots \\ \frac{\delta E_N}{\delta P_1}\Delta P_1 & \cdots & \cdots & \frac{\delta E_N}{\delta P_N}\Delta P_N \end{bmatrix} \quad (10)$$

N represents the total number of buses on the network and $n = 1,2 \ldots N$ represents any specific bus on the network. The rows represent the node voltages and the columns represent the BESS locations. When the voltage of a particular bus (along rows) is of interest for change, the column (representing BESS installation location) with the highest value is selected as the best suited for affecting the required voltage change. This selected BESS is designated $BESS_{sel}$ for the time instant that this evaluation is carried out. The selection according to ranking is carried out by the selection evaluator (SE) within the algorithm. When there is no BESS installation on a particular bus, the position of that bus in (10) is set to zero and therefore cannot be selected.

3.2. Description of sets used in formulation

The algorithm, during operation, maintains and updates the following sets at each time step.

3.2.1 Power rating set (P_{BES}): This is the set of active power ratings of all BESSs on the network.

$$P_{BES} = \{P_{BES_n} : n = 1,2, \ldots N\} \quad (11)$$

where P_{BES_n} is the active power rating of the BESS connected to bus n, N is the total number of buses on the network. Observe that $P_{BES_n} = 0 \; \forall n \in Z$ holds true, where Z is the set of all buses that have no BESS installation.

3.2.2 Selected BESS set (BES_{sel}): This is the set of all BESSs that have been selected by the SE and activated for charging or discharging.

$$BES_{sel} = \{BES_{sel_n} : \; n = 1,2, \ldots N\} \quad (12)$$

where BES_{sel_n} is an output from the SE which denotes the BESS that has been selected for charging. $BES_{sel} = \emptyset$ holds true as an initial condition at the start of operations. $BESS_{sel_l}$ is used to denote the last BESS that has been added to BES_{sel}.

3.2.3 Charge rates set (CR): This is a set of the charge or discharge rates of corresponding selected BESS contained in BES_{sel}

$$CR = \{CR_n : n = 1,2, \ldots N\} \quad (13)$$

where CR_n is the charge rate of the corresponding BES_{sel_n}. Similar to BES_{sel}, $CR = \emptyset$ holds true at the start of operations. CR_l is used to denote the charge rate of BES_{sel_l} and CR_{max} denotes the maximum charge rate of any BESS.

3.2.4 State of charge set (Ω_{soc}): This set contains the changing SOC of all the BESSs on the network. The algorithm uses this to have knowledge of which BESS are

fully charged, or nearly fully charged in order to take proactive actions. The latter is one of the objectives the scheme aims to achieve.

3.3. Flat structure sensitivity scheme operation

The flowchart in Fig. 2 shows the operation of the flat-structure sensitivity scheme (FSSS). In this work, the algorithm coordinates multiple BESS on a network with the objectives of mitigating overvoltage during periods of high PV generation and mitigating undervoltage during high loading periods. High loading periods often coincide with periods of low PV generation, usually in the evening. The bus voltages are maintained within set upper and lower limits, $V_{LTH} \leq V_m \leq V_{UTH}$. V_m is the monitored bus voltage, V_{LTH} is the statutory lower threshold voltage and V_{UTH} is the statutory upper threshold voltage. Fig. 2 shows the scheme for overvoltage alone, but the same flow of controls applies for undervoltage situations, with the BESS discharging instead of charging.

Following a scenario where the algorithm is initialised at the start of the day (midnight), then $V_m > V_{UTH}$ is likely to occur first as a result of possible overvoltage due to high PV power generation in the day when load demand is low. Upon overvoltage, the SE executes the evaluation and the output from the SE is BES_{sel_n}, and this BESS goes into charging mode. V_{diff} is the difference between the measured bus voltage V_m and the statutory threshold voltage V_{UTH} or V_{LTH}. CR_n, which is the amount of power that keeps V_{diff} at zero, is also derived for BES_{sel_n}. CR_n calculated as shown in (14), which is derived from (10).

$$CR_n = V_{diff} \cdot \left(\frac{\delta V_m}{\delta P_n}\right)^{-1} \tag{14}$$

$\left(\frac{\delta V_m}{\delta P_n}\right)$ is the sensitivity V_m to the bus where BES_{sel_n} is connected. During operation, given the situation where the CR of BES_{sel_n} stops being large enough to maintain $V_{diff} = 0$, possibly as a result of sustained increase in PV active power generation, new BESS are added, one at a time, to the BES_{sel} set. The selection this time will exclude from the ranking, any BESS that is already contained in BES_{sel}.

The SOC of participating BESSs are known since Ω_{SOC} is updated at every time step. With this information, new BESS are added to the BES_{sel} set just before any active BESS is charged or discharged to the maximum or minimum SOC, mitigating any unwanted voltage changes that could occur.

The BESS enters discharge mode anytime during operations that the condition $V_m < V_{LTH}$ is satisfied, or at set times for shaving operations during periods of high load demands. A similar procedure to charge operations is followed for the discharge operations. V_{UTH} is replaced by V_{LTH} in the algorithm for the evaluation of V_{diff}, causing V_{diff} to return negative values, and consequently negative values of CR_n. Negative CR_n values represent discharge signals to the BESS.

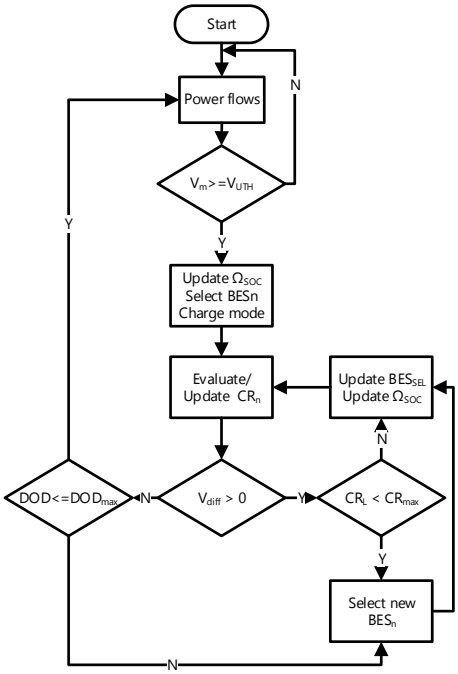

Fig. 2. *Flowchart of coordination scheme (overvoltage)*

4. Uniform neighbourhood participation scheme

The cost of BESS is the major limitation to increased installations on power networks. It then becomes necessary that initial cost of installation be justified, as well as delaying, as much as possible, any future replacement costs. Because the length of life of the battery is a function of the way it is operated during its lifetime, it then follows that the systematic operation in a manner to promote good health and prolong the lifetime, while satisfying the technical aims of installation of BESS, is an important objective.

One common scenario encountered in networks with BESS installations is where, due to network topology and structure, BESS connected to certain buses end up being cycled more frequently than others, as a result of their locations. Such BESS therefore reaches end-of-life quicker, thereby subjecting owners and operators to replacement costs, while some other BESS are not being put to use as much. Such replacements do not benefit from the advantages of economy of scale, among other undesirable consequences. The challenge encountered in the scenario, as described, and other cases that lead to wildly disproportionate cycling across multiple BESS in the same network, is what the uniform neighbourhood participation scheme (UNPS) aims to overcome.

In this scheme, the network is segmented into BESS operational zones. The BESSs in each zone operate in a cooperative and uniform manner to respond to events within the zone with charge and discharge operations as required. The sensitivity method introduced in section 3 is applied to determine the charge and discharge rates of the BESS for any active zone. A zone becomes active when the voltage on any bus in the zone exceeds the defined thresholds. This means that more than one zone can be active at any time. Zonal

neighbours (ZN) are zones configured with ability to respond to distress signals from each other, when the source zone for the distress is unable to sufficiently deal with the undesirable event. Every zone therefore possesses a hierarchical set, Z_{nbr}, that contains a list of every zone that it shares zonal neighbourhood with. The hierarchical structure of Z_{nbr} means that the first zone in the set is given priority appointment to attempt to resolve the distress. Only after the first element in Z_{nbr} is unable to resolve the problem is the second zone appointed, then the third, and so on. For example, the zonal neighbourhood set for zone B in a network is given in (15).

$$Z_{nbr|B} = [D, C, A, E] \tag{15}$$

Zone D is the priority zone to respond to distress signals from zone B when the BESSs in zone B are not sufficient to resolve the problem, followed by zone C and then zone E.

4.1. Network segmentation considerations

The segmentation of the network into zones for the implementation of the neighbourhood scheme considers a number of factors peculiar to the network. The first consideration is the electrical distances between the buses. With the increase in the length of the lines between buses comes a corresponding increase in the resistance between them.

The sensitivity values for buses electrically closer to each other are higher than that for buses that are farther apart, and therefore can more easily affect the voltages of each other. When using BESS active power for voltage control in the neighbourhood scheme, the aim therefore is to minimize the distances between the participating BESS in each zone. Areas of the network with shorter line distances apart are likely to be placed in the same zone while longer line distances are likely to form inter-zone boundaries. For implementation of the ZN feature, zones with shorter inter-zonal distances are likely to belong to the same zonal neighbourhoods. Segmentation of the test network used to demonstrate the scheme is shown in Fig. 9.

4.2. Operation of the uniform neighbourhood participation scheme

Let the network be segmented into Φ zones, where $\Phi = A, B, C \ldots$. Each zone can contain any number of BESS, depending on unique network features considered during segmentation, described in 4.1. Let the number of BESS in each zone be 1,2,3 ... K, so that if zone A and B, for example, have 4 and 5 BESS respectively, the zones will be:

$$\begin{aligned} A &= [A1, A2, A3, A4]; \\ B &= [B1, B2, B3, B4, B5] \end{aligned} \tag{16}$$

Z_{sel} is a set of all active zones and is updated at every time step of operations.

The scheme switches the BESSs into charge or discharge operation mode for any zone when the condition $V_{LTH} \leq V_m \leq V_{UTH}$ ceases to remain true for any bus in the zone. This means overvoltage or undervoltage on a single bus switches all the BESS in the zone from where the signal was sent. The BESS charge and discharge rates change in a uniform fashion until the distress signal discontinues.

The algorithm also updates the Z_{nbr} for each zone according to availability at any given time. The Z_{nbr} is used when distress signal persists in an operational zone, even when all the participating BESS in the operational zone are charging or discharging at maximum possible rates. When this happens, the first zone in Z_{nbr} for the zone in question is checked for availability and then appointed if available. If unavailable, the second zone in Z_{nbr} is checked, and so on. The newly-appointed zone is added into the Z_{sel} set. The zone goes into operation, despite the condition $V_{LTH} \leq V_m \leq V_{UTH}$ not violated on any of the buses in its zone.

5. Rotational neighbourhood participation scheme

The rotational neighbourhood participation scheme (RNPS) is a hybrid combination of the FSSS and UNPS. Like the UNPS, the segmentation of the network into zones, described in 4.1 is maintained; and like the FSSS, within each active zone, the BESSs charge and discharge in turns and not uniformly. 5.1 describes other features and operations of the RNPS.

5.1. Operation of the rotational neighbourhood participation scheme

In the RNPS, BESSs in each zone also belong to the same neighbourhood and only respond to events within the zones, except in cases where the Z_{nbr} is used to appoint a neighbour zone when an active zone is not able to deal with events independently. BESSs in the active zone are added to BES_{sel}, one at a time, depending on the severity of the event. The gradual addition of BESS in a zone to the BES_{sel} is similar to that seen in the FSSS. In other words, only the number of BESS required to make $V_{diff} = 0$ at every bus in the zone are sequentially added to the BES_{sel}. A unique feature of the RNPS is the use of a rotation array (RA) for charging and discharging operations in the zones. Each zone has two RAs; RA_C for charging operations and RA_D for discharging operations. The RA is the tool used by the RNPS to mitigate disproportionate cycling among BESS in any zone.

Each of RA_C and RA_D for each zone contains all the BESS in the zone, in the order to be followed for charging or discharging operations. The first BESS in RA_C and RA_D are the ones to respond to any charge or discharge signals respectively, received at any bus in the zone. This is followed by the second BESS in the RAs when the first is unable to make $V_{diff} = 0$, as a result of insufficient available capacity or persistence of distress signal despite charging or discharging at maximum rates. The third, then fourth, and so on, are subsequently appointed following same rules. Once a BESS has been added to BES_{sel}, the RA is updated with the same BESS moved from the first to the last position in the rank, while other BESSs move up one step in the rank. This sequence is the same for RA_C and RA_D.

For example, $RA_{C|B}$ is the rotation array for charging operations in zone B and contains the BESS in zone B, in the order in which they will respond to charge signals. On receipt of a charge signal on any bus in zone B, $BESS_{B1}$ is added to

B_{sel} and at the same time, moved to the last rank position in $RA_{C|B}$, which is then updated as shown in (17)

$$RA_{C|B} = \begin{bmatrix} BES_{B1} \\ BES_{B4} \\ BES_{B5} \\ BES_{B2} \\ BES_{B3} \end{bmatrix} \quad .. \text{ to } .. \quad \begin{bmatrix} BES_{B4} \\ BES_{B5} \\ BES_{B2} \\ BES_{B3} \\ BES_{B1} \end{bmatrix} \tag{17}$$

$BESS_{B4}$ becomes the next BESS to respond to charge signal from Zone B, and this happens when $BESS_{B1}$ is fully charged or B1 is unable to bring $V_{diff} = 0$ operating alone.

A similar sequence is maintained in $RA_{D|B}$. Note that in $RA_{D|B}$, the BESS can be ranked in an order different from $RA_{C|B}$, but must contain the same BESS as $RA_{C|B}$. The rotation of the BESS within the RA ensures that the charge/discharge responsibilities are evenly distributed among the participating BESS when assessed over a long period of time, such as during their entire lifetime.

6. Coordination algorithms implementation

This section describes the implementation of the three coordination algorithms presented in this work. The RNPS and UNPS are implemented on the same network while the FSSS is implemented on a different network.

6.1. *Implementation of flat structure sensitivity scheme*

The distribution network used as a case study in the implementation of the coordination scheme was developed using OpenDSS [9], an open source tool developed by Electric Power Research Institute (EPRI). The algorithm for the coordination control was developed in MATLAB. The Component Object Model (COM), which is made available in OpenDSS, was used as an interface to effect the controls on MATLAB to the network model on OpenDSS.

6.1.1 Case study network description: A 7-bus low voltage radial distribution network [20], located in Belgium, was used for the implementation. 4 out of the 7 buses (buses $2, 4, 5$ and 7) have PV installed on them and the feeder is supplied through a $22/0.4\ kV$ transformer rated $185 kVA$. 33 residential houses are connected to the feeder and total kWp installation of PV on the feeder is $42.6\ kWp$. 6 PV installations are on bus 7 while buses $2, 4, 5$ contain single installations each, as shown in Fig. 3. The BESS on the network are named, as shown in Fig. 3, according to the buses to which they are connected. Multiple BESS on bus 7 are numbered from 7 to 12.

6.1.2 Demand and generation profiles: The CREST tool [21] was used for the creation of the load profile used in the implementations. The tool was used to create load profiles for an aggregate of 100 houses, generating 50 different aggregations which were averaged out to obtain a typical representation of residential demand profile. The load shape was normalised and used as multipliers on the test network actual loads.

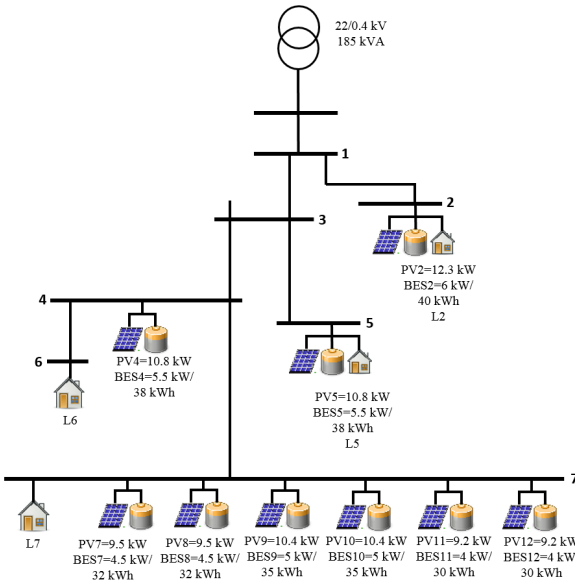

Fig. 3. *Diagram of test network*

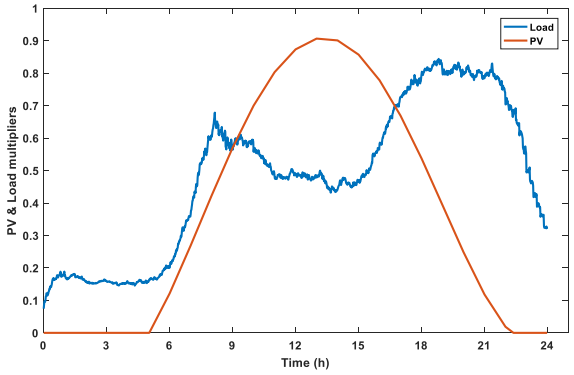

Fig. 4*. Load and demand profiles*

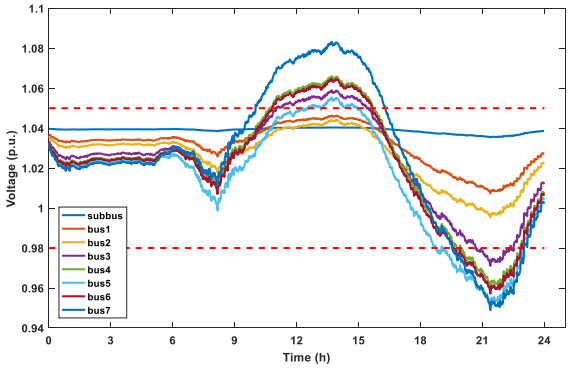

Fig. 5. *Feeder voltage profile without controls*

Summer-time load profile was generated to represent period of the year when PV generation is highest. This is shown in Fig. 4.

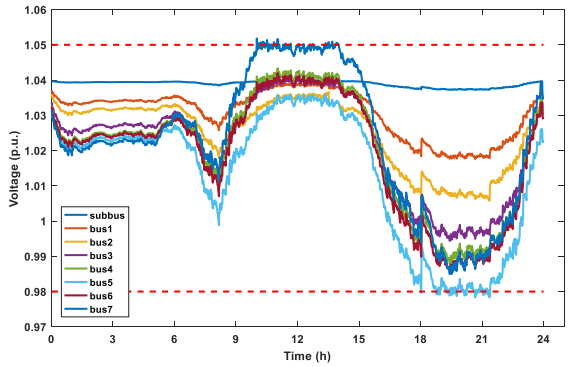

Fig. 6: *Feeder voltage profile with coordination control*

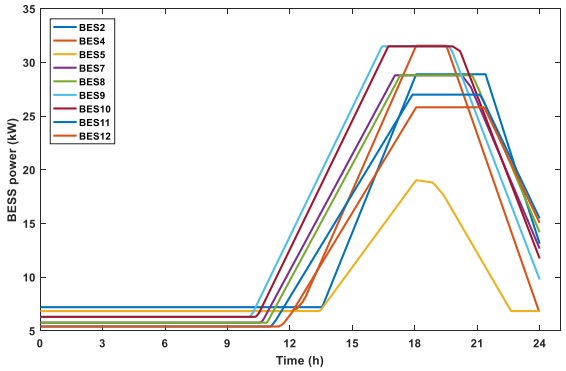

Fig. 7*. SOC of network BESS*

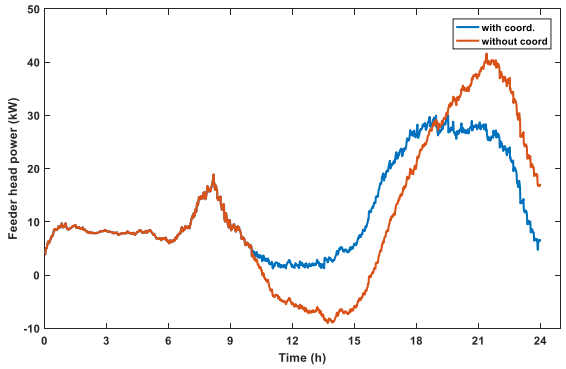

Fig. 8*. Power flows measured at the feeder head*

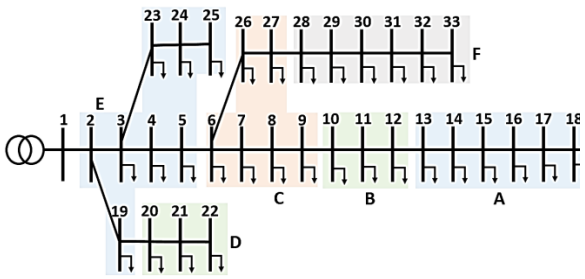

Fig. 9. *IEEE 33-bus distribution network*

A generic summer-time PV profile representing average typical PV behaviour was used as the generation profile. Similar to the demand profile, the generation profile is applied as a multiplier to the actual kWp values of the PV installations on the test network. The resolution for both generation and demand profiles is 1 minute.

6.1.3 Simulation results: Entire day simulations with a 1-minute resolution were run to demonstrate the operations of the algorithm, giving a total simulation time of 1440 minutes. The following values were used for other parameter configurations of the scheme: $V_{UTH} = 1.05$ p.u, $V_{LTH} = 0.98$ p.u, $CR_{max.} = 90\%$, $20\% \leq DOD \leq 90\%$. The substation voltage was set at 1.04 p.u in order to accommodate the voltage drop along the feeder.

The voltage profile of the network without any control scheme is shown in Fig. 5. It can be seen that both V_{UTH} and V_{LTH} are violated during periods of high PV generation and high demand respectively. The former leads to curtailment of excess active power generated, which undermines the economics of PV installation. With the FSSS in operation, Fig. 6 shows the voltage profile of the feeder. At about the 10th hour, bus 7 experiences a voltage violation ($V_{m_7} > V_{UTH}$) and BES_9 is switched to charging mode as it is the highest ranking on the SE. BES_{10} could also have been switched first since it has the same ranking as BES_9, given that they both have the same power ratings, availability according to Ω_{SOC} and are both positioned on the same bus. BES_{10} is switched to charging mode shortly after BES_9. This happens after CR_9 reaches CR_{max}, and $V_{diff} > 0$ still persists. With an increase in the PV generation, other BESS are sequentially switched to charging mode and the FSSS also ensures there are no sudden voltage changes, especially when a BESS is fully charged or discharged. It accomplishes this by monitoring the updated Ω_{SOC} in order to keep track of the SOC of active BESS.

In similar manner as in charging, discharge signals are sent to high ranking and available BESS during periods of heavy loading. In Fig. 6, $V_5 < V_{LTH}$ occurs around the 18th hour and BES_5 is the first to switch to discharge mode. Other BESSs are subsequently switched to discharge mode to ease loading on the network. ***Fig. 8*** shows reverse power flow from the LV to MV network without the FSSS, which is mitigated by application of FSSS.

6.2. Implementation of uniform neighbourhood participation scheme

6.2.1 Case study network description: The hypothetical IEEE 33-bus distribution network [22] is used for the implementation of the UNPS and RNPS. The network was developed in OpenDSS while the algorithm implementation was built in Python. The COM interface of the OpenDSS was used for connecting Python to the OpenDSS model.

The substation voltage is 12.66 kV with total load demand of 3715 kW. Each bus of the network has PV installation of $70kWp$ with co-located BESS of $50kW/50kWh$. The network is shown in Fig. 9. Following the considerations described in 4.1, the network is segmented as shown in Fig. 9. The load and generation profiles created in 6.1 are used as multipliers on the actual loads and PV respectively. The voltage at the feeder head is set at 1.05 pu.

The BESSs are named both according to their operational zones and the bus number to which they are connected. The bus number follows the zone identifier in this naming convention. For example, the BESSs in zone A are named as follows: $[BES_{A13}, BES_{A14}, BES_{A15}, BES_{A16}, BES_{A17}, BES_{A18}]$. The zonal neighbourhood sets for zones A and B, which are the zones used for illustration of the scheme, are: $Z_{nbr|A} = [B, C, E]$ and $Z_{nbrA|B} = [A, C, E]$.

6.2.2 Simulation results of UNPS: Simulations were run for an entire day with $1-$ minute resolution. The simulation was initialised with $SOC = 100\%$ for BES_{A18}, in order to capture variations that might be encountered in real operations where a BESS does not have capacity for charge prior to periods of high PV generation. Voltage profile of the network with UNPS in operation is shown in *Fig. 10*. Voltage violation ($V_{m18} > V_{UTH}$) occurs in zone A at about the 12th hour at bus 18 and the zone is switched to charge mode. The BESSs in zone A charge uniformly, with charge rates determined by the magnitude of V_{diff} on the overvoltage bus. Fig. 11 shows the SOC of the BESSs in zones A and B. The SOC for each zone can be seen varying uniformly throughout the duration of the simulation. In the evening during periods of high loading on the network, the BESSs are switched to discharge mode. Around the 22nd hour, zone A BESSs become fully charged, even though there is still need for maintaining the voltages in zone A within the set range. The algorithm, at this stage, uses $Z_{nbr|A}$, (the zonal neighbourhood set for zone A) to appoint a neighbour zone that switches into operation for the purpose of maintaining voltages. Zone B is the first element in Z_{nbr} and is appointed. As seen in Fig. 11, zone B BESSs ($BES_{B10}, BES_{B11}, BES_{B12}$) start discharging at about the same time that zone A BESSs become fully charged (around the 22nd hour).

6.3. Implementation of rotational neighbourhood participation scheme

The same network, zone segmentation, load and generation profiles used in 6.2 are also used in this section for the demonstration of the operations of the RNPS. To demonstrate the rotational sequencing of the BESSs using the RNPS, zone A will be focused on for simplicity. Behaviours in other zones of the network will be similar to zone A's. The initial RAs for zone A are given below:

$$RA_{C|A} = \begin{bmatrix} BES_{A18} \\ BES_{A17} \\ BES_{A16} \\ BES_{A15} \\ BES_{A14} \\ BES_{A13} \end{bmatrix} \quad RA_{D|A} = \begin{bmatrix} BES_{A17} \\ BES_{A18} \\ BES_{A16} \\ BES_{A15} \\ BES_{A14} \\ BES_{A13} \end{bmatrix} \qquad (18)$$

The initial SOC values of the BESS in zone A are 20% (minimum SOC), except BES_{A17} which starts at 100%.

6.3.1 Simulation results of RNPS: Fig. 12 shows the voltage profile of the feeder with the RNPS in operation.

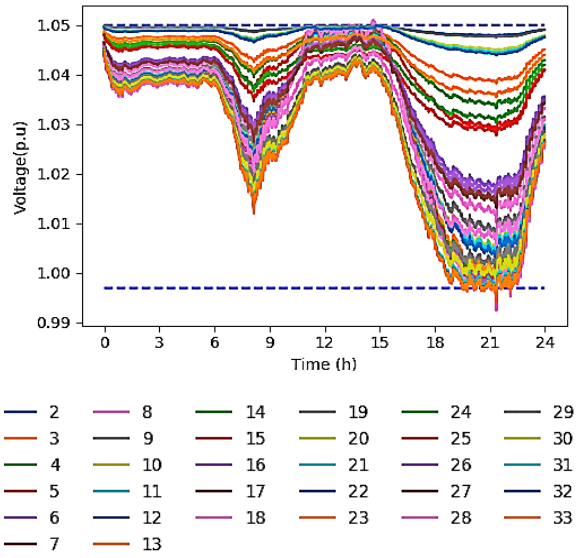

Fig. 10. *Feeder voltage profile with UNPS*

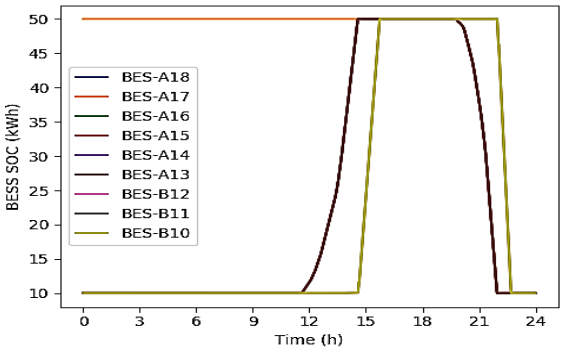

Fig. 11. *SOC of zone A with UNPS*

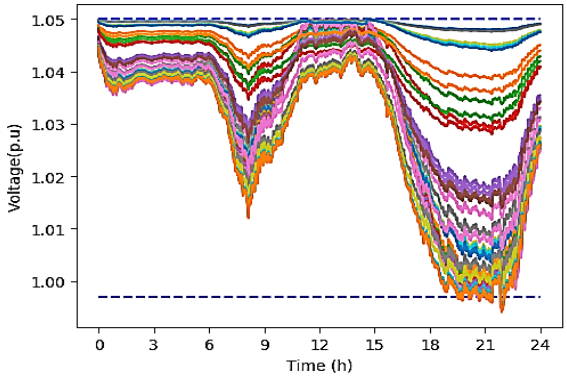

Fig. 12*. Feeder voltage profile with RNPS*

As PV power generation increases, bus 18 at the end of the feeder is the first to have its voltage exceed the upper threshold ($V_{m18} > V_{UTH}$) around the 12th hour. BES_{A18} is switched to charge mode, being the top ranked in $RA_{C|A}$.

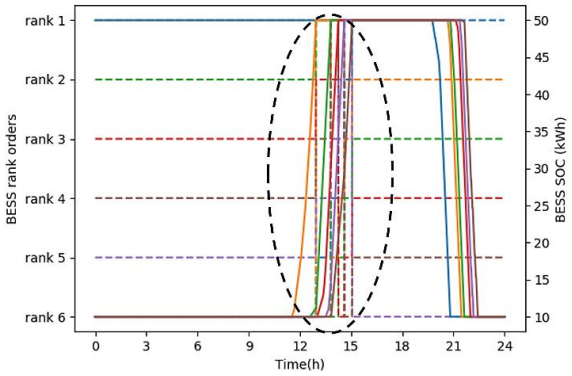

***Fig. 13**. Rotational order and SOC at zone A*

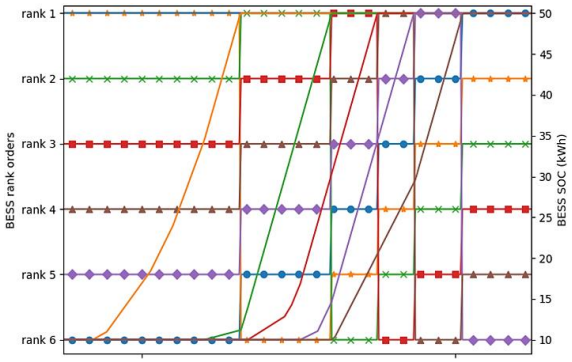

***Fig. 14.** Zoomed-in rotational order and SOC at zone A*

Fig. 13 shows how the orders of the BESSs are changing as their SOC change. A zoomed-in view is presented in Fig. 14 for clearer details. The magnified area is indicated by the block dotted oval on Fig. 13. The legend and colour schemes are the same as those used in Fig. 11. When BES_{A18} reaches maximum SOC, it is moved to the bottom of $RA_{C|A}$ and other BESSs in the set move up one step. The new highest-ranked BESS becomes BES_{A16} because the algorithm detects that $BESS_{A17}$ is fully charged (from initial settings), moves it to the bottom of the set and makes BES_{A16} the priority for charging. The BESSs are brought to charge sequentially according to the ranking in $RA_{c|A}$ until a signal for discharge is received around the 20th hour. $BESS_{17}$, being the highest-ranked in $RA_{D|A}$ is the first to start discharging. The other BESSs in the zone follow according to their positions on $RA_{D|A}$.

Around the 14th hour, a situation arises where all the BESSs in zone A are either fully charged, or charging at maximum rates but not able to mitigate the distress signal. The algorithm uses the Z_{nbr} of zone A, which has zone B as the first element, to solve the problem. BES_{B12} is switched to charging, followed by BES_{B11}. The voltage along the feeder is maintained during the period of high PV generation and high network loading. Two possible objectives could be set as target for the BESS discharge – a power threshold at the secondary of the substation or undervoltage at the buses. The latter has been used in this simulation and was set at $0.999V\ p.u.$

7. Conclusion and future work

In this paper, three different schemes for the coordination of multiple BESSs in a network were proposed. The schemes in operation mitigated the occurrence of overvoltage as a result of high PV generation on the network. During peak loading times on the network, the BESSs on the network were also coordinated to support the network. Voltage sensitivity was used for selection and charge rates estimation for the flat structure sensitivity scheme (FSSS). Segmentation of the network into BESS operational zones was performed in the uniform neighbourhood participation scheme (UNPS) and the rotational neighbourhood participation scheme (RNPS) to ensure more efficient and even cycling of the BESS on the network. Simulations were carried out using two different networks to demonstrate the performance of the schemes and results show that the schemes were able to mitigate overvoltage and that different schemes could be applied to different networks depending on specific network structure and techno-economic objectives. The schemes presented in this paper can be employed by utilities and owners of BESS to improve the lifetime of BESS while maximising the penetration of renewable energy resources in the network without technical challenges.

Future research will consider the implementation of the schemes on different networks and carrying out simulations to compare the performance of the schemes with other earlier-developed schemes in literature. In addition, performance of the schemes in managing the lives of the BESS will be evaluated individually by carrying out simulations for the entire lifetimes of the BESS.

8. Acknowledgement

The authors would like to acknowledge support by the following: a) Petroleum Technology Development Fund (PTDF), an initiative of the Federal Government of Nigeria; b) The British Council UK - India Education & Research Initiative & the Indian Department of Science & Technology under grant 16/17-98 (D-DIEM: Data-Driven Intelligent Energy Management for Environmentally Sustainable Energy Access); c) EPSRC through the National Centre for Energy Systems Integration, grant number EP/P001173/1.

9. References

[1] A. Jäger-Waldau, *European Commission PV Status Report 2017*. Publications Office of the European Union, Luxembourg, 2017.

[2] B. R. Pereira, G. R. M. Martins Da Costa, J. Contreras, and J. R. S. Mantovani, "Optimal Distributed Generation and Reactive Power Allocation in Electrical Distribution Systems," *IEEE Trans. Sustain. Energy*, vol. 7, no. 3, pp. 975–984, 2016.

[3] Sang Won Min, Seog-Joo Kim, Jae Woong Shim, Youngho Cho, and Kyeon Hur, "Synergistic Control of SMES and Battery Energy Storage for Enabling Dispatchability of Renewable Energy Sources," *IEEE Trans. Appl. Supercond.*, vol. 23, no. 3, pp. 5701205–5701205, 2013.

[4] B. Nykvist and M. Nilsson, "Rapidly falling costs of battery packs for electric vehicles," *Nat. Clim. Chang.*, vol. 5, no. 4, pp. 329–332, Apr. 2015.

[5] O. Schmidt, A. Hawkes, A. Gambhir, and I. Staffell, "The future cost of electrical energy storage based on experience rates," *Nat. Energy*, vol. 2, no. 8, p. 17110, Jul. 2017.

[6] J. F. Manwell *et al.*, "Hybrid2 - A Hybrid System Simulation Model Theory Manual," *Natl. Renew. Energy Lab.*, 2006.

[7] M. J. E. Alam, K. M. Muttaqi, and D. Sutanto, "Mitigation of rooftop solar PV impacts and evening peak support by managing available capacity of distributed energy storage systems," *IEEE Trans. Power Syst.*, vol. 28, no. 4, pp. 3874–3884, 2013.

[8] N. Jayasekara, M. A. S. Masoum, and P. J. Wolfs, "Optimal Operation of Distributed Energy Storage Systems to Improve Distribution Network Load and Generation Hosting Capability," *IEEE Trans. Sustain. Energy*, vol. 7, no. 1, pp. 250–261, Jan. 2016.

[9] O. Unigwe, D. Okekunle, and A. Kiprakis, "Economical distributed voltage control in low-voltage grids with high penetration of photovoltaic," *CIRED - Open Access Proc. J.*, vol. 2017, no. 1, pp. 1722–1725, 2017.

[10] I. Ranaweera, O.-M. Midtgård, and M. Korpås, "Distributed Control Scheme for Residential Battery Energy Storage Units Coupled With PV Systems."

[11] M. Y. Nguyen, D. H. Nguyen, and Y. T. Yoon, "A new battery energy storage charging/discharging scheme for wind power producers in real-time markets," *Energies*, vol. 5, no. 12, pp. 5439–5452, 2012.

[12] S.-J. Lee *et al.*, "Coordinated Control Algorithm for Distributed Battery Energy Storage Systems for Mitigating Voltage and Frequency Deviations," *IEEE Trans. Smart Grid*, vol. 7, no. 3, pp. 1713–1722, May 2016.

[13] L. Wang, D. H. Liang, A. F. Crossland, P. C. Taylor, D. Jones, and N. S. Wade, "Coordination of Multiple Energy Storage Units in a Low-Voltage Distribution Network," *IEEE Trans. Smart Grid*, vol. 6, no. 6, pp. 2906–2918, Nov. 2015.

[14] M. A. Abdullah, K. M. Muttaqi, D. Sutanto, and A. P. Agalgaonkar, "An Effective Power Dispatch Control Strategy to Improve Generation Schedulability and Supply Reliability of a Wind Farm Using a Battery Energy Storage System," *IEEE Trans. Sustain. Energy*, vol. 6, no. 3, pp. 1093–1102, Jul. 2015.

[15] O. Unigwe, D. Okekunle, and A. Kiprakis, "Smart coordination of battery energy storage systems for voltage control in distribution networks with high penetration of photovoltaics," pp. 1–6.

[16] R. Tonkoski, D. Turcotte, and T. H. M. El-Fouly, "Impact of High PV Penetration on Voltage Profiles in Residential Neighborhoods," *IEEE Trans. Sustain. Energy*, vol. 3, no. 3, pp. 518–527, Jul. 2012.

[17] "IEEE Standard for Interconnecting Distributed Resources with Electric Power Systems," *IEEE Std 1547-2003*, no. August, pp. 1–122, 2003.

[18] T. T. Teo, T. Logenthiran, W. L. Woo, and K. Abidi, "Advanced control strategy for an energy storage system in a grid-connected microgrid with renewable energy generation," *IET Smart Grid*, vol. 1, no. 3, pp. 96–103, 2018.

[19] M. Brenna *et al.*, "Automatic distributed voltage control algorithm in smart grids applications," *IEEE Trans. Smart Grid*, vol. 4, no. 2, pp. 877–885, Jun. 2013.

[20] M. Zeraati, M. E. Hamedani Golshan, and J. Guerrero, "Distributed Control of Battery Energy Storage Systems for Voltage Regulation in Distribution Networks with High PV Penetration," *IEEE Trans. Smart Grid*, pp. 1–1, 2016.

[21] E. McKenna and M. Thomson, "High-resolution stochastic integrated thermal–electrical domestic demand model," *Appl. Energy*, vol. 165, pp. 445–461, Mar. 2016.

[22] B. Venkatesh, R. Ranjan, H. B. Gooi, and S. Member, "Optimal Reconfiguration of Radial Distribution Systems to Maximize Loadability," *IEEE Trans. Power Syst.*, vol. 19, no. 1, pp. 260–266, 2004.

Towards benefit-stacking for grid-connected battery energy storage in distribution networks with high photovoltaic penetration

O. Unigwe[1] D. Okekunle[1] A. Kiprakis[1]

[1] School of Engineering, The University of Edinburgh, The King's Building, EH9 3DW, Edinburgh, UK.
{o.unigwe, d.okekunle, aristides.kiprakis} @ed.ac.uk

Abstract– This paper proposes an optimisation program for scheduling the operations of battery energy storage system (BESS) in a distribution network, in order to maximise energy arbitrage gains. BESS are increasingly being deployed for stationary applications in power systems globally. Due to the high capital cost of BESS deployment, it is necessary to have economic justification for investments. There are several applications of BESS in the power network such as frequency regulation, peak-shaving, voltage regulation, arbitrage and network upgrade deferral. Investors in BESS therefore aim to gain maximum 'stacked' benefits through the provision of these services. BESS, however, cannot be available to provide all these services at the same time and space. Commitment to one service often means inability to provide another at the same time. A linear program (LP) is used in this paper to schedule the charging and discharging of BESS in order to gain maximum benefit from energy arbitrage and peak shaving, while maximising the use of energy from installed photovoltaic (PV) systems. The objective also involves supplying network demand at the cheapest electricity cost at any time. The work in this paper is an integral part of a holistic optimisation of the BESS operations to participate in provision of multiple services. The aim is to create maximum economic benefits while maintaining operations in a system that promotes battery longevity. Simulations are carried out on a real low voltage (LV) distribution network to demonstrate the effectiveness of this approach.

Keywords– Battery energy storage system, distribution network, photovoltaic, distributed generation, linear program, optimisation.

I. INTRODUCTION

Battery energy storage systems (BESS) are increasingly being deployed across electric power networks globally. One of the major drivers for this development is the falling costs of renewable energy sources (RES), especially photovoltaic (PV) and wind. Another factor responsible for the increase in BESS usage across power networks is the falling costs of BESS due to increasing demand for batteries for transportation and consumer electronics [1]. BESS costs are expected to continue to decrease in the coming years [2], however, at present, the capital cost of BESS is still substantial. This necessitates justification for investment directed towards BESS, and thus a need to maximise benefits from installation.

Some of the value streams for BESS include energy arbitrage, frequency response, demand charge management, peak shaving, network upgrade deferral, loss reduction and voltage management [3]. BESS installation cannot commit to the provision of all the services at the same time, because commitment to one or a few often means the system is not available to provide other services. Therefore it is important to evaluate benefits from the various value streams available to the BESS and optimise its usage for maximum benefit.

Various studies have been carried out on cost-benefit assessment of BESS in power networks using different methods. Authors in [4] evaluated the use of BESS specifically for provision of primary and secondary frequency control. In [5], economic analysis was performed on different use cases of BESS, examining both lithium-ion and lead acid battery applications. The economic benefit of BESS due to deferral of network infrastructure upgrade was studied in [6]. Different methods are also employed in the solution of the BESS scheduling problem, with most of them involving some optimisation within constraints. In [7], mixed integer linear programming was used to evaluate economic benefits of BESS and PV in commercial buildings while interior point method was used in [8] to improve distributed generation and load hosting capability of distribution networks using BESS. The majority of work in this area focus on maximising the benefits gained by installation of BESS, while making the BESS operate in a way that prioritises longevity.

The work in this paper proposes a linear program (LP) optimisation technique to manage the scheduling of BESS in distribution networks with high PV penetration. This work forms an integral part of a holistic study of economic benefits of multiple value streams of BESS in power distribution networks – the 'benefits-stacking'. The focus of this part of the work is scheduling assignment by the optimiser to maximise the economic benefits gained through energy arbitrage, while simultaneously maximising the use of available PV power and satisfying network load demand using the cheapest energy sources available.

The paper is organised as follows: Section 2 presents the mathematical modelling of the BESS and the setup of the linear program. Implementation of the scheme is carried out in Section 3. Section 4 contains the results and discussions while Section 5 presents the conclusions and future work.

II. MATHEMATICAL MODEL

This section presents the mathematical modelling involved in the BESS scheduling problem. First, the modelling of the BESS operation and characteristics is presented, followed by the setting up of the linear program for optimisation.

1. Modelling the BESS

BESS operation in this paper is modelled considering the energy storage capacity, charge/discharge limits, maximum

and minimum depth of discharge (DOD), and efficiencies during charging/discharging. The DOD is the limit to which the BESS has been discharged, expressed as a percentage of the total capacity. Often, there is a specified constraint on the DOD to prevent damage of the energy storage.

The state of energy in the battery at any instant in time $E_{BESS}(t)$ is determined by the change in energy from the previous time instant, as expressed in (1).

$$\Delta E_{BESS} = E_{BESS}(t) - E_{BESS}(t-1) \tag{1}$$

The change in energy is dependent on the charge/discharge power of the BESS.

$$P_B(t) = \begin{cases} \frac{\Delta E_{BESS}}{\Delta t}.\eta_c^{-1} & P_B(t) > 1 \\ \frac{\Delta E_{BESS}}{\Delta t}.\eta_d & P_B(t) < 1 \end{cases} \tag{2}$$

where $P_{BESS}(t)$ is the charge or discharge power of BESS (positive for charging and negative for discharging), and Δt is the sampling or operation interval, η_d is the discharge efficiency and η_c is the charge efficiency. P_{BESS} will be the solution of the scheduling problem, containing the optimised power dispatch values for the period under consideration, given in (3).

$$P_B = \begin{bmatrix} P_B(1) \\ . \\ . \\ P_B(q) \end{bmatrix} \tag{3}$$

where q is the number of sampling instants within the period considered. For 15-minute and hourly sample intervals in a day, for example, q equals 96 and 24 respectively.

2. Linear program optimisation

A linear program is set up to optimise the scheduling of BESS in the network. The objective of the optimisation is to achieve maximum benefit from arbitrage, charging from cheapest electricity sources and discharging during high electricity prices, while obeying network constraints. This objective also coincides with peak shaving objective since peak load periods are also periods of higher electricity prices.

The objective function minimises the cost of delivering power to the network load, charging the BESS at minimum cost, especially during periods of high PV power production and discharging during peak demand periods. The objective function is presented in (4).

$$\min(C_j) = \sum_{t=1}^{q}\left[P_G(t).w_G(t) + \sum_{r=1}^{y} P_{PV}^{r}(t).w_{PV}^{r} + \sum_{s=1}^{z} P_B^s(t).w_B^s\right] \tag{4}$$

P_G is the power drawn from the grid, P_{PV} is the power from the PV while P_B is the charge or discharge power of the BESS. w_{PV} and w_B are the operating costs of the PV and the BESS respectively, while w_G represents the price of electricity purchased from the grid. y and z respectively are the total numbers of PVs and BESSs on the network. $r = 1,2 \ldots y$ and $s = 1,2 \ldots z$.

The objective function is subject to the following constraints:

$$SOC_{min}^{S}. \leq SOC^{S} \leq SOC_{max}^{S}. \tag{5}$$

$$P_L(t) = P_G(t) + \sum_{r=1}^{y} P_{PV}^{r}(t) + \sum_{s=1}^{z} P_B^s(t) \tag{6}$$

$$P_{PV}^{r}(t) \leq P_{PV\_PEAK}^{r} \tag{7}$$

$$P_{B,D\_MAX}^{S} \leq P_B^s \leq P_{B,C\_MAX}^{s} \tag{8}$$

$$P_{B,D}^{S}(t) = \frac{\Delta E_{BESS}}{\Delta t}.\eta_d \tag{9}$$

$$P_{B,C}^{S}(t) = \frac{\Delta E_{BESS}}{\Delta t}.\eta_c^{-1} \tag{10}$$

$$P_G(t) \leq P_{G\_PEAK} \tag{11}$$

$$\sum_{t=1}^{q}\left[\sum_{s=1}^{z}[P_{B,D}^{S}(t) \leq P_{B,C}^{S}(t)]\right] \tag{12}$$

The constraints for the DOD of the BESS are given in (5), where $SOC_{min}^{S}.$ and SOC_{max}^{S} are the minimum and maximum SOC of the s^{th} BESS. The power flow balance equation is given in (6), where P_L is the network load demand. The constraint on the amount of power produced by the PV is presented in (7), where P_{PV_PEAK} is the kilowatt peak rating of the PV. The constraint on the rate of charge or discharge of the BESS is given in (8), where P_{B,D_MAX}^{S} and P_{B,C_MAX}^{S} are the maximum discharge and charge rates respectively. The charge and discharge rates are given in (9) and (10) where η_d and η_c are the discharge and charge efficiencies respectively. In (11), the constraint for the maximum power drawn from the grid at the bulk supply point is given, where P_{G_PEAK} is the peak power. This constraint ensures peak shave. Constraint (12) specifies that during the given operation period, the amount of energy delivered by the BESS is not greater than the amount stored.

In this formulation, excess energy from the PV generators during high production periods are utilised for charging of the BESS, rather than exporting back to the grid after meeting the network load demand. In a time of use (TOU)

electricity market, electricity prices vary according to the cost of providing power during different times of the day. In this scheme, prices are highest during peak demand periods than otherwise. This means that overall, the BESS is charged at cheaper costs and discharged during peak periods when electricity prices are higher. This difference provides the energy arbitrage value, which is computed as given in (13).

$$\Omega_{TOU} = \sum_{t=1}^{q}\sum_{s=1}^{z}[P^{S}_{B,D}(t) - P^{S}_{B,C}(t)].w_G(t) \quad (13)$$

where Ω_{TOU} is the value obtained from arbitrage.

The lifetime of a BESS is represented by the total number of charge and discharge cycles of the unit before end-of-life is reached. This information is often provided by the manufacturer, and for most batteries, this represents the number of times the battery is cycled before it reaches 80 per cent of its initial energy capacity, expressed in (14).

$$E_t \leq 0.8E_{t_0} \quad (14)$$

In (14), E_t and E_{t_0} are the present and initial (first time) capacities, in Coulombs, of the BESS respectively.
The total number of cycles of BESS before (14) becomes satisfied is also a function of the DOD. The lower the DOD, the higher the number of cycles. Curves showing this relationship between the number of cycles to failure and the DOD are normally provided by the battery manufacturers, or can be estimated from field measurements. Figure 1 shows typical DOD/number of cycles relationship curve.

Depending on application, there could be varying and overlapping DOD during the operations of the BESS, rather than a constant DOD. For example, a cycle of 50% DOD could be followed by another cycle with 70% DOD. This makes it challenging to count accurately the number of cycles to end-of-life. In this situation, the rainflow counting algorithm [10] is used to capture the various cycle depths and therefore estimate more accurately the number of cycles to end-of-life. The expression for the rainflow counting is stated in (15).

$$C_F = a_1 + a_2 e^{a_3 R} + a_4 e^{a_5 R} \quad (15)$$

where C_F is the number of cycles to failure, $\{a_1, a_2, a_3, a_4\}$ are fitting constants, and R is the fractional depth of discharge (see Figure 1).

II. MATHEMATICAL MODEL

This section describes the test network and data used in the implementation of the linear program.

1. Network description

The distribution network shown in Figure 2 is used in this work [11]. It is a radial network with PV and BESS installations as shown. A 22/0.4 kV transformer supplies the feeder and 33 residential houses are connected to the feeder. For demonstrating the performance of the scheduling linear program, aggregate values for the load, PV and BESS are used in the simulations. The aggregate load values for the load and PV power respectively are $P_L = 66.75kW$ and $P_{PV} = 70kWp$. The BESS is also taken to be aggregated, with $P_B = 44kW$ and $E_{BESS} = 310kWh$. The discharge efficiency of the BESS is $\eta_d = 0.9$.

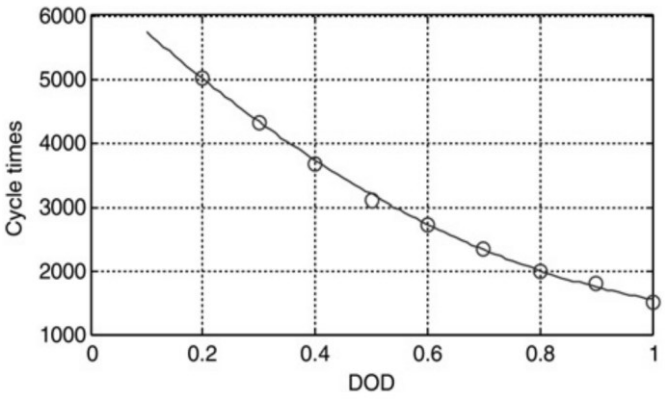

Figure 1: Number of cycles to failure vs depth of discharge [9]

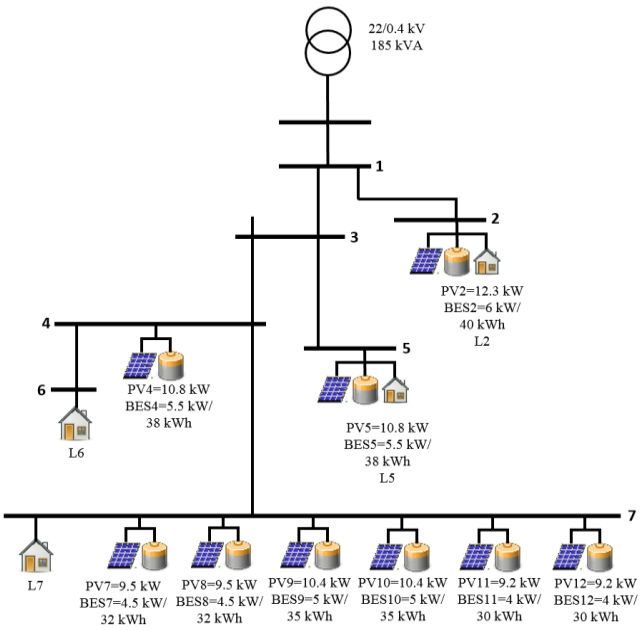

Figure 2: Diagram of test network

2. Description of profiles

The computational model developed by Centre for Renewable Energy Systems Technology (CREST) [12] was used to create the load profile. The tool was used to generate realistic demand profiles for 100 residential houses. Typical demand profile was obtained by averaging out 50 different profiles obtained from 100 residential houses. The resulting load shape was normalised and used as multiplier on the loads of the test network. Summer time profile generated using this method and used in this paper is shown in Figure 3.

A typical summer-time PV profile, also shown in figure 3 is used in the implementation. The values of the PV profile, like the load profile, are in per unit and used as multipliers for the actual kWp ratings of the PV units.

In the LP formulation, the prices of the electricity from the grid, PV and BESS are essential for decision making, since the objective is to supply load to the network using the cheapest available power resource. Day-ahead TOU prices for energy purchased from the grid is shown in Figure 4 [13].

III. Simulation Results and Discussions

Hourly simulations were carried out for a full day and the linear program was set up and solved using Matlab. The DOD of the BESS used is 0.9. Maximum charge and discharge rates were both $44kW$. The unsubsidised cost of energy for the PV used in this analysis was taken to be $w_{PV} = 4.6$ cents/kWh [14].

Figure 5 shows the voltage profile of the network without PV and BESS installations. It can be seen that before high penetration of PV and BESS, the voltage profile of the feeder fall within the regulatory upper and lower limits of 1.05 p.u and 0.95 p.u respectively (red dashed lines). In Figure 6, the power drawn from the grid, as measured at the feeder head, is shown. Relatively higher amount of power can be seen drawn during peak demand periods. Only the feeder head power profile is shown here since the study in this paper focuses on the aggregate demand.

Figure 7 shows plots of the optimal dispatch scheduling of the BESS, the power drawn from the grid, utilised PV power and the load. The optimisation aims to utilise all the available PV power produced during high solar irradiation, since this is cheaper, and also promotes the case for economic justification for PV installations. PV power is utilised, firstly to meet demand, followed by use for BESS charging. Any excess PV after this is either curtailed or has to be exported back to the grid. In this LP formulation, excess PV is exported to the grid. However, for the case study presented, all the PV power is fully utilised, and no power is returned back to the grid.

To maximise the arbitrage gain Ω_{TOU}, the BESS prioritises the use of the excess PV power for charging.

It can be seen that between 00:00 and 09:00, the BESS does not start charging with power from the grid. Charging only starts when excess PV power is available after meeting load demand. BESS is also incentivised to discharge during times of high electricity prices, which coincides with peak load periods, which is seen between 18:00 to 23:00.

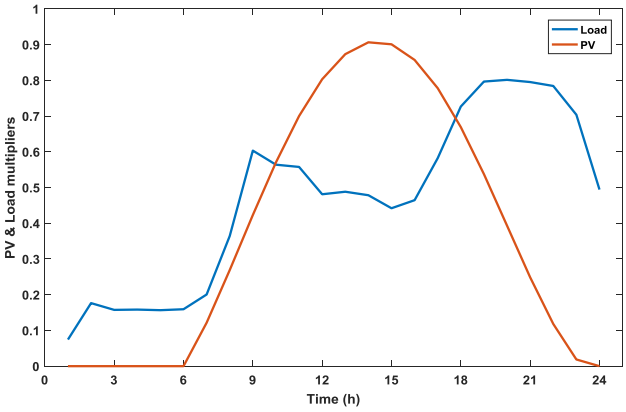

Figure 3: Load and PV generation profiles

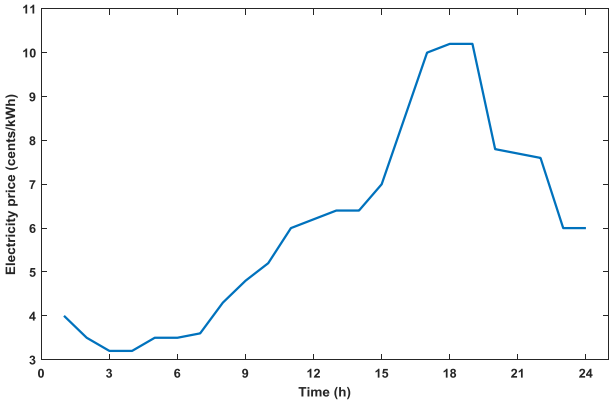

Figure 4: TOU electricity price profile [13]

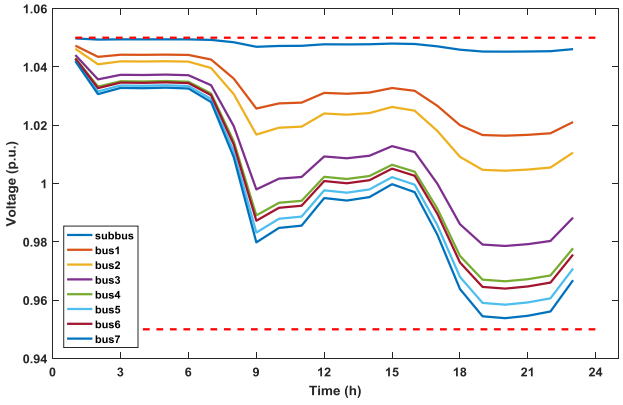

Figure 5: Feeder voltage profiles without PV and BESS

At 23:00, the maximum discharge power of the BESS ($44kW$) is not sufficient to meet demand, hence from this point, power is purchased from the grid. The minimal exchange of power between the network and the grid implies that the voltage profile of the network is maintained within regulatory limits, even with the high PV penetration, as there is no reverse power flow at any time.

The life characteristic curve for the typical lithium-ion battery used in this work adheres to the curve shown in Figure 1. With an average single cycle per day at 80% DOD, the number of cycles to failure is estimated as 2000,

corresponding to a period of 5.48 years. Hence, the rainflow algorithm given in (15) is not employed at this stage of the work. This will be utilised in future developments of this work, when daily simulations will be carried out using yearly data, for the lifespan of the BESS. The SOC of the BESS during the simulation period is shown in Figure 8.

For a 24-hour period and lifetime of the BESS, the arbitrage gain Ω_{TOU} is calculated by solving (13), and results are presented in Table 1. The results show a total energy arbitrage gain of USD 21,900. This is the value gained when exclusively considering purchasing energy at cheaper rates and delivering at higher rates.

III. CONCLUSION AND FUTURE WORK

This paper presented a linear program optimisation for scheduling BESS in a network with high penetration of PV, in order to maximise arbitrage gains. The algorithm achieved this while respecting all the BESS characteristic constraints and also meeting the network load demand using the cheapest available energy source at different times of the day. Overall, minimal energy was imported from the grid into the test network since the PV power was efficiently utilised by the optimisation.

The results obtained in this paper are based on the assumption that the day-ahead network load and PV power has been perfectly forecasted. However, this is hardly the case in real life and therefore is a limitation of this work. Practical systems will have to employ some control systems to handle variability of load and PV generation. The network losses are also assumed to be part of the base load demand, and are therefore not accounted for separately in this work.

As stated previously, BESS commitment to provision of one or more services results to unavailability to participate in the provision of some others. The work presented in this paper is a first step analysis which is integral to a holistic evaluation of stacked benefits of BESS on the power network. Future work involves the evaluation of other value streams, considering their benefits and peculiar inherent constraints. The end-goal is to develop a scheme that optimises the operation of the BESS to yield maximum benefit from several value streams in order to justify investment. Other factors that affect the overall economic valuation, such as load growth rate, cost of BESS installation and economies of scale will also be considered.

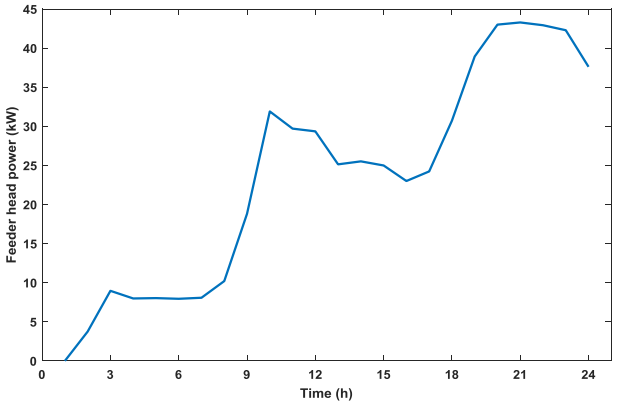

Figure 6: Power flows measured at the feeder head

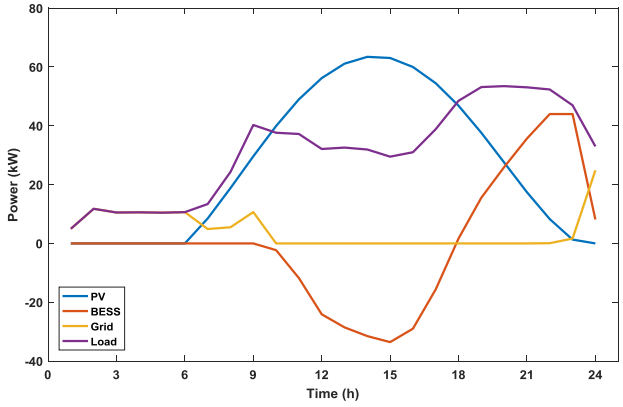

Figure 7: 24-hour BESS dispatch, grid energy import, load demand and PV power utilisation using LP algorithm

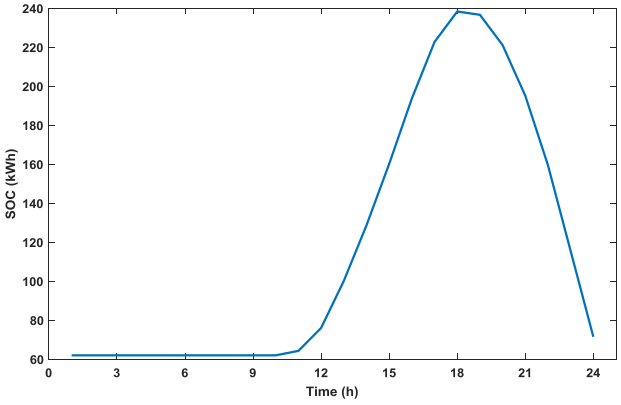

Figure 8: 24-hour profile of SOC of BESS

Table 1: Energy arbitrage values

	Daily ($)	Lifetime ($)
Cost of charging: $\sum_{t=1}^{q} P_{B,C}^{S}(t)$	8.04	16,080
Cost of discharging: $\sum_{t=1}^{q} P_{B,D}^{S}(t)$	18.99	37,980
Arbitrage gain: Ω_{TOU}	10.95	21900

IV. ACKNOWLEDGEMENTS

The authors would like to acknowledge support by the British Council UK - India Education & Research Initiative and the Indian Department of Science & Technology under grant 16/17-98 (D-DIEM: Data-Driven Intelligent Energy Management for Environmentally Sustainable Energy Access). Also the Petroleum Technology Development Fund (PTDF) by the Federal Government of Nigeria.

IV. REFERENCES

[1] B. Nykvist and M. Nilsson, "Rapidly falling costs of battery packs for electric vehicles," *Nat. Clim. Chang.*, vol. 5, no. 4, pp. 329–332, Apr. 2015.

[2] O. Schmidt, A. Hawkes, A. Gambhir, and I. Staffell, "The future cost of electrical energy storage based on experience rates," *Nat. Energy*, vol. 2, no. 8, p. 17110, Jul. 2017.

[3] C. A. Hill, M. C. Such, D. Chen, J. Gonzalez, and W. M. K. Grady, "Battery energy storage for enabling integration of distributed solar power generation," *IEEE Trans. Smart Grid*, vol. 3, no. 2, pp. 850–857, 2012.

[4] M. Benini, S. Canevese, D. Cirio, and A. Gatti, "Battery energy storage systems for the provision of primary and secondary frequency regulation in Italy," in *2016 IEEE 16th International Conference on Environment and Electrical Engineering (EEEIC)*, 2016, pp. 1–6.

[5] N. DiOrio, A. Dobos, and S. Janzou, "Economic Analysis Case Studies of Battery Energy Storage with SAM," *Natl. Renew. Energy Lab. Denver, CO, USA*, no. November, 2015.

[6] A. Thomas, T. K. Saha, S. R. Deeba, D. Chakraborty, and R. Sharma, "Evaluation of technical and financial benefits of battery-based energy storage systems in distribution networks," *IET Renew. Power Gener.*, vol. 10, no. 8, pp. 1149–1160, 2016.

[7] A. Mariaud, S. Acha, N. Ekins-Daukes, N. Shah, and C. N. Markides, "Integrated optimisation of photovoltaic and battery storage systems for UK commercial buildings," *Appl. Energy*, vol. 199, pp. 466–478, 2017.

[8] N. Jayasekara, M. A. S. Masoum, and P. J. Wolfs, "Optimal Operation of Distributed Energy Storage Systems to Improve Distribution Network Load and Generation Hosting Capability," *IEEE Trans. Sustain. Energy*, vol. 7, no. 1, pp. 250–261, Jan. 2016.

[9] J. Xiao, L. Bai, Z. Zhang, and H. Liang, "Determination of the optimal installation site and capacity of battery energy storage system in distribution network integrated with distributed generation," *IET Gener. Transm. Distrib.*, vol. 10, no. 3, pp. 601–607, Feb. 2016.

[10] J. F. Manwell *et al.*, "Hybrid2-A Hybrid System Simulation Model Theory Manual," 2006.

[11] M. Zeraati, M. E. Hamedani Golshan, and J. Guerrero, "Distributed Control of Battery Energy Storage Systems for Voltage Regulation in Distribution Networks with High PV Penetration," *IEEE Trans. Smart Grid*, pp. 1–1, 2016.

[12] E. McKenna and M. Thomson, "High-resolution stochastic integrated thermal–electrical domestic demand model," *Appl. Energy*, vol. 165, pp. 445–461, Mar. 2016.

[13] ComEd, "Real time hourly prices [Online]. Available: https://hourlypricing.comed.com/live-prices/."

[14] Lazard, "Levelised Cost of Energy Analysis," no. November, pp. 0–21, 2017.

The Journal of Engineering

The 7th International Conference on Renewable Power Generation (RPG 2018)

IET Journals
The Institution of Engineering and Technology

Smart coordination of battery energy storage systems for voltage control in distribution networks with high penetration of photovoltaics

eISSN 2051-3305
Received on 26th October 2018
Accepted on 10th January 2019
doi: 10.1049/joe.2018.9286
www.ietdl.org

Obinna Unigwe[1] ✉, Dahunsi Okekunle[1], Aristides Kiprakis[1]

[1]*School of Engineering, The University of Edinburgh, Edinburgh, UK*

✉ *E-mail: o.unigwe@ed.ac.uk*

Abstract: The use of battery energy storage systems (BESS) is one of the methods employed in solving the major challenge of overvoltage, experienced on low voltage (LV) distribution networks with high penetration of photovoltaics (PV). The overvoltage problem limits the penetration levels of PV into the LV network, and the benefits that could be gained. This paper presents a smart scheme for the coordination of multiple battery energy storage systems (BESS) in such networks. An approximate method was adopted for the evaluation of network voltage sensitivity, and the coordination algorithm was developed based upon this. Through the efficient selection, coordination and timing of charge and discharge operations of the BESS, the scheme maintains bus voltages within statutory ranges during both periods of high PV power generation and high network load demand. The scheme also prevents sudden voltage rise, which usually occurs in such networks immediately a BESS gets fully charged. Simulations were carried out on a real LV distribution network and results demonstrate the effectiveness of this approach.

1 Introduction

There has been an increasing acceptance and adoption of renewable energy sources (RES) globally, and there is an expectation that the penetration of low carbon technologies (LCT), especially in the low voltage distribution networks (LVDN), will continue to increase.

However, increased penetration of RES in the low voltage distribution networks can lead to power quality issues like reverse power flow and overvoltage, harmonics, line flickers and voltage unbalance [1]. Of these power quality issues, overvoltage presents a major challenge to increased penetration of RES. When there is more energy produced than consumed in a low voltage distribution network, overvoltage can occur – a situation where voltages rise beyond the statutory voltage levels.

A number of methods have been employed in solving the overvoltage problem. These include use of reactive power capability of the PV, active power curtailment, step voltage regulators, BESS and on-load tap changers. Many recent solutions for the increased adoption and penetration of PV in the distribution network are built around the use of BESS. This is because of the flexible active and reactive power control that BESS offers. Costs of BESS acquisition and installation are still high, but this is changing gradually. Costs have continued to drop in recent years due to the high interest in the development of batteries for electric vehicles and consumer electronics [2]. There is also an expectation that these falling prices will continue in the future [3].

There are, however, other challenges encountered in the use of BESS for the purpose of enabling higher penetration levels of PV energy, other than high costs. One of the challenges is the efficient coordination of operations of the BESS in the network. Different strategies have been proposed for solving this problem [4, 5]. Another challenge, according to the work in [6], is the sudden voltage rise when a significant BESS under charge reaches maximum state of charge (SOC) while there is still high active power generation from the PV.

This paper presents a scheme for the coordination of multiple BESS used in distribution networks with high PV penetration. An approximate method was adopted for the evaluation of network voltage sensitivity, upon which an algorithm was developed. The objective of the coordination scheme is to maintain network voltages within statutory range (mitigate overvoltage and undervoltage) through efficient selection and coordination of the operations of installed BESS, doing this in a manner that is healthy for the BESS.

The work is organised as follows: Section 2 provides methodology and description of the proposed algorithm. Section 3 describes the implementation of the scheme on a network. Section 4 presents the results followed by discussions and finally in Section 5, conclusions are drawn.

2 Methodology for coordination scheme

Before the operational flow of the coordination scheme is presented, the following subsections will describe some important components and operational structures of the scheme, and also factors considered in developing the algorithm.

2.1 Voltage sensitivity for BESS selection

Voltage sensitivity factor (VSF) provides the relationship between changes in bus voltage as result of changes in active or reactive power at various buses of a network. This relationship is determined normally by the Jacobian matrix given in (1).

$$\begin{bmatrix} \Delta\theta \\ \Delta|V| \end{bmatrix} = J^{-1} \begin{bmatrix} \Delta\theta \\ \Delta Q \end{bmatrix} \tag{1}$$

where

$$J = \begin{bmatrix} \frac{\delta P}{\delta\theta} & \frac{\delta P}{\delta V} \\ \frac{\delta Q}{\delta\theta} & \frac{\delta Q}{\delta V} \end{bmatrix}$$

$\Delta\theta$ is the change in bus voltage angle, ΔV is the change in bus voltage, ΔQ is the change in reactive power and ΔP is the change in active power. Equation (1) presents sensitivities for both voltage magnitude and angle. Focusing on ΔV, which is of more interest in the distribution network, the expression simplifies to (2).

$$\Delta|V| = \begin{bmatrix} \frac{\delta V}{\delta P} & \frac{\delta V}{\delta Q} \end{bmatrix} \cdot \begin{bmatrix} \Delta P \\ \Delta Q \end{bmatrix} \tag{2}$$

In relation to the work presented in this paper, voltage sensitivity is important for the initial selection of the BESS to be deployed for charge/discharge operations during overvoltage, under-voltage or peak-shaving conditions. ΔP here is represented by the charge or discharge power of the BESS under consideration and ΔV is considered at the node where the voltage change is targeted. Using the voltage sensitivity matrix ensures that the optimal BESS is selected, that has the most effective impact on the bus that is near, or already experiencing, voltage excursion.

The Jacobian matrix method of obtaining the sensitivities on the network, however, is computationally complex. Therefore an alternative method proposed in [7] is adopted in this work. This method is an approximate evaluation, with results that are very close to those obtained using (1) directly. This method is summarised in (3) and (4) as follows:

$$\frac{\delta E_i}{\delta P_j} = -\frac{1}{E_n}\left[\sum_{hk \in PT_{i,j}} R_{hk}\right] \tag{3}$$

$$\frac{\delta E_i}{\delta Q_j} = -\frac{1}{E_n}\left[\sum_{hk \in PT_{i,j}} X_{hk}\right] \tag{4}$$

where E_n is the approximate rated voltage of the network; R_{hk} and X_{hk} are the resistance and reactance of branch hk respectively; $PT_{i,j}$ is the set of nodes contained in the path connecting the medium voltage (MV) busbar to nodes i and j, and at the same time common to both nodes.

Sensitivity ranking matricesB_P for real power and B_Q for reactive power are formed using (3) and (4). Only B_P is shown in (5). B_Q is formed similarly to B_P but not shown as the work presented in this paper focuses only on active power dispatch by the BESS.

$$B_P = \begin{bmatrix} \frac{\delta E_1}{\delta P_1}\Delta P_1 & \cdots & \cdots & \frac{\delta E_1}{\delta P_N}\Delta P_M \\ \cdots & \cdots & \cdots & \cdots \\ \cdots & \cdots & \cdots & \cdots \\ \frac{\delta E_M}{\delta P_1}\Delta P_1 & \cdots & \cdots & \frac{\delta E_M}{\delta P_M}\Delta P_M \end{bmatrix} \tag{5}$$

M represents the total number of buses on the network and $m = 1,2 \ldots M$ represents any specific bus on the network.

On a particular row (representing the node whose voltage is of interest at the time), the column (representing BESS locations) with the maximum value is selected as the best suited for affecting voltage at that node of interest. The BESS on that column bus therefore is selected and designated BES_{sel}. This selection applies for the time instant during which this evaluation is executed by the algorithm. For the next time instant this ranking is evaluated, it excludes the BESS that has already been previously selected. The section of the algorithm that doses this selection is called the selection evaluator (SE) throughout the rest of this work. For the expression in (5), during the implementation of the algorithm, the buses without BESS installation are set as zero.

2.2 BESS state of health

The state of health (SOH) of a battery defines its remaining lifetime. For an estimation of the lifetime of the BESS, two factors relating to ageing are considered. The first is ageing as a result of number of cycles used up by the battery, and the second is capacity loss that occurs when BESS is in idle mode (not in operation).

The cycle life of BESS is the number of charge/discharge cycles that it experiences before it gets to a state where it can no longer meet basic minimum technical expectations. In many cases, a battery reaches its end-of-life when (6) holds true:

$$C_t \leq 0.8C_{t_0} \tag{6}$$

where C_t and C_{t_0} are present and initial (first time) battery capacities in Coulombs respectively. The larger the number of cycles on a BESS, the closer it gets to the end of its life. The depth of discharge (DOD) of a BESS, expressed as a percentage, is the difference between the minimum and maximum SOC during each cycle [8]. Some battery technologies are sensitive to DOD and higher DOD can reduce the life expectancy. In this work, therefore, the constraint on the DOD of the BESS is maintained according to (7).

$$0.2 \leq \text{DOD} \leq 0.9 \tag{7}$$

2.3 Description of sets used in algorithm formulation

The sets described below are maintained and updated by the algorithm at each time step as the operation advances.

a. a $\boldsymbol{P_{BES}}$**:** This is the set of active power ratings of all BESS on the network.

$$P_{BES} = \{P_{BES_n} : n = 1, 2, \ldots N\} \tag{8}$$

where P_{BES_n} is the active power rating of the BESS connected to bus n, N is the total number of buses on the network. Observe that $P_{BES_n} = 0 \forall n \in Z$ holds true, where Z is the set of all buses that have no BESS installation.

b. b $\boldsymbol{BES_{sel}}$**:** This is the set of all BESS that have been selected by the SE and activated for charging or discharging.

$$BES_{sel} = \{BES_{sel_n} : n = 1, 2, \ldots N\} \tag{9}$$

where BES_{sel_n} is an output from the SE which denotes the BESS that has been selected for charging. $BES_{sel} = 2205$ holds true as an initial condition at the start of operations. BES_{sel_l} is used to denote the last BESS that has been added to BES_{sel}.

c. c $\boldsymbol{CR}$**:** This is a set of the charge or discharge rates of corresponding selected BESS contained in BES_{sel}

$$CR = \{CR_n : n = 1, 2, \ldots N\} \tag{10}$$

where CR_n is the charge rate of the corresponding BES_{sel_n}. Similar to BES_{sel}, $CR = \emptyset$ holds true at the start of operations. CR_l is used to denote the charge rate of BES_{sel_l} and CR_{max} denotes the maximum charge rate of any BESS.

d. d $\boldsymbol{\Omega_{soc}}$**:** This set contains the changing SOC of all the BESS on the network. The algorithm uses this to have knowledge of which BESS are fully charged, or nearly fully charged in order to take proactive actions. The latter is one of the objectives the scheme aims to achieve.

2.4 Description of coordination algorithm operation

The flow of operations of the algorithm is shown in the flowchart of Fig. 1. The algorithm becomes operational from when the condition $V_{LTH} \leq V_m \leq V_{UTH}$ is violated, where V_m is monitored bus voltages, V_{LTH} is the statutory lower threshold voltage and V_{UTH} is the statutory upper threshold voltage. $V_m > V_{UTH}$ is more likely to occur first if the algorithm operation proceeds from the first hour of the day, as a result of possible overvoltage due to peak PV generation.

The SE outputs BES_{sel_n} (which goes into charging mode), and a corresponding CR_n is also evaluated. CR_n is the amount of power that keeps V_{diff} at zero. For the first time the algorithm calls a BESS into charge mode, BES_{sel_n} is designated BES_{sel_1}. Equation (12) derives from (5) for the evaluation of CR.

$$CR_n = V_{diff} \cdot \left(\frac{\delta V_m}{\delta P_n}\right)^{-1} \tag{11}$$

where $(\delta V_m/\delta P_n)$ in (11) is the sensitivity V_m to the bus of BES_{sel_n}

At any point while the algorithm executes, in the event that CR_l is no longer large enough to maintain V_{diff} at zero, possibly as a result of sustained increase in active power production from PV, a new BESS is added to the BES_{sel} set. This selection by the SE will exclude any BESS that is already contained in BES_{sel}. Updating the Ω_{SOC} informs the algorithm of the SOC status of each BESS as operations proceed. With this, new BESS are able to be appointed just before any battery is fully charged. The prevailing impact on bus voltages, of the BESS that most recently became fully charged, is also considered.

For the peak shaving operation, the algorithm switches the BESS to discharge mode when the condition $V_m < V_{LTH}$ is satisfied. This will usually occur during peak demand periods. A procedure similar to the charging operations is followed for the peak shave or discharging mode. In this mode, the algorithm replaces V_{UTH} with V_{LTH} (in the evaluation of V_{diff}), causing V_{diff} to return negative values, and consequently negative values of CR_n. Negative CR_n values represent discharge signals to the BESS.

3 Implementation of coordination algorithm

This section describes the tools, test network and implementation considerations made in demonstrating the performance of the coordination scheme.

3.1 Implementation tools

The distribution network used as a case study in the implementation of the coordination scheme was developed using OpenDSS [9], an open source tool developed by Electric Power Research Institute (EPRI). The algorithm for the coordination control was developed in MATLAB. The Component Object Model (COM), which is made available in OpenDSS, was used as an interface to effect the controls on MATLAB to the network model on OpenDSS.

3.2 Description of distribution network

The scheme is demonstrated using a Belgian low voltage residential network [10]. The network is a radial 7-bus feeder with 4 out of the 7 buses (buses 2, 4, 5 and 7) having PV installations. The feeder is supplied through a 22/0.4 kV transformer rated 185 kVA. The network diagram is shown in Fig. 2. 33 residential houses are connected on the feeder, with PV installations that total 42.6 kW. Six PV installations are located on bus 7 while buses 2, 4 and 5 contain single installations each. The values of the installations are as shown in Fig. 2. On each bus containing PV, BESS is installed and the capacities are also shown in Fig. 2.

For adaptation of the network to the structure of the algorithm, the BESS on the network are named according to the buses they are connected to. Multiple BESS on bus 7 are numbered from 7 to 12.

3.3 Demand and generation profiles

The load profile was created using the computational model developed by Centre for Renewable Energy Systems Technology (CREST) [11]. The CREST tool generates realistic daily profiles with one-minute resolution for residential loads. Load profiles for an aggregate of 100 houses were generated using the CREST tool. 50 different aggregations were averaged out to obtain a typical representation of demand in a residential low voltage distribution network. The resulting load shape was normalised and applied as multipliers on the test network loads. The demand profile is shown in Fig. 3. Summer-time load profile was generated to capture period of high PV generation.

The PV profile used in this work, also shown in Fig. 3, is a generic summer-time solar irradiation profile and represents average typical behaviour of PV output power. Similar to the demand profile, the PV profile is applied to the kWp values of the PV on the test network.

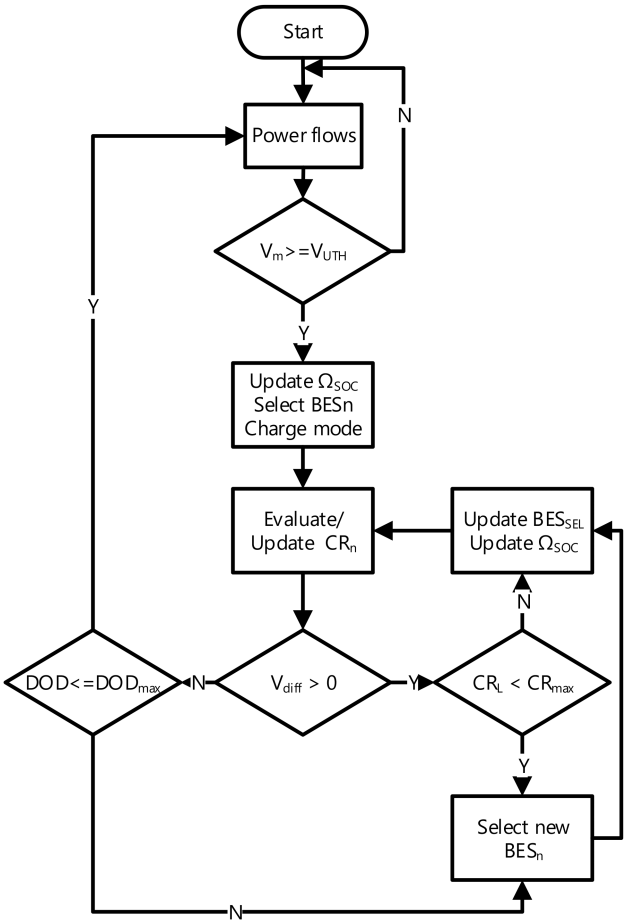

Fig. 1 *Flowchart of coordination scheme (overvoltage)*

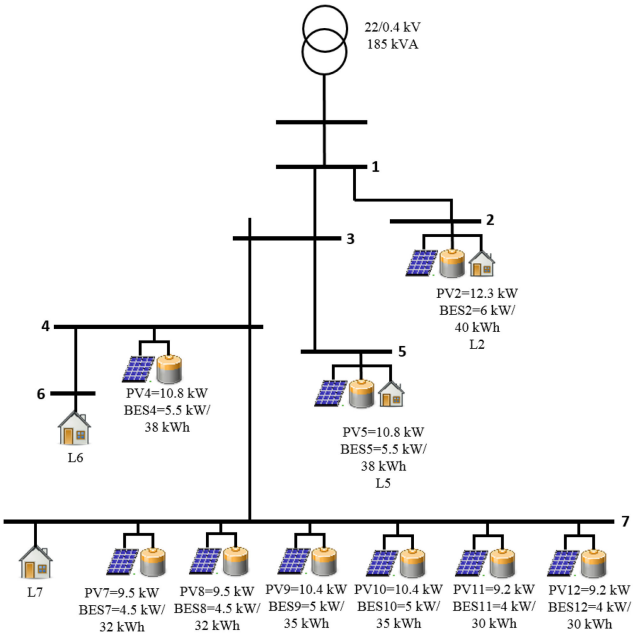

Fig. 2 *Diagram of test network*

4 Simulation results and discussions

Simulations were run for an entire day to demonstrate the operation of the algorithm, with a resolution of one minute. This also formed the time step for the algorithm – a total of 1440 time steps – since the PV and demand data were both obtained at resolutions of one minute. Other configuration parameters used in the simulations are as follows: $V_{UTH} = 1.05$ p.u, $V_{LTH} = 0.98$ p.u, $CR_{max} = 90\%$, $20\% \leq \text{DOD} \leq 90\%$. The substation voltage was set at 1.04 p.u in order to accommodate the voltage drop along the feeder.

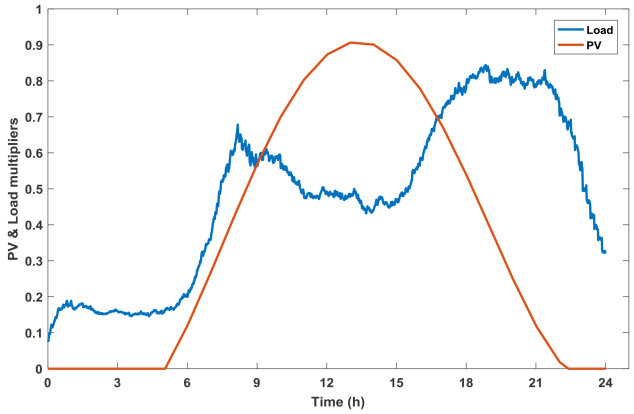

Fig. 3 *Load and demand profiles*

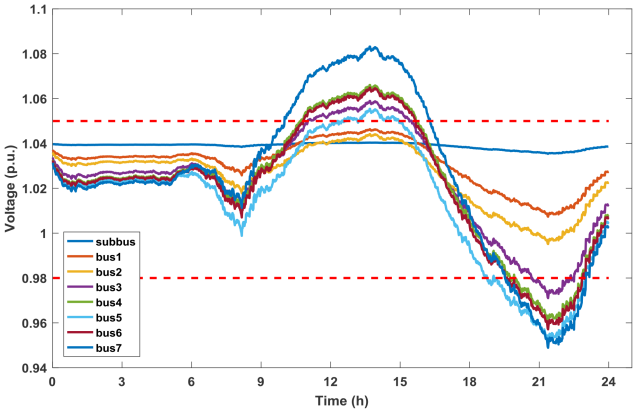

Fig. 4 *Feeder voltage profile without controls*

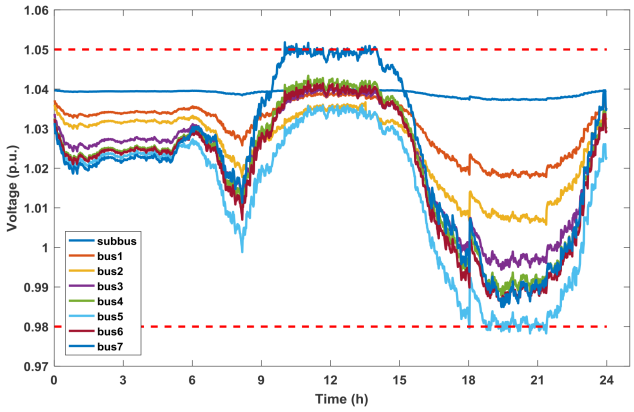

Fig. 5 *Feeder voltage profile with coordination control*

Fig. 4 shows the voltage profile of the network when there is no control scheme in place. It can be seen that the voltages exceed the statutory V_{TH} during the period of high PV production. This situation will lead to curtailment of excess active power, thereby reducing the economic benefits of PV installation. Also during the peak load period, there is occurrence of undervoltage on the network.

Fig. 5 shows the voltage profile of the network with the coordination algorithm in operation. Bus 7 is the end bus on this network and the first to experience voltage excursion. The coordination algorithm is activated when the voltage at bus 7 exceeds the upper threshold ($V_{m7} > V_{UTH}$). This occurs around the 10th hour, as shown in Fig. 5. BES_9 is switched to charging mode first as it is the highest ranking on the SE. BES_{10} could also have been switched first since it has the same ranking as BES_9, given that they both have the same power ratings, availability according to Ω_{SOC} and are both positioned on the same bus. BES_{10} is

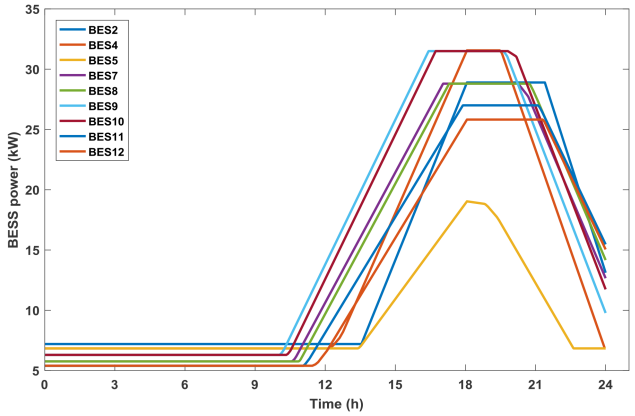

Fig. 6 *SOC of network BESS*

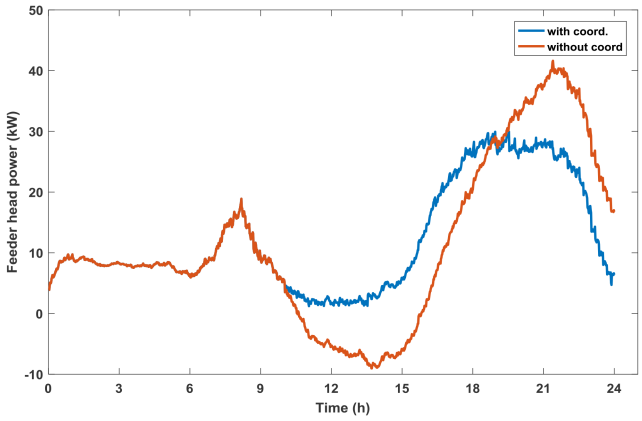

Fig. 7 *Power flows measured at the feeder head*

switched to charging mode shortly after BES_9. This happens after CR_9 reaches CR_{max}, and $V_{diff} > 0$ still persists.

The other BESS are sequentially switched to charging mode as PV power production continues to increase. The coordination control algorithm also ensures there are no sudden voltage rises, especially when a BESS charges to maximum capacity. This accomplishes one of the aims of this work. Fig. 5 also shows that the regulation of the voltage at the boundary is not exact but very close. One reason for this is that the method used to obtain the sensitivity matrix is an approximation. The benefit of the method, however, is its low computational complexity. Another reason is non-linearity of the elements of the distribution network.

During periods of heavy loading on the network, discharge signals are sent to appropriate BESS. As seen in Fig. 5, this is activated around the 18th hour when $V_5 < V_{LTH}$ occurs. BES_5, which is the most effective BESS for impact on bus 5, is switched to discharge mode first. Charging is discontinued for any BESS still in charging mode (BES_2 for example), and other BESS are sequentially switched to discharge mode according to the results of the evaluation in the SE at each time step. Undervoltage is prevented with the coordination control on the network (Fig. 6).

Fig. 7 shows that there is reverse power flow from the LV network to the MV network without the coordination control. There is also very large power drawn from the MV network during peak periods, which could lead to thermal ratings being exceeded or the need for infrastructure upgrade. There is a significant difference from this when the coordination control is deployed on the network.

5 Conclusion

In this work, an approximate method of voltage sensitivity evaluation was used to obtain a sensitivity ranking matrix, and based on this, a BESS coordination algorithm was developed for use in LV distribution networks with high PV penetration and multiple BESS. The algorithm was demonstrated to be effective in

coordinating the selection of BESS for charging or discharging at different times during operation.

The coordination control scheme also successfully mitigated overvoltage on the network during periods of high PV generation and prevented undervoltage from occurring during periods of high load demand on the network. Finally, the scheme was effective in preventing reverse power flows into the MV network and also reducing the power drawn from the MV network.

The latter benefits the network by ensuring thermal limits are not exceeded and that infrastructure upgrades are not needed immediately.

Since the method presented in this work is based on the voltage sensitivity characteristics of the network, the sensitivity matrix will need to be recomputed and updated in the event of any significant modifications on the network, or if the method were to be applied on a different network. Investigations on the performance of the method over the entire lifetime of the BESS, in comparison to other methods, is ongoing. This investigation will include performance evaluation as it relates to the health, economics and different technologies of BESS.

6 References

[1] Tonkoski, R., Turcotte, D., El-Fouly, T.H.M.: 'Impact of high PV penetration on voltage profiles in residential neighborhoods', *IEEE Trans. Sustain. Energy*, 2012, **3**, (3), pp. 518–527

[2] Nykvist, B., Nilsson, M.: 'Rapidly falling costs of battery packs for electric vehicles', *Nat. Clim. Chang.*, 2015, **5**, (4), pp. 329–332

[3] Schmidt, O., Hawkes, A., Gambhir, A.*, et al.*: 'The future cost of electrical energy storage based on experience rates', *Nat. Energy*, 2017, **2**, (8), p. 17110

[4] Alnaser, Sahban, Ochoa, L. F.: 'Optimal sizing and control of energy storage in wind power-rich distribution networks'. 2016 IEEE Power and Energy Society General Meeting (PESGM), 2016, pp. 1–1

[5] Lee, S.-J., Kim, J-H., Kim, C-H.*, et al.*: 'Coordinated control algorithm for distributed battery energy storage systems for mitigating voltage and frequency deviations', *IEEE Trans. Smart Grid*, 2016, **7**, (3), pp. 1713–1722

[6] Unigwe, O., Okekunle, D., Kiprakis, A.: 'Economical distributed voltage control in low-voltage grids with high penetration of photovoltaic', *CIRED – Open Access Proc. J.*, 2017, **2017**, (1), pp. 1722–1725

[7] Brenna, M., De Berardinis, E., Carpini, L.*, et al.*: 'Automatic distributed voltage control algorithm in smart grids applications', *IEEE Trans. Smart Grid*, 2013, **4**, (2), pp. 877–885

[8] Hutchinson, R.: 'Temperature effects on sealed lead acid batteries and charging techniques to prolong cycle life', 2004.

[9] Dugan, R.C., Montenegro, D.: 'Reference Guide the open distribution system simulator (OpenDSS)', 2018.

[10] Zeraati, M., Hamedani Golshan, M.E., Guerrero, J.: 'Distributed control of battery energy storage systems for voltage regulation in distribution networks with high PV penetration', *IEEE Trans. Smart Grid*, 2016, **9**, (4), pp. 1–1

[11] McKenna, E., Thomson, M.: 'High-resolution stochastic integrated thermal–electrical domestic demand model', *Appl. Energy*, 2016, **165**, pp. 445–461

24th International Conference & Exhibition on Electricity Distribution (CIRED)

12-15 June 2017

Session 4: Distributed energy resources and active demand integration

Economical distributed voltage control in low-voltage grids with high penetration of photovoltaic

ISSN 2515-0855
doi: 10.1049/oap-cired.2017.1227
www.ietdl.org

Obinna Unigwe ✉, *Dahunsi Okekunle*, *Aristides Kiprakis*

University of Edinburgh, Edinburgh, UK
✉ *E-mail: o.unigwe@ed.ac.uk*

Abstract: This study presents an economical distributed control scheme for operations in the low-voltage network. The scheme aims to keep bus voltages within the desired statutory range of values while increasing the penetration of solar photovoltaic (PV) renewable energy within the network. Rather than curtailment, battery energy storage system (BESS) is first brought to action by the controllers during periods of high output from PV. This is followed by reactive power action if overvoltage persists, and finally PV power curtailment as a last option. Simulations carried out on the test network show that in addition to successful overvoltage mitigation, the scheme is economical as it employs use of fewer BESS.

1 Introduction

In recent decades, considerable research and investment has gone into the development of cleaner renewable energy sources (RES) such as PV. However, increased penetration of RES into the traditional grid has lead to problems of power quality, especially in distribution networks where a significant portion of these RES are connected. The power quality issues include voltage unbalance, overvoltage, line flickering and harmonics. Of these problems, overvoltage presents the major limiting factor to increased levels of penetration of RES into the grid. Overvoltage arises when the consumption on a feeder is below the production, causing voltages to increase beyond statutory levels [1].

Use of the reactive power capabilities of the PV inverters alongside active power curtailment is one method for solving the overvoltage problem. For this method, reactive power absorption is employed during overvoltage, followed by active power curtailment if the reactive power absorption is insufficient [2]. The problem with this approach is that curtailment of active power means that the gains from investment in PV are not maximised.

Using step voltage regulators and on-load tap changers are traditional voltage control methods. However, these technologies, in the presence of high PV penetration, are exposed to stress, leading to degradation and reduced lifetimes [3]. Incorporating battery energy storage system (BESS) in networks with PV systems is a promising solution to the overvoltage problem as it provides flexible real power control within the network.

The inverters of PV systems are capable of providing reactive power services for the networks to which they are connected. This feature can be further explored in achieving voltage control together with the use of BESS.

This work presents a distributed control scheme for promoting greater penetration of PV on the distribution network while keeping voltages within the statutory range. In this scheme, during high PV generation that leads to overvoltage, the BESS is brought into action by the controllers. The reactive power resource of the PV inverters is then utilised if the BESS action fails to solve the overvoltage problem. Curtailment of PV active power (P_{PV}) is carried out as a last option if the previous two measures fail.

2 Distributed control scheme

Distributed control is used for the management of the network to keep voltages within designated limits. The controllers are located on every node where PV is installed. Minimal communication is required in this distributed control scheme as inverters on the same feeder only need to send distress signals across the feeder using cheap and available power line communication. An advantage of the distributed control is that there is no singular possible point of failure as is obtainable in centralised control schemes. Another advantage of the distributed scheme is that knowledge of the entire network state is not needed for the control. This scheme depends only on local measurement of voltages (V_{meas}) at the nodes for decisions and actions of the controllers. Fig. 1 illustrates the different sections of the control scheme.

The different parts of operation of this distributed control scheme are described in the following subsections.

2.1 Normal operations

In this state, the measured terminal voltage V_{meas} remains below the set voltage limit (V_{lim}) ($V_{meas} < V_{lim}$). No action is required by the controllers in this state since no set voltage limits are violated. This happens usually when P_{PV} is less than the total load demand P_{DEM}.

2.2 BESS charging

A local controller switches to this state of operation when V_{meas} reaches the V_{lim} ($V_{meas} \geq V_{lim}$). Usually, this happens in the day time when there are high values of P_{PV} that exceed load demand. When this occurs, an overvoltage signal is sent across the feeder by the controller located at the node of occurrence of overvoltage, to notify other controllers.

BESS charging starts in a bid to consume the excess PV power, thereby preventing overvoltage P_{BATT} refers to the total power consumed by the batteries at any time.

2.2.1 PV power curtailment: The controllers switch to this state as a result of one of two conditions. The first condition is when BESS charging occurs simultaneously with overvoltage. P_{PV} being higher than the sum of P_{BATT} and P_{DEM} ($P_{PV} > P_{BATT} + P_{DEM}$) is a common cause of this situation. The second condition is when batteries are full, reactive power action has been taken (described in the next section), yet an overvoltage signal persists.

For any of these two conditions, a curtailment algorithm is run by the controllers to determine the minimum amount of active power to curtail in order to mitigate the overvoltage.

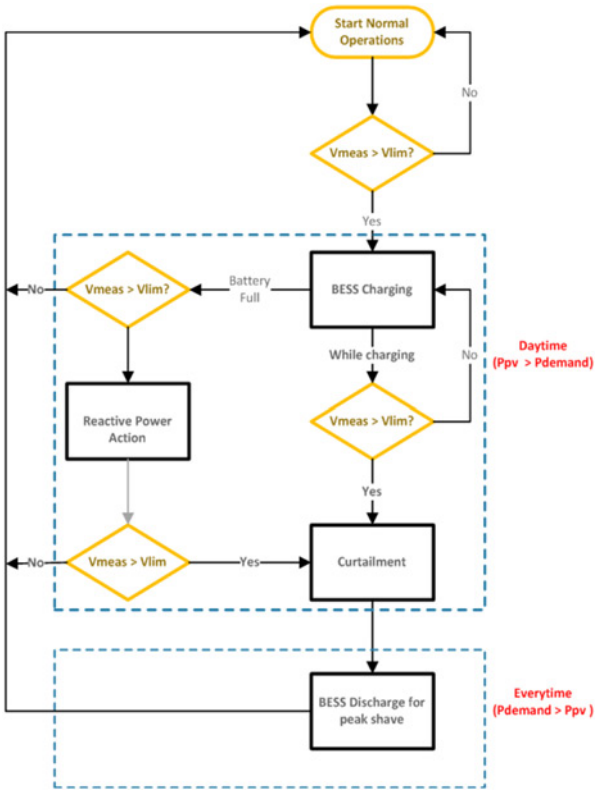

Fig. 1 *Distributed control scheme operation*

2.2.2 Reactive power absorption: This state is reached by the controllers when the batteries are fully charged and an overvoltage signal is still being received. Power quality – in this case appropriate voltage levels – on the distribution network can be improved by the use of PV inverters. The use of PV inverters for this purpose, however, comes under regulations by different countries. The specific country grid code defines whether this feature is allowed or not, as well as the permitted capability curve to be used. Fig. 2 shows the capability curve of for a typical PV inverter.

PV inverters do not infinitely sink or source reactive power [4]. The maximum reactive power $q_{\max}$ that can be provided by the inverter is limited by the inverter's rated apparent power s_{PV} and the current active power generation $P_{(k)}$.

The relationship between these quantities is given as

$$q_{(k)} \leq \sqrt{(s_{\mathrm{PV}}^2 - p_{(k)}^2)} \equiv q_{\max} \tag{1}$$

where $q_{(k)}$ is the reactive power available during real power output $p_{(K)}$. An oversized inverter, indicated by the dashed semi-circle in Fig. 2, is capable of reactive power support even when active power production is at maximum.

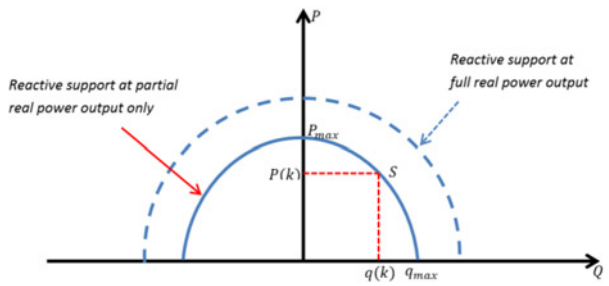

Fig. 2 *Inverter capability curve*

2.2.3 BESS peak-shave discharging: The controllers switch to this state when the power demand on the network exceeds a set power threshold P_{TH}. This usually occurs during times when P_{DEM} is much higher than P_{PV}. The BESS are made to start discharging during this peak loading period. Peak-shaving is important as it avoids the installation of additional capacity in the network to for the purpose of meeting peak demands.

3 Implementation of control scheme

This section describes the tools, data and test network used to illustrate the distributed control scheme.

3.1 Implementation tools

The algorithm for the distributed control scheme was developed in MATLAB and the distribution network models and resources were developed using OpenDSS. OpenDSS is an open source distribution network systems tool developed by Electric Power Research Institute. It has the component object model which enables it to interact with MATLAB and other similar programming tools. MATLAB was further utilised for all the analysis carried out in this work.

3.2 Test network

The operation of the control scheme is illustrated using a single feeder distribution network, which is a section of the network presented in [5]. It has been modified for the purpose of this implementation. The diagram of this single feeder is shown in Fig. 3.

The single feeder consists of ten nodes with PV units and loads installed on each of the nodes. The PV units are each rated 32.5 kWp and the equivalent load on a single node is rated at maximum 15 kVA apparent power. Different numbers of BESS are added on different nodes of the network to create different scenarios as discussed in the next sections. Each BESS is rated at 120 kWh with state of charge of 30% and an external dispatch mode $V_{\mathrm{lim}} = 1.07$ p.u. is used as the voltage limit for this study.

3.2.1 Load demand and PV profile inputs: The load demand and PV power profiles used for the simulations are shown in Fig. 4.

The maximum PV value is 32.5 kWp while the maximum load value is 15 kVA. Both profiles are generic, representing typical characteristics of daily PV power output and daily residential demand. The profiles have not considered the fast variability and intermittent nature of load demand and PV output power,

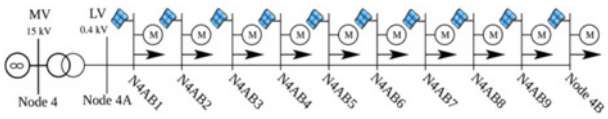

Fig. 3 *Single distribution network feeder*

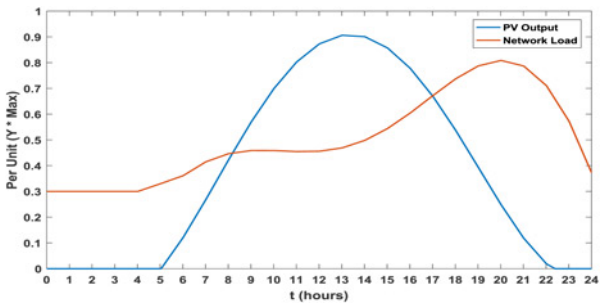

Fig. 4 *Load demand and PV profiles*

respectively. This notwithstanding, the profiles provide a fair representation.

4 Simulation results

Daily simulations of 1 min resolution (1440 min) are used throughout the study P_{PV} and demand data are therefore also in 1 min resolutions. The simulation cases highlight effects on the network characteristics (especially voltage) for different combinations of control. Knowledge of the amount of active power curtailed for each case is also important as this highlights the benefits of having this control.

4.1 Case 1

In this case, the network behaviour is observed with the penetration of PV, without application of the distributed control scheme. A plot of the voltage profile is shown in Fig. 5.

Overvoltage occurs on most of the nodes when no control actions are taken. Fig. 6 shows the voltage profile when the excess P_{PV} is curtailed in order to avoid overvoltage. This is achieved by employing the algorithm for curtailment only. Fig. 7 shows the amount of active power curtailed.

V_{meas} for Node4B reaches V_{lim} at $t = 485$ min (just after the 8th hour). The total energy curtailed is 94.5 kWh

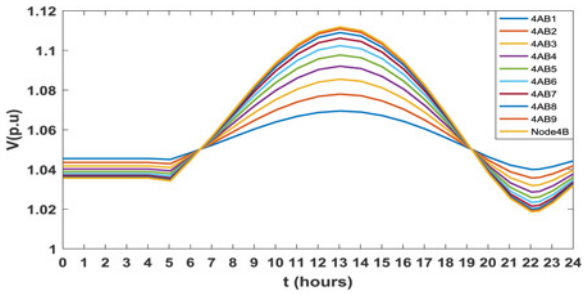

Fig. 5 *Feeder voltage profile without controls*

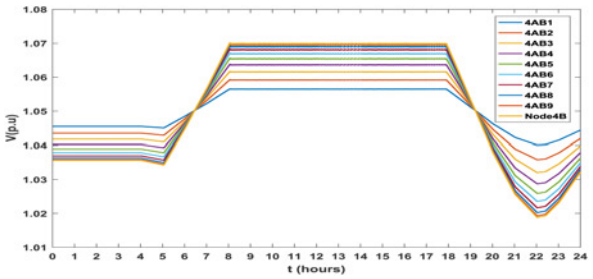

Fig. 6 *Feeder voltage profile with curtailment only*

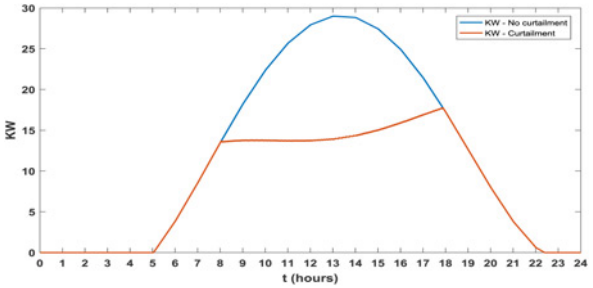

Fig. 7 *PV active power curtailment*

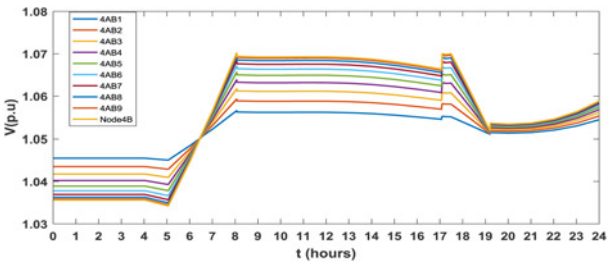

Fig. 8 *Feeder voltage profile for case 2*

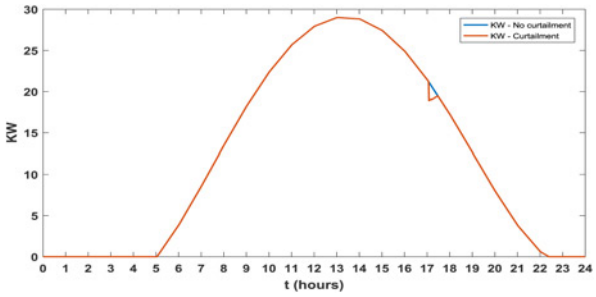

Fig. 9 *PV active power curtailment for case 2*

4.2 Case 2

In this case, the distributed control algorithm is deployed with BESS installed on all the nodes on the feeder. The reactive power action has been disabled for this case, to represent a possible real life scenario where the PV systems do not have this capability. Fig. 8 shows the voltage profile for this case, while Fig. 9 shows the curtailment.

Again, V_{meas} for Node4B reaches V_{lim} at $t = 485$ min (after the 8th hour) and the controllers switch to the BESS charging state. The batteries are fully charged at time $t = 1024$ min (just after the 17th hour) and a small curtailment is observed in this case (Fig. 9). The curtailment is small because at this time of the day, P_{PV} is decreasing and tending towards zero.

Peak shaving to ease loading on the network starts at time $t = 1025$ min (after the 17th hour), when the P_{TH} is reached as a result of high load demands around this time (see Fig. 3).

4.3 Case 3

In this case, the distributed control scheme is again deployed on the test feeder as in Case 2, but this time, with the reactive power action enabled. Another difference this case has from Case 2 is that fewer BESS have been installed on the nodes of the test feeder. BESS installations for this case are only on nodes 4AB2, 4AB4, 4AB6, 4AB8 and Node4B. This is to represent a possible real life scenario where an attempt is made to cut the cost of installation of BESS units. The voltage profile is shown in Fig. 10.

The batteries start charging and are fully charged at times $t = 485$ min (after the 8th hour) and $t = 774$ min (before the 13th

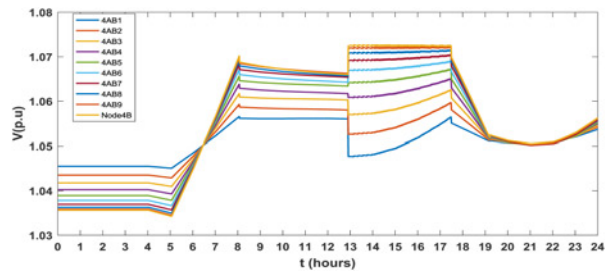

Fig. 10 *Feeder voltage for case 3*

CIRED, Open Access Proc. J., 2017, Vol. 2017, Iss. 1, pp. 1722–1725

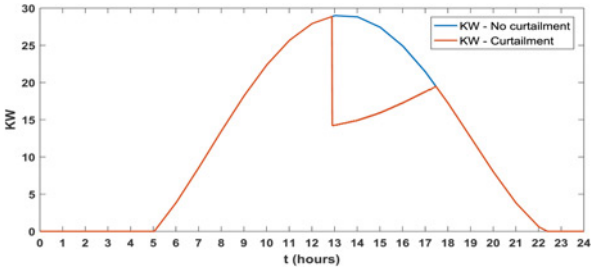

Fig. 11 *Curtailment for case 3 without reactive power action*

hour), respectively. The reactive power action takes up the control immediately the batteries get full. The maximum amount of reactive power that can be absorbed by the inverters at this time is given by (1). The voltage dip that can be observed at the point of reactive power action, especially for the nodes closer to the substation, is as a result of the controller operating uniformly and absorbing the same amount of reactive power. This therefore has different impacts on the terminal voltage of different nodes on the feeder. If the reactive power action was not activated for this case, a large amount of energy would be curtailed as shown in Fig. 11.

5 Discussion

This scheme has demonstrated the use of BESS and reactive power to mitigate overvoltage on the distribution network. The tests, however, were carried out without consideration of the variability of load and intermittency of PV power. The illustration was made simplistic to obtain preliminary results and information for further development.

Using this scheme, it is possible to have no curtailment of active power. This maximises the benefits of investment in PV systems and reduction in greenhouse gas emissions, but it comes at the cost of having to install BESS, which are expensive. Holistic cost–benefit assessments are important in order to ascertain the exact economic benefits of using BESS versus curtailing active power.

Optimum BESS sizing and location are also important factors to consider if this scheme is to be deployed in a larger network. This is to avoid situations where BESS may be oversized, as this would lead to greater cost.

Losses on the power lines due to use of reactive power for voltage control is a factor that should also be considered.

6 Conclusion

This paper presented a distributed control scheme for mitigation of overvoltage on low-voltage distribution networks with high penetration of PV. The scheme was tested on a single feeder distribution network. BESS was employed to accommodate excess PV production, especially during the day when there is light loading and high PV power production. Simulations show that this scheme successfully keeps voltages within statutory limits. Fewer numbers of BESS were installed on critical nodes and this achieves almost the same results as when BESS are installed on all the nodes. The control scheme therefore is economical in this sense.

7 References

1 B. EN, "50160: 'Voltage characteristics of electricity supplied by public distribution systems' (British Standards Institution, 2000)
2 Olivier, F., Aristidou, P., Ernst, D., *et al.*: 'Active management of low-voltage networks for mitigating overvoltages due to photovoltaic units', *IEEE Trans. Smart Grid*, 2016, **7**, pp. 926–936
3 Yang, Y., Li, H., Aichhorn, A., *et al.*: 'Sizing strategy of distributed battery storage system with high penetration of photovoltaic for voltage regulation and peak load shaving', *IEEE Trans. Smart Grid*, 2014, **5**, pp. 982–991
4 Turitsyn, K., Sulc, P., Backhaus, S., *et al.*: 'Options for control of reactive power by distributed photovoltaic generators', *Proc. IEEE*, 2011, **99**, pp. 1063–1073
5 Otomega, B., Van Cutsem, T.: 'Distributed load interruption and shedding against voltage delayed recovery or instability'. 2013 IEEE Grenoble PowerTech (POWERTECH), 2013, pp. 1–6